Visually guided motion through complex environments



Natalia Pérez-Campanero Antolín

St John's College

University of Oxford

A thesis submitted for the degree of

Doctor of Philosophy

Hilary 2022

Abstract

The ability of animals to swiftly move through cluttered environments has inspired biologists interested in understanding its underlying mechanisms and engineers interested in applying its underpinning principles. To avoid colliding with obstacles, animals first need to detect that an object may be in their way. A decision then needs to be made about avoiding contact with the object so that locomotor strategies can be adjusted accordingly. In this thesis, I break down the problem of how animals negotiate clutter into three distinct, but related questions: 1) What information is needed to avoid collisions, and how do animals perceive it?; 2) how do animals choose between alternative paths to take?; 3) how are such choices implemented? I study these questions in two model species that inhabit open spaces but regularly encounter clutter: the homing pigeon (*Columba livia*) and the Picasso triggerfish (*Rhinecanthus aculeatus*). I frame their clutter negotiation behaviour as a process of sequential gap selection, allowing me to decompose it into components that can be independently evaluated. In Chapter 2, I use a combined experimental and modelling approach to model pigeons' steering behaviour algorithmically in a two-alternative forced-choice task. The birds are tracked flying inside a large hall whose open exit was separated from the release point by a curtain creating two vertical gaps. I find that their flights are best modelled by delayed proportional navigation, the same steering controller that has been used to implement all basic geometries observed in pursuit behaviour. In Chapter 3, I use a high-speed motion capture system to track pigeons flying through an artificial forest of vertical poles. I find bird gap choices are best captured by an autoregressive model, including information about the exit location, the cartesian distance between the closest obstacles, and the apparent visual gaps between all the obstacles ahead. In Chapter 4, I use a similar experimental paradigm to investigate how fish negotiate clutter, a behaviour which has never been studied in fish before. I find evidence of fish choosing clearances most directly aligned with their target based on egocentric visual cues. Finally, I show how these components can be combined to simulate realistic animal trajectories through clutter. Overall, the results of my thesis provide a valuable new framework for looking at how animals move through complex environments.

Contributions

The work within this thesis is primarily my own. None of the content has been submitted, in whole or in part, in any previous application for a degree. Other authors contributed towards one or more data chapters as follows:

Graham Taylor oversaw the project and provided feedback on all data chapters of this thesis.

Chapter 2: This chapter is presented as a journal manuscript. The experiment was designed between myself and Graham Taylor. I collected, formatted and analysed the data and wrote the manuscript, which was edited and modified by my supervisor Graham Taylor. The published manuscript is available at: doi.org/10.1242/jeb.244215

Chapter 3: Lucy Larkman assisted with data collection. Cait Newport provided feedback.

Chapter 4: Cait Newport aided with behavioural training and the construction of the experimental set-up, and provided feedback. Abhishek Dutta processed video data collected during experiments in Chapter 4. As noted in the chapter, this is not used for the analysis presented in this thesis but forms the basis of a submitted manuscript on using computer vision methods for processing behavioural data. Preliminary results of what this process looks like are presented as supplementary information, as they will form the basis of data analysed for publication in an additional manuscript that is currently *in prep*.

This thesis is submitted in an integrated format. Chapters, therefore, have stand-alone introductions and discussions.

Acknowledgements

Throughout my DPhil, I have received guidance, support, and companionship from countless sources, for which I am endlessly grateful. Before thanking individuals, I would first like to acknowledge the BBSRC, ERC, St John's College and AFOSR for their financial support. Their generous funding has provided me academic freedom under trying circumstances.

My primary supervisor Graham Taylor has played a fundamental part in this thesis: allowing me to become an independent researcher through punctuated feedback, and securing the ERC grant that ensured I had access to state-of-the-art equipment for my work. Thanks to this, we were able to bring to life a purpose-built experimental facility even when most of the department was struggling to find building space. It has been an honour to be welcomed into the Oxford Flight Group. I would also like to thank my secondary supervisor, Cait Newport, for joining the project halfway through and taking me on as her first student. She has been a constant source of support and inspiration, both on an academic and a personal level. Thank you also to my examiners, Adrian Thomas, who has seen many stages of my work, and Andrea Gaede, for their valuable and insightful comments.

Life and work at the Wytham Field Station would have been a lot harder without the wonderful colleagues in it. I would particularly like to thank Marco and Sofia for their sunny disposition, always being willing to lend a helping hand and assuaging the many issues with the mocap system. Thank you as well to James S, Leo, and Indira for providing many laughs, interesting conversations, and much needed breaks. Caroline, Lydia, the Jameses, Emma, Robin, Kyu Minh and Alex have also all made the Flight lab a great group to work in. Lucy and John have been fantastic in supporting my work, and I have learnt a lot about animal husbandry and carpentry from them both – most importantly that it's best to leave some things to the professionals.

On a personal level, I would first like to thank my parents and sister for their constant support and encouragement, as well as their valiant efforts to relate to my life. To the many friends and connections, I have made in Oxford: thank you for enriching my life. I have many fond memories in and around St John's College and its properties with a lot of MCR members. Anna and Alix particularly have been absolute rocks – I wouldn't have wanted to go through the ups and downs

of PhD life with anyone else. The DTP crowd, and everyone who I have met through them, has also been a fantastic group to be part of, and I am excited to see where everyone ends up. My more artistically inclined friends have provided some much-needed balance - I am indebted to Maria, Tiffany, Bex and the others for rekindling my love for painting, music and dress-up. The community I have found through pole and yoga has given me more than I could ever have imagined, and I will forever be grateful for them coming into my life. Their practice has kept me sane during building closures -whether asbestos or lockdown related- and the writing-up stages. I have somehow managed to spend a large portion of my PhD in London – much love to everyone who has made weekends there so fun and provided some necessary perspective away from the Oxford bubble.

Finally, I would like to thank the deities of academia and scholarship, which I evidently offended in a past life, for providing me with more examples of how to deal with difficult situations than I could possibly use in a lifetime of job interviews.

Contents

List of Figures **x**

List of Tables **xii**

1 Introduction **1**
1.1 Framing the thesis problem 5
1.2 Sensing clutter in the environment 5
1.2.1 Vision 6
1.3 Processing of sensory information relevant to negotiating complex surroundings 10
1.3.1 Avian vision 11
1.3.2 Fish vision 14
1.3.3 Spatial information 15
1.4 Engineering approaches to negotiating cluttered environments . . . 17
1.4.1 Path planning: dealing with obstacles from an engineering perspective 18
1.5 How are obstacle-laden spaces perceived while navigating? 24
1.6 Why these study species? 26
1.6.1 Pigeons 26
1.6.2 Trigger fish 27
1.7 Structure of thesis 28
References 31

2 Gap selection and steering during obstacle avoidance in pigeons **40**
2.1 Abstract 41
2.2 Introduction 41
2.3 Algorithmic framework 43
2.4 Methods 49
2.4.1 Subjects and training 49
2.4.2 Experimental set-up and protocol 49
2.4.3 Motion capture 51
2.4.4 Flight trajectory analysis 53

2.4.5 Steering controller simulations . . . 54
2.4.6 Statistical analysis . . . 56
2.5 Results . . . 56
2.5.1 Pigeons select gaps on the basis of handedness, not size . . . 57
2.5.2 Simulations of steering behaviour . . . 58
2.5.3 Extension of model fitting to entire measured trajectory . . . 67
2.6 Discussion . . . 67
2.6.1 Limitations . . . 73
2.7 Supplementary Information . . . 76
2.7.1 Characteristics of animals used during data collection and recorded flights . . . 76
2.7.2 Results of simulations treating the midpoint of the gap as the target of the bird's guidance. . . . 80
2.7.3 Results of simulations treating the point 0.35 m from the edge of the curtain as the target of the bird's guidance. . . . 85
References . . . 89

3 Pigeon gap selection in forest-like obstacle field 92
3.1 Abstract . . . 93
3.2 Introduction . . . 93
3.3 Methods . . . 98
3.3.1 Ethics statement . . . 98
3.3.2 Subjects and training . . . 98
3.3.3 Experimental setup . . . 98
3.3.4 Experimental design . . . 101
3.3.5 Motion capture . . . 102
3.3.6 Marker reconstruction and labelling . . . 102
3.3.7 Statistical analysis . . . 103
3.4 Results . . . 106
3.4.1 Different individuals select similar routes through the same clutter . . . 106
3.4.2 Pigeons select gaps most aligned with the exit roller door . . . 107
3.4.3 Initial flight direction relates to gap choice, not handedness . . . 109
3.4.4 Modelling gap choice . . . 110
3.5 Discussion . . . 111
3.5.1 Estimating the size of apertures . . . 113
3.5.2 Determining targets . . . 115
3.5.3 Limitations . . . 118
3.6 Supplementary Information . . . 120

3.6.1 Characteristics of animals used during data collection 120
3.6.2 2D histograms of routes taken through obstacle configurations 121
3.6.3 2D histograms of routes taken by individual 127
3.6.4 Performance of candidate binomial generalised linear models of pigeon gap choice in an artificial forest of obstacles task. . 129
3.6.5 Performance of candidate binomial generalised linear models of pigeon gap choice in an artificial forest of obstacles task. . 131
References 131

4 Fish gap selection in rubble-like obstacle field 134
4.1 Abstract 134
4.2 Introduction 135
4.3 Methods 139
4.3.1 Subjects 139
4.3.2 Experimental tank 140
4.3.3 Experimental procedure 141
4.3.4 Data processing 143
4.3.5 Data analysis 144
4.4 Results 148
4.5 Discussion 153
4.5.1 Visual cues for clutter negotiation 153
4.5.2 Gap selection and individual characteristics 154
4.5.3 Limitations 155
4.6 Supplementary Information 157
References 157

5 General discussion 160
5.1 Modelling decision-making in space 161
5.2 Spatial decision-making in distinct taxa 164
5.2.1 Limitations 164
5.2.2 State dependence 167
5.2.3 Timing and geometry of decisions 168
5.3 Concluding remarks 170
References 170

Appendices

A Visual and vestibular input use in perching **173**
A.1 Abstract . . . 173
A.2 Introduction . . . 174
A.3 Materials and methods . . . 175
A.3.1 Animals . . . 175
A.3.2 Videography . . . 176
A.3.3 Treatment . . . 178
A.3.4 Torque measurements . . . 178
A.3.5 Statistical analysis . . . 179
A.4 Results . . . 179
A.5 Discussion . . . 180
References . . . 182

List of Figures

1.1 Coordinate system for description of optic flow 8
1.2 Patterns of optic flow experienced in the retina from different movements. 9
1.3 Perceiving clutter 25

2.1 Geometry of pursuit 44
2.2 Experimental set-up 52
2.3 Gap negotiation behaviour in pigeons 59
2.4 Gap selection behaviour in pigeons. 60
2.5 Box plots showing root mean square (RMS) error (ϵ) of simulations under each fitted guidance model 63
2.6 Distributions of parameter estimates for guidance models fitted independently to each flight 64
2.7 Optimization surfaces for steering controllers fitted globally for all flights 66
2.8 Simulations of gap-oriented steering in pigeons under proportional navigation guidance 68

3.1 Patterns of optic flow generated by corridors and gaps. 96
3.2 Experimental set-up and illustrations of variables captured in the model. 100
3.3 2D histograms of 17 flight tracks in a single obstacle configuration (left, i) and for a single bird (right, ii-iii) 108
3.4 Gaps selected by pigeons in the forest-of-obstacles arrangement and ROC curve of best performing model of pigeon gap choice. 109
3.5 Model variables included in the top performing models 112
3.6 2D histograms of routes taken through obstacle configurations 1-10 121
3.7 2D histograms of routes taken through obstacle configurations 11-20 122
3.8 2D histograms of routes taken through obstacle configurations 21-30 123
3.9 2D histograms of routes taken through obstacle configurations 31-40 124
3.10 2D histograms of routes taken through obstacle configurations 41-50 125
3.11 2D histograms of routes taken through obstacle configurations 51-62 126
3.12 2D histograms of routes taken by individuals A27-B80. 127

3.13 2D histograms of routes taken by individuals D00-S86 128

4.1 The natural habitat of Picasso triggerfish 137
4.2 Experimental tank 142
4.3 Depiction of trial variables captured in statistical model 146
4.4 Alluvial plot depicting frequency of gap choices. 149
4.5 Fish trajectories during recorded trials included in the analysis . . . 150
4.6 Example output of processing recorded video data using a deep learning pipeline 157

5.1 Incorporating models of gap choice and steering into a simulated trajectory 163
5.2 Determining the mid-point of gaps to aim towards 166

A.1 Diagram of sensory modalities associated with maintaining upright posture and how these translate into a motor output. 175
A.2 Top-down schematic view of experimental set-up. 177
A.3 Bird cage set-up for social input 177
A.4 Histograms of root mean square (RMS) values of torque in light and dark conditions 180
A.5 Example of power spectral density estimate for one individual. . . . 181

List of Tables

2.1 Guidance laws used to model target-oriented steering behaviour in animal flight. . . . 46
2.2 Parameter estimates for steering controllers fitted globally for all flights. . . . 67
2.3 Birds used for experiments. . . . 76
2.4 Obstacle positions and gap choices of all recorded flights. . . . 76
2.5 Flight characteristics. . . . 80
2.6 Individually fitted one-parameter simulations with the target as the middle of the gap. . . . 81
2.7 Individually fitted two-parameter simulations with the target as the middle of the gap. . . . 82
2.8 Globally fitted simulations of one-parameter models with the target as the middle of the gap. . . . 83
2.9 Globally fitted simulations of two-parameter models with the target as the middle of the gap. . . . 84
2.10 Individually fitted simulations of one-parameter models with the target one wing-length from the curtain edge. . . . 85
2.11 Individually fitted simulations of two-parameter models with the target one wing-length from the curtain edge. . . . 86
2.12 Globally fitted simulations of one-parameter models with the target one wing-length from the curtain edge 87
2.13 Globally fitted simulations of two-parameter models with the target one wing-length from the curtain edge. . . . 88

3.1 Variables extracted from each flight for further analysis 104
3.2 Model structures used for analysis. . . . 106
3.3 Analysis of variance of factors included in the top-performing model of pigeon gap choice. . . . 113
3.4 Birds used for experiments. . . . 120
3.5 Performance of candidate binomial generalised linear models of pigeon gap choice in an artificial forest of obstacles task. . . . 129

3.6 Odds ratios of individual birds choosing a gap on the first row based on handedness, gap size or alignment with roller door. 131

4.1 Association between variables extracted from each trial 152
4.2 Odds ratios of fish choosing a gap given the same gap was crossed in the row before, that the gap is the largest available, and that the gap contains a view of the food target 152

Caminante, no hay camino, se hace camino al andar...

Traveler, there is no road; you make your own path as you walk...

— in Antonio Machados's *Caminante, no hay camino*

1 Introduction

Contents

1.1 Framing the thesis problem 5
1.2 Sensing clutter in the environment 5
1.2.1 Vision 6
1.3 Processing of sensory information relevant to negotiating complex surroundings 10
1.3.1 Avian vision 11
1.3.2 Fish vision 14
1.3.3 Spatial information 15
1.4 Engineering approaches to negotiating cluttered environments 17
1.4.1 Path planning: dealing with obstacles from an engineering perspective 18
1.5 How are obstacle-laden spaces perceived while navigating? 24
1.6 Why these study species? 26
1.6.1 Pigeons 26
1.6.2 Trigger fish 27
1.7 Structure of thesis 28
References 31

As Machado's poem beautifully illustrates, the path our lives take is shaped by the accumulated decisions we make over time. Animals, too, face constant choices every day, from deciding between alternative food sources to choosing a mate. Even the most basic of these require multiple systems within an organism

to work in tandem to find a solution. For instance, to choose between alternative food sources, an individual must first decide that moving to one of these sources is a better outcome than doing nothing. In other words, it must set reaching food as a goal. Once this goal has been established, the animal must identify its available options to achieve such a goal: how many food sources are available, where are they, and how do they differ? Assuming the location is clear, and one of the options is superior, the individual must then figure out how to get to that goal. Breaking such simple decisions down thus starts to unpack some of the complexity behind them. Yet, animals with the simplest of brains execute these almost instantaneously while swiftly moving through the complex environment that the world presents. How do they achieve such feats? This is what I have tried to answer over the course of my DPhil. In the complex, three-dimensional environments animals live in, how do they make their way to their target location while avoiding colliding with the many obstacles in their way? What follows is an account of how I have thought about this problem and what I have learned.

Animal movement has fascinated researchers for centuries at various spatial and temporal scales. Writers as far back as Homer and Aristotle have pondered the seasonal disappearance and reappearance of birds that we now know as migration. An organism's ability to get to a desired location implies at least two key capabilities: first, the capacity to form an internal representation of the identities and locations of significant objects in one's environment, and second, being able to orient oneself with respect to such objects [1]. The problem of navigating space to reach a goal is so common that many disciplines have approached it through their own lens, often leading to ambiguous or conflicting terminology being used to describe the same phenomena. Therefore, for clarity, I shall first outline how some common terms will be used in this thesis. Attempts at breaking down navigation elements such as homing have mostly opted to distinguish based on the range and type of information used. In terms of information range, the component of navigation that utilises environmental information that is directly accessible by an organism's sensory and motor systems is known as locomotion or guidance. In contrast, a goal-directed

movement towards a destination beyond the local surroundings, what ethologists traditionally think of as "navigation", can be referred to as wayfinding. Regarding the type of information being used, available cues can be divided into allothetic (external to the body of an animal) and idiothetic (self-referential) cues.

Idiothetic cues can be generated from an organism's proprioceptive and vestibular system [2], sensory flow [3], or efferent copies of movement commands [4]. The navigational strategy that involves using self-generated cues to monitor a navigator's displacement over time relative to a starting position is termed path integration. First observed in gerbils, which were found to be capable of carrying displaced pups in a straight line path from the pick-up point to their nest even in complete darkness [5], path integration has since been demonstrated across taxa (ants [6], spiders [7], rats [8], humans [9], [10], goldfish [11], mantis shrimp [12]). Animals commonly use path integration to take a direct vector home at any point in an outward journey by integrating their velocity -containing information about both speed and direction of travel- as deduced from idiothetic cues.

In contrast, navigational strategies that rely on allothetic cues typically involve the use of landmarks, defined as cues that are salient and stable in the environment. These can be used by navigating animals as a reference point for the desired location ("beaconing") or to identify a route. Such landmarks can take the form of visual, auditory or olfactory features in the environment. Examples of each of these have been observed in animals moving across aquatic (e.g. Pacific salmon swimming towards the odour of their home stream water [13]), aerial (e.g. big brown bats using a frog chorus as an auditory beacon) and terrestrial environments (mice, humans, ants). A single landmark is used in beaconing, and animals often take the shortest possible route towards it, a straight-line path. When a sequence of landmarks or well-marked routes is used to navigate to a target, the strategy is termed route following, as is often observed in ants and termites following pheromone trails. This is also called piloting in animal navigation, with pigeons [14] and brown surgeonfish [15] providing notable examples.

A further distinction is made between the navigational strategies above and those thought to require an enduring external or internal spatial representation (a map or cognitive map), that is, knowledge of landmarks, routes, distances and directions that is spatially unified. The exact form such a "map" takes has been extensively studied, with two key ideas emerging from the ethological literature: the grid and the mosaic maps. Based on observations of pigeon homing, Wallraff [16] suggested that birds determine their position with respect to home by using local scalar values of environmental gradients, referenced against a mental representation of the spatial distribution of such gradients. It is suggested that by extrapolating gradients beyond the range of direct experience, such a "gradient map" allows birds to estimate distances and navigate at unfamiliar sites. Possible cues that have been suggested to form gradient maps include odour, magnetic intensity and gravity (reviewed in [17]). Within familiar sites where the difference in such gradients may become unusable for navigation, Wallraff proposed that birds remember the position of prominent landmarks with respect to each other, forming a directionally oriented representation of the home area. Confusingly, the term piloting is also used in the cognitive neurobiology and psychology literature to describe navigational strategies involving landmark-based cognitive maps. Still, we will limit its meaning here to following a sequence of landmarks or well-known cues for clarity.

To successfully reach its target, an organism needs to keep track of its location relative to some reference point as it moves to remain oriented. Spatial orientation is always relative to something, and the system used for defining relational systems consisting of spatial relations between objects is termed a reference system. Reference systems can be divided in a myriad of ways, but for navigation, it is useful to distinguish between egocentric and environment-based reference frames broadly. Location and orientation can be specified relative to the observer's position (egocentric); for instance, the pigeon loft is 80 m the left and behind the flight hall; or relative to the environment, such as the sun's azimuth or landmarks (the pigeon loft is to the east of Wytham Hill). These can of course be further subdivided, such as into eye, head and body-based coordinate systems in the case of egocentric reference frames,

or intrinsic and absolute in the case of allocentric reference frames, amongst others. Levinson [18] defined absolute reference systems as those coding directions relative to global features that function over large areas. Features animals are thought to make use of to provide a global (azimuthal) reference include the position of the sun [19], celestial bodies [20] or geomagnetic cues [21]. In Kramer's [22] two-step "map-and-compass" navigation model, this process is known as the "compass" step.

1.1 Framing the thesis problem

To avoid colliding with obstacles, animals first need to detect that an object may be in their way. A decision then needs to be made about how to avoid contact with the object so that locomotor strategies can be adjusted accordingly. The problem of successful navigation through complex environments is common in fields as varied as robotics, psychology and biomechanics. The advances in areas adjacent to animal behaviour have been instrumental in developing biologists' thinking about how animals may achieve feats similar to those studied in humans and man-made systems. Biological systems have heavily influenced obstacle avoidance in robotics, and in turn, this thesis draws on how engineers have dealt with controlling machine movement in cluttered spaces. In this spirit, I think of my question of study in terms of 1) the information needed to avoid collisions and how this is perceived and processed by animals; 2) how this information informs decisions about what path to take; 3) how such decisions are implemented. I address this question in two species that move in 3D environments differently: the pigeon and the triggerfish. Therefore in briefly outlining some background relevant to the thesis below, I focus primarily on that most pertinent to my study species.

1.2 Sensing clutter in the environment

Information about the environment is available in the form of electromagnetic energy, chemicals, vibrations, temperature and physical contact, amongst others. For an animal to determine whether an obstacle may be obstructing its path, it must first be

able to separate objects in the environment from the background. Information about these objects' position, size, or velocity must then be collected to establish whether the agent might be on a collision course. How can this information be obtained?

Animals have developed highly specialised sensory systems to extract information relevant to their survival, such as avoiding collisions while moving at high speed. Such systems include those well-studied in humans (vision, hearing, smell, touch, taste, equilibrium), and some, to the best of my knowledge, beyond human capabilities, such as electric and magnetic field detection or infrared "vision". The sensory modality of information inevitably limits its use in specific scenarios, and so at any given point, an animal is likely to be utilising inputs from several modalities [23]. For instance, vibrational information obtained from echolocation can provide high angular, and depth resolution [24] and is commonly used by bats and dolphins, amongst others. However, it has an intermittent sampling rate and relatively short range due to relying on high frequencies that attenuate rapidly in air [25]. Accordingly, bats have been found to complement auditory cues from echolocation with visual cues during navigation to enhance obstacle avoidance capabilities [26]. Nevertheless, spatial navigation tasks, including negotiating cluttered environments, tend to depend mainly on vision [27]. This is particularly true in organisms whose primary sense is vision, including pigeons and triggerfish. Therefore, this thesis will consider vision as the primary source of information relevant to navigating complex environments.

1.2.1 Vision

Animals can perceptually integrate the 2D stimuli received by retinal surfaces to obtain information about the third dimension of the visual environment in which they operate. Reconstructing this third dimension facilitates the estimation of relative positions of points, planes or features with respect to a fixation plane (or another relative position). This process is referred to as depth perception and allows observers to segregate unambiguous surfaces into figure and ground, facilitating object detection. Additionally, a three-dimensional frame of reference can allow

observers to estimate the egocentric absolute distance of an object (i.e. the absolute distance of an object to the observer).

Mechanisms that enable 3D visual perception from 2D retinal projections typically exploit geometric spatial relations or some form of prior knowledge. Sampling the same point in space from two vantage points, such as from two separate eyes (known as stereopsis), allows a direct angular measure of depth with respect to a fixation point. In stereopsis, such information is based on horizontal retinal disparity. Additionally, visual geometry can be combined with proprioception to perceive three-dimensional space by measuring the oculomotor adjustment needed to maintain a sharp image on the photoreceptors of each or both eyes - known as accommodation and convergence, respectively. An alternative approach to estimating depth from visual cues relies on the cognitive interpretation of previously explored static images. Cues such as occlusion, relative size, perspective, shading, texture gradients and blur are valuable in interpreting scene structure. However, these can generally not provide the precise quantitative information necessary in situations at the limits of depth resolution, such as flight manoeuvres in a cluttered environment.

The above cues can all provide information while an observer is stationary. However, as an observer moves through an environment, the visual information created by motion provides several additional cues. Similar geometry to that used for binocular depth perception can be exploited by sampling the same point from different positions in time instead, due to the difference in image motion between objects at different depths known as motion parallax. As an animal moves relative to its environment, the rays connecting object points to the animal's vantage point move in a predictable way. The pattern of angular velocities generated in the retina when an animal moves through space contains a wealth of information that can be used while navigating 3D environments, including that relating to the orientation of surfaces [28], the direction of heading [29], and time to contact an approaching object [30]. Gibson [31] was among the first to notice this, referring to this pattern as "optic flow". In this section, I will use the coordinate system of the animal's eye depicted in figure 1.1 to illustrate some important features of

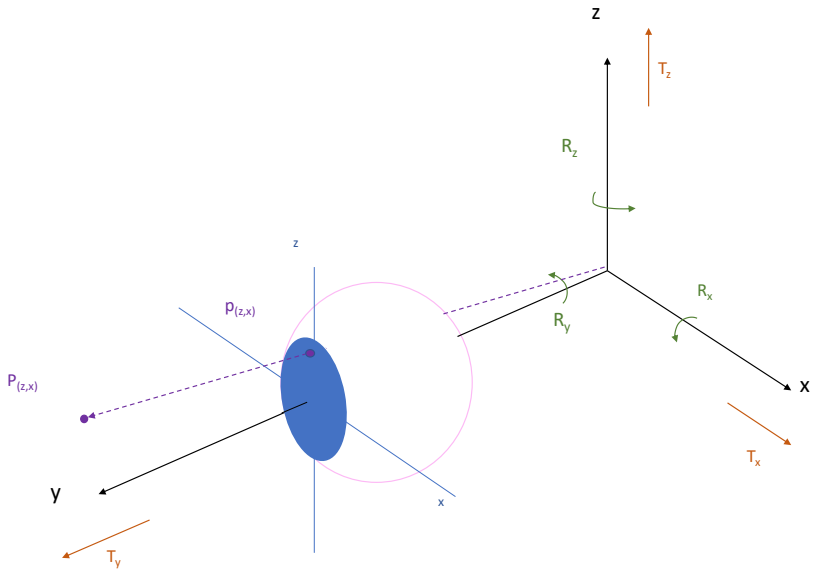


Figure 1.1: Coordinate system for description of optic flow used in this thesis. Note depth information is contained in the axis labelled Y. Other authors have also referred to this as the Z axis in the context of optics, but this thesis shall use the coordinate system depicted here.

optic flow and how depth information can be obtained from it. I will treat the retina as a planar projection plane (xz) for simplification, but the same principles apply when projections are onto the spherical shape of animal retinas. Note in the diagram, the Y-axis represents depth.

The motion of an observer relative to the environment is described by a translational and a rotational component, with elements in each of the axis (yaw, pitch and roll). These components of relative motion between observer and environment are experienced as rotational and translational optic flow in the observer's retina ($T_xT_yT_z$ and $R_xR_yR_z$). Only the translational component of optic flow provides depth information. This happens because, in pure rotation about the eye, all points move with the same angular velocity regardless of depth. The perception of depth of environmental points along the y-axis in figure 1.1 therefore arises from translation rather than rotation. This is depicted in figure 1.2, which shows the patterns of flow generated by each type of movement when looking at two planes at different depths (the left plane is closer than the right plane). In figure 1.2B, the vectors at corresponding eccentricities on the left and right have

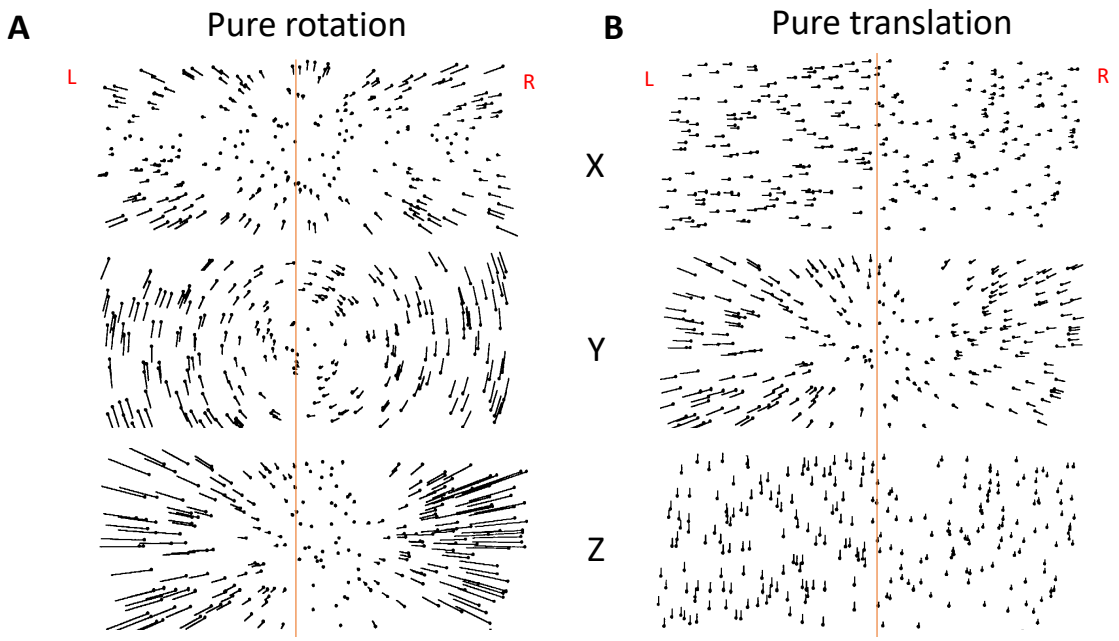


Figure 1.2: Patterns of optic flow experienced in the retina from different movements. **A** Pattern of optic flow experienced during pure rotational movement when looking at two planes at different depths. The left plane is closer (less deep) than the right plane. Despite the different depths of the planes, corresponding vectors in the left and right have equal lengths, as angular velocity depends on the position of the retina only. **B** Pattern of optic flow experienced during pure translational movement when looking at two planes at different depths. The left plane is closer (less deep) than the right plane. The vectors at corresponding eccentricities in the left and right have different lengths. Thus relative depth of the left and right can be obtained from the relative difference in velocities of of the moving points.

different lengths. Thus the relative depth of the left and right can be obtained from the relative difference in velocities of the moving points. Meanwhile, for rotational movements (fig 1.2A), corresponding vectors in the left and right have equal lengths, as angular velocity depends on the position of the retina only.

Naturalistic movement almost always involves both translational and rotational optic flow components, and therefore filtering out rotational optic flow from the apparent image motion experienced in the retina is the key to recovering depth information from motion. Birds have been shown to maximise the time during which they can perceive depth information from optic flow by reducing rotational gaze shift to short saccadic head turns, and keeping their head orientation constant relative to the environment while moving around obstacles [32]. For purely translational optic flow along the X or Z planes, the relative depth of two objects is given by the ratio of the retinal velocities between those objects. Differentiating the retinal vectors in

space provides the rate at which these change in the X and Z directions, which can be used to recover the orientation and curvature of a surface. When the flow is in the Y plane, retinal coordinates are also needed to calculate depth. Assuming the relative velocity of the observer stays constant, the depth of environmental points obtained from Y-translation also provides information about time to collision (TTC) independent of object size. This is a particularly helpful cue for avoiding collisions, and has been linked to escape, landing, and pursuit behaviours in several species (e.g. [33] [34] amongst others). As well as providing information about the structure and layout of objects in the world, translational optic flow provides information about the observer's movement in an environment. This can be understood most simply when considering the view from a car while driving on a motorway. In this situation, there is an outflow of global visual information from the end of the road (the focus of expansion, assuming the road is straight) in the direction of the observer's movement. This pattern of expansion provides information about the direction and speed of the observer's translation. Animals have been shown to use information from optic flow in this way to help estimate flight distance, for instance, during homing [35].

1.3 Processing of sensory information relevant to negotiating complex surroundings

Visual processing in vertebrates can be loosely divided into three parts: the eye (including the retina), retinal projections connecting the retina to visual centers in the brain, and visual centers in the brain receiving and processing sensory information. Work on bird and fish visual systems has revealed that the fundamental principles that allow key aspects of visual perception are well conserved across vertebrates, despite vast disparity in available circuity between clades [36]. For instance, in the natural environment, motion detection is dominated by luminance-based motion cues. These are referred to as first-order or Fourier motion. Second-order (also known as non-Fourier) motion cues, such as movement of contrast, flicker or texture can also be used to perceive complex environments. The processing of such second-order motion cues is linked to higher-level cognitive phenomena such as attention,

and was traditionally considered to be unique to the mammalian neocortex due to the computational challenge it poses. Despite that, we now know both fish and birds perceive second-order motion [37] [38]. This suggests that either second-order motion is processed in earlier stages of the vertebrate visual system, or similar computations to those thought to happen in the neocortex take place in homologous structures in fish and birds (the pallium). Beyond its inherent interest, this account thus illustrates how furthering our knowledge of animal visual systems can develop our understanding of vision in humans.

1.3.1 Avian vision

Birds are highly visual animals, relying more heavily on vision than any other terrestrial vertebrate [39]. Pigeons, in particular, have been the subject of a large amount of work on avian vision, thanks to which we now better understand birds' extensive visual abilities. These include good detection of static and dynamic stimuli in noise, detection of biological and other complex motion, colour and UV vision, as well as stereopsis.

Avian vision is achieved by several neurovisual systems originating in the retina but varying in their destination within the brain. Two of these systems have been widely studied: that carrying information from the retina to the optic tectum, and that moving information from the retina to the principal visual nucleus of the dorsal thalamus [40]. In birds, these are known as the tectofugal and thalamofugal pathways. However, other neurovisual systems exist, such as those carrying information from the retina to nuclei in the accessory optic system (AOS), the pretectum, and the hypothalamus, all of which are highly conserved in vertebrates [41].

Differences in the relative sizes of visual nuclei are often correlated to the visual behaviour of a species. For instance, hummingbirds tend to have enlarged pretectal nuclei, nucleus lentiformis mesencephali (LM). The LM is associated with the optokinetic response and the analysis of optic flow, both of which are critical to hovering [42]. Meanwhile, the size of the visual Wulst seems to be correlated with

the amount of binocular overlap of a species. Owls and other species thought to possess global stereopsis tend to have particularly enlarged visual Wulsts [43] [44].

Nevertheless, the tectofugal pathway tends to be the most prominent in birds and is considered the primary visual system of the clade, with most optic fibres projecting onto the optic tectum, which is generally large compared to that of other vertebrates [41]. The optic tectum is thought to control the localisation of objects in space; it is responsible for orienting an animal's movement to stimuli of interest and is thus involved in identifying and judging the importance of focussed objects [45]. Neurons in the optic tectum and further upstream of the tectofugal pathway respond to objects moving towards the eye of the bird (looming stimuli) relative to the background, but not when the motion of the object and background are identical [46] [47].

Meanwhile, the role of the visual Wulst, the telencephalic target of the thalamofugal pathway, is less well understood. The visual Wulst is analogous to the mammalian primary visual cortex (V1) – both receive visual information from the retina via the nucleus geniculatus pars dorsalis of the thalamus (Gld), and project onto thalamic and midbrain structures, amongst other similarities [48]. However, the physiological function of the visual Wulst in pigeons cannot be extrapolated from our knowledge of it in the many studies of the owl Wulst, due to each processing qualitatively different information: pigeons receive mainly monocular information from the lateral visual field, while owls' input is predominantly binocular. In laterally-eyed birds, the Wulst seems to be principally involved in analysing visual information in the lateral visual field [49]. GLd neurons projecting onto the Wulst respond preferentially to motion within 60° of the optic axis, with receptive fields generally larger than those in the tectum [50]. There is also evidence that the Wulst is engaged in representing and remembering global spatial information [51] [52].

The neurovisual systems connecting the retina with nuclei in the accessory optic system and pretectum are often considered the third major visual pathway in birds. These constitute a highly conserved brainstem visual pathway that processes the optic flow pattern resulting from self-motion and generates the optokinetic

nystagmus (OKN) that facilitates gaze stabilisation [53]. The two principal retinal recipient nuclei of this pathway are the nucleus of the basal optic root (nBOR), and the pretectal nucleus lentiformis mesencephali (LM). The nBOR and LM both have extensive projections to other brain structures involved in motor control and to nuclei of other visual pathways such as the Gld [54].

Neurons in nBOR and LM have large receptive fields, as would be expected of a system that analyses patterns of visual motion across the retina, such as those caused by self-motion. Additionally, nBOR and LM neurons are directionally sensitive to large moving patterns, with preferred directions in the nBOR corresponding to upward, downward and backward directions and forward motion in the LM [55] [56]. Neurons in these nuclei are, however, unable to distinguish between translational and rotational components of optic flow. For an illustration of why this is the case, refer back to figure 1.2A: rotational optic flow about the Y axis appears as upward and downward motion along the equator, in the left and right of the image, respectively. The large receptive fields of neurons in the nBOR and LM preferring upward motion would therefore respond equally well to downwards translation and a rightwards roll of the head. A solution to this for lateral-eyed animals, such as pigeons, is to integrate information from the visual fields of each eye.

Information about optic flow is processed and disambiguated in the LM and nBOR's projections to, as well as inside of, the cerebellum. In particular, signals from the direction-selective neurons of nBOR and LM are integrated in the inferior olive. The inferior olive in turn projects to the vestibullocerebellum (VbC), which is involved in making compensatory eye movements [57]. In the VbC, information from ipsilateral and contralateral visual fields is integrated to disambiguate rotational and translational components of optic flow. Neurons in the VbC show a clear topographic organisation, with separate regions responsive to each component of optic flow [58]. Generally, rotational optic flow is encoded in the lateral VbC, known as the flocculus, and translational optic flow is encoded in the medial VbC, known as the uvula. The responses of visual climbing fibres to the flocculus are organised in a three-axis system along the vertical (R_z in fig 1.1) and horizontal

directions, with the two horizontal axes (R_x equivalent) oriented 45° to the midline. The orientation of this axis system matches that of the semicircular canals of the vestibular system, the other sensory system involved in the analysis of self-rotation [57]. It also coincides with the spatial reference system used by the output of the visual system, the eye muscles which generate compensatory eye movements [59]. These systems work in tandem to guide and stabilise flight behaviour.

1.3.2 Fish vision

Multiple fish species rely on vision to guide their behaviour, and accordingly have well-developed visual capabilities [60]. Amongst teleosts, zebrafish and goldfish have traditionally been the species of choice for studying visual systems, with studies on the perception of shape and colour being mostly on the latter, and research on motion vision carried out mainly using zebrafish.

As in avian visual systems, and indeed those of all vertebrates, retinal ganglion cells (RGCs) in fish retina project to several targets in the brain, including the thalamus, hypothalamus, pretectum and optic tectum. While the projections to and from each of these retinorecipient targets have traditionally been considered individual pathways, they are often interconnected and linked to both primary and higher-order sensory and motor structures [61].

In teleosts, the optic tectum receives 98% of the axon projections of RGCs [62]. The pathway connecting the retina to the optic tectum, known as the retinotectal pathway, is thus thought to be the primary visual pathway in fish. The tectal projections from RGCs follow a topographic organisation, with axons from neighbouring ganglion cells terminating in neighbouring positions in the contralateral tectum, thus forming a complete optic chiasm [63]. Neurons in the fish optic tectum respond preferentially to image motion corresponding to temporal-to-nasal, nasal-to-temporal, up and down directions [64]. Evidence suggests the tectum is likely to have a role in visual orientation, discrimination and grasp behaviour rather than in motion detection [65]. Information from the optic tectum is then transmitted to motor nuclei, where it is used to form orientation-based motor reactions such

as turning to a prey object or away from a large potentially dangerous stimulus [66]. The fish optic tectum also receives sensory inputs from other sensory systems and is thus suggested to be involved in multi-sensory integration [67].

As in mammals, birds, reptiles and amphibians, the fish accessory optic system constitutes another major visual pathway that is fundamental to gaze stabilisation, which is essential for the proper functioning of other visual systems [68]. Despite this pathway's key role in mediating visuomotor behaviours, it took much longer to recognise it in fish than in other vertebrates, in part due to the huge variation in fish species, and ongoing debate about the number and exact location of presumed AOS nuclei in different species [69]. The pretectum -part of the diencephalon- is essential for the fish optokinetic reflex and optomotor responses, suggesting it is the principal brain area associated with the processing of optic flow information in the taxa [70]. Neurons of retinorecipient nuclei in the pretectum -presumed to be AOS nuclei- are highly responsive to whole-field motion in four orthogonally arranged preferred directions, and have relatively large receptive fields [71]. These cells have been shown to differentially represent rotational and translational components of optic flow in zebrafish. Two broad classes of pretectal neurons have been identified: "simple" monocular and "complex" binocular neurons. Each of the four types of monocular pretectal neurons preferentially respond to either a nasal or temporal direction of motion in the left or right visual field. Meanwhile, binocular neurons seem to be tuned to translational optic flow, responding strongly to translational forwards and backward motion [72], but being inhibited during rotational motion. The inhibition is likely provided by the eye opposite to the one that activates the cell. Hence these cells are considered binocular [73]. Pretectal neurons in turn project to the cerebellum and lower part of the midbrain, where visual information is processed further.

1.3.3 Spatial information

The information gathered about the environment from external sensory cues must then be integrated with sensory cues derived from self-motion (vestibular or mechanosensory cues, optic flow, proprioceptive feedback and motor efference

copy from limbs) to form an inner representation of the space in which an animal is operating [74]. This internal representation can then be used to determine what motor commands would lead to optimally negotiating an environment in a particular behavioural context.

At a neural level, spatial representations have been strongly linked to the hippocampal formation in fish, reptiles, birds and mammals. The neural mechanisms that facilitate spatial navigation have been most extensively studied in mammals. Specialised cells have been found to encode the internal representation of the animal's location, head direction and various aspects of movement such as speed and angular velocity. The four main types of cells identified are grid cells, place cells, border cells and head direction cells, but others, such as speed cells, have also been found. Together, these encode the two main components required for guided movement: position and orientation. Of these, head direction cells, which encode orientation, are found most commonly across taxa, having been reliably found in birds [4] and fish [75] as well as mammals [76]. Head direction cells are tuned to single preferred head orientations. Their firing rate reaches a maximum when the animal faces the cell's preferred direction, independent of the animal's location or the head's pitch or roll [77].

Place cells, grid cells and border cells encode location information. Place cells become active when an animal passes through a particular location in the environment, called the place field [78]. Meanwhile, grid cells can provide information about both location and distance due to becoming active when an animal traverses one of the vertices of the hexagonal lattice that tiles an animal's mental representation of the environment [79]. Despite the apparent lack of clear place or grid cells in non-mammalian vertebrates, there is evidence of other spatially modulated, if more broadly tuned, cells in both fish [80] and birds [81]. These findings are most commonly thought to indicate that non-mammalian spatial cognition operates through mechanisms that are fundamentally distinct from those in mammals and do not require place cells or the wave patterns characteristic of mammalian spatial cognition [82].

The fourth primary type of cell associated with spatial cognition, boundary/border cells, fire when an animal is located at the boundaries of an environment, thus encoding its shape [83]. Similar cells encoding borders of an environment have been found in the relatively few studies of neural activity in the non-mammalian hippocampus. Fish's lateral pallium [75][84] and birds' hippocampal formation [82] are both considered functional homologues of the mammalian hippocampal formation. The firing fields of cells in the hippocampal formation are anchored to the external environment (ie they are in a world-centred or allocentric reference frame). This makes such cells suitable for a longer-term memory of spatial relationships that do not require continuous transformations between visual and body reference frames as online control of action can [85]. Accordingly, the hippocampal formation is strongly linked to spatial memory and cognition more broadly on top of spatial perception [86]. This contrasts with neurons that carry information about the source of a sensory cue, such as a neuron in the visual cortex responding to a stimulus in a particular part of the visual field relative to the head (i.e. in an egocentric reference frame).

1.4 Engineering approaches to negotiating cluttered environments

Until recently, the strategies and mechanisms underlying negotiating obstacle-laden environments in animals had received surprisingly little attention despite their clear ecological importance. Meanwhile, obstacle avoidance has been a key problem in robotics for some time. As a result, thinking developed in the robotics path planning literature has helped develop biologists' understanding of how animals navigate complex environments. As the name indicates, obstacle avoidance has traditionally been thought of in terms of repellence: objects in the environment the animal or robot (hereafter "agent") aims to stay clear of. This is reflected in the strategies that have been employed to implement obstacle avoidance in engineered systems, briefly reviewed here to place the problem this thesis is trying to solve within the broader literature. In man-made systems, approaches used to solve the problem of collision

avoidance whilst driving the agent towards the target location can be broadly divided into two categories based on the amount of information they require. Global path planning methods require full knowledge of the environment, while sensor-based methods respond to local information only (reactive navigation). In the robotics literature, these are known as classical and reactive path planning, respectively. The advantage of the former is that entire trajectories can be computed offline. Still, it suffers from obvious drawbacks of being computationally challenging (and therefore slow) and models of the world being inaccurate. Reactive approaches, on the other hand, have much lower computational complexity due to only using a portion of the world model. Reactive approaches are clearly more directly relevant to animal systems, as full, up-to-date knowledge of a dynamic natural environment beyond the sensory range of animals is unfeasible. Even if it were, the sensory uncertainty inherent in any biological system would render such methods inaccurate over long timescales. Collecting sensory information directly from the local environment is, therefore, necessary for robust movements in real-world environments. A full review of obstacle avoidance and path planning methods in robotics is beyond the scope of this thesis. Nevertheless, some background on how thinking about the sorts of spatial problems that animals face daily has developed from an engineering perspective can help shed some light on possible underlying mechanisms. The reader is directed to [87] [88] for more comprehensive reviews.

1.4.1 Path planning: dealing with obstacles from an engineering perspective

Path planning algorithms can be classified in a multitude of ways. Several authors divide them into classical (also known as exact) algorithms and heuristic-based algorithms [89] [90]. Classical algorithms look for a navigation solution, typically based on full prior knowledge of the environment, which can be computationally intensive. Meanwhile, heuristic algorithms usually create a set of temporary paths at each iteration, taking in local environmental information at each step and recursively

taking the agent closer to its goal location. Such methods are more competent at dealing with unfamiliar environments.

1.4.1.1 Classical methods

Some of the classical methodologies used in the 1980s and 1990s to determine the most efficient and collision-free route from the current to the goal location include cell decomposition, potential field, sampling-based methods and their many iterations. These usually require global knowledge of the environment, based on which a path is planned, rather than reacting to environmental information as it is encountered.

Cell decomposition

The basic idea behind cell decomposition methods is to transform a continuous problem into a discrete graph search. First proposed by [91], the cell decomposition approach divides space into non-overlapping grids (cells), and forms a connectivity graph that captures the structure of the space by representing each cell as a node in the graph. In its simplest form, each node is marked as full -if it contains obstacles- or empty – if it has no obstacles. The nodes containing the start position and goal are determined, and the algorithm looks for a sequence of free nodes to connect the two. This provides a collision-free path to reach the target. However, as the dimensions of the space an agent is moving through increase, cell decomposition methods suffer from large numbers of cells, eventually making them impracticable [92].

Potential field

The family of models that are referred to as potential field methods were originally proposed by [93]. In this approach, targets are modelled as attractors and obstacles as repellers. Repulsive and attractive forces are then combined to create a potential field which gives the model its name. Using this method, the agent is modelled as a particle moving in a space under the influence of a force field. The force (potential) field is used to guide the agent's movement towards a goal while avoiding obstacles. This method thus requires a priori knowledge of the positions of all obstacles and can rapidly increase in complexity as more obstacles are added. In

its original form, this model predicts oscillating trajectories in narrow passages and with paths disproportionately influenced by lateral obstacles. Moreover, the agent can get trapped in local minima. A number of studies have attempted to address this issue, but ultimately none guarantee local minima can be avoided [94]. These characteristics make it unlikely to be used by animals, but the method has nonetheless been implemented to model prey-approaching behaviour in toads [95]. A related potential field reactive model used on human path selection experiments approaches the problem as a dynamical system, with steering decisions generated online by solving differential equations [96], instead of explicitly path planning. This dynamical model predicts smoother paths and does not get stuck in local minima. It also has lower computational requirements than local path planning approaches but continues to suffer from non-optimal trajectories being generated (eg oscillatory paths in narrow corridors).

The concept of a potential field is applied slightly differently in vector field histogram (VFH) algorithms. These compute a set of suitable motion commands and select amongst these based on a given navigation strategy (e.g. avoid areas of the highest obstacle density). They have several stages, with the first stage involving the generation of a 2D Cartesian histogram as a continuously updated world model. This grid is reduced to a 1D polar histogram around the agent representing polar obstacle density in each direction. In the final step, the algorithm selects the polar sector with the lowest obstacle density and calculates the steering angle and velocity necessary for the agent to move in that direction. This method always selects the sector which is in the same direction as the goal, but the selected sector is not always optimal. An improved version of this, the nearness diagram approach, uses a divide-and-conquer strategy to reduce the difficulty of the task. This method discretises the possible relationships between an agent, its goal, and any potential obstacles on the way into five states (low safety 1 or 2, depending on whether there are obstacles on one or both sides of the agent; high safety with the goal in the obstacle-free region, high safety with a wide obstacle-free area, or

high safety with a narrow obstacle-free region) [97]. The strategy employed to command agent steering will in turn depend on the state.

Sampling-based motion planning

The above methods rely on an explicit representation of obstacles in the available space, which is used to find a solution. As mentioned, this can be computationally intensive in high-dimensional spaces or spaces with many obstacles. To avoid this problem, a series of sampling-based methods emerged in the 1990s [98] [99]. Instead of formulating a complete map of the available space, these methods connect points sampled randomly from the available space in order to build a graph of feasible trajectories. The way such a graph is built is what differentiates alternative sampling-based methods. For instance, two of the most widely used algorithms in this class are probabilistic roadmaps (PRM) and rapidly exploring random trees (RRTs). The probabilistic roadmap approach is one where coordinates in space are picked at random. Samples that contain obstacles are discarded, and collision-free samples are retained as waypoints. Each waypoint is linked by straight paths to its nearest neighbours, and obstacle-free links are retained as possible paths. Thus space is represented as a network graph of possible paths, which can be used to search for a path from any given start point to a target location. Meanwhile, RRTs form a tree-like graph connecting sampled points, where every node is connected to a single parent, and the tree has a root at the start location. Similar to PRM, as new positions are sampled, they are connected to the existing graph if they represent free space. Another tree is grown rooted at the target location following this procedure, and after every new node is added to a tree, the algorithm attempts to bridge the node with the closest node of the tree rooted at the start position to create an obstacle-free path between the start and goal locations. RRTs can find a feasible motion plan relatively quickly, even in high-dimensional space, making them a popular option in robotics applications.

1.4.1.2 Heuristic methods

Unlike classical methods, heuristic methods do not rely on a priori knowledge on the environment an agent is moving through. Instead, they use simple, predefined behaviours to solve complex scenarios, making them reliable in dynamic environments. Heuristic methods are less computationally intensive and tend to find a solution more rapidly than classical approaches. However, heuristic-based algorithms do not always reach a solution. Many heuristic algorithms have been inspired by nature at a variety of scales, from gene to whole organism behaviour.

Bug algorithms

Despite their name suggesting a biological origin, bug algorithms are only loosely inspired by alleged insect behaviour and in fact, evolved from maze-solving algorithms [100]. They are a non-optimal method to find the route between two points, and assume only local knowledge of the environment - but global knowledge of the goal position. In the standard bug algorithm, an agent moves directly towards the goal state. If an obstacle is encountered, the boundary of said obstacle is followed until the beeline to the target is once again unobstructed, at which point the agent resumes its trajectory towards the target. These work well for avoiding a single obstacle but are slow and do not extend to complex environments.

Genetic algorithms

Genetic algorithms (GAs) fall under the broader category of evolutionary algorithms. They are a search and optimisation technique modelled on the process of natural selection, with their first application to computer science proposed by [101] in 1975. Evolutionary algorithms can provide global solutions to complex optimisation problems, and increase the probability of exploring near-optimal solutions early on. In the robotics application, a population of randomly generated individuals each represent a specific solution to the problem. Individuals that provide a better solution to the problem – i.e. have higher fitness – are more likely to pass their information to subsequent generations by crossover. Mutations maintain the

diversity in the population and prevent premature convergence. In an unfamiliar environment, GA path planners represent a robust search method, requiring little information about the environment to search efficiently. The algorithm is terminated when the population has converged.

Swarm intelligence

In ethology, we think of swarm intelligence as a collective behaviour where individuals interact with each other in a decentralised system. Applying this to path planning, such an approach divides the problem into an exploration and a search phase. Individuals communicate data to others and combine self-generated data and data generated by others to determine the direction in which each agent should travel. We observe this type of behaviour most clearly in colonial animals such as bees and ants, which has resulted in path planning algorithms named after such organisms, with the best known being the ant colony optimisation (ACO), based on ants' use of pheromones for decision-making [102], and the artificial bee colony (ABC) algorithms, based on bees' waggle dance [103].

Gap arrays

In 2012, Sezer and Gokasan [94] proposed an alternative way of approaching movement through cluttered environments, framing the problem as gaps in the environment to aim towards rather than obstacles to avoid. In this way, sensors detect gap arrays instead of obstacle arrays. The resulting algorithm, named follow-the-gap (FGM) selects the gap around the agent with maximum angle size as a target and steers the robot towards the midpoint of that gap. This FGM method has proved to be one of the safest and most efficient algorithms for obstacle avoidance [104] and has been used to model pigeons negotiating cluttered environments [105]. Nonetheless, calculating the heading angle to the centre of a gap based on angular size can put the agent at risk of collision in certain scenarios, such as when obstacles are not stationary [106].

The brief account of obstacle avoidance algorithms above illustrates how most reactive approaches generate motion commands for an agent, that is, in stages. First, a desired direction of motion is determined, and then a steering command is generated to move the agent in the required direction. Similarly, in this thesis, I break down the problem of negotiating cluttered spaces into two steps, with the first being how to decide on a direction of travel amongst available options and the second being how this decision is then implemented. Steering controller implementation in biological systems is reviewed in chapter 2. In the general discussion (chapter 5), I pick up on how elements of the above algorithms have influenced the thinking in this thesis.

1.5 How are obstacle-laden spaces perceived while navigating?

In order to determine how animals decide on a direction of travel, it is important first to understand how complex environments may be perceived. Collisions while moving at high speed have severe fitness consequences, so safety is likely to be prioritised by animal systems. As established, the follow-the-gap algorithm is among the safest models of obstacle avoidance in man-made systems. But reframing the problem of moving through cluttered spaces from perceiving objects (repellers) to sensing available opportunities (gaps) opens up a further question: how does an animal choose between potential gaps (targets)?

Visual systems can segregate objects in the environment from the background to perceive potential obstacles. Gaps, on the other hand, represent negative space (a lack of obstacles). Their definition is therefore arbitrary and will depend on which elements of the scene an animal perceives as separate from the background. This is illustrated in figure 1.3. Depending on the distance at which objects in the environment are considered to be relevant to a decision, the gap to be targeted is likely to change. For instance, assuming an animal is aiming to maximise the distance to obstacles it moves past, it would make sense to follow the rule proposed in the FGM method: aiming for the middle of the largest gap. Such a rule has

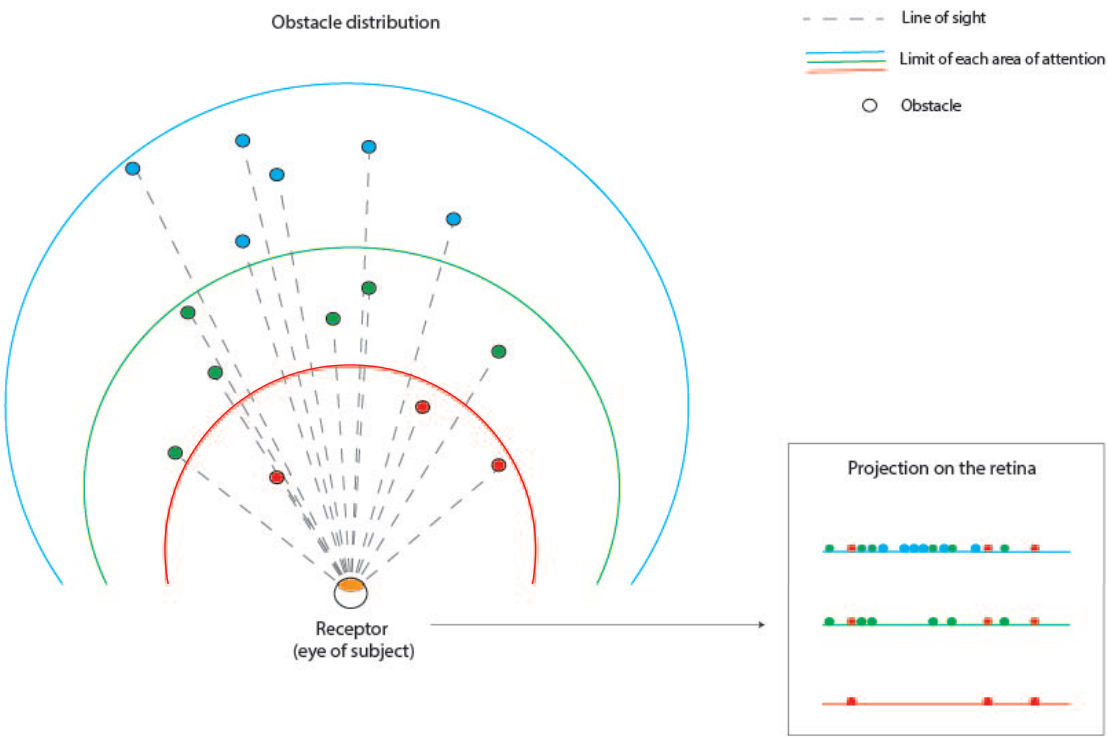


Figure 1.3: Perceiving clutter An example obstacle distribution, with the agent at the bottom looking on. Coloured semi-circles represent "areas of attention": the area around the agent in which objects are considered to be separate from the background. Obstacles are shaded according to the area of attention they would fall under. The dashed line is the line of sight from the agent to each obstacle. The projections of the obstacles that would result in the observer's retina are shown in the box at the bottom right. Again, each circle corresponds to an obstacle in the sample distribution. Depending on how far ahead the observer looks, the largest gap is in different positions.

been previously used to model pigeon flight in obstacle-laden environmental set-ups [105]. However, the diagram in figure 1.3 illustrates how ambiguous such a rule is. Depending on how gaps are defined, the resulting steering aim would be in different positions. If only the obstacles shaded in red are considered in determining what the largest available gap is, the steering aim would be roughly perpendicular to the agent at the midpoint between the two leftmost red obstacles. However, if the area of attention of the agent extends beyond the three closest obstacles to the green line, for instance, this would no longer be the case. As can be seen on the retinal projection diagram on the right, the largest visual gap in the green area of attention is in fact, mostly to the left of the midpoint of the largest gap in the red area of attention. In turn, the steering aim would be roughly 30° to the left of the agent if

it were to aim at the midpoint of the largest visual gap available in the green area. The position the agent ends up in based on this initial steering aim would then affect what is considered the largest gap at the next time step. Thus trajectories can diverge quite significantly based on the distance at which obstructions between the agent and its goal are considered to form visual gaps rather than being part of the background. Moreover, selecting the largest available gaps based on the positions of obstacles close by is likely to lead to zig-zagging trajectories, as has been noted in robotic systems applying FGM methods [106].

Determining what is perceived as a gap and how animals make decisions between available clearances is thus not a trivial question. To the best of my knowledge, this has not been addressed in previous work with animals. In chapters 3 and 4, I explicitly address this question, attempting to model how two species choose between available gaps in ecologically relevant tasks.

1.6 Why these study species?

1.6.1 Pigeons

The homing pigeon (*Columba livia*) has long been a favourite subject for research on the sensory and spatial representation mechanisms that guide avian navigation, as well as animal cognition, more broadly. Domestic pigeons offer a range of favourable traits that makes them suitable for use in behavioural and neuroscientific experiments. They are a long-lived species, living up to 20 years in captivity, and as a result, can be trained, tested and even re-trained for extended periods. They are easily available and quickly adapt to human handling, minimising the effect of stress on experiments relative to wild populations. Moreover, they respond well to training via operant conditioning and are highly motivated by food. Like other birds, they are highly visual, with a major portion of the endbrain dedicated to visual processing, and their visual system has been studied in detail. They have also shown impressive cognitive abilities, such as forming complex perceptual categories to enable them to discriminate unfamiliar paintings from two artists [107]. Their spatial abilities have been widely studied both through release studies looking at their navigational

abilities and laboratory experiments exploring the mechanisms by which they form cognitive maps (for reviews of each of these, see [108], and [109] respectively).

Pigeons' eyes occupy approximately 50% of their skull volume, compared to roughly 5% in humans [110]. Like other prey species, pigeons have lateral eyes with panoramic visual fields spanning roughly 300° [111], which allows for increased acuity in the visual field, as larger images can be focussed on the retina. They have rich colour vision, and colour perception, with four cone receptors with spectral sensitivities ranging from the ultraviolet (320 nm) to the far red (650 nm) [112]. Their retina contains red, orange and yellow eye droplets, which anatomists have used to distinguish between retinal areas. Thus, the area of the retina with a high concentration of red and orange oil droplets was given the inventive name of the red field. This field has an area of enhanced acuity corresponding to the binocular section of the visual field directly below the beak. It is linked with behaviours requiring short-range vision, such as feeding and pecking [113]. The aptly-named yellow field projects instead into the lateral monocular visual fields and contains its own high acuity area with high ganglion density (the fovea centralis) associated with monitoring predators and conspecifics [113].

1.6.2 Trigger fish

Teleost fish inhabit almost every aquatic niche on earth [114], making them a valuable study system in investigating how aquatic animals have evolved to solve spatial problems relative to their terrestrial counterparts. My study species for Chapter 4, Picasso triggerfish (*Rhinecanthus aculeatus*), is a marine fish from the order Tetraodontiformes typically found in shallow reef flats throughout the Indo-Pacific ocean. The inter-tidal zones occupied by this species are usually shallow (<20m depth) and brightly lit. Still, the tidal movements to which they are exposed also makes this an unstable environment due to irregular water currents disturbing sediment and sometimes breaking up and displacing coral reef or other environmental structures. The high availability of visual information this species can extract from their environment relative to teleosts that occupy dark environments

in deeper waters or caves, together with a habitat that naturally provides complex spatial navigation problems, therefore, makes triggerfish a promising candidate to study visual decision-making in space.

Their territorial behaviour means they can be kept in isolated tanks whilst maintaining natural behaviour [115], making them easy to keep in laboratory aquaria. They have also proven to be bold, highly responsive to food rewards, and well inclined to train for complex tasks using operant conditioning, making them an excellent study species for behavioural experiments. As such, they have recently been used in studies investigating how fish collect, process and use spatial information to navigate through their environment accurately [116], as well as many studies investigating visual processes, including the segregation of objects [117], the effect of caustics on object detection [118] and perception of visual illusions [117] amongst others. The knowledge acquired from these studies forms an invaluable basis for considering the sensory cues and mechanisms that may enable fish to move through complex environments. Still, the question of how they choose between available options in space remains largely unanswered.

1.7 Structure of thesis

This thesis is structured into a series of papers, each with a self-contained introduction and discussion. Accordingly, supplementary materials to each self-contained chapter are included per chapter. The main chapters included in the thesis each tackle different aspects of how to solve the problem of moving through structured space. This represents the work carried out in the second half of my DPhil.

In the first half of my DPhil, I worked primarily on perching in zebra finches. The work involved two parts, with the first considering the relative importance of the visual and vestibular systems to balancing on a perch, and the second looking at how birds approach a perch. The first part of the work was carried out at a collaborator's lab at the University of Washington due to facilities at Oxford being unavailable as a result of the Tinbergen crisis (who knew a building hosting two entire Oxford University departments could become unusable from one day to

the next!). Zebra finches were assessed for their ability to perch using high-speed infrared videography and perch torque measurements in light and dark conditions over several weeks. Birds were treated with an antibiotic that had been previously used in humans and other birds to disable the vestibular system temporarily. Sadly, we struggled with getting the correct dosage for the zebra finches, resulting in some of the birds dying and the birds on which the rest of the data was collected not having a high enough dose to draw any meaningful conclusions about the importance of the vestibular system.

In the second half of the work, we recorded zebra finches flying towards a moving perch in a purpose-built aviary fit with motion capture cameras. We initially expected the zebra finches to respond as a linear system would, where the frequency of the input (perch movement) would have been represented in the output (bird movement, e.g. horizontal velocity towards perch). The experiments were thus designed to test this hypothesis, with a perch attached to a rotary motor to enable us to vary the speed and amplitude of the oscillation independently. The second part of the experiment, which introduced multi-sines, was designed to test whether the birds were making use of any forward planning. However in practice, it was not possible to get both multiple oscillations and the birds to land, and we found the birds landed on a very small subset of the conditions we had planned to test even after extensive training. Due to the motion capture cameras only being available for me to use for part of the year, this resulted in a much smaller sample size than we would have liked. This was the first time mocap had been used on such a small bird, and sadly the tracking was not anywhere near as good as we expected. Moreover, I later developed an allergy to pigeons which meant that going back to repeat or extend data collection with the zebra finches -or indeed pigeons- was no longer an option.

As a result of one of the three species that I had intended to work with during my thesis proving to be an unfruitful avenue, and the work being less directly related to that of fruitful experiments, I have excluded work relating to zebra finches from the main body of my thesis. I instead provide a small sample of this work as a self-contained short appendix chapter. While the research I carried out with

finches proved to be inconclusive, the abortive attempts at processing the data from a force-balance sensor as well as the motion capture system proved instrumental in developing the data pipeline for the work that is included in the main body of the thesis. Below, I provide a brief summary of the motivation and aims driving the work in each chapter that did make it into the thesis.

In Chapter 2, I take a guidance approach to study how birds steer towards a gap. I borrow terminology from the missile guidance literature to frame this problem in the same context as pursuit behaviour but using a stationary target. Pigeons were recorded manoeuvring through a gap with the aim of determining their steering dynamics. This was the first of a series of two experiments trying to establish a model of obstacle avoidance. The experimental design simplifies the problem of moving through complex environments to selecting between two available gaps, using homing pigeons tracked through motion capture and guidance-based simulations to help understand the underlying steering mechanism used while moving through complex environments.

The overarching goal of Chapters 2 and 3 was to develop a full model of how pigeons navigate cluttered environments, by combining the steering controller we established in Chapter 2 with the model of how pigeons choose between available clearances. To establish a decision model, in chapter 3 I record 17 pigeons flying through an artificial forest of obstacles using motion capture. For the purposes of analysis, the trajectories are discretised into a series of 7 choices in each flight, corresponding to established transitions in the obstacle arrangement. At each time point, features the animals may be attending to are extracted from the trajectory data and experimental set-up, and their relative impact on the birds' decisions is analysed.

In Chapter 4, I consider another species that habitually travels through highly structured environments in a very different medium: water. The experiment was designed to echo the experimental design of Chapter 3 (looking at gap selection in pigeons), to allow broad comparisons to be made between the two systems. I pick up on these in the general discussion but focus the discussion in this chapter on

the data collected in the fish experiment. Five triggerfish were recorded moving through an obstacle field consisting of vertical poles resembling their natural habitat in coral rubble. We test how environmental and individual characteristics affect the gaps the fish swim through, and relate this to their ecology.

The last chapter of this thesis is a general discussion of the common themes between the chapters. I synthesise the findings of my thesis, discuss the limitations and implications of the research and provide recommendations for future research.

References

[1] John M McNamara and Alasdair I Houston. "Optimal Annual Routines: Behaviour in the Context of Physiology and Ecology". In: *Philosophical Transactions of the Royal Society B: Biological Sciences* 363.1490 (Jan. 2008), pp. 301–319. (Visited on 05/19/2022).

[2] Douglas G. Wallace et al. "Vestibular Information Is Required for Dead Reckoning in the Rat". In: *Journal of Neuroscience* 22.22 (Nov. 2002), pp. 10009–10017. (Visited on 05/19/2022).

[3] Douglas R. W. Wylie and Barrie J. Frost. "Complex Spike Activity of Purkinje Cells in the Ventral Uvula and Nodulus of Pigeons in Response to Translational Optic Flow". In: *Journal of Neurophysiology* 81.1 (Jan. 1999), pp. 256–266. (Visited on 05/19/2022).

[4] Elhanan Ben-Yishay et al. "Directional Tuning in the Hippocampal Formation of Birds". In: *Current biology: CB* 31.12 (June 2021), 2592–2602.e4.

[5] M. -L. Mittelstaedt and H. Mittelstaedt. "Homing by Path Integration in a Mammal". In: *Naturwissenschaften* 67.11 (Nov. 1980), pp. 566–567. (Visited on 05/06/2022).

[6] Martin Müller and Rüdiger Wehner. "Path Integration in Desert Ants, Cataglyphis Fortis". In: *Proceedings of the National Academy of Sciences* 85.14 (July 1988), pp. 5287–5290. (Visited on 05/19/2022).

[7] null Collett. "Insect Navigation En Route to the Goal: Multiple Strategies for the Use of Landmarks". In: *The Journal of Experimental Biology* 199.Pt 1 (1996), pp. 227–235.

[8] Carole Parron and Etienne Save. "Evidence for Entorhinal and Parietal Cortices Involvement in Path Integration in the Rat". In: *Experimental Brain Research* 159.3 (Dec. 2004), pp. 349–359. (Visited on 05/19/2022).

[9] Soyun Kim et al. "Contrasting Effects on Path Integration after Hippocampal Damage in Humans and Rats". In: *Proceedings of the National Academy of Sciences* 110.12 (Mar. 2013), pp. 4732–4737. (Visited on 05/06/2022).

[10] Xiaoli Chen et al. "Bias in Human Path Integration Is Predicted by Properties of Grid Cells". In: *Current biology: CB* 25.13 (June 2015), pp. 1771–1776.

[11] Ehud Vinepinsky, Opher Donchin, and Ronen Segev. “Wireless Electrophysiology of the Brain of Freely Swimming Goldfish”. In: *Journal of Neuroscience Methods* 278 (Feb. 2017), pp. 76–86. (Visited on 05/06/2022).

[12] Rickesh N. Patel and Thomas W. Cronin. “Mantis Shrimp Navigate Home Using Celestial and Idiothetic Path Integration”. In: *Current Biology* 30.11 (June 2020), 1981–1987.e3. (Visited on 05/06/2022).

[13] null Dittman and null Quinn. “Homing in Pacific Salmon: Mechanisms and Ecological Basis”. In: *The Journal of Experimental Biology* 199.Pt 1 (1996), pp. 83–91.

[14] Dora Biro, Jessica Meade, and Tim Guilford. “Familiar Route Loyalty Implies Visual Pilotage in the Homing Pigeon”. In: *Proceedings of the National Academy of Sciences* 101.50 (Dec. 2004), pp. 17440–17443. (Visited on 05/06/2022).

[15] Anthony Inder Mazeroll and W. Linn Montgomery. “Daily Migrations of a Coral Reef Fish in the Red Sea (Gulf of Aqaba, Israel): Initiation and Orientation”. In: *Copeia* 4 (Dec. 1998), pp. 893–905. (Visited on 05/06/2022).

[16] Hans G. Wallraff. “The Effect of Directional Experience on Initial Orientation in Pigeons”. In: *The Auk* 91.1 (1974), pp. 24–34. JSTOR: 4084658. (Visited on 05/19/2022).

[17] Roswitha Wiltschko and Wolfgang Wiltschko. “Avian Navigation: From Historical to Modern Concepts”. In: *Animal Behaviour* 65.2 (Feb. 2003), pp. 257–272. (Visited on 05/19/2022).

[18] Stephen C. Levinson. “Language and Space”. In: *Annual Review of Anthropology* 25.1 (1996), pp. 353–382. (Visited on 05/19/2022).

[19] Tim Guilford and Dora Biro. “Route Following and the Pigeon’s Familiar Area Map”. In: *Journal of Experimental Biology* 217.2 (Jan. 2014), pp. 169–179. (Visited on 05/19/2022).

[20] Stephen T. Emlen. “The Influence of Magnetic Information on the Orientation of the Indigo Bunting, Passerina Cyanea”. In: *Animal Behaviour* 18 (May 1970), pp. 215–224. (Visited on 05/19/2022).

[21] Roswitha Wiltschko. “Über Den Einfluß Statischer Magnetfelder Auf Die Zugorientierung Der Rotkehlchen (Erithacus Rubecula)”. In: *Zeitschrift für Tierpsychologie* 25 (Apr. 2010), pp. 537–558.

[22] Kramer. “EXPERIMENTS ON BIRD ORIENTATION AND THEIR INTERPRETATION. - Kramer - 1957 - Ibis - Wiley Online Library”. In: (1957). (Visited on 05/19/2022).

[23] Eberhard Dodt and Alberto Wirth. “Differentiation Between Rods and Cones by Flicker Electroretinography in Pigeon and Guinea Pig”. In: *Acta Physiologica Scandinavica* 30.1 (1954), pp. 80–89. (Visited on 05/19/2022).

[24] James A. Simmons, Michael J. Ferragamo, and Cynthia F. Moss. “Echo-Delay Resolution in Sonar Images of the Big Brown Bat, Eptesicus Fuscus”. In: *Proceedings of the National Academy of Sciences of the United States of America* 95.21 (Oct. 1998), pp. 12647–12652. (Visited on 05/20/2022).

[25] Lasse Jakobsen, Signe Brinkløv, and Annemarie Surlykke. “Intensity and Directionality of Bat Echolocation Signals”. In: *Frontiers in Physiology* 4 (2013). (Visited on 05/17/2022).

[26] Te K. Jones and Cynthia F. Moss. “Visual Cues Enhance Obstacle Avoidance in Echolocating Bats”. In: *Journal of Experimental Biology* 224.9 (May 2021), jeb241968. (Visited on 05/14/2022).

[27] Robert B. Welch and David H. Warren. “Immediate Perceptual Response to Intersensory Discrepancy”. In: *Psychological Bulletin* 88.3 (1980), pp. 638–667.

[28] Jan J. Koenderink. “Optic Flow”. In: *Vision Research* 26.1 (Jan. 1986), pp. 161–179. (Visited on 05/19/2022).

[29] J. J. Gibson. “The Perception of Visual Surfaces. By James J. Gibson, 1950”. In: *The American Journal of Psychology* 100.3-4 (1987 Fall-Winter), pp. 646–664.

[30] D. N. Lee et al. “The Optic Flow Field: The Foundation of Vision”. In: *Philosophical Transactions of the Royal Society of London. B, Biological Sciences* 290.1038 (July 1980), pp. 169–179. (Visited on 05/19/2022).

[31] James J. Gibson. *The Ecological Approach to Visual Perception*. New York: Psychology Press, 1979.

[32] Dennis Eckmeier et al. “Gaze Strategy in the Free Flying Zebra Finch (Taeniopygia Guttata)”. In: *PLOS ONE* 3.12 (Dec. 2008), e3956. (Visited on 05/09/2022).

[33] David N Lee. “A Theory of Visual Control of Braking Based on Information about Time-to-Collision”. In: *Perception* 5.4 (Dec. 1976), pp. 437–459. (Visited on 05/19/2022).

[34] Lance F. Tammero and Michael H. Dickinson. “Collision-Avoidance and Landing Responses Are Mediated by Separate Pathways in the Fruit Fly, Drosophila Melanogaster”. In: *Journal of Experimental Biology* 205.18 (Sept. 2002), pp. 2785–2798. (Visited on 05/18/2022).

[35] Melissa J Kearns et al. “Path Integration from Optic Flow and Body Senses in a Homing Task”. In: *Perception* 31.3 (Mar. 2002), pp. 349–374. (Visited on 05/18/2022).

[36] Jonathan C Horton and Daniel L Adams. “The Cortical Column: A Structure without a Function”. In: *Philosophical Transactions of the Royal Society B: Biological Sciences* 360.1456 (Apr. 2005), pp. 837–862. (Visited on 05/19/2022).

[37] Michael B. Orger et al. “Perception of Fourier and Non-Fourier Motion by Larval Zebrafish”. In: *Nature Neuroscience* 3.11 (Nov. 2000), pp. 1128–1133. (Visited on 05/17/2022).

[38] Erich D. Jarvis et al. “Avian Brains and a New Understanding of Vertebrate Brain Evolution”. In: *Nature Reviews Neuroscience* 6.2 (Feb. 2005), pp. 151–159. (Visited on 05/17/2022).

[39] Michael P. Jones, Kenneth E. Pierce, and Daniel Ward. “Avian Vision: A Review of Form and Function with Special Consideration to Birds of Prey”. In: *Journal of Exotic Pet Medicine* 16.2 (Apr. 2007), pp. 69–87. (Visited on 05/04/2022).

[40] Scott Husband and Toru Shimizu. “Evolution of the Avian Vision”. In: *Avian Visual Cognition* (Jan. 2001).

[41] Ann B. Butler and William Hodos. *Comparative Vertebrate Neuroanatomy: Evolution and Adaptation*. John Wiley & Sons, Sept. 2005.

[42] Andrew N. Iwaniuk and Douglas R.W. Wylie. "Neural Specialization for Hovering in Hummingbirds: Hypertrophy of the Pretectal Nucleus Lentiformis Mesencephali". In: *Journal of Comparative Neurology* 500.2 (2007), pp. 211–221. (Visited on 03/18/2023).

[43] J. D. Pettigrew, K. J. Sanderson, and W. R. Levick. *Visual Neuroscience*. CUP Archive, Dec. 1986.

[44] Robert van der Willigen, Barrie Frost, and Hermann Wagner. "Stereoscopic Depth Perception in the Owl". In: *Neuroreport* 9 (May 1998), pp. 1233–7.

[45] H J Bischof and S Watanabe. "On the Structure and Function of the Tectofugal Visual Pathway in Laterally Eyed Birds". In: *European journal of morphology* 35.4 (Oct. 1997), pp. 246–254. (Visited on 05/19/2022).

[46] B. J. Frost, D. R. Wylie, and Y. -C. Wang. "The Processing of Object and Self-Motion in the Tectofugal and Accessory Optic Pathways of Birds". In: *Vision Research*. Optics Physiology and Vision 30.11 (Jan. 1990), pp. 1677–1688. (Visited on 05/17/2022).

[47] Qian Xiao and Barrie J. Frost. "Looming Responses of Telencephalic Neurons in the Pigeon Are Modulated by Optic Flow". In: *Brain Research* 1305 (Dec. 2009), pp. 40–46. (Visited on 05/17/2022).

[48] E. Pascal Malkemper et al. "Neuronal Circuits and the Magnetic Sense: Central Questions". In: *Journal of Experimental Biology* 223.21 (Nov. 2020), jeb232371. (Visited on 03/18/2023).

[49] Dom Miceli et al. "Distribution of Ganglion Cells in the Pigeon Retina Labeled via Retrograde Transneuronal Transport of the Fluorescent Dye Rhodamine β-Isothiocyanate from the Telencephalic Visual Wulst". In: *Brain Research* 1098.1 (July 2006), pp. 94–105. (Visited on 05/19/2022).

[50] Jin Yang, Chuan Zhang, and Shu-Rong Wang. "Comparisons of Visual Properties between Tectal and Thalamic Neurons with Overlapping Receptive Fields in the Pigeon". In: *Brain, Behavior and Evolution* 65.1 (2005), pp. 33–39. (Visited on 05/13/2022).

[51] Cheri A. Budzynski et al. "Participation of the Homing Pigeon Thalamofugal Visual Pathway in Sun-Compass Associative Learning". In: *European Journal of Neuroscience* 15.1 (2002), pp. 197–210. (Visited on 02/18/2023).

[52] P. Chand, R. C. Maurya, and U. C. Srivastava. "Neuronal Morphology and Spine Density of the Visual Wulst of the Strawberry Finch, Estrilda Amandava". In: *Proceedings of the National Academy of Sciences, India Section B: Biological Sciences* 83.4 (Dec. 2013), pp. 627–642. (Visited on 02/18/2023).

[53] Nathan A. Crowder and Douglas R. Wylie. "Responses of Optokinetic Neurons in the Pretectum and Accessory Optic System of the Pigeon to Large-Field Plaids". In: *Journal of Comparative Physiology A* 188.2 (Mar. 2002), pp. 109–119. (Visited on 02/18/2023).

[54] J. Martin Wild. “Pretectal and Tectal Projections to the Homologue of the Dorsal Lateral Geniculate Nucleus in the Pigeon: An Anterograde and Retrograde Tracing Study with Cholera Toxin Conjugated to Horseradish Peroxidase”. In: *Brain Research* 479.1 (Feb. 1989), pp. 130–137. (Visited on 02/18/2023).

[55] Nathan A. Crowder, Michael R.W. Dawson, and Douglas R.W. Wylie. “Temporal Frequency and Velocity-Like Tuning in the Pigeon Accessory Optic System”. In: *Journal of Neurophysiology* 90.3 (Sept. 2003), pp. 1829–1841. (Visited on 02/18/2023).

[56] B. J. Winterson and S. E. Brauth. “Direction-Selective Single Units in the Nucleus Lentiformis Mesencephali of the Pigeon (Columba Livia)”. In: *Experimental Brain Research* 60.2 (1985), pp. 215–226.

[57] W. Graf, J. I. Simpson, and C. S. Leonard. “Spatial Organization of Visual Messages of the Rabbit’s Cerebellar Flocculus. II. Complex and Simple Spike Responses of Purkinje Cells”. In: *Journal of Neurophysiology* 60.6 (Dec. 1988), pp. 2091–2121. (Visited on 05/17/2022).

[58] David J. Graham and Douglas R. Wylie. “Zebrin-Immunopositive and -Immunonegative Stripe Pairs Represent Functional Units in the Pigeon Vestibulocerebellum”. In: *The Journal of Neuroscience* 32.37 (Sept. 2012), pp. 12769–12779. (Visited on 05/17/2022).

[59] Curtis Hardyck et al. “The Eyes Have It: Exposure Times and Saccadic Movements in Visual Half-Field Experiments”. In: *Brain and Cognition* 4.4 (Oct. 1985), pp. 430–438. (Visited on 05/19/2022).

[60] Kevin Laland, Jens Krause, and Culum Brown. *Fish Cognition and Behavior*. John Wiley & Sons, June 2011.

[61] K. V. Fite. “Pretectal and Accessory-Optic Visual Nuclei of Fish, Amphibia and Reptiles: Theme and Variations”. In: *Brain, Behavior and Evolution* 26.2 (1985), pp. 71–90.

[62] Alexey T. Aliper et al. “Updated Functional Segregation of Retinal Ganglion Cell Projections in the Tectum of a Cyprinid Fish—Further Elaboration Based on Microelectrode Recordings”. In: *Fish Physiology and Biochemistry* 45.2 (Apr. 2019), pp. 773–792. (Visited on 03/04/2023).

[63] Greg Lemke and Michaël Reber. “RETINOTECTAL MAPPING: New Insights from Molecular Genetics”. In: *Annual Review of Cell and Developmental Biology* 21.1 (2005), pp. 551–580. (Visited on 05/19/2022).

[64] Tobias Roeser and Herwig Baier. “Visuomotor Behaviors in Larval Zebrafish after GFP-Guided Laser Ablation of the Optic Tectum”. In: *Journal of Neuroscience* 23.9 (May 2003), pp. 3726–3734. (Visited on 05/19/2022).

[65] Ethan Gahtan, Paul Tanger, and Herwig Baier. “Visual Prey Capture in Larval Zebrafish Is Controlled by Identified Reticulospinal Neurons Downstream of the Tectum”. In: *Journal of Neuroscience* 25.40 (Oct. 2005), pp. 9294–9303. (Visited on 05/19/2022).

[66] Estuardo Robles, Stephen Smith, and Herwig Baier. “Characterization of Genetically Targeted Neuron Types in the Zebrafish Optic Tectum”. In: *Frontiers in Neural Circuits* 5 (2011). (Visited on 03/04/2023).

[67] M Van Der Marel et al. “Changes in Skin Mucus of Common Carp, Cyprinus Carpio L., after Exposure to Water with a High Bacterial Load”. In: *Journal of Fish Diseases* 33.5 (2010), pp. 431–439. (Visited on 05/19/2022).

[68] J I Simpson. “The Accessory Optic System”. In: *Annual Review of Neuroscience* 7.1 (1984), pp. 13–41. (Visited on 03/04/2023).

[69] Olivia Andrea Masseck and Klaus-Peter Hoffmann. “Question of Reference Frames: Visual Direction-Selective Neurons in the Accessory Optic System of Goldfish”. In: *Journal of Neurophysiology* 102.5 (Nov. 2009), pp. 2781–2789. (Visited on 03/04/2023).

[70] Kun Wang et al. “Parallel Channels for Motion Feature Extraction in the Pretectum and Tectum of Larval Zebrafish”. In: *Cell Reports* 30.2 (Jan. 2020), 442–453.e6. (Visited on 03/04/2023).

[71] Kun Wang et al. “Selective Processing of All Rotational and Translational Optic Flow Directions in the Zebrafish Pretectum and Tectum”. In: *BMC Biology* 17.1 (Mar. 2019), p. 29. (Visited on 05/19/2022).

[72] Hongyuan Wu, Xiaoye Michael Wang, and Jing Samantha Pan. “Perceiving Blurry Scenes with Translational Optic Flow, Rotational Optic Flow or Combined Optic Flow”. In: *Vision Research* 158 (May 2019), pp. 49–57. (Visited on 05/19/2022).

[73] Eva A. Naumann et al. “From Whole-Brain Data to Functional Circuit Models: The Zebrafish Optomotor Response”. In: *Cell* 167.4 (Nov. 2016), 947–960.e20. (Visited on 05/19/2022).

[74] Adrienn G. Varga et al. “Spatial Navigation and the Central Complex: Sensory Acquisition, Orientation, and Motor Control”. In: *Frontiers in Behavioral Neuroscience* 11 (2017). (Visited on 05/06/2022).

[75] Ehud Vinepinsky et al. “Representation of Edges, Head Direction, and Swimming Kinematics in the Brain of Freely-Navigating Fish”. In: *Scientific Reports* 10.1 (Sept. 2020), p. 14762. (Visited on 05/06/2022).

[76] Js Taube, Ru Muller, and Jb Ranck. “Head-Direction Cells Recorded from the Postsubiculum in Freely Moving Rats. I. Description and Quantitative Analysis”. In: *The Journal of Neuroscience* 10.2 (Feb. 1990), pp. 420–435. (Visited on 05/06/2022).

[77] Jeffrey S. Taube. “The Head Direction Signal: Origins and Sensory-Motor Integration”. In: *Annual Review of Neuroscience* 30 (2007), pp. 181–207.

[78] J. O’Keefe and D. H. Conway. “Hippocampal Place Units in the Freely Moving Rat: Why They Fire Where They Fire”. In: *Experimental Brain Research* 31.4 (Apr. 1978), pp. 573–590. (Visited on 05/19/2022).

[79] Torkel Hafting et al. “Microstructure of a Spatial Map in the Entorhinal Cortex”. In: *Nature* 436.7052 (Aug. 2005), pp. 801–806. (Visited on 05/19/2022).

[80] James G. Canfield and Sheri J. Y. Mizumori. “Methods for Chronic Neural Recording in the Telencephalon of Freely Behaving Fish”. In: *Journal of Neuroscience Methods* 133.1-2 (Feb. 2004), pp. 127–134.

[81] Jennifer J. Siegel, Douglas Nitz, and Verner P. Bingman. “Lateralized Functional Components of Spatial Cognition in the Avian Hippocampal Formation: Evidence from Single-Unit Recordings in Freely Moving Homing Pigeons”. In: *Hippocampus* 16.2 (2006), pp. 125–140.

[82] H. L. Payne, G. F. Lynch, and D. Aronov. “Neural Representations of Space in the Hippocampus of a Food-Caching Bird”. In: *Science* 373.6552 (July 2021), pp. 343–348. (Visited on 05/19/2022).

[83] Francesco Savelli, JD Luck, and James J Knierim. “Framing of Grid Cells within and beyond Navigation Boundaries”. In: *eLife* 6 (Jan. 2017). Ed. by Upinder S Bhalla, e21354. (Visited on 05/19/2022).

[84] Haleh Fotowat et al. “Neural Activity in a Hippocampus-like Region of the Teleost Pallium Is Associated with Active Sensing and Navigation”. In: *eLife* 8 (Apr. 2019). Ed. by Vatsala Thirumalai, Timothy E Behrens, and Maurice J Chacron, e44119. (Visited on 05/06/2022).

[85] Tom Hartley et al. “Space in the Brain: How the Hippocampal Formation Supports Spatial Cognition”. In: *Philosophical Transactions of the Royal Society B: Biological Sciences* 369.1635 (Feb. 2014), p. 20120510. (Visited on 05/06/2022).

[86] Bruce L. McNaughton et al. “Path Integration and the Neural Basis of the ’Cognitive Map’”. In: *Nature Reviews. Neuroscience* 7.8 (Aug. 2006), pp. 663–678.

[87] Bruno Siciliano and Oussama Khatib, eds. *Springer Handbook of Robotics*. Springer Handbooks. Springer, 2016.

[88] Steven M. LaValle. *Planning Algorithms*. Cambridge University Press, May 2006.

[89] A. Elshamli, H.A. Abdullah, and S. Areibi. “Genetic Algorithm for Dynamic Path Planning”. In: *Canadian Conference on Electrical and Computer Engineering 2004 (IEEE Cat. No.04CH37513)*. Vol. 2. May 2004, 677–680 Vol.2.

[90] Adham Atyabi and David Powers. “Review of Classical and Heuristic-Based Navigation and Path Planning Approaches”. In: *International Journal of Advancements in Computing Technology (IJACT)* 5 (Jan. 2013), pp. 1–14.

[91] Rodney A. Brooks. “Planning Collision- Free Motions for Pick-and-Place Operations”. In: *The International Journal of Robotics Research* 2.4 (Dec. 1983), pp. 19–44. (Visited on 04/05/2023).

[92] Sertac Karaman and Emilio Frazzoli. “Sampling-Based Algorithms for Optimal Motion Planning”. In: *The International Journal of Robotics Research* 30.7 (June 2011), pp. 846–894. (Visited on 03/20/2023).

[93] Oussama Khatib. “Real-Time Obstacle Avoidance for Manipulators and Mobile Robots”. In: *The International Journal of Robotics Research* 5.1 (Mar. 1986), pp. 90–98. (Visited on 05/20/2022).

[94] Volkan Sezer and Metin Gokasan. “A Novel Obstacle Avoidance Algorithm: “Follow the Gap Method””. In: *Robotics and Autonomous Systems* 60.9 (Sept. 2012), pp. 1123–1134. (Visited on 05/19/2022).

[95] A Arbib. “Sensorimotor Transformations in the Worlds of Frogs and Robots”. In: (1995), p. 27.

[96] Brett R Fajen et al. “A Dynamical Model of Visually-Guided Steering, Obstacle Avoidance, and Route Selection | SpringerLink”. In: 54 (2003), pp. 13–34. (Visited on 05/18/2022).

[97] J. Minguez and L. Montano. “Nearness Diagram (ND) Navigation: Collision Avoidance in Troublesome Scenarios”. In: *IEEE Transactions on Robotics and Automation* 20.1 (Feb. 2004), pp. 45–59. (Visited on 05/20/2022).

[98] L. Kavraki and J.-C. Latombe. “Randomized Preprocessing of Configuration Space for Path Planning: Articulated Robots”. In: *Proceedings of IEEE/RSJ International Conference on Intelligent Robots and Systems (IROS'94)*. Vol. 3. Sept. 1994, 1764–1771 vol.3.

[99] Steven M. LaValle and James J. Kuffner. “Randomized Kinodynamic Planning”. In: *The International Journal of Robotics Research* 20.5 (May 2001), pp. 378–400. (Visited on 03/20/2023).

[100] Vladimir J. Lumelsky and Alexander A. Stepanov. “Path-Planning Strategies for a Point Mobile Automaton Moving amidst Unknown Obstacles of Arbitrary Shape”. In: *Algorithmica* 2.1 (Nov. 1987), pp. 403–430. (Visited on 05/19/2022).

[101] John H. Holland. *Adaptation in Natural and Artificial Systems: An Introductory Analysis with Applications to Biology, Control, and Artificial Intelligence*. Adaptation in Natural and Artificial Systems: An Introductory Analysis with Applications to Biology, Control, and Artificial Intelligence. Oxford, England: U Michigan Press, 1975, pp. viii, 183.

[102] M. Dorigo and L.M. Gambardella. “Ant Colony System: A Cooperative Learning Approach to the Traveling Salesman Problem”. In: *IEEE Transactions on Evolutionary Computation* 1.1 (Apr. 1997), pp. 53–66.

[103] Dervis Karaboga. “An Idea Based on Honey Bee Swarm for Numerical Optimization, Technical Report - TR06”. In: *Technical Report, Erciyes University* (Jan. 2005).

[104] M. Zohaib et al. *Control Strategies for Mobile Robot With Obstacle Avoidance*. June 2013. arXiv: 1306.1144 [cs]. (Visited on 05/13/2022).

[105] Huai-Ti Lin, Ivo G. Ros, and Andrew A. Biewener. “Through the Eyes of a Bird: Modelling Visually Guided Obstacle Flight”. In: *Journal of The Royal Society Interface* 11.96 (July 2014), p. 20140239. (Visited on 05/04/2022).

[106] Hosein Houshyari and Volkan Sezer. “A New Gap-Based Obstacle Avoidance Approach: Follow the Obstacle Circle Method”. In: *Robotica* (Nov. 2021), pp. 1–24. (Visited on 05/19/2022).

[107] Shigeru Watanabe, Junko Sakamoto, and Masumi Wakita. “Pigeons' Discrimination of Paintings by Monet and Picasso”. In: *Journal of the Experimental Analysis of Behavior* 63.2 (Mar. 1995), pp. 165–174. (Visited on 05/06/2022).

[108] Wolfgang Wiltschko and Roswitha Wiltschko. “Magnetic Compass Orientation in Birds and Its Physiological Basis”. In: *Naturwissenschaften* 89.10 (Oct. 2002), pp. 445–452. (Visited on 05/19/2022).

[109] Ken Cheng et al. “Small-Scale Spatial Cognition in Pigeons”. In: *Behavioural Processes* 72.2 (May 2006), pp. 115–127.

[110] Jerry A. Waldvogel. “The Bird’s Eye View”. In: *American Scientist* 78.4 (1990), pp. 342–353. JSTOR: 29774120. (Visited on 05/20/2022).

[111] Kevin J Rounsley and Sally A McFadden. “Limits of Visual Acuity in the Frontal Field of the Rock Pigeon (Columba Livia)”. In: *Perception* 34.8 (Aug. 2005), pp. 983–993. (Visited on 05/06/2022).

[112] Monika Remy and Jacky Emmerton. “Directional Dependence of Intraocular Transfer of Stimulus Detection in Pigeons (Columba Livia)”. In: *Behavioral Neuroscience* 105.5 (1991), pp. 647–652.

[113] Melvyn A. Goodale. “Visuomotor Organization of Pecking in the Pigeon”. In: *Advances in Vertebrate Neuroethology* (1983), pp. 349–357. (Visited on 05/20/2022).

[114] Thomas J. Near et al. “Resolution of Ray-Finned Fish Phylogeny and Timing of Diversification”. In: *Proceedings of the National Academy of Sciences* 109.34 (Aug. 2012), pp. 13698–13703. (Visited on 05/20/2022).

[115] Karen L. Cheney et al. “Colour Vision and Response Bias in a Coral Reef Fish”. In: *Journal of Experimental Biology* 216.15 (Aug. 2013), pp. 2967–2973. (Visited on 05/19/2022).

[116] C. Karlsson et al. *Teleost Fish Can Accurately Estimate Distance Travelled*. Nov. 2019. (Visited on 03/18/2023).

[117] Laurie Mitchell et al. “Triggerfish Uses Chromaticity and Lightness for Object Segregation”. In: *Royal Society Open Science* 4.12 (), p. 171440. (Visited on 05/19/2022).

[118] S. R. Matchette et al. “Underwater Caustics Disrupt Prey Detection by a Reef Fish”. In: *Proceedings of the Royal Society B: Biological Sciences* 287.1924 (Apr. 2020), p. 20192453. (Visited on 05/19/2022).

2

Gap selection and steering during obstacle avoidance in pigeons

Contents

2.1 Abstract 41
2.2 Introduction 41
2.3 Algorithmic framework 43
2.4 Methods 49
2.4.1 Subjects and training 49
2.4.2 Experimental set-up and protocol 49
2.4.3 Motion capture 51
2.4.4 Flight trajectory analysis 53
2.4.5 Steering controller simulations 54
2.4.6 Statistical analysis 56
2.5 Results 56
2.5.1 Pigeons select gaps on the basis of handedness, not size 57
2.5.2 Simulations of steering behaviour 58
2.5.3 Extension of model fitting to entire measured trajectory 67
2.6 Discussion 67
2.6.1 Limitations 73
2.7 Supplementary Information 76
2.7.1 Characteristics of animals used during data collection and recorded flights 76
2.7.2 Results of simulations treating the midpoint of the gap as the target of the bird's guidance. 80
2.7.3 Results of simulations treating the point 0.35 m from the edge of the curtain as the target of the bird's guidance. 85
References 89

2.1 Abstract

The ability of birds to fly through cluttered environments has inspired biologists interested in understanding its underlying mechanisms, and engineers interested in applying its underpinning principles. To analyse this problem empirically, we break it down into two distinct, but related, questions: How do birds select which gaps to aim for? And, how do they steer through them? We answered these questions by using a combined experimental and modelling approach, in which we released pigeons *(Columbia livia domestica)* inside a large hall whose open exit was separated from the release point by a curtain creating two vertical gaps—one of which was obstructed by an obstacle. We tracked the birds using a high-speed motion capture system, and found that their gap choice seemed to be biased by their intrinsic handedness, rather than determined by extrinsic cues such as the size of the gap or its alignment with the destination. We modelled the pigeons' steering behaviour algorithmically by simulating their flight trajectories under a set of six candidate guidance laws, including those used previously to model target-oriented flight behaviours in birds. We found that their flights were best modelled by delayed proportional navigation commanding turning in proportion to the angular rate of the line-of-sight from the pigeon to the midpoint of the gap. Our results are consistent with this being a two-phase behaviour, in which the pigeon heads forward from the release point before steering towards the midpoint of whichever gap it chooses to aim for under closed-loop guidance. Our findings have implications for the sensorimotor mechanisms that underlie clutter negotiation in birds, uniting this with other kinds of target-oriented behaviours including aerial pursuit.

2.2 Introduction

When B.F. Skinner proposed using pigeons to guide flying vehicles in World War II [119], he may have been onto something. Pigeons have colonized complex, cluttered

urban environments throughout the world, which they negotiate successfully at high speeds. They achieve this visually, aided by their panoramic (300°) field of view, and by visual processing some three times faster than a human's [39]. However, rather than using operant conditioning to train pigeons to pilot vehicles by pecking at a screen as Skinner proposed, a better approach might have been to study the guidance algorithms by which they steer their flight. Here, we set out to do just that, using a combined experimental and modelling approach to investigate how pigeons steer towards gaps. This work is closely inspired by previous research on pigeons flying through a dense forest of vertical poles [105], but reduces the problem to its simplest level, by presenting the birds with a binary choice between an obstructed or unobstructed gap through which to fly.

Algorithmic approaches to the study of goal-directed behaviours [120] have been successful in explaining the detailed flight trajectories of pigeons negotiating clutter [105], and bats [121], raptors [122–124], and flies [125] intercepting prey. These studies use differential equations to build simple phenomenological models that are capable of accurately describing complex behavioural data. This approach models behaviour as a dynamical input-output relationship governed by a guidance law treating the animal's motion (e.g. its horizontal turn rate) as a control input that is commanded by feeding back the sensory output the behaviour produces (e.g. information on the target's relative position or motion). Different guidance laws will in general produce different behaviours. For instance, guidance laws using different sensory information typically generate trajectories from different families of curves, yielding variation that can be used for model selection and identification in relation to empirical data.

The sensory information that is most relevant to guiding target-oriented behaviour describes the direction of the line-of-sight vector connecting the subject to its target. This is characterised by two angles: the line-of-sight angle (λ), defined as the angle between the line-of-sight and some arbitrary inertial reference (e.g. true North); and the deviation angle (δ), defined as the angle between the line-of-sight and the subject's velocity vector (Fig. 2.1). Driving the deviation angle δ to zero causes

the subject to fly directly at its target, whereas driving δ to some non-zero angle produces a spiralling approach. It can therefore make sense to use both the deviation angle δ and its time derivative $\dot{\delta}$ to control turning. In contrast, unless there is a reason to drive an approach towards some particular bearing, the line-of-sight angle λ is not itself used to control turning in target-oriented flight. On the other hand, because λ remains constant for any pair of objects on a direct collision course, driving its time derivative $\dot{\lambda}$ to zero leads naturally to interception. For this reason, the line-of-sight rate $\dot{\lambda}$ is often used to control turning in target-oriented flight.

Apart from shaping the resulting flight trajectory, the choice of what sensory information to use has implications for how it is obtained. For instance, if head movements are used to look directly at the target, then the output of the vestibular system can be used to estimate the line-of-sight rate $\dot{\lambda}$. Identifying which input variables best model an animal's steering output therefore has important implications for understanding the underlying physiological mechanisms. Moreover, because it is only the motion of the subject relative to its target that matters in target-oriented flight, the same guidance laws can be applied to both stationary and moving targets. This opens the possibility of unifying target chasing and clutter negotiation behaviours under one common algorithmic framework. To this end, we begin by reviewing the guidance laws that have been used to model target-oriented behaviours of both kinds to date.

2.3 Algorithmic framework

Inspired by the types of controllers used in the engineering literature, early attempts to model the steering of animal flight [126] looked for a proportional relationship between the subject's turn rate ($\dot{\gamma}$) and the deviation angle (δ). The simplest form of this proportionality corresponds to the guidance law $\dot{\gamma}(t) = k_P \delta(t - \tau)$, called pure or proportional pursuit [123], where $k_P < 0$ is the guidance gain, t is time, and $\tau \geq 0$ denotes a fixed delay. Pure pursuit drives the deviation angle δ towards zero, thereby causing the subject to aim its flight directly at its target. A simple variant called deviated pursuit drives the deviation angle δ towards some nonzero constant

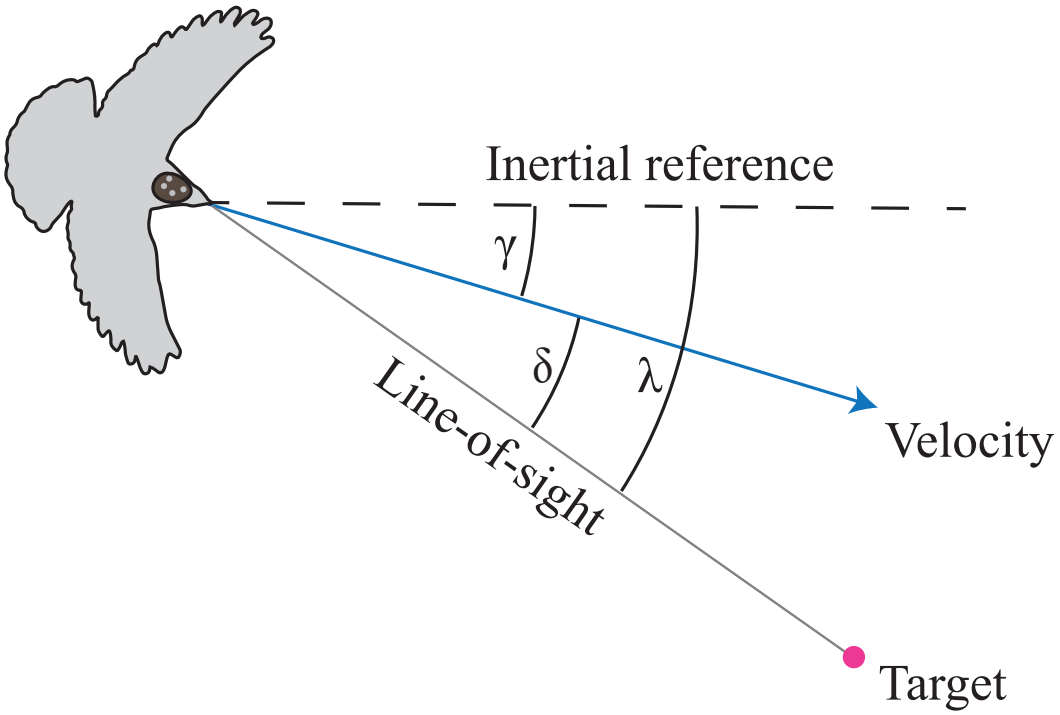


Figure 2.1: Geometry of target-oriented guidance behaviour. Definition sketch showing: the line-of-sight angle λ measured between the line-of-sight (grey line) from pigeon to target, and some arbitrary inertial reference direction (dashed line); the track angle γ measured between the bird's ground velocity vector (blue arrow) and the inertial reference direction (dashed line); the deviation angle δ measured between the line-of-sight from bird to target (grey line), and the pigeon's velocity vector (blue arrow). The arrangement of the tracked headpack markers is shown schematically.

δ_0 with $\dot{\gamma}(t) = k_P[\delta(t-\tau) - \delta_0]$. This causes flight to be aimed at a point ahead of a moving target, which promotes effective interception of a moving target (cf. pure pursuit, which leads directly to a tail chase), but produces a spiraling trajectory about a stationary target, which could help to steer flight around, rather than into, an obstacle (cf. pure pursuit, which leads directly to a collision).

Because the performance of a proportional controller can often be improved by adding derivative feedback, several studies have looked for the involvement of an additional derivative term $k_D\dot{\delta}(t-\tau)$, where $\dot{\delta}$ is the rate of change of the deviation angle, and $k_D < 0$ is the associated guidance gain [105, 126]. The addition of this derivative term anticipates the changes in deviation angle that are the basis of proportional pursuit, but commands high turning rates if the deviation angle

changes rapidly, which can cause instability at high gain. Because derivative control has no inherent tendency to correct for any constant offset in the deviation angle, it is usually only used in combination with proportional control, but we also test it in isolation to aid in statistical inference. Adding an integral term to the controller is not expected to be useful in this context, given that driving the deviation angle δ to any small angle is sufficient to bring the subject to its target (see above).

Guidance law	Abbreviation	Name	Examples
$\dot{\gamma}(t) = k_N \dot{\lambda}(t-\tau)$	k_N	proportional navigation*	pursuit in falcons [122, 124], hawks [127, 128], bats [121], killerflies, robberflies [125]
$\dot{\gamma}(t) = k_P \delta(t-\tau)$	k_P	pure/proportional pursuit*	pursuit in hawks [127], blowflies [129], tiger beetles [130], honey bees [131]
$\dot{\gamma}(t) = k_P[\delta(t-\tau) - \delta_0]$	k_P	deviated pursuit	pursuit in hoverflies [132], bluefish [133], dragonflies [134]
$\dot{\gamma}(t) = k_D \dot{\delta}(t-\tau)$	k_D	derivative control*	not modelled previously
$\dot{\gamma}(t) = k_N \dot{\lambda}(t-\tau) + k_P \delta(t-\tau)$	$k_N k_P$	mixed guidance*	pursuit in hawks [123]
$\dot{\gamma}(t) = k_P \delta(t-\tau) + k_D \dot{\delta}(t-\tau)$	$k_N k_D$	proportional-derivative controller*	pursuit in houseflies [135]
$\dot{\gamma}(t) = k_N \dot{\lambda}(t-\tau) + k_D \dot{\delta}(t-\tau)$	$k_P k_D$	proportional navigation with derivative controller*	not modelled previously
$\dot{\gamma}(t) = k_P \delta(t-\tau) + k_D \dot{\delta}(t-\tau) + k_S \dot{\gamma}(t-\tau)$	$k_P k_D k_S$	proportional-derivative controller with inertia	gap aiming in pigeons [105]

Table 2.1: Guidance laws used to model target-oriented steering behaviour in animal flight. Here we model the six alternative guidance laws marked with an asterisk; see Introduction for rationale and definitions of terms.

Other plausible steering controllers command turning in proportion to the angular rate of the subject's line-of-sight to its target ($\dot{\lambda}$), measured in an inertial frame of reference. The simplest form of this proportionality corresponds to the classical guidance law of homing missiles, $\dot{\gamma}(t) = k_N\dot{\lambda}(t-\tau)$, called proportional navigation [122]. This guidance law has been used to explain the attack trajectories of raptors [122, 124, 127, 128], and effectively combines a proportional controller's tendency to correct a constant error signal with a derivative controller's tendency to anticipate changes in the error signal. It achieves this by driving a constant-bearing approach to the target, which typically leads to interception, rather than tail-chasing, of moving targets at $k_N > 1$. This guidance gain k_N is usually called the navigation constant and is conventionally denoted N, but we write it here as k_N for consistency with our notation for k_P and k_D.

In contrast to proportional pursuit, proportional navigation is considered an optimal guidance strategy, in the sense that it can be tuned to minimize the steering effort needed to hit a non-manoeuvring target [136]. Here, steering effort is defined as the sum of the squared lateral acceleration command, and non-manoeuvring means that the target is either stationary or flying in a straight line. These properties make proportional navigation an appealing candidate for gap-oriented steering, but previous research on gap-aiming behaviours in birds has focused only on guidance laws involving the proportional-derivative guidance terms k_P and k_D [105]. Proportional navigation can also be used to model deviated pursuit when $k_N = 1$, which matches the subject's turn rate $\dot{\gamma}$ to its line-of-sight rate $\dot{\lambda}$, and therefore tends to keep the deviation angle δ constant at its initial value $\delta_0 = \delta(0)$ (see Fig. 2.1). We make use of this fact to avoid having to fit δ_0 as a second free parameter in this single-input guidance law and do not model deviated pursuit explicitly here (Table 2.1).

Different linear combinations of these k_P, k_D, and k_N terms have been used to formulate mixed guidance laws of the forms shown in Table 2.1. For example, mixed k_Nk_P-guidance has been used to explain the attack trajectories of hawks pursuing manoeuvring targets [123], whereas proportional-derivative k_Pk_D-guidance has been

used to model pigeons steering through clutter [105]. Finally, the $k_P k_D$ controller that Lin *et al.* [105] used to model gap aiming behaviour in pigeons was originally tested with the addition of a delayed damping term $k_S\dot{\gamma}(t-\tau)$ that we do not model here.

Whereas guidance laws can be used straightforwardly to model the target chasing behaviours of birds [122–124], using them to model clutter negotiation behaviour poses several new challenges. A key contribution of the pioneering work by Lin *et al.* (2014) was to treat clutter negotiation not as an obstacle avoidance behaviour, but as a gap targeting behaviour, thereby enabling its treatment as a classical guidance problem [105]. Framing an animal's movement through a field of obstacles as a sequence of consecutive gap-aiming events [105] avoids the need to model more complex attractor-repeller type behaviours, but risks over-fitting if there are many obstacles, and hence multiple gaps, present. Moreover, a key challenge in applying this framework is the need to define what constitutes a target, and—following from this—the extent to which obstacle avoidance behaviour can be described as target oriented movement at all. This is because an animal's perception of what constitutes a gap may be different to how an experimenter defines it [137]. How an animal perceives a gap will depend not only on the visual angles subtended by the objects in the environment [105], but also on background brightness [137], and the subjective distance at which the animal treats an object as an obstacle relevant to gap choice. It follows that the gaps between obstacles are virtual constructs that are liable to change as an animal moves.

In this paper, we therefore use a simplified experimental setup to identify the mechanisms of gap choice and gap steering independently. Using a forced binary choice protocol in which one of the gaps was partially obstructed allowed us to test whether the birds flew towards the gap providing the greatest clearance, or whether they used some alternative method of gap selection. Forcing the birds to manoeuvre towards one of two divergent positions also gave us sufficiently varied trajectory data to test alternative guidance laws modelling their steering (Table 2.1), and to test whether pigeons target the physical centre of the gap between obstacles as Lin *et al.* proposed [105].

2.4 Methods

2.4.1 Subjects and training

We used $N = 12$ homing pigeons *(Columba livia domestica)* aged from 2 to 10 years as subjects (Supplementary Data S1-S2), choosing this sample size to be at least twice that of related studies of gap negotiation behaviours in birds [105, 138]. The sex of these individuals is unknown, owing to the lack of unambiguous external sex characteristics in this species. The birds were reared at the John Krebs Field Station, Wytham, Oxford, UK, as members of a free-ranging population provided with *ad libitum* access to food and water in the home loft to which they returned voluntarily. The most experienced non-retired individuals of the population were selected for experiments in order to minimise distress to the animals.

Experiments took place over a four week period from mid-November to mid-December 2018. The birds were caught from their loft immediately before the experiment, and released by an experimenter in a large indoor flight hall with one of its ends open to the outside. The birds usually returned directly to their home loft, which was located within 80 m of the exit. Each subject was released in the empty flight hall on five consecutive days prior to experimentation, to ensure familiarity with the location and its relationship to the home loft before introducing any obstructions. All testing was approved by the Animal Welfare and Ethical Review Board of the University of Oxford's Department of Zoology (permit number APA/1/5/ZOO/NASPA), and we monitored the feather condition and flight behaviour of the birds throughout the study for any signs of stress.

2.4.2 Experimental set-up and protocol

Experiments were undertaken in a flight hall measuring 20.2 m by 6.1 m, with a minimum ceiling height of 3.8 m. The walls of the hall were covered with camouflage netting to provide homogeneous visual contrast. Flicker-free LED lights provided a mixture of direct 4000 K illumination and indirect 5000 K illumination at approximately 1000 lux, which was designed to mimic overcast morning or

evening light conditions. Most of the back wall of the building comprised an open roller shutter door providing natural daylight illumination, presenting a much brighter scene than the interior of the flight hall. The ambient weather conditions and position of the sun's disc were a source of uncontrolled variation in brightness during the experiments. To minimise such variation, experiments were only undertaken during overcast days.

On each day of experiments, the pigeons were collected from their home loft, and fitted with a rigid plate attached to their head using eyelash glue (Duo Quick Set Strip Lash Adhesive Clear Tone). This was fitted just before the start of each recording session, and was removed at the end of the release. Each plate had a unique asymmetrical configuration of three or four 4 mm diameter spherical retro-reflective markers for motion capture purposes (Vicon Motion Systems Ltd, Oxford, UK). Each pigeon was taken out of its carrier box individually in the flight hall, held for a minute at the release point to acclimatise, and then released to fly freely by the experimenter opening their hands. The next pigeon was only taken out of its carrier box once the preceding bird had exited the flight arena and was out of sight. After all the pigeons had been released, they were collected from the loft to be released again. On a typical test day, we would carry out three releases per pigeon. Testing was only conducted on clear days, and the markers were removed from the pigeons at the end of each day.

Pigeons were released at 1.2 m height approximately 2 m from the front wall of the hall, within ± 1 m of the midline. From there, they flew through one of two floor-to-ceiling gaps created to either side of a heavy black curtain hung across the hall, approximately 7 m ahead of the release point (Fig. 2.2A). These symmetric vertical gaps were approximately 1.2 m wide, and hence up to roughly twice the wingspan of the birds. The aperture of the roller door was not visible to the birds at the point of release, but flying through either gap enabled the pigeons to see and reach this aperture, from where they could exit the building (Fig. 2.2C). Their home loft was located a short distance (approximately 80 m) behind and to the left of the building (Fig. 2.2B), so was occluded from view until the birds had exited the flight hall.

We placed a 4.0 m high obstacle in one of two fixed positions in each of the front and back sections of the hall (Fig. 2.2A). Each obstacle consisted of a pair of 0.3 m diameter white expanded polystyrene cylinders taped together side-by-side, giving high visual contrast against the background. The two obstacles were placed 2 m away from the curtain along the longitudinal axis of the flight arena to obstruct the most direct path from (i) the release point to either the right or left gap (front obstacle); and (ii) either the right or left gap of the curtain to the midpoint of the open shutter doors (back obstacle). We randomised the side on which the front and back obstacles were placed at the start of each release, and maintained the same obstacle positions for all the individuals on a given release to minimise the time that they were kept waiting in their carrier boxes. The back obstacle was not visible to the pigeon until it had reached the gaps on either side of the curtain, and is not considered further here. Here we focus exclusively on the behaviour of the birds in the front section of the hall, between the release point and the curtain. Given that the curtain was located 9.0 m into the hall, we assume that both gaps would have appeared similarly bright to the birds were it not for the placement of the front obstacle (Fig. 2.2).

2.4.3 Motion capture

We used an array of 22 high-speed motion capture cameras (Vantage 16, Vicon Motion Systems Ltd, Oxford, UK) and 4 reference video cameras (Vue, Vicon Motion Systems Ltd, Oxford, UK) to record the flights. Cameras were mounted 3.0 m above the floor on scaffolding fixed around the perimeter of the room. The cameras were arranged so that any marker within the recording volume would be visible to at least three cameras, which enabled automatic reconstruction of its 3D coordinates by the motion capture system. Sensor resolution for the Vantage cameras was 4096×4096 pixels at a 200 Hz frame rate and 1 ms shutter speed. A strobe unit on each camera emitted infrared light at 850 nm, which falls outside the visible spectrum of the birds [139]; an optical filter blocked light at other

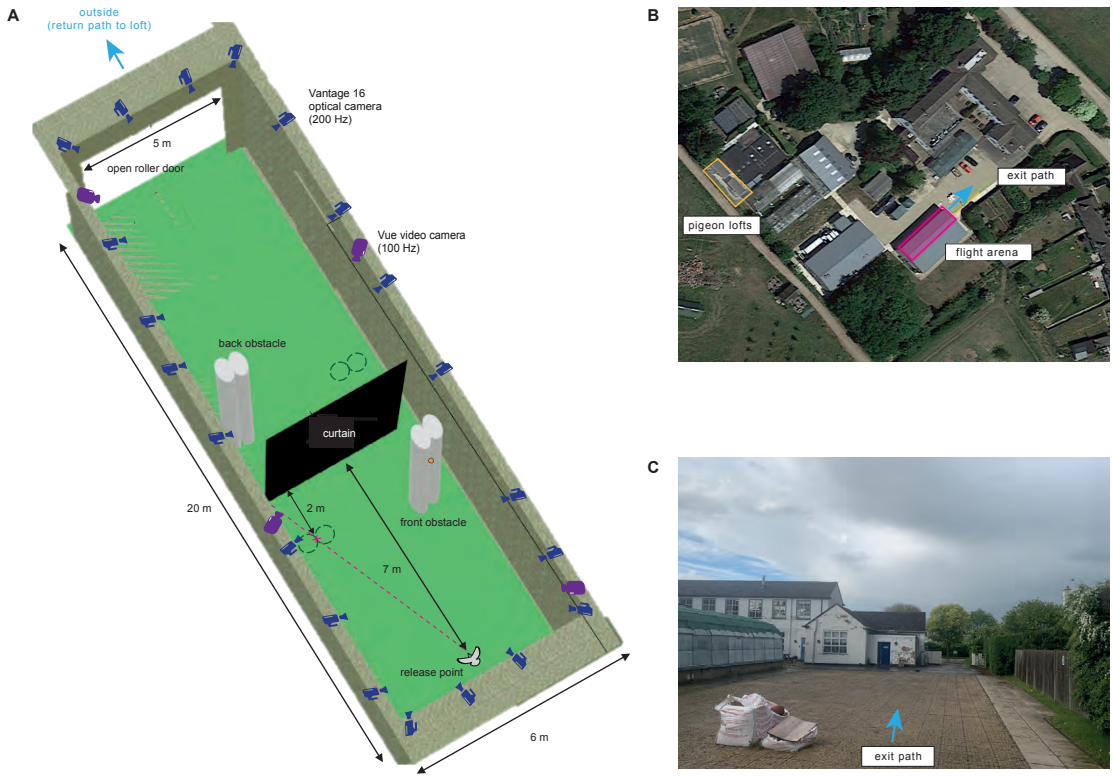


Figure 2.2: Experimental setup. (A) Flight arena viewed from above. Pigeons flew from the release point (marked as grey a bird outline) to the outside through the open roller door. The path was obstructed by a curtain, creating gaps on either side for the pigeons to fly through. The area from the release point to the curtain covers the region of interest in which target-oriented steering flight was modelled, from release point to gap. Obstacles were placed in front of (and behind) the curtain on alternate sides. The positions of these are represented as either a white obstacle formed by two circular columns or two dashed dark green circles signalling the position at which there was no obstacle in this sample trial. (B) Aerial view of experimental area relative to pigeon home lofts. (C) View out of the experimental area from the open shutter door. Note that buildings are visible to the left.

wavelengths. For the Vue cameras, the sensor resolution was 1920 x 1080 pixels at a frame rate of 100 Hz and a shutter speed of 2 ms.

The camera system was calibrated at the start of each day of experiments. Experiments only went ahead after each camera had been calibrated to an image error accuracy of $\leq$0.4 pixels for the motion capture cameras, and $\leq$1.2 pixels for the reference video cameras. Flights were recorded using Vicon Nexus software, which was manually triggered for each pigeon release, with calibration error being checked at the start of each experimental session. The accuracy of the calibration decreased gradually through the day, but the mean three-dimensional reconstruction accuracy for all trials was 0.7 mm (Q1, Q3: 0.57, 1.26 mm). In addition to the

retro-reflective markers fitted to the pigeons, we placed 6 mm diameter markers at fixed positions on the edges of the curtain, walls, and obstacles, to record the positions of these features accurately for each trial. These markers were removed temporarily for calibration of the motion capture system.

The Vicon Nexus software outputs the 3D coordinates of all of the markers found within the imaging volume throughout the trial. We labelled each of the recorded markers using custom-written software in MATLAB v9.6 (MathWorks, Inc., Natick, MA, USA), which used clustering algorithms to group markers within and between frames (e.g. to distinguish markers on the pigeon from markers on the obstacles, based on their speeds). The marker labelling procedure was designed to eliminate the false positives that can arise from spurious reflections, but inevitably resulted in some data drop-out; particularly in the less-well visualised part of the flight volume near the ceiling, and in the partially occluded regions of the flight volume close to the curtain. Marker positions were defined relative to the principal axes of the room, as determined through the calibration of the motion capture system. Any minor discrepancies in the alignment of this global axis system between trials were corrected by applying a Procrustes transformation to the camera coordinates prior to further analysis, so that the global axis definitions for all trials were the same.

2.4.4 Flight trajectory analysis

We recorded a total of $n = 105$ flights, of which $n = 96$ were judged suitable for further analysis in the sense that the pigeon was recorded flying through one of the gaps without landing or loitering. Of these, $n = 76$ flights were tracked for ≥ 1 s and were used for the purposes of quantitative trajectory analysis. We determined pigeon head position as the mean position of the identified head markers, and fitted a quintic smoothing spline to remove the noise associated with occasional missing or merged markers. The smoothing tolerance was set such that the mean distance between the spline and the data was kept below the maximum span of the head markers, in order to preserve the detail of the head motion. We dropped any flights for which the recorded markers were insufficient for coordinate reconstruction, or

where the bird did not fly to the exit point (e.g. perching on a camera instead of exiting the flight hall). Although the trajectory data are fully three-dimensional, we analyse only their horizontal components here, on the basis that the gaps we treat as the targets of the bird's guidance are extended objects in the vertical dimension.

2.4.5 Steering controller simulations

We modelled the horizontal steering behaviour of our pigeons using the same trajectory simulation approach used to study target-oriented attack flights in hawks and falcons [122–124], but tested a broader set of candidate steering controllers comprising all single-input and two-input guidance laws involving linear combinations of k_N, k_P, and k_D (Table 2.1). We did not model deviated pursuit explicitly, because proportional navigation with $k_N = 1$ simulates a deviated pursuit trajectory in which the deviation angle δ remains constant at its initial value $\delta_0 = \delta(0)$, thereby avoiding the need to treat the commanded deviation angle as another free parameter. Because the presence of an obstacle is expected to have modified the bird's perception of the obstructed gap, we only consider the subset of flights taken through the unobstructed gap for the purposes of modelling the steering controller. With this restriction, and to avoid overfitting any very short recordings, we analysed only the subset of $n = 23$ flights from $N = 10$ individuals with ≥ 1 s of continuous recording during which the pigeons were tracked to within ≤ 1 m of the unobstructed gap through which they flew. It is important to note that this 1.0 s period of flight typically does necessarily extend to the point at which the bird finally reached the gap, owing to marker occlusion in the vicinity of the curtain.

For these $n = 23$ flights, we fitted the candidate guidance laws under two alternative definitions of the target of the pigeons' gap-aiming behaviour: (i) the midpoint between the curtain edge and the wall (i.e. the point corresponding to the physical centre of the gap); and (ii) the point approximately half a wingspan (0.35 m) into the gap from the edge of the curtain (i.e. the point minimising the clearance with the wings fully spread). The former target definition maximizes the bird's minimum clearance from the physical structures in its environment, whereas the

latter minimizes the clearance on the inside of the turn without risking a collision. Pigeons can fly through gaps as narrow as 0.11 m by closing their wings, but doing so compromises their efficiency and manoeuvrability [140]. Given that the physical size of the gap would not oblige the birds to close their wings, and given that we saw no evidence of them doing so, we opted for a target definition that would allow the birds to turn as tightly as possible without closing their wings.

Given the initial conditions recorded for each flight, we simulated the best-fitting flight trajectory commanded under the various guidance models shown in Table 2.1. For each steering controller, we estimated the guidance parameters and delay for a given flight, or collection of flights, by minimising the mean squared distance between the measured and simulated trajectories over all of the fitted sample points, which we report as the root mean square (RMS) error (ϵ). However, because the birds did not necessarily begin their target-oriented steering behaviour immediately upon release, we only use the data from the last 1.0 s of flight recorded before the pigeon entered the gap for the purposes of model selection and statistical inference; we later extend the simulated section of flight back in time to cover the entire recorded trajectory. Whereas we used the guidance law to simulate the bird's turning, we matched the simulated flight speed to the bird's measured flight speed, to ensure proper determination of the time derivatives of the line-of-sight angle λ and deviation angle δ.

To account for sensorimotor delay, we lagged the input variables by $0 \leq \tau \leq 0.4$ s. The upper end of this range of values exceeds the latency of the pectoralis muscles to the firing of the looming-sensitive neurons in the pigeon's tectofugal pathway by at least a factor of 4 [141], but is intended to accommodate the possibility that pigeon steering responses in flight might also be delayed by one wingbeat period (approximately 0.15 s inside the flight hall), as observed in turning flight [142]. Taking time $t = 0$ as the first data point, we therefore modelled the bird's flight trajectory beginning from time $t = \tau_{max}$, to ensure that the same section of flight was simulated for all tested values of τ. We were thereby able to model each two-dimensional flight trajectory given knowledge of the pigeon's initial track

angle and position, the time history of the pigeon's speed, and the location of the unobstructed gap formed by the edge of the curtain and the wall. See Supplementary Information for methodological details and supporting code.

2.4.6 Statistical analysis

We use a generalized linear mixed effects (GLME) model with binomial link function in R [**R**] to analyse the factors affecting left versus right gap choice over all $n = 105$ flights and all $N = 12$ birds, treating bird identity as a random effect and including the side of the obstructed gap as a fixed factor. We report these means of quantities estimated directly from the trajectory data together with their standard deviation (mean $\pm$ s.d.) for the $n = 95$ flights in which the pigeons flew through one or other gap without landing loitering, and use two-sample t-tests to test for differences in these means between samples. Note that we treat each flight as an independent datapoint when analysing the detailed properties of the trajectories, which means that some of the analyses risk pseudo-replication within birds.

For the subset of $n = 23$ flights included in the guidance analysis, we use hat notation to refer to the least squares estimates of the guidance model parameters (e.g. $\hat{k}_N$ denotes a unique estimate of k_N), and tilde notation to denote their median across all flights (e.g. $\tilde{k}_N$ denotes the median value of $\hat{k}_N$ over all flights). We report these medians together with their associated 1st and 3rd quartiles (Q1, Q3), and use sign tests to test whether the fitted guidance constants were consistently positive or negative, or lower than some critical numerical value (see Discussion). We use Wilcoxon signed rank tests to test for differences in the median RMS error of the fitted guidance models, treating each flight as an independent data point. Unless stated otherwise, we report two-tailed p-values throughout.

2.5 Results

Upon release, the pigeons flew in the direction of the open roller shutter door, even though its aperture was not directly visible from the release point, and despite this being in a different direction to the home loft. Most birds flew directly to

the outside via one of the two gaps, but a few began circling in the section of the hall before the curtain. For the purposes of our analyses of gap selection (Fig. 2.4) and steering (Fig. 2.3), we only consider data collected between the release point and the curtain. The mean speed of flights through the unobstructed gap (4.0 ± 0.8 m s^{-1}) was significantly higher than for flights through the obstructed gap (3.6 ± 0.7 m s^{-1}; two-sample t-test: $t_{(93)} = 2.37$, $p = 0.02$). These speeds are slow compared to the cruising speeds of pigeons flying in the open, which can exceed 10 m s^{-1} [143], but are similar to the flight speeds observed previously under similarly cluttered experimental conditions [105].

2.5.1 Pigeons select gaps on the basis of handedness, not size

The pigeons usually flew forwards upon release, before steering towards one of the two available gaps, resulting in a characteristic goblet-shaped distribution of flight trajectories (Fig. 2.3). We interpret this initial flight behaviour as an escape response, with the first unambiguous evidence of gap selection coming later in the flight. The pigeons flew through the unobstructed gap on 53% of the $n = 105$ flights (overall odds of selecting the unobstructed gap: 1.14). The presence of an obstacle had no statistically significant effect on gap choice (GLME: $z = 1.84$, $p = 0.07$), so there is no evidence that the pigeons headed for the unobstructed, and hence larger, of the two gaps. However, comparing the detailed flight trajectories associated with flight through obstructed versus unobstructed gaps, it appears that birds flying through the obstructed gap may have made the decision to do so later than birds flying through the unobstructed gap, since the bifurcation of the goblet-shaped distribution occurs noticeably closer to the curtain for the subset of flights through the obstructed gap (Fig. 2.3).

The pigeons also displayed a statistically significant tendency to fly through the right-hand gap (GLME: $z = 2.13$, $p = 0.03$), which they took on 65% of the 105 flights (overall odds of selecting the right-hand gap: 1.84; marginal odds of selecting the right-hand gap: 1.67 when unobstructed; 2.86 when obstructed). Since the home

loft was located to the left of the exit, it follows that the birds were not choosing the gap that was most closely aligned with their intended flight direction. Instead, they appear to have been flying with a specific handedness. Importantly, the direction of this handedness was not universal to all birds: some individuals displayed a strong preference for flying towards the right-hand side independent of obstacle placement (e.g. pigeons B01, B65, S57, X41), as indicated by marginal odds ratios significantly larger than 1, whereas a smaller number of individuals (e.g. pigeons D10, X53, C68) displayed a strong preference for flying to the left independent of obstacle placement, with marginal odds ratios significantly below 1 (Fig. 2.4). There is also a possibility that the right preference observed was in response to the left side of the room behind the release point being more cluttered. For example, the computer controlling the motion capture system was located in the far left corner of the room. Because the birds were released 2 m ahead of the wall, the placement of this equipment would not have interfered with the appearance of their frontal visual field, but their peripheral vision is such that the computer station would still have been in sight.

2.5.2 Simulations of steering behaviour

The birds tended to fly upwards from the release point, with a mean altitude gain of 0.73 ± 0.48 m. The mean transverse clearance of the pigeons from the curtain was 0.47 ± 0.30 m, or approximately two thirds of an average wingspan, with 0.80 ± 0.48 m mean transverse clearance from the wall. Although the pigeons therefore tended to fly closer to the curtain than to the wall, the fit of the guidance simulations with parameters fitted independently to each flight was closer when the target was defined as the midpoint of the gap than when the target was defined as the point 0.35 m from the edge of the curtain (Wilcoxon signed rank test: $z = -2.17$, $p = 0.030$; test of mean RMS error over all six guidance models fitted independently to each flight). The quantitative results reported below (see Supplementary Data S1 for summary) are therefore for simulations targeting the midpoint of the gap, which is the same definition used in previous work on pigeon gap-steering behaviour [105]. The quantitative results of the simulations targeting the point 0.35 m from the

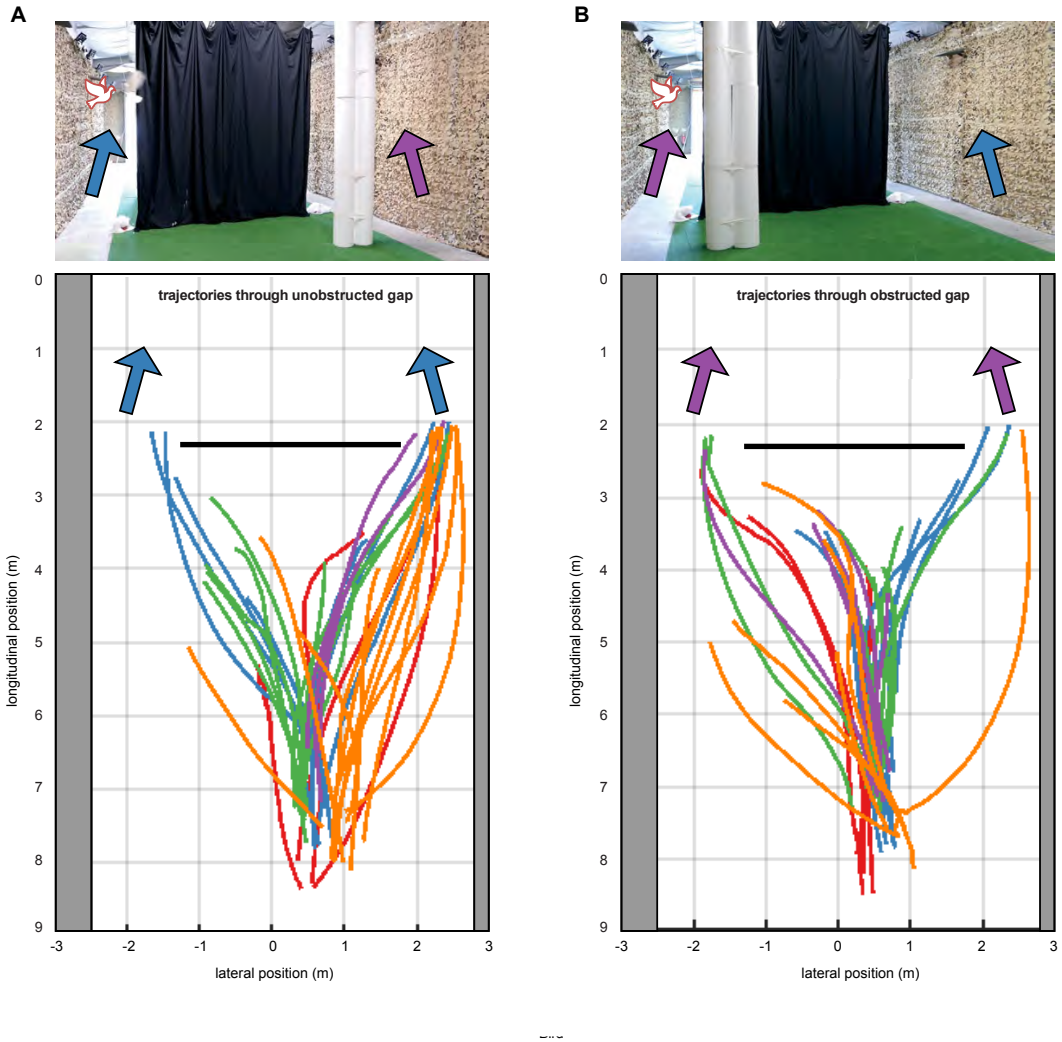


Figure 2.3: Gap negotiation behaviour in pigeons. All $n = 96$ flight trajectories, viewed from above and colour-coded by day of data collection. Obstacle position was randomised throughout, and pigeons were free to fly through either gap. Trials in which the pigeon flew through the non-obstructed gap (left) are shown separately from trials in which the pigeon flew through the obstructed gap (right). The images above show typical flight behaviour and illustrate the experimental setup.

edge of the curtain are provided as Supplementary Data S2, and are qualitatively similar in the patterns that they display.

2.5.2.1 Guidance parameters fitted independently to each flight

All six steering controllers that we tested (Table 2.1) were capable of simulating the flight trajectories closely if their parameters were fitted independently to the last 1.0 s of each flight (Fig. 2.5A). The associated estimates of the delay spanned

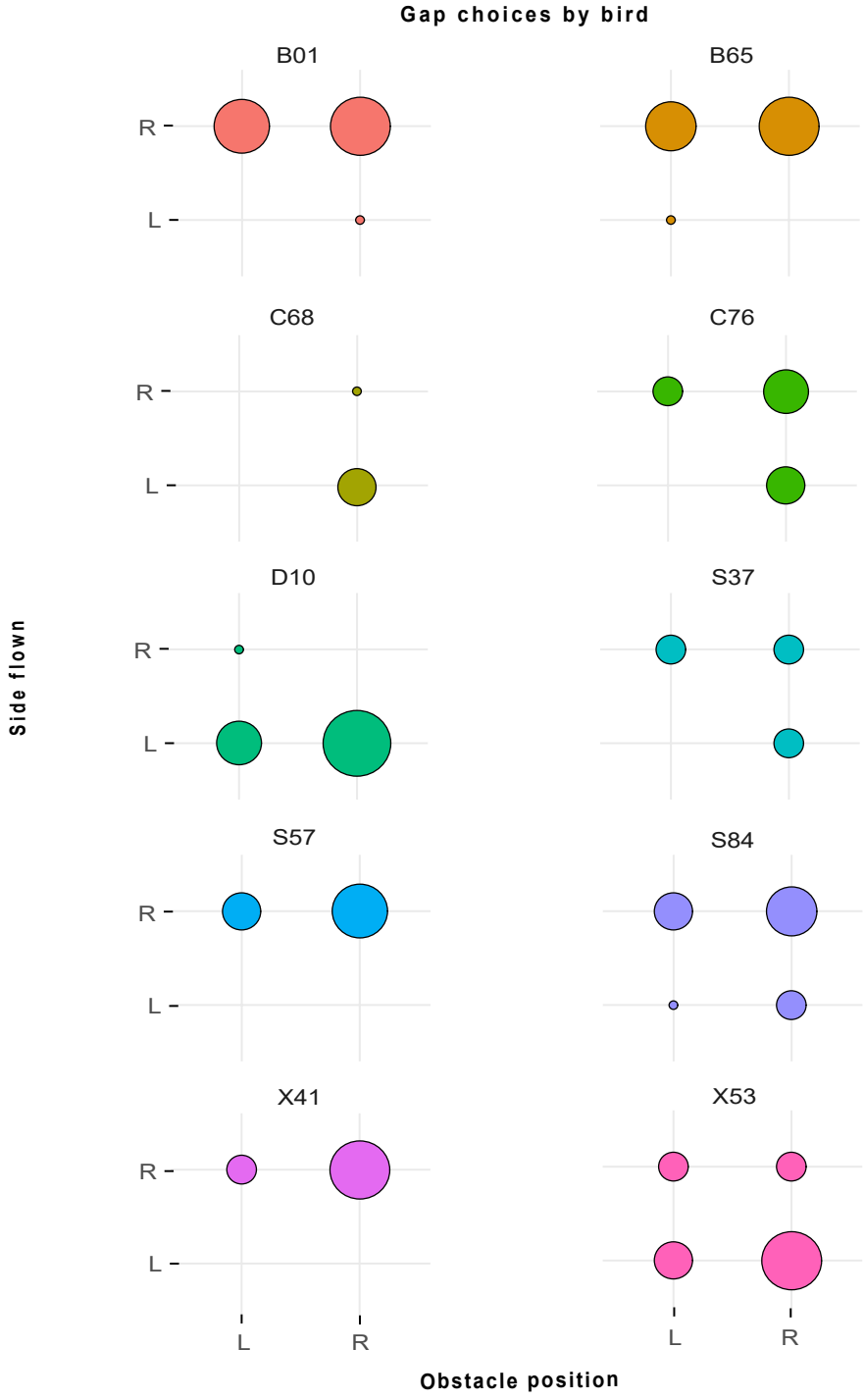


Figure 2.4: Gap selection behaviour in pigeons. Distribution of gap choice comparing side flown to side on which obstacle was placed for all $n = 96$ flights; the area of the plotted circle is shown proportional to the frequency of choice. Most pigeons display a clear preference for flying on one or another side of the curtain—most often the right-hand side. In the figure, this manifests as larger circles in either the top or bottom positions instead of circles of equal area in all four positions. This idiosyncratic preference does not seem to be affected by the placement of an obstacle between the release point and the gap.

a broad range of values (Fig. 2.6), with a model-average of $\tilde{\tau} = 0.24$ s (Q1, Q3: 0.07, 0.36 s) over all six guidance laws. Among the three single-input guidance laws that we tested, k_N-guidance modelled the data most closely (Fig. 2.5A), with a median RMS error of $\tilde{\epsilon} = 0.015$ m (Q1, Q3: 0.007, 0.056 m). The other single-input controllers that we tested had a higher median RMS error, with $\tilde{\epsilon} = 0.018$ m for k_P-guidance (Q1, Q3: 0.011, 0.042 m) and $\tilde{\epsilon} = 0.045$ m for k_D-guidance (Q1, Q3: 0.020, 0.101 m), but in neither case was this difference statistically significant across flights (Wilcoxon signed rank test: $z = 0.37$, $p = 0.72$; $z = 1.86$, $p = 0.06$). As expected, our estimates of the guidance constants were consistently positive under k_N-guidance ($\tilde{k}_N = 2.6$; Q1, Q3: 1.9, 4.2; sign test: $p < 0.001$; Fig. 2.6B), and consistently negative under k_P-guidance ($\tilde{k}_P = -2.3$ s^{-1}; Q1, Q3: -3.7, -1.9 s^{-1}; sign test: $p < 0.001$; Fig. 2.6D). In contrast, they were inconsistently signed under k_D-guidance ($\tilde{k}_D = 0.7$; Q1, Q3: -1.0, 1.1; sign test: $p = 0.40$; Fig. 2.6F), which reflects the over-fitting expected for a controller with no inherent tendency to steer towards a target. In summary, either proportional navigation (i.e. k_N-guidance) or proportional pursuit (i.e. k_P-guidance) is capable of providing a reasonable model of the data, with proportional navigation providing a marginally better fit.

Introducing a second input variable reduced the error between the measured and simulated trajectories by at least a factor of two (Fig. 2.5A). Of the various two-input controllers that we tested, $k_N k_D$-guidance provided the closest fit (Fig. 2.5A), with a median error of $\tilde{\epsilon} = 0.005$ m (Q1, Q3: 0.003, 0.007 m) that was significantly lower than for the best-fitting of the single-input guidance laws (Wilcoxon signed rank test: $z = -4.20$, $p < 0.001$). The other two-input controllers that we tested had a higher median RMS error, with $\tilde{\epsilon} = 0.006$ m for $k_N k_P$ (Q1, Q3: 0.004, 0.010 m) and $\tilde{\epsilon} = 0.008$ m for $k_P k_D$ (Q1, Q3: 0.005, 0.011 m). However, in neither case was this difference statistically significant across flights (Wilcoxon signed rank tests: $z = 1.00$, $p = 0.32$; $z = 1.43$, $p = 0.15$), and in both cases the fit was significantly closer than for the best-fitting of the single-input guidance laws (Wilcoxon signed rank test: $z = -3.56$, $p < 0.001$; $z = -2.43$, $p = 0.015$). Notwithstanding their improved fit over single-input k_N- or k_P-guidance, there is clear evidence that

all of the two-input guidance models were over-parameterized. Specifically, the estimates of both guidance constants under $k_N k_P$-guidance were inconsistently signed ($\tilde{k}_N = 2.5$; Q1, Q3: -1.6, 5.2; sign test: $p = 0.21$; $\tilde{k}_P = -0.3$ s^{-1}; Q1, Q3: -5.4, 1.7 s^{-1}; sign test: $p = 1.0$; Fig. 2.6H). There is therefore no evidence that proportional navigation and proportional pursuit are combined under $k_N k_P$-guidance. In contrast, although the estimates of k_N and k_P remained consistently signed when fitted in combination with k_D, the associated estimates of k_D were inconsistently signed ($\tilde{k}_D = 0.5$ under $k_N k_D$; Q1, Q3: -0.6, 1.0; sign test: $p = 0.40$; Fig. 2.6J; $\tilde{k}_D = 0.3$ under $k_P k_D$; Q1, Q3: -0.5, 0.7; sign test: $p = 0.40$; Fig. 2.6L). There is therefore no evidence that derivative control is combined with proportional navigation or proportional pursuit under $k_N k_D$- or $k_P k_D$-guidance.

In summary, when the guidance parameters were fitted independently to the last 1.0 s of each flight, proportional navigation (i.e. k_N-guidance) gave the best fit of all the single-input steering controllers, but fitted the data only marginally better than proportional pursuit (i.e. k_P-guidance). Whilst it was always possible to achieve a closer fit by adding a second guidance term, the parameter estimates for the second guidance term were always inconsistently signed. The guidance simulations fitted independently to the last 1.0 s of each flight therefore provide no evidence for the involvement of a second guidance term, but do not allow us to distinguish unambiguously between single-input proportional navigation or proportional pursuit.

2.5.2.2 Guidance parameters fitted globally for all flights

Fitting the guidance parameters independently to each flight is appropriate if the true underlying guidance gains vary within or between individuals [122], but risks over-parameterization otherwise. To mitigate this risk, we searched for the unique combinations of parameter settings (Table 2.2) that minimised the median RMS error for each candidate guidance law over the last 1.0 s of all $n = 23$ flights (Fig 2.7). We did this using an exhaustive search procedure in which we computed the RMS error on every flight, for all combinations of $k_N \in [-0.5, 5.5]$, $k_P \in [-5.5, 0.5]$, and $k_D \in [-2, 2]$ at 0.1 spacing, and $\tau \in [0, 0.4]$ at 0.005 spacing (SI units). We

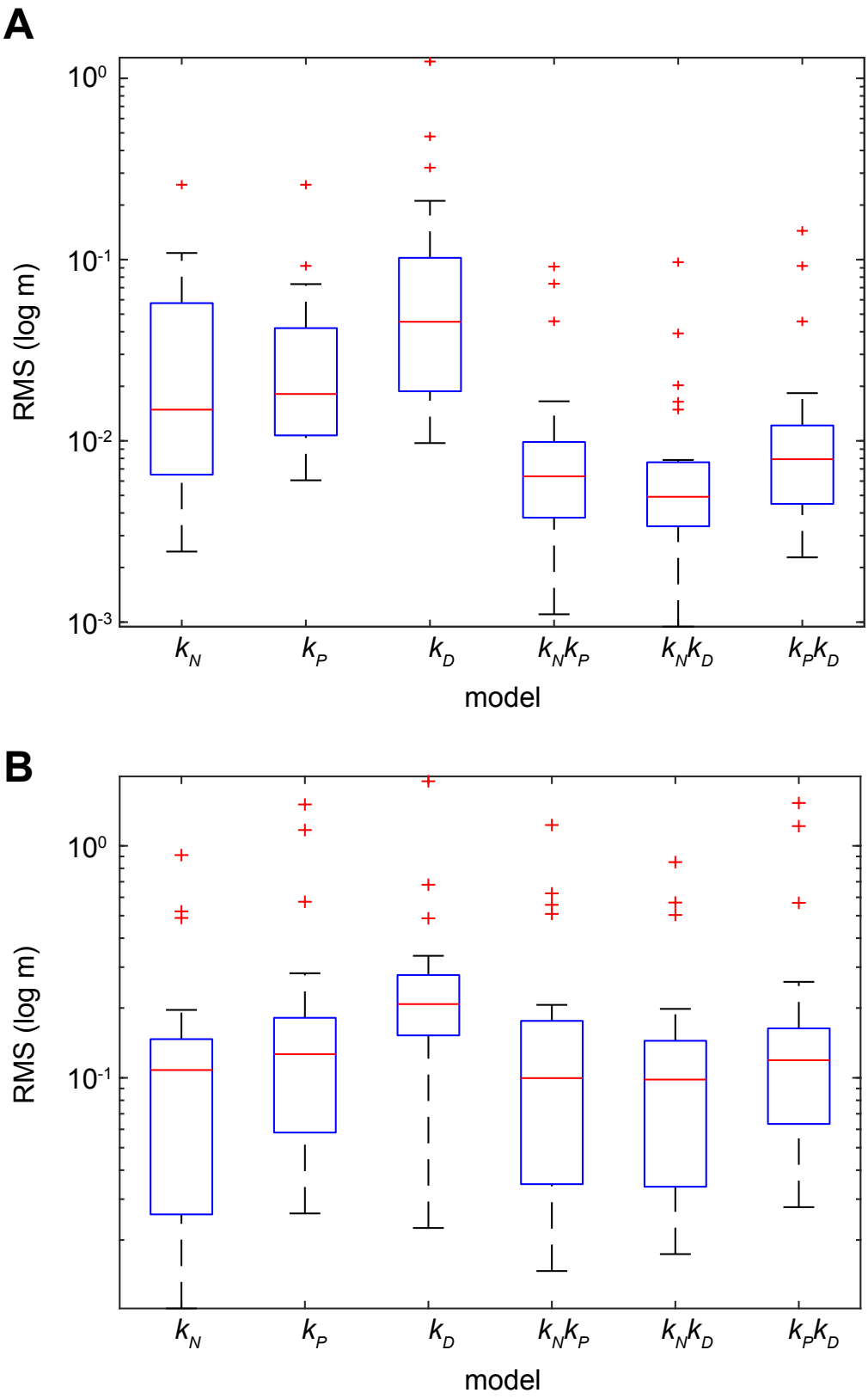


Figure 2.5: Box plots showing root mean square (RMS) error (ϵ) of simulations under each fitted guidance model. (A) Models with parameters fitted independently to each of the $n = 23$ flights through the unobstructed gap. (B) Models with parameters fitted globally to these same flights. The blue box encloses the middle half of the data, with Q1 at the bottom and Q3 at the top; the red line denotes the median; red crosses denote outliers.

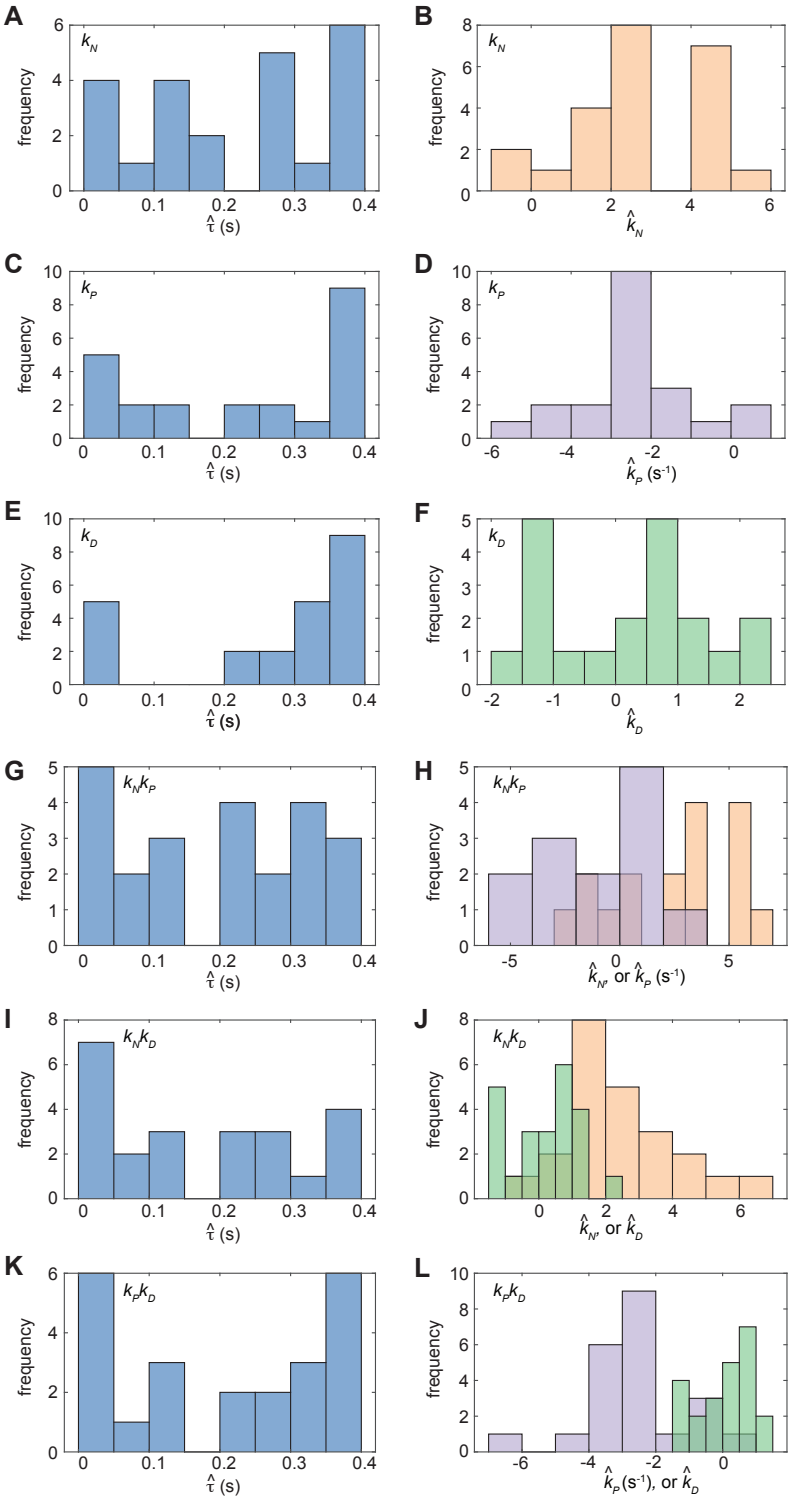


Figure 2.6: Distributions of parameter estimates for guidance models fitted independently to each flight. Results shown for all $n = 23$ flights through the unobstructed gap, but with some outlying values of the guidance parameters not shown for the few cases where the fitting did not converge on a value within the axis limits (see Supplementary Data S1 for all values including these outliers). Left column: histograms of parameter estimates for time delay τ (blue); right column: histograms of parameter estimates for guidance constants k_N (orange), k_P (lilac), and k_D (green), for all $n = 23$ flights. (A,B) k_N-guidance; (C,D) k_P-guidance; (E,F) k_D-guidance; (G,H) $k_N k_P$-guidance; (I,J) $k_N k_D$-guidance; (K,L) $k_P k_D$-guidance.

chose these intervals in light of the ranges of the parameter estimates that we had identified by fitting all flights independently, and used the resulting simulations to identify the global optimum minimising the median RMS error over all flights. Having identified this global optimum at coarse parameter spacing, we then refined the search spacing by a factor of 5 in the vicinity of the coarse global optimum. Fitting the parameters of these steering controllers globally for all flights reduced the total number of fitted parameters by a factor of 23, but also increased the median RMS error by an order of magnitude (Fig. 2.5B).

Among the three single-input steering controllers that we tested, k_N-guidance once again provided the best fit to the data, with a median RMS error of $\tilde{\epsilon} = 0.108$ m (Q1, Q3: 0.026, 0.144 m; Fig. 2.5B). The parameter estimate for the navigation constant in this globally-fitted model ($\hat{k}_N = 2.05$) was somewhat lower than the median of the parameter estimates for the navigation constants fitted independently to each flight ($\tilde{k}_N = 2.6$), but well within the typical range of fitted values (Q1, Q3: 1.9, 4.2). The associated parameter estimate for the time delay $\hat{\tau} = 0.27$ s was also in the middle of the range of values fitted independently to each flights (see above). The other single-input controllers that we tested performed significantly less well than k_N-guidance when fitted globally to all fits (Fig. 2.5B), with a median RMS error of $\tilde{\epsilon} = 0.127$ m for k_P-guidance (Q1, Q3: 0.058, 0.178 m; Wilcoxon signed rank test: $z = 2.13$, $p = 0.033$) and $\tilde{\epsilon} = 0.208$ m for k_D-guidance (Q1, Q3: 0.156, 0.275 m; Wilcoxon signed rank test: $z = 2.83$ $p = 0.005$).

Adding a second input variable produced only a marginal improvement in the goodness-of-fit of the globally fitted models (Table 2.2; Fig. 2.5B). Indeed, although $k_N k_D$-guidance once again emerged as the best of the two-input models, with a median RMS error of $\tilde{\epsilon} = 0.098$ m (Q1, Q3: 0.035, 0.140 m), it provided no statistically significant improvement in fit over single-input k_N-guidance in the globally-fitted analysis (Wilcoxon signed rank test: $z = -0.90$, $p = 0.37$). The results of the globally-fitted guidance models therefore confirm without ambiguity that single-input proportional navigation is the best supported of the six alternative steering controllers when fitting these to the last 1.0 s of each flight.

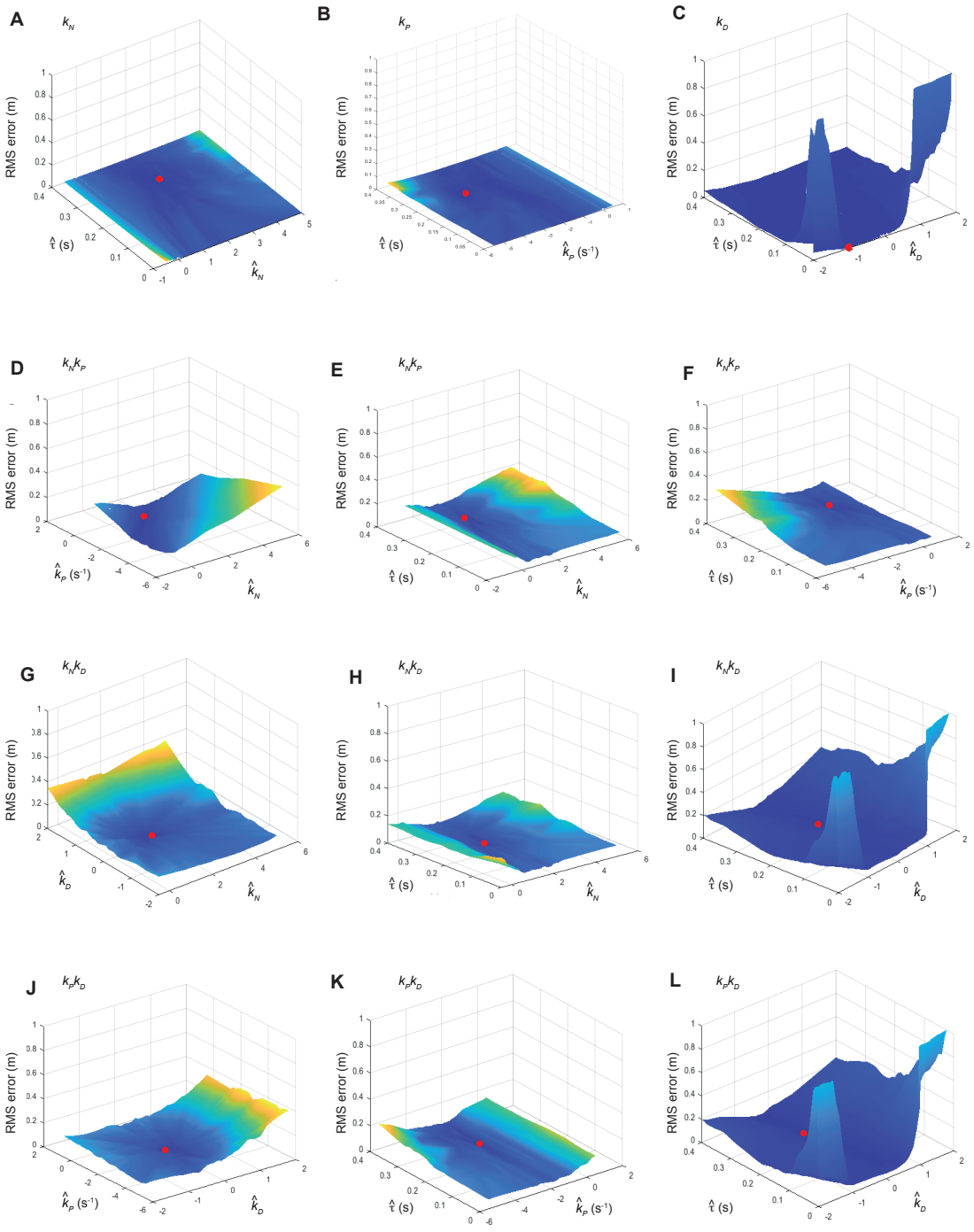


Figure 2.7: Optimization surfaces for steering controllers fitted globally for all flights. The height of each surface displays the median RMS error for the $n = 23$ flights through the unobstructed gap, as a function of the fitted guidance parameters. (A-C) Single-input guidance laws, plotting median RMS error against the relevant guidance constant (k_N, k_P, or k_D) and time delay τ. (D-L) Two-input guidance laws, plotting median RMS error against the relevant pair of guidance constants (k_N, k_P, and/or k_D), or their pairings with the time delay τ. Surface colour scaled according to surface height; red dot denotes location of global minimum (see Supplementary information 2.7.2 for values).

model	$\hat{k}_N$	$\hat{k}_P$	$\hat{k}_D$	$\hat{\tau}$ (s)	median RMS error (m)
k_N	2.05	-	-	0.27	0.108 (0.025, 0.146)
k_P	-	-1.90	-	0.19	0.127 (0.058, 0.181)
k_D	-	-	-1.00	0.01	0.208 (0.152, 0.277)
$k_N k_P$	1.50	-0.55	-	0.29	0.100 (0.035, 0.176)
$k_N k_D$	1.90	-	0.10	0.24	0.098 (0.033, 0.144)
$k_P k_D$	-	-1.90	-0.10	0.27	0.119 (0.063, 0.163)

Table 2.2: Parameter estimates for steering controllers fitted globally for all flights. Results shown for guidance models fitted to all $n = 23$ flights through the unobstructed gap. Median root mean square (RMS) error ($\tilde{\epsilon}$) stated with 1st and 3rd quartiles (Q1, Q3) displayed in parentheses. Results for the two-input controllers are stated subject to the constraint that neither guidance constant can be zero.

2.5.3 Extension of model fitting to entire measured trajectory

Having identified delayed proportional navigation targeting the midpoint of the gap as the best supported of the six candidate guidance laws over the last 1.0 s of each flight, we finally used the same model to simulate the entire measured length of the same $n = 23$ trajectories, from time $t = \tau$ to the end of the flight (Fig. 2.8). Because the values of the navigation constant k_N and time delay τ were inherited from the simulations that we had already fitted over the last 1.0 s of each flight (Fig. 2.6A,B), they are no longer expected to be strictly optimal, and would only be expected to result in a close fit to the data if the birds were engaged in consistent gap-oriented steering behaviour for the entire duration of the measured trajectory. This appears to be the case in general, because with only a few exceptions, the simulations still capture the curvature of the measured flight trajectories closely (Fig. 2.8), with a median RMS error of $\tilde{\epsilon} = 0.015$ m (Q1, Q3: 0.007, 0.072 m).

2.6 Discussion

Our analysis shows that the horizontal flight trajectories of pigeons steering towards vertical gaps are best modelled by the same proportional navigation guidance law that best models falcons attacking stationary or manoeuvring targets [122, 124]. There are several lines of evidence that support this conclusion. Firstly, proportional navigation (i.e. k_N-guidance) fitted the trajectory data more closely

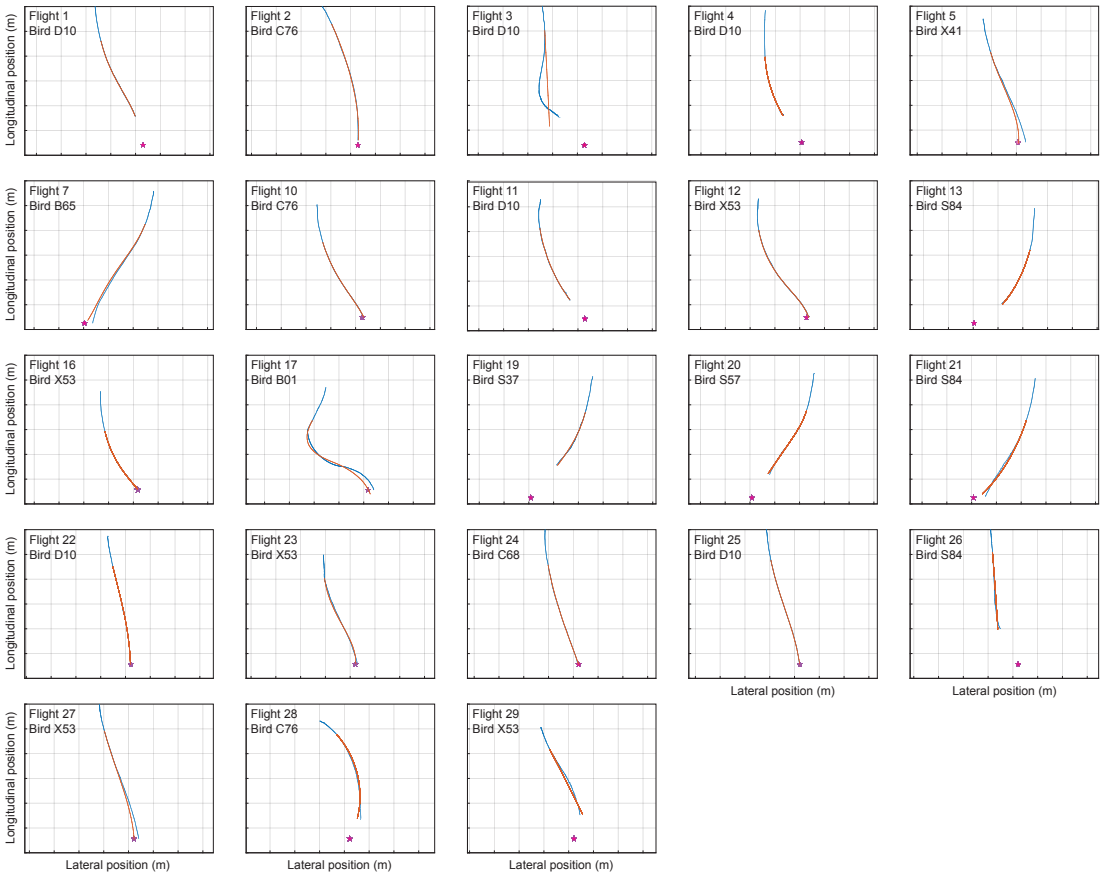


Figure 2.8: Simulations of gap-oriented steering in pigeons under proportional navigation guidance. Two-dimensional trajectory data (blue dotted lines) are shown for all $n = 23$ flights lasting ≥ 1 s, together with simulations under delayed k_N-guidance (orange line) inheriting the values of the navigation constant k_N and time delay τ from the simulations fitted independently to the last 1.0 s of each flight. Note that the simulations are plotted beginning from time $t = \tau$ after the start of the recorded trajectory, which is why some trajectories begin with a section of flight for which no simulation is shown.

than any other single-input steering controller that we tested in simulations fitting the guidance parameters independently to each flight, albeit not significantly so at $\alpha = 0.05$. Secondly, proportional navigation fitted the data significantly more closely than any other single-input guidance law that we tested in simulations fitting the guidance parameters globally for all flights. Thirdly, adding a second input to this proportional navigation controller (i.e. adding either a k_P or k_D guidance term) resulted in a marginal and non-significant improvement in fit when the parameters were fitted globally to all flights, and was associated with inconsistently-signed parameter estimates. Our results further show that the pigeons' steering behaviour is significantly better modelled by treating the target of its guidance as the midpoint

of the gap, rather than the point falling approximately half a wingspan from the nearside edge. This result holds on average across all of the guidance models that we fitted independently to each flight, and also holds for the proportional navigation controller in particular—albeit that the qualitatively better fit of the model treating the midpoint of the gap as the target of the bird's guidance is not quite significant in this specific case (Wilcoxon signed rank test: $z = -1.89$, $p = 0.059$).

Our results therefore support Lin *et al.*'s conclusion [105] that feeding back the rate of change of the deviation angle ($\dot{\delta}$) through derivative control (k_D) is unimportant to modelling gap steering behaviour in pigeons. However, they also show that this behaviour is better modelled by a proportional navigation (k_N) controller feeding back the line-of-sight rate ($\dot{\lambda}$) of the midpoint of the gap, than by a proportional pursuit (k_P) controller feeding back the deviation angle of the midpoint of the gap (δ) as Lin *et al.* originally proposed. This conclusion has implications for our assumptions regarding the underlying sensory mechanism. Specifically, whereas measurement of the deviation angle (δ) is expected to require knowledge of the retinal coordinates of the target and angular position of the head with respect to the body or its velocity, measurement of the line-of-sight rate ($\dot{\lambda}$) is expected to require knowledge of the retinal drift rate of the target and angular rate of the head in an inertial frame of reference. The sensory requirements of these two guidance laws are therefore quite different, although either could in principle be used to model the data satisfactorily. More importantly, our results confirm the possibility of uniting the study of target-oriented steering behaviours of all kinds under one common algorithmic framework. Specifically, we have now shown that the same proportional navigation guidance law that best models attack behaviours in falcons [122, 124] and some hawks [128] also provides the best model of gap-oriented steering behaviour in pigeons. This is consistent with our emerging hypothesis that target-oriented guidance behaviours of birds of all kinds share a common evolutionary origin deep in their phylogeny [123].

In fact, our numerical estimates of the navigation constant k_N in the proportional navigation simulations fitted independently to the obstacle avoidance flights of our

pigeons ($\tilde{k}_N = 2.6$; Q1, Q3: 1.9, 4.2) were quantitatively similar to those found previously in peregrine falcons attacking stationary targets ($\tilde{k}_N = 2.6$; Q1, Q3: 1.7, 3.3). This has several further implications, which we elaborate here utilising some classical results describing the behaviour of proportional navigation at different values of the navigation constant k_N [136]. The statistically significant result that $\tilde{k}_N > 0$ in the guidance models fitted independently to each flight (one-tailed sign test: $p < 0.001$) confirms that the pigeons engaged in target-oriented steering behaviour immediately before passing through the gap, because proportional navigation produces turning towards a stationary target at $k_N > 0$. Likewise, the statistically significant result that $\tilde{k}_N > 1$ in these simulations (one-tailed sign test: $p < 0.001$) confirms that the pigeons were not using any form of pure or deviated pursuit, which is the flight behaviour that proportional navigation describes at $k_N = 1$. More generally, proportional navigation produces a turn of ever-decreasing radius against a stationary target at $k_N < 2$, with a turn of constant radius produced at $k_N = 2$. Hence, the statistically significant result that $\tilde{k}_N > 2$ in the guidance models fitted independently to each flight (one-tailed sign test: $p = 0.047$) confirms that the pigeons usually made a turn of increasing radius as they approached the gap. This is an appropriate behaviour for flight aimed at a narrow gap, because it causes flight to straighten out as the bird passes through the gap, avoiding the need for manoeuvring when flying through the confines of the gap itself, and ensuring visibility of any obstacles beyond it. Proportional navigation at $k_N > 2$ may therefore be a better guidance law for negotiating a narrow gap than proportional pursuit, which produces a tightening turn. Indeed, the median value of $\tilde{k}_N = 2.6$ that we found is not significantly lower (sign test: $p = 0.11$) than the theoretical optimum of $k_N = 3$ that commands the most efficient turn towards a stationary target, in the sense of minimising the control effort measured by the time integral of the squared acceleration command.

It is interesting to note that the goblet-shaped spatial distribution of our pigeons' flight trajectories (Fig. 2.3) closely resembles the results of experiments from flies and locusts presented with a choice between two spatially distinct options [144].

In both these cases, the animal appears to adopt the average path between the options until some critical phase transition occurs, at which point the system decides spontaneously between them. Our pigeons likewise displayed a centered response initially, flying forwards from the point of release, before turning in the direction of one of the two gaps and then steering through it (Fig. 2.3). Theoretical modelling of this two-option spatial decision making process [144] associates the moment at which turning begins with the timing of the decision to turn towards one or other option, but the results of our guidance modelling suggest a more nuanced interpretation in the case of our pigeons. Specifically, because the line-of-sight rate of a stationary target will only be non-zero if the subject is moving, it follows that the subject must already be moving in order to generate a steering command under proportional navigation. In the presence of sensorimotor delay, this means that the animal may not begin turning at all until after it has begun moving. Hence, whereas proportional navigation can only produce monotonic turning towards a stationary target in the absence of delay, it can produce a sinuous turn in the presence of a delay. This is already sufficient to explain the sinuous nature of some of the measured trajectories plotted in Fig. 2.8. Nevertheless, as these trajectories do not begin from the moment of take-off, it remains possible that the pigeons did not make their targeting decision until after they had already begun flying forwards from the release point. This would be consistent with Lin et al's [105] argument that pigeons rely on short-range guidance, based on the observation that the pigeons in their study showed no evidence of steering toward gaps until 1.5 m (*c.* 0.33 s) before encountering vertical clutter. Any such delay in their decision making may also explain why the pigeons did not show any clear preference for flying through the unobstructed gap (Fig. 2.4). This is because the obstacle was placed between the release point and the gap (Fig. 2.2), so may not have obstructed either gap from the perspective of the subject at the point where its targeting decision was finally taken (Fig. 2.3).

The preceding account points to the importance of determining both the outcome and the timing of targeting decisions when modeling movement through complex

environments. In cluttered environments requiring multiple targeting decisions, the timing of every decision will be critical to determining the overall shape of the trajectory [105]. The general question of how a chain of spatial decisions structures trajectories through complex environments clearly merits further investigation, because the portion of a trajectory over which steering can occur under closed-loop guidance is obviously limited to the interval between the point at which a targeting decision is made and the point at which the animal reaches its target. Fast decision making is therefore critical when flying through clutter, and open-loop turning commands may be important to ensuring that flight is directed appropriately during the period of any delay between target acquisition and the onset of closed-loop guidance. One method of increasing the speed of decision making when choosing between similar alternatives is to introduce a bias in the decision making process. There is clear evidence of biased choice in our data, because at the population level our birds displayed a clear preference for selecting the right hand gap, whilst at the individual level most birds displayed their own idiosyncratic preference for choosing the right or left gap. This is consistent with individual biases observed in budgerigars choosing between two apertures of differing sizes [138]. We speculate that such biases may aid decision making when flying through clutter, which is a situation in which making and committing to a decision quickly may be at least as important as the decision that is made [105]. This hypothesised enhancement of speed and safety when flying through clutter has been shown to be advantageous for flocks of birds as well as individuals [138], but how might such biased choices arise? There is widespread evidence of handedness in animals [145], which has already been shown to accelerate homing over longer distances in swimming and flying animals [146]. Handedness can be of mechanical, sensory, or neural origin, but based on the information available here, we cannot distinguish whether the biased choice that we observed reflects the intrinsic handedness of different individuals, or an idiosyncratic response to extrinsic cues. For instance, as the preference to fly down the right hand side of the hall continued after the pigeons had passed through the gap, it is plausible that individual birds simply used their visual memory to

recapitulate the fine scale route that they had followed on their initial release, as has already been shown in large-scale homing behaviours [147].

Finally, the guidance framework that we have applied has implications for understanding the sensory information that animals use to structure their goal-directed behaviours. The steering behaviour that we observed in our pigeons was best explained by assuming that they targeted the midpoint of the gap (which would maximise the clearance on both sides), rather than the point half-a-wingspan in from the near edge (which would have minimised the nearside clearance with the wings spread). It is therefore reasonable to assume that this behaviour would not have required metric estimation of the physical width of the gap. On the other hand, as the midpoint of the gap represents a virtual target, it is an open question how its line-of-sight rate ($\dot{\lambda}$) would have been estimated by the birds. One possibility is that the birds could have centred the gap in their visual field, and estimated its line-of-sight rate from the angular rate of their head by integrating the angular accelerations sensed by their vestibular system. Another possibility is that they could have made use of the rotational optic flow cues produced by the head's self-motion relative to a fixed visual background. A gap-centering response of this kind would differ from the mechanism observed in birds avoiding single obstacles, which appear to fixate their gaze on the edge of the obstacle that they are aiming to avoid [148, 149]. This again raises the question of whether animals perceive clutter as a set of gaps to be aimed at, or a set of obstacles to stay clear of. Establishing a guidance model for gap-oriented steering behaviour in pigeons, as we have done here, reduces the problem to one of determining how and when they select which clearances to fly through.

2.6.1 Limitations

Although the number of individuals that we tested was twice that of other similar studies [105, 138], our sample size is small in absolute terms, and involves repeated measures from the same individuals that could not always be controlled for statistically. It follows that our results cannot necessarily be assumed to generalise

more broadly. The sections of flight that were fitted under the guidance models are also quite short, which is inevitable when modelling flight through clutter, but explains why the observed flight trajectories can often be modelled successfully by more than one guidance model. Hence, although proportional navigation was the best supported of the various guidance models that we tested in pigeons negotiating a single gap from a choice of two, it is plausible that a different result might emerge given a larger sample size, a longer flight duration, or a greater number of gaps. Future studies could usefully increase the total number of individuals tested, the distance between the release point and the gap, and the number of gaps, explicitly testing the role of handedness in the context of an experimental setup more like the forest of vertical obstacles employed by Lin *et al.* [105]. Finally, it is important to note that the experimenter who released the birds by hand could not be made blind to the experimental condition (Fig. 2.2). However, as there was no evidence of any effect of obstacle placement on gap choice, this is unlikely to have affected the experimental results. Other possible biases such as the handedness of the experimenter would have affected different birds similarly, so they are unlikely to explain their idiosyncratic preference for choosing the right or left gap.

Footnotes

Acknowledgements

We thank Lucy Larkman for her assistance with the bird experiments and animal husbandry. We thank Marco Klein-Heerenbrink and Sofia Minano-Gonzalez for their assistance with data processing.

Contributions

Conceptualization: N.P.-C., G.T.; Methodology: N.P.-C.; Investigation: N.P.-C.; Software: N.P.-C., G.T.; Data curation: N. P.-C.; Formal Analysis: N.P.-C., G.T.; Visualization: N.P.-C.; Writing - original draft: N.P.-C. Funding acquisition: N.P.-C., G.T.; Project administration: G.T.; Supervision: G.T.; Writing - review & editing: G.T.

Funding

This work was supported by the Biotechnology and Biological Sciences Research Council (BBSRC) grant (BB/M011224/1) to N.P.-C. This project has received funding from the European Research Council (ERC) under the European Union's Horizon 2020 research and innovation programme (Grant Agreement No. 682501) to G.T.

Data

Flight trajectory data and code is available on figshare at

https://doi.org/10.6084/m9.figshare.19285289.

2.7 Supplementary Information

Supplementary information 2.7.1 contains further information about the characteristics of recorded flights and pigeons used. Supplementary information 2.7.2 contains the results of simulations treating the midpoint of the gap as the target of the bird's guidance. Supplementary information 2.7.3 contains the results of simulations treating the point 0.35 m from the edge of the curtain as the target of the bird's guidance.

2.7.1 Characteristics of animals used during data collection and recorded flights

Name	Ring number	Colour	Year	Weight (g)
B65	B46865	BB Pied	2012	493
C68	C07768	Black	2018	530
C76	C07776	White/ Red	2018	500
D10	D44810	BB	2010	501
S37	S18837	Red	2017	586
S57	S19557	BB	2016	502
S84	S21284	BB Pied	2014	510
X41	X44941	Black, White knees	2015	563
X53	X44953	White Blk Tip	2015	543
B01	B46901	B DK CH	2012	508
S28	S21328	B CH	2014	502
C67	C07767	BB	2018	478

Table 2.3: Birds used for experiments.

Table 2.4: Obstacle positions and gap choices of all recorded flights.

Date	**Bird**	**Side flown**	**Obstacle position**	**Release number**	**Flight duration**
11.12.2018	B01	right	right	AM1	2.095
11.12.2018	B01	right	left	AM2	1.89
11.12.2018	B01	right	left	AM3	not analysed
11.12.2018	B65	right	right	AM1	3.65
11.12.2018	B65	right	left	AM2	1.45
11.12.2018	B65	left	left	AM3	1
11.12.2018	C67	left	right	AM1	not analysed
11.12.2018	C68	left	right	AM1	0.695
11.12.2018	D10	left	right	AM1	1.13

Table 2.4 – continued from previous page

Date	Bird	Side flown	Obstacle position	Release number	Flight duration (s)
11.12.2018	D10	left	left	AM2	4.525
11.12.2018	D10	left	left	AM3	12.405
11.12.2018	S37	right	right	AM1	2.73
11.12.2018	S57	right	right	AM1	1.43
11.12.2018	S57	right	left	AM2	0.935
11.12.2018	S84	right	right	AM1	5.055
11.12.2018	S84	left	left	AM3	not analysed
11.12.2018	X41	right	right	AM1	1.525
11.12.2018	X41	right	left	AM3	1
11.12.2018	X53	left	right	AM1	1.39
11.12.2018	X53	left	left	AM2	3.76
11.12.2018	X53	right	left	AM3	1.03
12.12.2018	B01	right	right	AM1	2.585
12.12.2018	B01	right	right	AM2	2.77
12.12.2018	B01	right	left	AM3	not analysed
12.12.2018	B65	right	right	AM1	3.23
12.12.2018	B65	right	left	AM3	0.78
12.12.2018	C68	right	right	AM1	3.23
12.12.2018	C76	left	right	AM1	1.43
12.12.2018	C76	right	left	AM3	1.315
12.12.2018	D10	left	right	AM1	1.36
12.12.2018	D10	left	right	AM2	not analysed
12.12.2018	D10	left	left	AM3	1.855
12.12.2018	S37	left	right	AM1	1.33
12.12.2018	S37	right	left	AM3	1.72
12.12.2018	S57	right	right	AM1	3.335
12.12.2018	S57	right	right	AM2	2.015
12.12.2018	S57	right	left	AM3	1.04
12.12.2018	S84	left	right	AM1	0.92
12.12.2018	S84	right	right	AM2	2.095
12.12.2018	S84	right	left	AM3	1.14
12.12.2018	X41	right	right	AM1	1.585
12.12.2018	X41	right	right	AM2	not analysed
12.12.2018	X41	right	left	AM3	not analysed
12.12.2018	X53	left	right	AM1	1.03
12.12.2018	X53	right	right	AM2	3.51
12.12.2018	X53	right	left	AM3	6.355
13.12.2018	B01	right	right	AM1	2.495
13.12.2018	B01	left	right	AM2	2.615
13.12.2018	B01	right	left	AM3	0.56

Table 2.4 – continued from previous page

Date	Bird	Side flown	Obstacle position	Release number	Flight duration (s)
13.12.2018	B01	right	left	AM4	0.505
13.12.2018	B65	right	right	AM1	6.615
13.12.2018	B65	right	right	AM2	3.485
13.12.2018	B65	right	left	AM3	0.64
13.12.2018	B65	right	left	AM4	0.555
13.12.2018	C68	left	right	AM1	1.045
13.12.2018	C76	right	right	AM1	2.19
13.12.2018	C76	right	right	AM2	2.265
13.12.2018	C76	right	left	AM3	0.495
13.12.2018	C76	right	left	AM4	0.54
13.12.2018	D10	left	right	AM1	0.83
13.12.2018	D10	left	right	AM2	1.135
13.12.2018	D10	left	left	AM3	6.375
13.12.2018	S28	right	right	AM2	not analysed
13.12.2018	S37	right	right	AM1	2.745
13.12.2018	S37	right	left	AM4	1.34
13.12.2018	S57	right	right	AM1	2.995
13.12.2018	S57	right	left	AM4	1.14
13.12.2018	S84	right	right	AM1	15.905
13.12.2018	S84	right	right	AM2	3.655
13.12.2018	S84	right	left	AM4	1.105
13.12.2018	X41	right	right	AM1	1.61
13.12.2018	X41	right	right	AM2	3.955
13.12.2018	X41	right	left	AM3	1.26
13.12.2018	X53	left	right	AM1	1.28
13.12.2018	X53	left	right	AM2	1.07
13.12.2018	X53	left	left	AM3	2.185
13.12.2018	X53	left	left	AM4	5.16
14.12.2018	B01	right	right	AM1	1.97
14.12.2018	B01	right	right	AM2	4.12
14.12.2018	B01	right	left	AM3	not analysed
14.12.2018	B65	right	right	AM1	5.935
14.12.2018	B65	right	right	AM2	3.485
14.12.2018	B65	right	left	AM3	0.92
14.12.2018	C68	left	right	AM2	1.315
14.12.2018	C76	right	right	AM1	3.83
14.12.2018	C76	left	left	AM3	8.62
14.12.2018	D10	left	right	AM1	1.185
14.12.2018	D10	left	right	AM2	1.355
14.12.2018	D10	right	left	AM3	1.285

Table 2.4 – continued from previous page

Date	Bird	Side flown	Obstacle position	Release number	Flight duration (s)
14.12.2018	S57	right	left	AM3	1.085
14.12.2018	S84	right	right	AM1	2.91
14.12.2018	S84	left	right	AM2	1.17
14.12.2018	X41	right	right	AM1	2.575
14.12.2018	X53	left	right	AM1	1.395
14.12.2018	X53	left	right	AM2	1.54
14.12.2018	X53	right	left	AM3	1.365
30.11.2018	X53	left	right	AM1	not analysed
4.12.2018	B01	right	right	AM2	3.28
4.12.2018	B65	right	right	AM2	3.26
4.12.2018	C76	left	right	AM1	1.41
4.12.2018	D10	left	right	AM1	2.045
4.12.2018	D10	left	right	AM2	1.445
4.12.2018	S37	left	right	AM1	1.21
4.12.2018	S57	right	right	AM2	4.595
4.12.2018	S84	right	right	AM2	2.59

Date	Bird ID	Flight ID	Duration (s)	Distance (m)
4.12.2018	D10	1	1.45	4.76
4.12.2018	C76	2	1.41	6.10
4.12.2018	D10	3	2.05	5.16
11.12.2018	D10	4	1.13	4.37
11.12.2018	X41	5	1.32	5.36
11.12.2018	B65	7	1.42	5.86
12.12.2018	C76	10	1.38	5.13
12.12.2018	D10	11	1.36	4.34
12.12.2018	X53	12	1.63	5.49
12.12.2018	S84	13	1.14	4.17
13.12.2018	X53	16	1.12	4.38
13.12.2018	B01	17	2.47	5.77
13.12.2018	S37	19	1.34	3.91
13.12.2018	S57	20	1.14	4.53
13.12.2018	S84	21	1.11	5.22
14.12.2018	D10	22	1.13	5.28
14.12.2018	X53	23	1.31	4.70
14.12.2018	C68	24	1.23	5.65
14.12.2018	D10	25	1.30	5.65
14.12.2018	S84	26	1.17	4.14
14.12.2018	X53	27	1.43	5.66
14.12.2018	C76	28	1.30	5.32
14.12.2018	X53	29	1.40	4.87
Median			1.32	5.16
Q1			1.16	4.45
Q3			1.41	5.57
Flights shorter than 1 second, and therefore not modelled				
11.12.2018	B01	6	0.58	1.58
11.12.2018	S57	8	0.94	4.31
11.12.2018	X53	9	0.95	4.52
12.12.2018	C68	14	0.94	4.17
13.12.2018	D10	15	0.83	3.34
13.12.2018	X53	18	0.97	4.30

Table 2.5: Flight characteristics of the $n = 29$ recorded flights where the bird flew through the unobstructed side of the curtain.

2.7.2 Results of simulations treating the midpoint of the gap as the target of the bird's guidance.

Flight	k_N **simulation**			k_P **simulation**			k_D **simulation**		
	k_N	tau	RMS (m)	k_P	tau	RMS (m)	k_D	tau	RMS (m)
1	5.60	0.40	0.03	-13004.28	0.00	0.15	1.07	0.40	0.04
2	1.38	0.07	0.01	-1.59	0.00	0.03	0.82	0.40	0.06
3	-0.01	0.00	0.26	-0.02	0.35	0.26	0.05	0.10	0.26
4	3.12	0.21	0.01	-3.55	0.25	0.01	2.78	0.40	0.03
5	-1.28	0.22	0.11	1.48	0.17	0.09	0.39	0.28	0.06
7	4.03	0.28	0.01	-12897.61	0.00	0.06	0.51	0.40	0.07
10	3.01	0.40	0.01	-2.61	0.40	0.01	0.82	0.27	0.03
11	2.34	0.40	0.01	-1.43	0.40	0.03	0.97	0.35	0.01
12	3.38	0.40	0.02	-2.36	0.40	0.03	-1.00	0.00	0.52
13	1.48	0.13	0.00	-1.56	0.40	0.01	-1.18	0.02	0.14
16	2.98	0.36	0.01	-3.31	0.40	0.02	1.57	0.34	0.02
17	2.91	0.40	0.21	-2.27	0.40	0.15	-1.61	0.34	1.26
19	2.41	0.40	0.02	-1.92	0.40	0.02	1.74	0.31	0.01
20	4.71	0.23	0.00	-4.23	0.23	0.01	3.17	0.38	0.10
21	2.96	0.00	0.03	-3.76	0.10	0.02	2.44	0.36	0.05
22	2.54	0.40	0.01	-2.86	0.40	0.01	-0.36	0.00	0.01
23	6.35	0.36	0.04	-4.28	0.32	0.02	-1.00	0.00	0.36
24	3.17	0.40	0.02	-2.06	0.40	0.02	0.56	0.40	0.01
25	6.94	0.40	0.05	-137.99	0.00	0.16	0.64	0.18	0.05
26	-0.45	0.40	0.03	0.29	0.40	0.03	0.13	0.06	0.03
27	-1.26	0.18	0.09	1.27	0.08	0.07	0.24	0.40	0.04
28	1.88	0.16	0.11	-1.64	0.28	0.01	-1.00	0.00	0.54
29	1.00	0.40	0.07	-0.84	0.40	0.09	-0.35	0.00	0.07
median	2.91	0.36	0.02	-2.27	0.35	0.03	0.51	0.31	0.05
Q1	1.43	0.19	0.01	-3.65	0.13	0.02	-0.36	0.04	0.03
Q3	3.27	0.40	0.07	-1.50	0.40	0.08	1.02	0.39	0.13

Table 2.6: Individually fitted one-parameter simulations with the target as the middle of the gap.

Flight	$k_N k_P$ **simulation**				$k_N k_D$ **simulation**				$k_P k_D$ **simulation**			
	k_N	k_P	tau	RMS (m)	k_N	k_D	tau	RMS (m)	k_P	k_D	tau	RMS (m)
1	1482.21	-1757.80	0.00	0.15	13.62	-1.42	0.24	0.12	-10.20	-1.57	0.25	0.13
2	2.28	0.47	0.27	0.01	2.38	-0.29	0.40	0.01	-2.54	-1.18	0.37	0.00
3	23.22	16.65	0.40	0.05	1.00	1.00	0.00	0.04	-0.83	0.99	0.01	0.05
4	-2.72	-5.93	0.40	0.01	1.00	1.00	0.00	0.01	-1.37	0.99	0.01	0.01
5	1.22	3.28	0.00	0.03	1.49	0.73	0.26	0.01	-3.05	0.91	0.31	0.01
7	3.81	-0.17	0.28	0.01	4.54	-0.30	0.35	0.01	-3.97	-0.60	0.39	0.01
10	3.84	0.73	0.40	0.00	2.94	0.03	0.40	0.00	-2.39	0.11	0.40	0.01
11	4.83	1.81	0.26	0.01	1.13	0.96	0.03	0.01	-0.98	0.49	0.38	0.01
12	2.73	-0.46	0.40	0.01	3.28	0.04	0.40	0.01	-2.19	0.26	0.33	0.02
13	2.29	1.00	0.21	0.00	1.65	-0.25	0.21	0.00	-2.86	-1.25	0.07	0.00
16	5.88	3.67	0.30	0.00	2.15	0.81	0.17	0.00	-3.54	0.71	0.16	0.01
17	-4.45	-5.74	0.32	0.12	2.97	0.18	0.40	0.17	-1.83	0.57	0.19	0.14
19	-45.84	-39.03	0.31	0.00	0.94	1.05	0.03	0.01	-0.57	1.41	0.23	0.01
20	6.41	1.51	0.23	0.00	1.00	1.00	0.00	0.00	-4.39	-0.70	0.36	0.00
21	-5.02	-7.15	0.40	0.01	4.73	-2.62	0.40	0.01	-2.31	0.81	0.02	0.01
22	2.22	-0.42	0.40	0.00	2.91	0.30	0.36	0.00	-3.89	0.61	0.33	0.00
23	330.37	-391.56	0.00	0.19	221.86	1.00	0.00	0.19	-4.27	0.00	0.32	0.02
24	210.51	-249.61	0.00	0.10	0.73	0.43	0.40	0.01	0.00	0.56	0.40	0.01
25	271.77	-322.37	0.00	0.16	1.99	0.77	0.19	0.00	-3.82	0.07	0.40	0.00
26	8.90	6.35	0.32	0.00	1.84	1.19	0.08	0.00	-2.25	1.37	0.07	0.00
27	-3.55	-5.02	0.40	0.02	1.35	0.56	0.28	0.00	-1.88	0.54	0.28	0.01
28	0.17	-1.49	0.30	0.00	0.99	0.99	0.02	0.00	-1.31	0.18	0.40	0.00
29	4.41	3.18	0.39	0.04	0.97	0.88	0.01	0.02	-2.11	0.94	0.13	0.01
Median	3.81	-0.42	0.30	0.01	1.84	0.73	0.21	0.01	-2.31	0.54	0.31	0.01
Q1	0.70	-6.54	0.22	0.00	1.00	0.04	0.02	0.00	-3.68	0.04	0.15	0.00
Q3	7.66	1.66	0.40	0.04	2.95	0.99	0.38	0.01	-1.60	0.86	0.38	0.01

Table 2.7: Individually fitted two-parameter simulations with the target as the middle of the gap.

Flight	k_N **simulation**			k_P **simulation**			k_D **simulation**		
	k_N	tau	RMS (m)	k_P	tau	RMS (m)	k_D	tau	RMS (m)
1	2.90	0.40	0.14	-1.70	0.40	0.15	0.60	0.24	0.21
2	2.90	0.40	0.19	-1.70	0.40	0.20	0.60	0.24	0.21
3	2.90	0.40	0.51	-1.70	0.40	0.47	0.60	0.24	0.39
4	2.90	0.40	0.03	-1.70	0.40	0.14	0.60	0.24	0.33
5	2.90	0.40	0.32	-1.70	0.40	0.26	0.60	0.24	0.14
7	2.90	0.40	0.07	-1.70	0.40	0.06	0.60	0.24	0.09
10	2.90	0.40	0.01	-1.70	0.40	0.13	0.60	0.24	0.18
11	2.90	0.40	0.08	-1.70	0.40	0.07	0.60	0.24	0.08
12	2.90	0.40	0.07	-1.70	0.40	0.18	0.60	0.24	0.52
13	2.90	0.40	0.20	-1.70	0.40	0.02	0.60	0.24	0.24
16	2.90	0.40	0.01	-1.70	0.40	0.17	0.60	0.24	0.30
17	2.90	0.40	0.21	-1.70	0.40	0.36	0.60	0.24	3.18
19	2.90	0.40	0.05	-1.70	0.40	0.03	0.60	0.24	0.20
20	2.90	0.40	0.08	-1.70	0.40	0.15	0.60	0.24	0.33
21	2.90	0.40	0.09	-1.70	0.40	0.09	0.60	0.24	0.31
22	2.90	0.40	0.01	-1.70	0.40	0.03	0.60	0.24	0.17
23	2.90	0.40	0.21	-1.70	0.40	0.23	0.60	0.24	0.50
24	2.90	0.40	0.02	-1.70	0.40	0.04	0.60	0.24	0.03
25	2.90	0.40	0.11	-1.70	0.40	0.10	0.60	0.24	0.07
26	2.90	0.40	0.09	-1.70	0.40	0.11	0.60	0.24	0.04
27	2.90	0.40	0.19	-1.70	0.40	0.12	0.60	0.24	0.18
28	2.90	0.40	0.12	-1.70	0.40	0.17	0.60	0.24	1.10
29	2.90	0.40	0.27	-1.70	0.40	0.16	0.60	0.24	0.62
Median			0.093			0.140			0.210
Q1			0.051			0.076			0.148
Q3			0.201			0.180			0.377

Table 2.8: Globally fitted simulations of one-parameter models with the target as the middle of the gap.

Flight	$k_N k_P$ **simulation**				$k_N k_D$ **simulation**				$k_P k_D$ **simulation**			
	k_N	k_P	tau	RMS (m)	k_N	k_D	tau	RMS (m)	k_P	k_D	tau	RMS (m)
1	3.80	1.10	0.40	0.18	1.80	0.60	0.24	0.09	-1.90	0.50	0.15	0.14
2	3.80	1.10	0.40	0.04	1.80	0.60	0.24	0.30	-1.90	0.50	0.15	0.25
3	3.80	1.10	0.40	0.43	1.80	0.60	0.24	0.39	-1.90	0.50	0.15	0.56
4	3.80	1.10	0.40	0.05	1.80	0.60	0.24	0.10	-1.90	0.50	0.15	0.12
5	3.80	1.10	0.40	0.31	1.80	0.60	0.24	0.17	-1.90	0.50	0.15	0.31
7	3.80	1.10	0.40	0.09	1.80	0.60	0.24	0.15	-1.90	0.50	0.15	0.06
10	3.80	1.10	0.40	0.05	1.80	0.60	0.24	0.05	-1.90	0.50	0.15	0.13
11	3.80	1.10	0.40	0.05	1.80	0.60	0.24	0.24	-1.90	0.50	0.15	0.11
12	3.80	1.10	0.40	0.17	1.80	0.60	0.24	0.05	-1.90	0.50	0.15	0.10
13	3.80	1.10	0.40	0.17	1.80	0.60	0.24	0.15	-1.90	0.50	0.15	0.13
16	3.80	1.10	0.40	0.02	1.80	0.60	0.24	0.04	-1.90	0.50	0.15	0.18
17	3.80	1.10	0.40	0.36	1.80	0.60	0.24	0.59	-1.90	0.50	0.15	0.20
19	3.80	1.10	0.40	0.02	1.80	0.60	0.24	0.03	-1.90	0.50	0.15	0.03
20	3.80	1.10	0.40	0.12	1.80	0.60	0.24	0.12	-1.90	0.50	0.15	0.08
21	3.80	1.10	0.40	0.07	1.80	0.60	0.24	0.07	-1.90	0.50	0.15	0.07
22	3.80	1.10	0.40	0.01	1.80	0.60	0.24	0.01	-1.90	0.50	0.15	0.02
23	3.80	1.10	0.40	0.28	1.80	0.60	0.24	0.23	-1.90	0.50	0.15	0.11
24	3.80	1.10	0.40	0.07	1.80	0.60	0.24	0.06	-1.90	0.50	0.15	0.06
25	3.80	1.10	0.40	0.13	1.80	0.60	0.24	0.04	-1.90	0.50	0.15	0.08
26	3.80	1.10	0.40	0.06	1.80	0.60	0.24	0.07	-1.90	0.50	0.15	0.12
27	3.80	1.10	0.40	0.21	1.80	0.60	0.24	0.06	-1.90	0.50	0.15	0.18
28	3.80	1.10	0.40	0.40	1.80	0.60	0.24	0.11	-1.90	0.50	0.15	0.31
29	3.80	1.10	0.40	0.22	1.80	0.60	0.24	0.05	-1.90	0.50	0.15	0.20
Median				0.116				0.088				0.118
Q1				0.049				0.051				0.082
Q3				0.218				0.167				0.191

Table 2.9: Globally fitted simulations of two-parameter models with the target as the middle of the gap.

2.7.3 Results of simulations treating the point 0.35 m from the edge of the curtain as the target of the bird's guidance.

Flight	k_N simulation			k_P simulation			k_D simulation		
	k_N	tau	RMS (m)	k_P	tau	RMS (m)	k_D	tau	RMS (m)
1	4.13	0.38	0.01	-307.52	0.01	0.07	1.16	0.40	0.04
2	1.59	0.00	0.01	-2.08	0.00	0.04	0.79	0.40	0.06
3	-0.01	0.00	0.26	-0.01	0.35	0.26	-1.44	0.40	0.21
4	2.28	0.00	0.01	-2.73	0.08	0.01	-7.70	0.33	0.10
5	5.75	0.40	0.10	-5.41	0.40	0.04	0.49	0.27	0.05
7	4.86	0.19	0.06	-2.93	0.13	0.06	0.72	0.22	0.07
10	2.65	0.25	0.01	-2.15	0.37	0.01	0.94	0.27	0.02
11	2.12	0.12	0.01	-2.40	0.00	0.02	1.04	0.35	0.01
12	2.93	0.30	0.01	-2.06	0.39	0.02	-1.00	0.00	0.48
13	1.42	0.13	0.00	-1.41	0.40	0.01	-1.18	0.02	0.14
16	2.17	0.15	0.01	-2.53	0.40	0.01	2.06	0.35	0.02
17	2.95	0.40	0.11	-2.15	0.38	0.09	-1.72	0.33	1.24
19	2.03	0.40	0.02	-1.53	0.40	0.02	2.03	0.31	0.01
20	4.86	0.11	0.01	-4.23	0.12	0.02	3.88	0.38	0.10
21	1.81	0.28	0.05	-2.13	0.23	0.03	3.19	0.37	0.05
22	4.30	0.33	0.00	-4.65	0.30	0.01	-1.00	0.00	0.02
23	4.91	0.26	0.03	-3.61	0.23	0.01	-1.00	0.00	0.32
24	2.84	0.07	0.01	-3.79	0.07	0.01	0.66	0.36	0.01
25	4.43	0.26	0.00	-614.29	0.00	0.04	0.84	0.20	0.04
26	-0.16	0.18	0.03	0.19	0.40	0.03	-0.85	0.37	0.01
27	4.15	0.40	0.07	-2.30	0.40	0.01	0.26	0.40	0.03
28	2.00	0.00	0.04	-1.78	0.28	0.01	1.51	0.37	0.03
29	0.19	0.40	0.06	0.01	0.04	0.06	-0.02	0.00	0.06
Median	2.645	0.250	0.015	-2.303	0.280	0.018	0.660	0.330	0.045
Q1	1.902	0.110	0.007	-3.702	0.073	0.011	-1.001	0.210	0.019
Q2	4.225	0.353	0.058	-1.921	0.393	0.042	1.100	0.370	0.102

Table 2.10: Individually fitted simulations of one-parameter models with the target one wing-length (0.35 m) from the curtain edge.

Flight	$k_N k_P$ **simulation**				$k_N k_D$ **simulation**				$k_P k_D$ **simulation**			
	k_N	k_P	tau	RMS (m)	k_N	k_D	tau	RMS (m)	k_P	k_D	tau	RMS (m)
1	352.36	-417.73	0.00	0.07	2.92	0.50	0.25	0.00	-2.58	0.27	0.31	0.00
2	3.03	0.84	0.28	0.01	2.94	-0.41	0.40	0.01	-3.37	-1.41	0.36	0.01
3	-51.58	-42.21	0.00	0.05	1.00	1.00	0.00	0.04	-0.80	0.98	0.00	0.05
4	-2.27	-5.16	0.21	0.01	3.58	-1.18	0.03	0.01	-4.78	-1.14	0.02	0.01
5	-3.85	-7.96	0.40	0.01	2.03	0.59	0.27	0.01	-3.47	0.46	0.31	0.01
7	-11.35	-12.72	0.14	0.02	6.48	-1.24	0.37	0.02	0.77	1.06	0.05	0.02
10	3.92	1.36	0.24	0.00	1.08	0.96	0.02	0.00	-2.60	0.50	0.13	0.01
11	3.08	1.01	0.00	0.01	3.74	-1.06	0.12	0.01	-3.25	-0.90	0.30	0.01
12	2.54	-0.31	0.31	0.01	1.04	0.98	0.01	0.00	-2.06	0.13	0.32	0.02
13	2.24	0.93	0.21	0.00	1.58	-0.25	0.21	0.00	-2.42	-1.22	0.07	0.00
16	5.72	6.20	0.07	0.00	3.11	-1.08	0.25	0.00	-2.79	0.51	0.15	0.01
17	-1.71	-3.40	0.34	0.09	2.96	0.08	0.40	0.10	-2.15	0.00	0.38	0.09
19	-28.03	-22.84	0.34	0.00	0.94	1.07	0.03	0.01	-0.63	1.42	0.23	0.01
20	18.87	12.76	0.12	0.00	4.87	-1.31	0.37	0.00	-3.75	-1.04	0.36	0.00
21	-1.50	-5.68	0.00	0.01	-0.66	2.35	0.21	0.01	-2.03	0.73	0.02	0.01
22	6.65	2.03	0.35	0.00	2.41	0.73	0.14	0.00	-6.97	-0.21	0.40	0.00
23	0.14	-3.53	0.23	0.01	5.38	-0.43	0.34	0.02	-3.64	-0.01	0.23	0.01
24	5.26	3.06	0.08	0.00	4.41	-0.81	0.13	0.00	-2.81	0.61	0.04	0.00
25	5.21	0.63	0.27	0.00	1.85	0.83	0.07	0.00	-3.54	-0.45	0.36	0.01
26	5.23	5.30	0.11	0.00	1.68	1.21	0.08	0.00	-0.51	-0.55	0.40	0.01
27	-0.33	-2.39	0.40	0.01	1.84	0.47	0.28	0.00	-23.47	0.98	0.01	0.14
28	0.51	-1.29	0.40	0.00	0.98	1.00	0.02	0.00	-1.38	0.45	0.27	0.00
29	3.86	5.00	0.00	0.02	1.03	0.92	0.01	0.01	-2.19	0.84	0.13	0.00
Median	0.045	-0.315	0.210	0.006	2.032	0.496	0.135	0.005	-2.602	0.272	0.225	0.008
Q1	0.019	-5.417	0.075	0.004	1.061	-0.623	0.030	0.003	-3.503	-0.500	0.058	0.005
Q2	0.102	1.695	0.320	0.010	3.342	0.971	0.270	0.008	-2.045	0.670	0.338	0.012

Table 2.11: Individually fitted simulations of two-parameter models with the target one wing-length (0.35 m) from the curtain edge.

Flight	k_N **simulation**			k_P **simulation**			k_D **simulation**		
	k_N	tau	RMS (m)	k_P	tau	RMS (m)	k_D	tau	RMS (m)
1	2.90	0.40	0.15	-1.70	0.40	0.15	0.60	0.24	0.27
2	2.90	0.40	0.03	-1.70	0.40	0.06	0.60	0.24	0.20
3	2.90	0.40	0.52	-1.70	0.40	0.57	0.60	0.24	0.32
4	2.90	0.40	0.03	-1.70	0.40	0.06	0.60	0.24	0.21
5	2.90	0.40	0.18	-1.70	0.40	0.19	0.60	0.24	0.21
7	2.90	0.40	0.09	-1.70	0.40	0.07	0.60	0.24	0.22
10	2.90	0.40	0.05	-1.70	0.40	0.13	0.60	0.24	0.24
11	2.90	0.40	0.01	-1.70	0.40	0.03	0.60	0.24	0.23
12	2.90	0.40	0.14	-1.70	0.40	0.19	0.60	0.24	0.49
13	2.90	0.40	0.11	-1.70	0.40	0.06	0.60	0.24	0.14
16	2.90	0.40	0.02	-1.70	0.40	0.13	0.60	0.24	0.19
17	2.90	0.40	0.49	-1.70	0.40	0.28	0.60	0.24	1.90
19	2.90	0.40	0.02	-1.70	0.40	0.03	0.60	0.24	0.16
20	2.90	0.40	0.12	-1.70	0.40	0.12	0.60	0.24	0.28
21	2.90	0.40	0.07	-1.70	0.40	0.06	0.60	0.24	0.18
22	2.90	0.40	0.02	-1.70	0.40	0.03	0.60	0.24	0.02
23	2.90	0.40	0.20	-1.70	0.40	0.17	0.60	0.24	0.34
24	2.90	0.40	0.02	-1.70	0.40	0.05	0.60	0.24	0.12
25	2.90	0.40	0.07	-1.70	0.40	0.07	0.60	0.24	0.13
26	2.90	0.40	0.12	-1.70	0.40	0.15	0.60	0.24	0.07
27	2.90	0.40	0.13	-1.70	0.40	0.14	0.60	0.24	0.15
28	2.90	0.40	0.13	-1.70	0.40	1.17	0.60	0.24	0.68
29	2.90	0.40	0.91	-1.70	0.40	1.51	0.60	0.24	0.23
Median			0.108			0.127			0.208
Q1			0.026			0.058			0.172
Q2			0.147			0.181			0.277

Table 2.12: Globally fitted simulations of one-parameter models with the target one wing-length (0.35 m) from the curtain edge.

Flight	$k_N k_P$ **simulation**				$k_N k_D$ **simulation**				$k_P k_D$ **simulation**			
	k_N	k_P	tau	RMS (m)	k_N	k_D	tau	RMS (m)	k_P	k_D	tau	RMS (m)
1	3.80	1.10	0.40	0.17	1.80	0.60	0.24	0.15	-1.90	0.50	0.15	0.14
2	3.80	1.10	0.40	0.04	1.80	0.60	0.24	0.04	-1.90	0.50	0.15	0.07
3	3.80	1.10	0.40	0.56	1.80	0.60	0.24	0.50	-1.90	0.50	0.15	0.57
4	3.80	1.10	0.40	0.02	1.80	0.60	0.24	0.03	-1.90	0.50	0.15	0.06
5	3.80	1.10	0.40	0.21	1.80	0.60	0.24	0.18	-1.90	0.50	0.15	0.19
7	3.80	1.10	0.40	0.10	1.80	0.60	0.24	0.08	-1.90	0.50	0.15	0.07
10	3.80	1.10	0.40	0.09	1.80	0.60	0.24	0.05	-1.90	0.50	0.15	0.12
11	3.80	1.10	0.40	0.01	1.80	0.60	0.24	0.02	-1.90	0.50	0.15	0.03
12	3.80	1.10	0.40	0.17	1.80	0.60	0.24	0.13	-1.90	0.50	0.15	0.16
13	3.80	1.10	0.40	0.06	1.80	0.60	0.24	0.10	-1.90	0.50	0.15	0.07
16	3.80	1.10	0.40	0.03	1.80	0.60	0.24	0.02	-1.90	0.50	0.15	0.13
17	3.80	1.10	0.40	0.51	1.80	0.60	0.24	0.57	-1.90	0.50	0.15	0.26
19	3.80	1.10	0.40	0.03	1.80	0.60	0.24	0.02	-1.90	0.50	0.15	0.03
20	3.80	1.10	0.40	0.13	1.80	0.60	0.24	0.13	-1.90	0.50	0.15	0.11
21	3.80	1.10	0.40	0.07	1.80	0.60	0.24	0.06	-1.90	0.50	0.15	0.05
22	3.80	1.10	0.40	0.03	1.80	0.60	0.24	0.02	-1.90	0.50	0.15	0.03
23	3.80	1.10	0.40	0.18	1.80	0.60	0.24	0.20	-1.90	0.50	0.15	0.16
24	3.80	1.10	0.40	0.03	1.80	0.60	0.24	0.02	-1.90	0.50	0.15	0.05
25	3.80	1.10	0.40	0.08	1.80	0.60	0.24	0.06	-1.90	0.50	0.15	0.07
26	3.80	1.10	0.40	0.15	1.80	0.60	0.24	0.12	-1.90	0.50	0.15	0.15
27	3.80	1.10	0.40	0.15	1.80	0.60	0.24	0.12	-1.90	0.50	0.15	0.13
28	3.80	1.10	0.40	0.62	1.80	0.60	0.24	0.12	-1.90	0.50	0.15	1.22
29	3.80	1.10	0.40	1.23	1.80	0.60	0.24	0.85	-1.90	0.50	0.15	1.53
Median				0.006				0.005				0.008
Q1				0.004				0.003				0.005
Q2				0.010				0.008				0.012

Table 2.13: Globally fitted simulations of two-parameter models with the target one wing-length (0.35 m) from the curtain edge.

References

[39] Michael P. Jones, Kenneth E. Pierce, and Daniel Ward. "Avian Vision: A Review of Form and Function with Special Consideration to Birds of Prey". In: *Journal of Exotic Pet Medicine* 16.2 (Apr. 2007), pp. 69–87. (Visited on 05/04/2022).

[105] Huai-Ti Lin, Ivo G. Ros, and Andrew A. Biewener. "Through the Eyes of a Bird: Modelling Visually Guided Obstacle Flight". In: *Journal of The Royal Society Interface* 11.96 (July 2014), p. 20140239. (Visited on 05/04/2022).

[119] J. H. Capshew. "Engineering Behavior: Project Pigeon, World War II, and the Conditioning of B. F. Skinner". In: *Technology and Culture* 34.4 (Oct. 1993), pp. 835–857.

[120] Andrew M. Hein et al. "An Algorithmic Approach to Natural Behavior". In: *Current Biology* 30.11 (June 2020), R663–R675. (Visited on 05/04/2022).

[121] Kaushik Ghose et al. "Echolocating Bats Use a Nearly Time-Optimal Strategy to Intercept Prey". In: *PLOS Biology* 4.5 (Apr. 2006), e108. (Visited on 05/04/2022).

[122] Caroline H. Brighton, Adrian L. R. Thomas, and Graham K. Taylor. "Terminal Attack Trajectories of Peregrine Falcons Are Described by the Proportional Navigation Guidance Law of Missiles". In: *Proceedings of the National Academy of Sciences* 114.51 (Dec. 2017), pp. 13495–13500. (Visited on 05/04/2022).

[123] Caroline H. Brighton and Graham K. Taylor. "Hawks Steer Attacks Using a Guidance System Tuned for Close Pursuit of Erratically Manoeuvring Targets". In: *Nature Communications* 10.1 (June 2019), p. 2462. (Visited on 05/04/2022).

[124] Caroline H. Brighton et al. "Attack Behaviour in Naive Gyrfalcons Is Modelled by the Same Guidance Law as in Peregrine Falcons, but at a Lower Guidance Gain". In: *Journal of Experimental Biology* 224.5 (Mar. 2021), jeb238493. (Visited on 05/04/2022).

[125] Samuel T. Fabian et al. "Interception by Two Predatory Fly Species Is Explained by a Proportional Navigation Feedback Controller". In: *Journal of The Royal Society Interface* 15.147 (Oct. 2018), p. 20180466. (Visited on 05/04/2022).

[126] T. S. Collett and M. F. Land. "How Hoverflies Compute Interception Courses". In: *Journal of Comparative Physiology ? A* 125.3 (1978), pp. 191–204. (Visited on 05/04/2022).

[127] Suzanne Amador Kane, Andrew H. Fulton, and Lee J. Rosenthal. "When Hawks Attack: Animal-Borne Video Studies of Goshawk Pursuit and Prey-Evasion Strategies". In: *Journal of Experimental Biology* 218.2 (Jan. 2015), pp. 212–222. (Visited on 03/20/2023).

[128] Caroline H. Brighton et al. "Raptors Avoid the Confusion Effect by Targeting Fixed Points in Dense Aerial Prey Aggregations". In: *Nature Communications* 13.1 (Aug. 2022), p. 4778. (Visited on 03/24/2023).

[129] Norbert Boeddeker and Martin Egelhaaf. "Steering a Virtual Blowfly: Simulation of Visual Pursuit". In: *Proceedings. Biological Sciences* 270.1527 (Sept. 2003), pp. 1971–1978.

[130] Andreas F. Haselsteiner, Cole Gilbert, and Z. Jane Wang. “Tiger Beetles Pursue Prey Using a Proportional Control Law with a Delay of One Half-Stride”. In: *Journal of The Royal Society Interface* 11.95 (June 2014), p. 20140216. (Visited on 05/04/2022).

[131] S. W. Zhang et al. “Visual Tracking of Moving Targets by Freely Flying Honeybees”. In: *Visual Neuroscience* 4.4 (Apr. 1990), pp. 379–386.

[132] Bart R. H. Geurten et al. “A Syntax of Hoverfly Flight Prototypes”. In: *The Journal of Experimental Biology* 213.Pt 14 (July 2010), pp. 2461–2475.

[133] Matthew J. McHenry et al. “The Pursuit Strategy of Predatory Bluefish (Pomatomus Saltatrix)”. In: *Proceedings of the Royal Society B: Biological Sciences* 286.1897 (Feb. 2019), p. 20182934. (Visited on 05/04/2022).

[134] R. M. Olberg et al. “Eye Movements and Target Fixation during Dragonfly Prey-Interception Flights”. In: *Journal of Comparative Physiology. A, Neuroethology, Sensory, Neural, and Behavioral Physiology* 193.7 (July 2007), pp. 685–693.

[135] M. F. Land and T. S. Collett. “Chasing Behaviour of Houseflies (Fannia Canicularis)”. In: *Journal of comparative physiology* 89.4 (Dec. 1974), pp. 331–357. (Visited on 05/06/2022).

[136] N. A. Shneydor. *Missile Guidance and Pursuit: Kinematics, Dynamics and Control*. Elsevier, Jan. 1998.

[137] Emily Baird and Marie Dacke. “Finding the Gap: A Brightness-Based Strategy for Guidance in Cluttered Environments”. In: *Proceedings of the Royal Society B: Biological Sciences* 283.1828 (Apr. 2016), p. 20152988. (Visited on 05/04/2022).

[138] Partha S. Bhagavatula et al. “Behavioral Lateralization and Optimal Route Choice in Flying Budgerigars”. In: *PLOS Computational Biology* 10.3 (Mar. 2014), e1003473. (Visited on 05/04/2022).

[139] M. Remy and J. Emmerton. “Behavioral Spectral Sensitivities of Different Retinal Areas in Pigeons”. In: *Behavioral Neuroscience* 103.1 (Feb. 1989), pp. 170–177.

[140] C. David Williams and Andrew A. Biewener. “Pigeons Trade Efficiency for Stability in Response to Level of Challenge during Confined Flight”. In: *Proceedings of the National Academy of Sciences* 112.11 (Mar. 2015), pp. 3392–3396. (Visited on 05/04/2022).

[141] Yongchang Wang and Barrie J. Frost. “Time to Collision Is Signalled by Neurons in the Nucleus Rotundus of Pigeons”. In: *Nature* 356.6366 (Mar. 1992), pp. 236–238. (Visited on 05/04/2022).

[142] Ivo G. Ros et al. “Rules to Fly by: Pigeons Navigating Horizontal Obstacles Limit Steering by Selecting Gaps Most Aligned to Their Flight Direction”. In: *Interface Focus* 7.1 (Feb. 2017), p. 20160093. (Visited on 05/09/2022).

[143] C. J. PENNYCUICK. “Power Requirements for Horizontal Flight in the Pigeon Columba Livia”. In: *Journal of Experimental Biology* 49.3 (Dec. 1968), pp. 527–555. (Visited on 05/04/2022).

[144] Vivek H. Sridhar et al. “The Geometry of Decision-Making in Individuals and Collectives”. In: *Proceedings of the National Academy of Sciences* 118.50 (Dec. 2021), e2102157118. (Visited on 05/04/2022).

[145] J. M. Warren. “Handedness and Laterality in Humans and Other Animals”. In: *Physiological Psychology* 8.3 (Sept. 1980), pp. 351–359. (Visited on 05/04/2022).

[146] Promode R. Bandyopadhyay, Henry A. Leinhos, and Aren M. Hellum. “Handedness Helps Homing in Swimming and Flying Animals”. In: *Scientific Reports* 3.1 (Jan. 2013), p. 1128. (Visited on 05/04/2022).

[147] Dora Biro, Jessica Meade, and Tim Guilford. “Route Recapitulation and Route Loyalty in Homing Pigeons: Pilotage From 25 Km?” In: *Journal of Navigation* 59 (Jan. 2006), pp. 43–53.

[148] Daniel Kress, Evelien van Bokhorst, and David Lentink. “How Lovebirds Maneuver Rapidly Using Super-Fast Head Saccades and Image Feature Stabilization”. In: *PLOS ONE* 10.6 (June 2015), e0129287. (Visited on 05/04/2022).

[149] Sofía Miñano and Graham K. Taylor. *Through Hawks’ Eyes: Reconstructing a Bird’s Visual Field in Flight to Study Gaze Strategy and Attention during Perching and Obstacle Avoidance*. June 2021. (Visited on 05/19/2022).

3

Pigeon gap selection in forest-like obstacle field

Contents

3.1 Abstract 93
3.2 Introduction 93
3.3 Methods 98
3.3.1 Ethics statement 98
3.3.2 Subjects and training 98
3.3.3 Experimental setup 98
3.3.4 Experimental design 101
3.3.5 Motion capture 102
3.3.6 Marker reconstruction and labelling 102
3.3.7 Statistical analysis 103
3.4 Results 106
3.4.1 Different individuals select similar routes through the same clutter 106
3.4.2 Pigeons select gaps most aligned with the exit roller door 107
3.4.3 Initial flight direction relates to gap choice, not handedness 109
3.4.4 Modelling gap choice 110
3.5 Discussion 111
3.5.1 Estimating the size of apertures 113
3.5.2 Determining targets 115
3.5.3 Limitations 118
3.6 Supplementary Information 120
3.6.1 Characteristics of animals used during data collection . 120
3.6.2 2D histograms of routes taken through obstacle configurations 121
3.6.3 2D histograms of routes taken by individual 127

3.6.4 Performance of candidate binomial generalised linear models of pigeon gap choice in an artificial forest of obstacles task. 129
3.6.5 Performance of candidate binomial generalised linear models of pigeon gap choice in an artificial forest of obstacles task. 131
References 131

3.1 Abstract

Solving spatial problems is fundamental to the survival of any animal: finding food and mates both involve moving from A to B, often through unfamiliar or changing environments. Here, we ask what factors affect how birds move between two known locations through an unfamiliar structured environment. We use high-speed motion capture cameras to track pigeons flying out of a familiar flight hall through a set of obstacles arranged on a chevron matrix, randomising the position of the obstacles between trials. We find systematic variance in the paths taken to negotiate environmental obstacles linked to the distribution of obstacles. We then ask what mechanisms might generate such variance by modelling the free-flight behaviour as a process of sequential gap selection. This method allows us to independently evaluate how different components affect the observed behaviour. We find bird gap choices are best captured by an autoregressive model, including information about the exit location, the cartesian distance between the closest obstacles, and the apparent visual gaps between all the obstacles ahead. Our decision model can, in turn, be combined with established models of pigeon steering to provide a complete picture of how birds guide their flight through complex environments.

3.2 Introduction

The resilience and adaptability of pigeons have made them a popular species for scientific study for centuries. From their original habitat of cliff edges, they have adapted to living in highly three-dimensional urban ecosystems. Moving through

such structurally complex environments requires combining rapid processing of sensory cues with aerodynamic manoeuvring on the fly. This remarkable ability of flying animals to manoeuvre through obstacle-laden areas has become a growing focus of attention [137][142]. Still, our understanding of how animals detect and recognize elements in their environment as areas to avoid and modify their path around them is far from complete. In longer-range navigational tasks, pigeons are thought to plan routes from their current to their desired location based on an internal representation of environmental features [150]. Such an approach makes sense in a largely stable environment when the goal is beyond an animal's perceptual range. However, it is less useful at smaller scales, where environments change more rapidly, and the information perceived by one's senses is sufficient -and likely more accurate- than an internal representation based on previous experiences.

In this study, we set out to investigate how pigeons negotiate obstacles positioned between their starting and goal locations, when both the target and obstacles are within their perceptual range - and therefore no internal representation of the environment is strictly necessary. We limit the obstacles presented to the vertical axis, as this emulates the structure of complex environments that pigeons habitually encounter, such as forests and cities. If birds' movements are a reaction to information being perceived as they move through their environment, rather than based on an internal representation of their environment or other factors, clarifying *what* information is being used and *how* birds perceive the space around them becomes key to predicting their reactions. Here, we explore these questions by testing how different features the animals may be responding to affect the birds' flight paths.

Birds are well-known for using vision to guide their flight [151], and it is essential to consider their visual abilities when analysing their movement behaviour. Pigeons have lateral eyes, allowing for a panoramic field of view covering almost 340° [111]. Panoramic fields facilitate the detection of objects while the animal remains still, and are typical of granivorous birds attempting to avoid the motion detectors of potential predators. However, they are also associated with narrower binocular fields and thus limited stereoscopic depth perception. The binocular field of the

pigeon, for example, is approximately 20° and their stereoscopic depth perception is limited 10-20 cm [111]. Despite adaptations to maintain resolution across central and peripheral vision [152], their broad field of view also reduces pigeons' visual acuity to approximately 12 cycles/degree in the lateral visual field, declining further towards the frontal visual field. While this resolution is much lower than that of humans ($\sim$ 70 cycles/degree), pigeons' visual systems are keenly sensitive to moving stimuli, with flicker fusion frequencies over twice as high as humans' at about 130 Hz [23] [111]. High flicker fusion frequencies are often observed in animals that move through their environments quickly [153].

When an animal is in motion, spatial information must be gathered and updated quickly. Information-gathering mechanisms used when an animal is still, or moving slowly, are not always suitable. For example, retinal images incur motion blur when an animal is moving quickly, reducing the efficacy and reliability of sharp retinal images for distance estimation or edge detection. Similarly, oculomotor mechanisms for distance and depth estimation -such as accommodation and convergence- are too slow to be used while flying through unfamiliar environments [154]. Our knowledge of the pigeon visual system also indicates that stereopsis would not help extract depth cues during flight. Fast detection of information during visually guided locomotion is thus more likely to be obtained using motion-based visual cues.

Motion-based visual cues are known to be used by other fast-moving species -such as honeybees (*Apis mellifera*) [155], bumblebees (*Bombus terrestris*) [156], and budgerigars (*Melopsittacus undulatus*) [157]- to avoid collisions. When flying through corridors, these animals are thought to use wide-field image motion generated on their retinas to maximize their distance from corridor walls. This pattern of visual motion is known as optic flow. Balancing the angular velocity of optic flow experienced by each eye results in the animals centering their flight through corridors [157]. The use of optic flow for centering in a corridor is made possible by the nature of the relationship between the distance to the walls (d), the viewing angle at which optic flow is measured (θ), and the animal's velocity (V): $V/d \cdot sin\theta$. As animals translate, the images of distant objects move slower than those of objects close by,

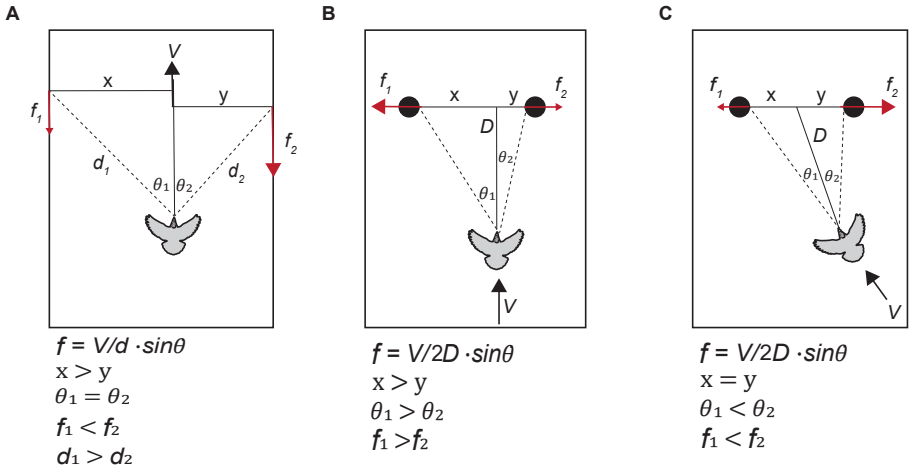


Figure 3.1: Patterns of optic flow generated by corridors and gaps. (A) As the bird translates through a corridor off-center, each wall is at a different distance from the bird's retina. The optic flow experienced from the more distant wall (f_1) is thus smaller than that experienced from the closest wall (f_2). The relationship between the direction and magnitude of optic flow on the retina of a bird flying on a perpendicular but off-centre trajectory (B) or diagonally towards the centre of an aperture (C). θ: angle at which optic flow to a point is measured. x,y: lateral distance to the point generating optic flow. D: perpendicular distance to the aperture.

which, in a corridor, means that the angular velocity of optic flow experienced in the retina will be greater in the eye closer to the wall (Fig 3.1A). This illustrates how using areas of different image speeds and directions of motion obviates the need for detailed edge or object recognition.

While birds have been shown to centre their flight through corridors [157] and gaps [158], apertures in a cluttered environment generate very different patterns of visual motion to corridors. Previous studies have re-framed the problem of avoiding obstacles, which is challenging to model, as a gap-aiming task, and have found that pigeons tend to aim for the centre of the largest visual gaps [105]. If an obstacle field is indeed perceived as a set of apertures to aim towards, an animal approaching a gap will experience a pattern of expanding images in its frontal visual field (Fig 3.1B,C), with the focus of expansion corresponding to the projection of the animal's velocity vector onto the image field. This account assumes that the animal fixates its heading point, which in this case would serve to remove any rotational component of the optic flow. Such image motion is thus characterised by the animal's velocity (V), perpendicular distance to the aperture (D), and the angle at which optic flow of the

edge is measured (θ), such that $V/2D \cdot sin\theta$. A key consequence of this relationship is that the relative difference in angular velocities generated by contiguous objects changes with different approach trajectories (Fig. 3.1B,C). Therefore, unless the bird is flying perpendicular to the plane of the aperture and with its velocity vector directed towards the centre of the gap, balancing optic flow will not result in the animal's position being centred between two obstacles in the same way as it would in a corridor. This derivation illustrates that such a strategy would not be robust to the variation present in naturalistic environments.

A strategy involving balancing optic flow to fly towards the centre of gaps is further complicated in situations with multiple obstacles where visual gaps are not clearly defined. As the previous account illustrates, based on optic flow cues, the apparent size of an aperture will depend on the animal's velocity and angle of approach. Additionally, the locations that are perceived as apertures may change depending on an animal's path. This can manifest in several ways. An aperture identified based on the physical distance between two objects is clearly defined. However, that same aperture would appear and possibly map differently onto physical space depending on the bird's perspective at any given point - including its geometry relative to other obstacles as well as the objects it perceives as relevant. This is depicted in Fig. 3.2. The top-down view of the obstacle arrangement Fig. 3.2B shows how, in the sixth row (obstacles **g**-**i**, shown in violet), the physical distance between obstacles **g** and **h** is larger than that between obstacles **h** and **i**. The mid-point of this larger gap (**g**-**h**, depicted as a violet cross) is clearly defined. However, the simulated bird view in Fig. 3.2D shows that from this vantage point, the spatial relationships change: the visual gap between obstacles **h** and **i** appears bigger than that between obstacles g and h, and the physical midpoint between obstacles **h** and **i** doesn't map onto the middle of the visual gap. Similarly, depending on the depth at which obstacles are considered when evaluating a scene, the space that constitutes the largest visual gap will change, as shown in the simulated subject view from just before the fourth row of obstacles in Fig. 3.2C. This raises the question of what information the animals are utilising.

Here, we address this question by presenting pigeons with an artificial forest of obstacles to traverse, testing different definitions of environmental gaps to better understand how pigeons choose between available options and what cues might influence the birds' decisions while flying.

3.3 Methods

3.3.1 Ethics statement

The animal husbandry and experimental procedures outlined in this section were approved by the local ethical review committee of the University of Oxford's Department of Zoology (permit number APA/1/5/ZOO/NASPA).

3.3.2 Subjects and training

Seventeen homing pigeons *(Columba livia domestica)* ages 2-10 years were used for this experiment (see Supplementary Data 2.7.1 for further details). The pigeons were housed with approximately 120 other free-ranging pigeons in 2 neighbouring lofts at the John Krebs Field Station, Wytham, Oxford, UK, to which they returned voluntarily. Access to water, grit and a standard pigeon feed mix was available *ad libitum* at all times in the loft. The heaviest birds from one loft were chosen to participate in the experiment to minimise the effect of the weight of the markers on their flight behaviour. The condition of the pigeons was monitored every day of experiments for any changes in health conditions. If any pigeon was found to be physically unwell, it was excluded from further experiments. Only one bird had to be excluded from the study for health reasons.

3.3.3 Experimental setup

Flights were recorded in a windowless hall measuring 20.2 m $\times$ 6 m, with a minimum ceiling height of 3.8 m and walls hung with camouflage netting to provide visual contrast. Flicker-free LED lights provided a mixture of direct 4000 K lighting and indirect 5000 K lighting at approximately 1000 lux, designed to mimic overcast morning or evening light conditions. Most of the front wall of the building comprised

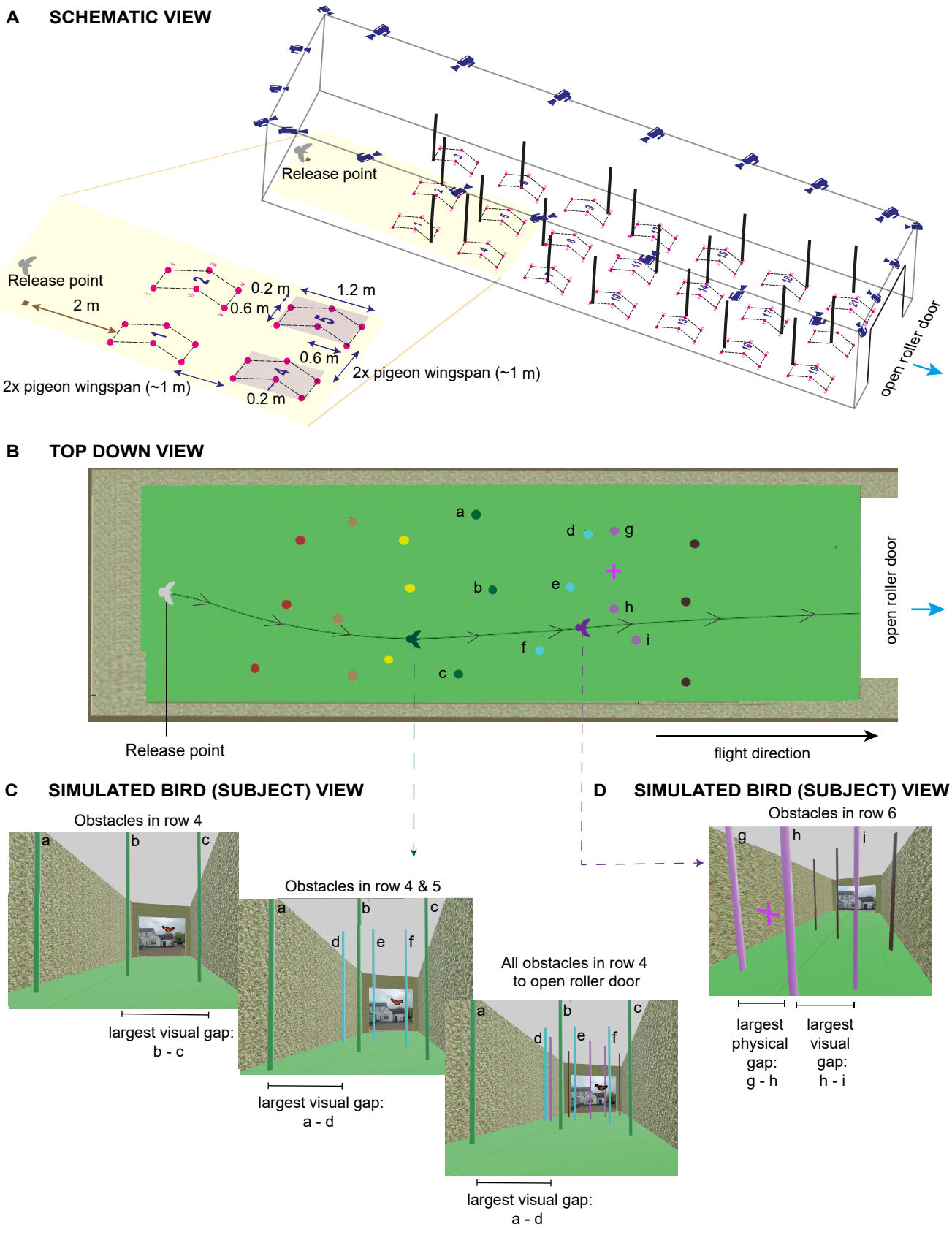

A SCHEMATIC VIEW
Release point
Release point
2 m
0.2 m
0.6 m
1.2 m
0.6 m
0.2 m
2x pigeon wingspan (~1 m)
2x pigeon wingspan (~1 m)
open roller door
B TOP DOWN VIEW
a
b
c
d
e
f
g
h
i
open roller door
Release point
flight direction
C SIMULATED BIRD (SUBJECT) VIEW
Obstacles in row 4
largest visual gap:
b - c
Obstacles in row 4 & 5
largest visual gap:
a - d
All obstacles in row 4
to open roller door
largest visual gap:
a - d
D SIMULATED BIRD (SUBJECT) VIEW
Obstacles in row 6
largest
physical
gap:
g - h
largest
visual
gap:
h - i

Figure 3.2: Experimental set-up. A Schematic depicting the experimental area with high-speed motion cameras used to track pigeons flying down a flight hall through an obstacle arrangement leading to an open shutter door. Obstacles are randomly distributed in the room through a hexagonal lattice arrangement. Contiguous obstacles form rows (e.g. row 1: obstacles 1-3, row 2: obstacles 4-6 etc.). **B** Top-down illustration of flight hall during a sample trial. Obstacle positions are shown as dots coloured by row. The flight path is shown as a black line from the release point to the left, marked as a grey bird outline, to the open roller door to the right. The green bird outline and dashed green line mark the position of the "decision point" for row 4 from which polar angles were measured to determine model predictors (V2a), (V2b), (V2c) and (V3) (see main text section 3.3.7). The purple bird outline and dashed purple line mark the position of the "decision point" for row 6 from which polar angles were measured to determine model predictors. A purple cross has been overlaid to mark the midpoint between obstacles **g** and **h** - see (D). **C** View of the obstacle configuration depicted in (B) from the bird's vantage point at the decision point for row_t=4. As seen in (B), the bird flew through the right-hand gap in this instance. This is depicted as a red bird outline in C (bird outline not to scale). From this vantage point, the side containing the largest physical gap (V1) and the side containing the largest visual gap (V2a) are the same when only the fourth row of obstacles is considered: they are both the right-hand gap. This is because $\overline{\text{ab}} < \overline{\text{bc}}$ and $\angle ab < \angle bc$. However, adding obstacles in subsequent rows means the largest visual gap changes location (second and third images). With an additional row of obstacles taken into account, five gaps form between the two outermost obstacles: $\angle ad, \angle db, \angle be, \angle ef, \angle fc,$. The largest visual gap (between obstacles **a** and **d**) then falls to the left of the central obstacle (**b**) instead of to the right - i.e. the side not flown through. The same is the case when all the remaining obstacles in the room are considered (third image). **D** View of the obstacle configuration depicted in (B) from the bird's vantage point at the decision point for row_t=6. From this vantage point, the side containing the largest physical gap (V1) is different to the side containing the largest visual gap (V2a). This is because $\overline{\text{gh}} > \overline{\text{hi}}$ and $\angle gh < \angle hi$. The midpoint between obstacles **g** and **h**, marked by a purple cross, does not appear to be at the visual centre between the two obstacles from this vantage point (compare to the position of the purple cross in (B), and see main text). Explanatory model variables for this obstacle configuration would be recorded as: 1) largest physical distance between obstacles ($\overline{\text{ab}} > \overline{\text{bc}}$): left gap (gap not flown through); (V2a) largest visual distance between obstacles ($\angle ab > \angle bc$): left gap; (V2b) largest visual distance between obstacles in the row to be crossed and the row after (row 5) ($\angle ad > \angle ef$): left gap; (V2c) largest visual distance between obstacles when all obstacles ahead of the bird are considered: left gap; (V3) gap most aligned with the roller door (containing the largest angle of roller door opening): right gap; (V4a) gap choice at $\text{row}_{\text{t-1}}$: right gap; (V4b) gap at $\text{row}_{\text{t-2}}$: right gap. (V5) bird crossed right-hand gap (formed by obstacles b-c).

an open roller shutter door providing natural daylight illumination, presenting a much brighter scene than the interior of the flight hall. The ambient weather conditions and position of the sun's disc were a source of uncontrolled variation in brightness during experiments. To minimise such variation, experiments were only undertaken on overcast days, and releases happened at roughly the same time each day during a two week experimental period.

3.3.4 Experimental design

We collected trajectory data over a period of approximately two weeks. All subjects completed a minimum of 10 training flights in the empty flight hall preceding the start of the experiment. On each day of training and experimental flights, the pigeons were collected from their home loft and fitted with a rigid plate attached to their head using Velcro (Velcro IP Holdings LLC). This was fitted just before the start of the first recording session of the day, and removed at the end of the last release of the day. Each plate had a unique asymmetrical configuration of four 4 mm diameter spherical retro-reflective markers for motion capture (Vicon Motion Systems Ltd, Oxford, UK). Each bird was individually taken out of its carrier box in the flight hall, held for a minute at the release point to acclimatise, and then released to fly freely by the experimenter opening their hands. A pigeon was only taken out of its carrier box once the preceding bird had exited the flight arena and was out of sight. After all pigeons had been released, they were collected from the loft to be re-released. Each bird's number of releases per day was variable up to a maximum of 10 per day.

After each bird had completed their 10 training flights through an empty flight hall, 21 obstacles were positioned in the flight hall between the release point of the pigeons and the open roller shutter door. Each obstacle consisted of a 50 mm diameter, 3.5 m height black plastic pole with three 10 mm retro-reflective markers (Vicon Motion Systems Ltd, Oxford, UK) stuck on each side at three set heights. The obstacles were arranged in a regular grid so that a bird's trajectory could be divided into distinct decision points at each row. However, we also wanted to have the obstacles change positions from trial to trial to allow for variation in environmental features. Therefore, the grid locations consisted of chevrons with six available positions, where an obstacle was pseudo-randomly placed in each trial (Fig. 3.2B). Thus the overall configuration of obstacles in each trial was semi-random. The grid had 21 chevrons arranged in seven rows of three over a 4 m x 18.8 m area (Fig. 3.2A). Black netting was hung from the ceiling to ensure the birds did not fly above the obstacles. Experimental flights consisted of birds being individually

released from the end of the flight hall opposite an open roller door and allowed to fly freely in the flight hall, following the same steps as with training flights. The release point of the pigeons was 2 m from the foremost grid position of the first row of obstacles, at 1.2m height and within 1m of the midline of the hall. From there, they flew through the obstacle arrangement to the aperture created by the open roller door at the end of the flight hall, from where they could exit the building. Their home loft was located a short distance (approximately 80 m) behind to the left of the building (see Fig. 3.2B,C for reference), so it was occluded from view until the birds had exited the flight hall.

3.3.5 Motion capture

The birds' flight trajectories were reconstructed using a motion capture system of 22 high-speed cameras (Vantage 16, Vicon Sytems Ltd, Oxford, UK) and four reference video cameras (Vue, Vicon Sytems Ltd, Oxford, UK). Cameras were mounted on 3.5 m scaffolding fixed around the hall's perimeter. The motion capture cameras were set to record at 200 Hz under stroboscopic 850 nm infrared illumination, well outside the visible spectrum of these birds [139], with an optical filter blocking light at other wavelengths. At this frame rate, the sensor resolution for the Vantage cameras was 4096 $\times$ 4096 pixels, with a 1 ms shutter speed. The four definition video cameras recorded reference video at 100 Hz, with a sensor resolution of 1920 $\times$ 1080 pixels and a shutter speed of 2 ms. The motion capture system was turned on at least one hour before the start of the experiments and calibrated without the obstacles present shortly before the first session (Vicon Active Calibration Wand), using Vicon Nexus 2 software for data acquisition. Experiments only went ahead after each camera had been calibrated to an image error accuracy of $\leq$0.4 pixels for the motion capture cameras and $\leq$1.2 pixels for the reference video cameras.

3.3.6 Marker reconstruction and labelling

We used Vicon Nexus 2.7.6 software to reconstruct the positions of the markers within the flight volume, using a coordinate system corresponding to the principal

axes of the flight hall. However, the proprietary marker tracking algorithm was not always able to label each marker reliably due to a combination of intermittent marker occlusion, high-speed motion and patches of specular reflection sometimes appearing as ghost markers. We, therefore, labelled each of the recorded markers using custom-written software in MATLAB v9.6 (MathWorks, Inc., Natick, MA, USA). The software used clustering algorithms to group markers within and between frames (e.g. to distinguish markers on the pigeon from markers on the obstacles, based on their speeds). The centroid of the resulting set of candidate head markers was used as an initial estimate of head position and fitted a quintic spline to interpolate its position on frames with missing data. We then used our initial or interpolated estimate of the head position on each frame to define a search volume matched to the size and distribution of the head markers and labelled any other markers falling within this search volume as candidate head markers. This two-stage marker labelling procedure was designed to accommodate missing markers while eliminating the ghost markers that can arise from spurious reflections. However, it inevitably resulted in some data dropout, particularly in the less-well visualised part of the flight volume near the ceiling. Only flights where the birds did not contact obstacles or the floor were accepted for analysis, resulting in a sample of n = 916 flight trajectories (approximately 50 per bird for N = 17 birds).

3.3.7 Statistical analysis

We modelled each flight as a sequence of seven consecutive gap choices (Fig 3.2), with four possible outcomes per row according to whether the bird flew through the gap formed by a pair of adjacent obstacles or between an obstacle and the wall. In practice, the birds rarely flew between the obstacles and the wall (7% of choices), so we simplified the analysis by considering only those cases where the bird flew between adjacent obstacles. This reduced the problem to a binary choice between the gaps formed by the middle obstacle and the left or right obstacle, making it amenable to analysis as the response variable in a logistic regression. To assess the factors predicting this binary choice, we recorded the bird's position as it crossed

the preceding row of obstacles, which we censused at the row's mean longitudinal position (Fig 3.2). When modelling the bird's first gap choice, we censused its position at the release point. Whilst these census points may not correspond to the birds' actual decision points, they do provide an objective and consistent definition of where the bird was committed to its current gap choice, and hence of where it was likely to have made or been preparing to make its next choice.

Making use of the bird's position at each census point, we classified the upcoming left and right gaps according to which: (V1) had the largest physical width; (V2a) subtended the largest angular width; and (V3) contained the largest angular width of the open roller door. Because the pigeons might have attended to obstacles in subsequent rows at the same time, we also classified the upcoming left and right gaps according to which: (V2b) contained the largest angular sub-gap between obstacles in this and the following row; (V2c) contained the largest angular sub-gap between obstacles in this and all subsequent rows. Variables V2a, V2b and V2c are designed to provide insight into how forward-looking a bird is in the choices it makes, with V2a representing the most myopic-view and V2c the most far-sighted. Likewise, variable V1 is intended to test whether birds estimate the absolute size of a gap, whereas variable V3 can be considered as a proxy for the relative brightness of the gap, given the light that flooded in through the open roller door.

Variable	Measured as:	Abbreviation
(1) Largest gap	distance between Cartesian coordinates of contiguous obstacles in row_t	gC
(V2a) Largest gap	distance between polar coordinates of contiguous obstacles in row_t	gP
(V2b) Largest gap	distance between polar coordinates of contiguous obstacles in row_t + row_{t+1}	sg1
(V2c) Largest gap	distance between polar coordinates of contiguous obstacles in rows= row_t to row_7	sg7
(V3) Most roller door subtended	distance between polar coordinates of roller door edges and middle obstacle of row_t	ex
(V4a) Previous choice	gap traversed at row_{t-1}	AR1
(V4b) Previous choice	gap traversed at row_{t-2}	AR02
(V5) Side flown	left or right of middle obstacle in row_t	sf
(V6) Bird identity	as recorded	ID

Table 3.1: Variables extracted from each flight for further analysis

We used these gap classification variables to model left versus right gap choice in a mixed effects logistic regression model, including pigeon identity as a random effect (intercept only) to control for the repeated measures structure of the data at the population level. We then fitted individual identity as a fixed effect in order to capture any handedness of specific individuals, as was found in a previous study of

binary gap choices in pigeons antolin2022b. In each case, we included a first-order autoregressive (AR1) to control for the time-series structure of the data. This serves to capture any tendency of the birds to select the closest gap, noting that a bird's behaviour will be perfectly predicted by the AR1 term if it always remains on the same side. We also tested the effect of including a second-order autoregressive (AR2) term, which in combination with the AR1 term provides information on the bird's overall direction of travel. Note that because two preceding gap choices are needed to form the AR1 and AR2 terms in the model, we are only able to model the birds' choices in rows three to seven.

The explanatory variables were determined as follows: (V1) was calculated based on the Cartesian coordinates of the obstacles in the row to be crossed; (V2a), (V2b) and (V2c) were calculated using the polar coordinates of the obstacles ahead, taken from the bird's vantage point at the defined decision coordinate; (V3) the polar coordinates of the roller door edges were used to determine which gap subtended the broadest view of the roller door leading to the outside; gap choices were determined by identifying the positions at which the bird's trajectory intersected virtual lines connecting contiguous obstacles within a row; (Fig. 3.2).

Statistical analyses were conducted in R version 4.1.1 (RCoreTeam 2021), using the packages lme4 to construct generalised mixed effects models (GLMMs), bblme to estimate generalised linear model (GLM) parameters using maximum likelihood, and pROC for visualising model performance. Odds ratios from the logistic regressions were computed by exponentiating the logistic regression coefficients. We used likelihood ratio tests to assess the significance of the model factors at $\alpha = 0.05$, Wald tests to compute the significance of differences between levels, and profile-likelihood 95% confidence intervals to quantify the uncertainty in the parameter estimates. We tested each combination of explanatory variables. Akaike Information Criterion (AIC) and Akaike Weights were used for model selection. Model assumptions were verified by plotting residuals versus fitted values, each covariate in the model and each covariate not in the model.

We only used data from the initial response after release to indicate pigeon handedness.

Model+type	Data	Response variable	Explanatory variables	
			Fixed	Random
1 Binomial GLM	Row 1	Gap choice (L/R)	Bird ID	
2 Binomial GLM	Row 1	Gap choice (largest: Y/N)	Bird ID	
3 Binomial GLM	Row 1	Gap choice (most roller door: Y/N)	Bird ID	
4 Binomial GLMM	Row 1	Gap choice (largest: Y/N)		Bird ID
5 Binomial GLMM	Row 1	Gap choice (most roller door: Y/N)		Bird ID
6 Binomial GLMM	Rows 3-7	Gap choice (L/R)	Gap choice$_{(t-1)}$ + Gap choice$_{(t-2)}$	Bird ID
7 Binomial GLMM	Rows 3-7	Gap choice (L/R)	roller door contained (largest angle: Y/N)	Bird ID
8 Binomial GLMM	Rows 3-7	Gap choice (L/R)	Gap choice (largest: Y/N)	Bird ID

Table 3.2: Model structures used for analysis.

3.4 Results

We recorded the flight trajectories of $N = 17$ pigeons traversing a forest of vertical obstacles as they flew individually from their release point at the back of a 20 m $\times$ 6 m motion capture studio to exit through an open roller shutter door at the front. The 21 obstacles were arranged in an irregular grid comprising seven rows of three obstacles whose exact position was varied randomly between releases, such that all the birds within a release experienced the same obstacle configuration (see Methods). When crossing each row of obstacles, the bird was forced to choose to fly through one of four gaps created between adjacent obstacles or an obstacle and the wall. We recorded $n = 916$ flights in total, leading to a total of 6412 choices, of which 5418 could be observed reliably after accounting for data dropout.

3.4.1 Different individuals select similar routes through the same clutter

To visualize how obstacle placement affected pigeon gap choice, we plotted spatial histograms of the horizontal flight trajectories taken by: (i) different individuals in the same obstacle configuration; and (ii) the same individual in different obstacle configurations (Fig. 3.3; see also Supplementary Information). These histograms show a clear effect of obstacle configuration on gap choice by pigeons, with different individuals converging on similar flight trajectories in response to the same obstacle field. The consistency observed across flights from different birds negotiating the

same obstacle field is especially striking in comparison to the variability seen across flights from the same individual negotiating different obstacle fields (Fig. 3.3; see also Supplementary Information). This repeatability implies that obstacle placement, rather than individual idiosyncrasy, is the primary determinant of route choice in pigeons negotiating a novel clutter configuration.

3.4.2 Pigeons select gaps most aligned with the exit roller door

Mixed effect general linear models indicated the likelihood of observations at both the previous time step ($row_{t\text{-}1}$) and the time-step before that ($row_{t\text{-}2}$) are statistically significant predictors of gap choice ($z = 19.79, p << 0.001$ and $z = 15.40, p << 0.001$ respectively). We found the odds of a bird choosing the right-hand gap given it chose the right gap at $row_{t\text{-}1}$ to be 5.1 (CI: 4.3, 6.0), and the odds of a pigeon choosing the right gap given it chose the gap on the right at $row_{t\text{-}2}$ to be 3.4 (CI: 2.9, 4.1). The proportion of roller door a gap contained (variable 3) seemed to have the second most impact on gap choice ($z = 26.45, p << 0.001$) after time history effects were taken into account (variables 4a, 4b). The odds of selecting the gap containing the most roller door -thus containing the most view of the outside, making it the brightest gap- were 3.21 (CI: 2.94, 3.50). Similarly, all four definitions of gap (variables 1, 2a, 2b, 2c) showed a statistically significant effect of gap size on path choice ($p << 0.001$, $z_{1)} = 18.03, z_{2a)} = 21.02, z_{2b)} = 20.68, z_{2c)} = 4.66$). The odds of a bird flying through the largest gap were 2.03 (CI: 1.88, 2.20) when measured based on the cartesian coordinates of the row of obstacles to be crossed (1) and 2.05 (CI: 1.90, 2.22) when measured based on the polar coordinates of that same row of obstacles (2a). When the largest gap was identified based on additional obstacles, the odds of flying through the side containing the largest visual gap became 2.33 (CI: 2.15, 2.56) when obstacles in row_t and row_{t+1} were taken into account (2b); and 1.18 (CI: 1.10, 1.27) when all the obstacles remaining ahead of the bird were factored in (2c).

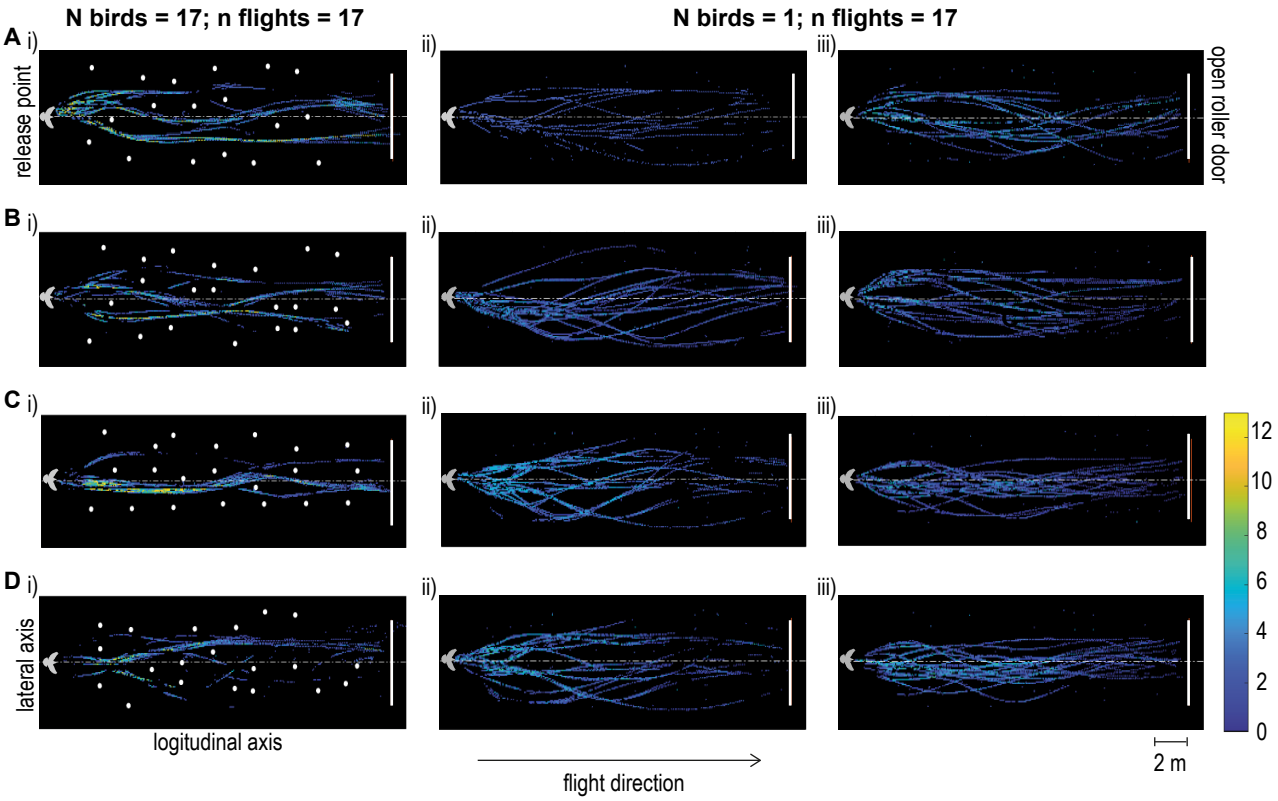


Figure 3.3: 2D histograms of 17 flight tracks in a single obstacle configuration (left, i) and for a single bird (right, ii-iii). Obstacle configurations were randomly selected from the subset of obstacle configurations that all 17 birds experienced. Two birds were randomly selected to show the consistent contrast between the collected trajectories taken by all birds in a single obstacle configuration (left, i) and those taken by an individual bird across several obstacle configurations (right, ii-iii). Flights for individual birds were selected semi-randomly so that the same flight was represented in the left (i) and right (ii or iii) plots in each panel. White dots represent obstacle positions. The white dashed line marks the midpoint along the transverse of the flight hall. The pigeon release point is to the left end of the histogram (represented by an orange star sign), with the roller door opening at the right (represented by a red line). **A** Flight in common to plots i) and ii) is bird D12 flying through obstacle configuration 10. Flight in common to plots i) and iii) is bird K03 flying through obstacle configuration 10. **B** Flight in common to plots i) and ii) is bird D12 flying through obstacle configuration 25. Flight in common to plots i) and iii) is bird K03 flying through obstacle configuration 25. **C,D** As above for obstacle configurations 37 and 43, respectively.

In practice, the birds only flew between a wall and an obstacle on 7% of their observed choices, and we, therefore, reduce the problem to a binary choice between the left or right gaps between obstacles by dropping.

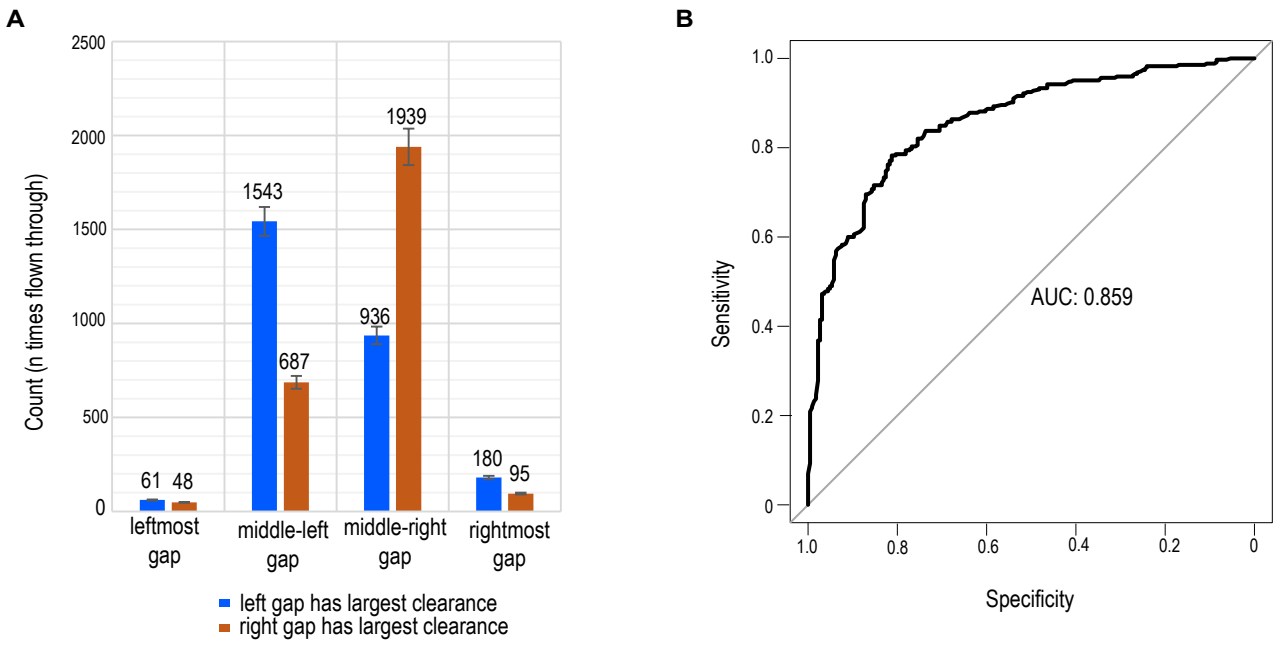


Figure 3.4: Gaps selected by pigeons in the forest-of-obstacles arrangement and ROC curve of best performing model of pigeon gap choice. A Distribution of gap choices across all rows (1-7) for all recorded flights ($n = 916$) showing the outermost gaps are rarely chosen (outer gaps account for only 7% of observations). Gaps are ordered from left to right along the x-axis, and bar colour indicates which side of the central obstacle contained the largest absolute clearance to the external obstacles in the row a bird was flying through at the decision point (see main text). Most pigeons display a clear preference for flying to the side with the largest gap, as can be seen by the blue bars being significantly larger than the orange bars when the birds chose gaps to the left of the central obstacle, and vice versa. **B** The Receiver Operating Characteristics (ROC) curve, a standard performance measurement for classification problems, is a probability curve plotting true positive rate (sensitivity) against false positive rate (1 - specificity). The 45° diagonal line serves as the reference line, since it is the ROC curve of random classification. The associated AUC (area under the curve) indicates the ability of the model to distinguish between a gap choice of the left or the right-hand gap. AUC values fall within the range [0.5–1.0], where 0.5 represents the performance of a random classifier and 1 would correspond to a perfect classifier (e.g., with a classification error rate equivalent to zero). Curve shown for binomial GLM with structure $Gapchoice \sim Gapchoice_{(t-1)} + Gapchoice_{(t-2)} + rollerdoor + subgap_{(row+1)} + subgap_{(allrowsahead)} + Gapsize_{cartesian} + BirdID$.

3.4.3 Initial flight direction relates to gap choice, not handedness

In an earlier study antolin2022b, we found pigeons displayed individual handedness when selecting between two gaps in the same flight hall, and seemed to choose gaps on this basis rather than gap size. To determine whether this held in our current set-up, we first examined the responses to the first row of obstacles in the 871 incidences of the birds crossings the first row of obstacles in which the birds

were observed flying through the middle two gaps. In this first row, the pigeons flew through the right-hand gap on 58% of the 871 flights included in the analysis (odds of selecting a gap on the right: 1.2, CI: 1.09, 1.47), and through the biggest gap on 79% of flights (odds of selecting the largest gap: 2.5, CI: 2.11, 2.93). While there was some evidence of individual handedness, it was only statistical significant for two of the 17 birds tested (A27, B01, table 3.6). At an individual level, the effect of gap size on gap choice was somewhat more consistent, as reflected in odds ratios significantly higher than one, but, based on data from the first row only, not universal to all birds. The statistical significance of the effect of gap size remained strong whether the size of the gap between the obstacles in the first row was measured in cartesian (2a) or polar (2b) coordinates (GLME: $z = 16.0$ and 16.2, respectively, $p << 0.001$ for both at group level). In 85% of the choices in the first row, birds chose the gap that contained the largest amount of roller door (odds of choosing gap most aligned with roller door: 5.7, CI: 4.63, 7.01). Again, the effect of variable 3 (most roller door subtended) was statistically significant at the group level (GLME: $z = 16.4$, $p << 0.001$), but not universal to all birds. We found the position at which the birds crossed two adjacent obstacles to follow a normal distribution. Birds mostly centred their position between obstacles (normalised median position of bird, where 0 represents a centred response and 1 and -1 the positions of adjacent obstacles: -0.02, Q1: -0.23, Q3: 0.23), consistent with previous results antolin2022b.

3.4.4 Modelling gap choice

All three models that captured the data best (Akaike weights > 0.001) included a second-order autoregressive (AR[2]) term (variables V4a+V4b), the term indicating alignment with the open roller door (V3), cartesian gap size (V1), and the side containing the largest visual gap amongst all obstacles ahead of the bird (V2c). All model results are available in Table 3.5. Adding information about the proportion of roller door subtended by a gap (variable 3) resulted in the largest drop in the residual deviance in the top model (Table 3.3), suggesting this factor had the greatest influence in the gap birds flew through. The odds of choosing the gap subtending

the most roller door were 2.91 (CI: 2.31, 3.68). Associations tests between variables showed only medium to weak associations between roller door subtended (V3) and other explanatory variables (Cramer's V < 0.5 for variable 3 with variables V1, V2a, V2b, V2c, bird identity and previous gap choices), indicating the large decrease in residuals relative to other variables was not due to co-linearity. Moreover, this term was present in the top 50% of models. This was also true of gap size. The estimates of the top model further indicated that larger gaps are positively related to gap choice ($p << 0.001$, $z_{cartesian} = 9.08, z_{subgaprowahead} = 4.98, z_{subgapallrows} = 4.07$). The definition of gap size that accounted for the most variability of the data was based on cartesian coordinates of the obstacle positions. Based on this definition, the odds of choosing the largest gap were 3.06 (CI: 2.41,3.90), controlling for other factors. Together, these strongly suggest that target position (correlated with brightness in our set-up) and gap size both play an important role in determining how pigeons choose gaps when flying through structured environments. The superior performance of AR[2] models relative to AR[1] models further suggests that the time history of the bird's trajectory is important in informing about where a bird came from and how it got there. In our top model, both time-steps before showed a significant effect on gap choice at the current time-step ($p << 0.001$, $z_{t-1} = 7.12, z_{t-2} = 5.11$), with the adjusted odds of choosing the right gap given a bird chose the right gap on the previous time step (2.24, CI: 1.79, 2.79) slightly higher than the adjusted odds of the bird choosing the right if it had chosen the right in the ante-previous row (1.72, CI: 1.40, 2.12), as expected. Simple holdout cross-verification of the top model with an 80/20 split resulted in an F1 of 82.7% (precision=81.5%, recall=84.1%) and an accuracy of 85.9%, as determined from the AUC-ROC of the top model (Area Under the Curve of the Receiver Operating Characteristics curve, Fig. 3.4).

3.5 Discussion

In this study, we investigated the ability of birds to fly through a forest-like obstacle field in a collision-free manner. We find greater consistency in trajectories across individuals when responding to matching configurations of obstacles than in the

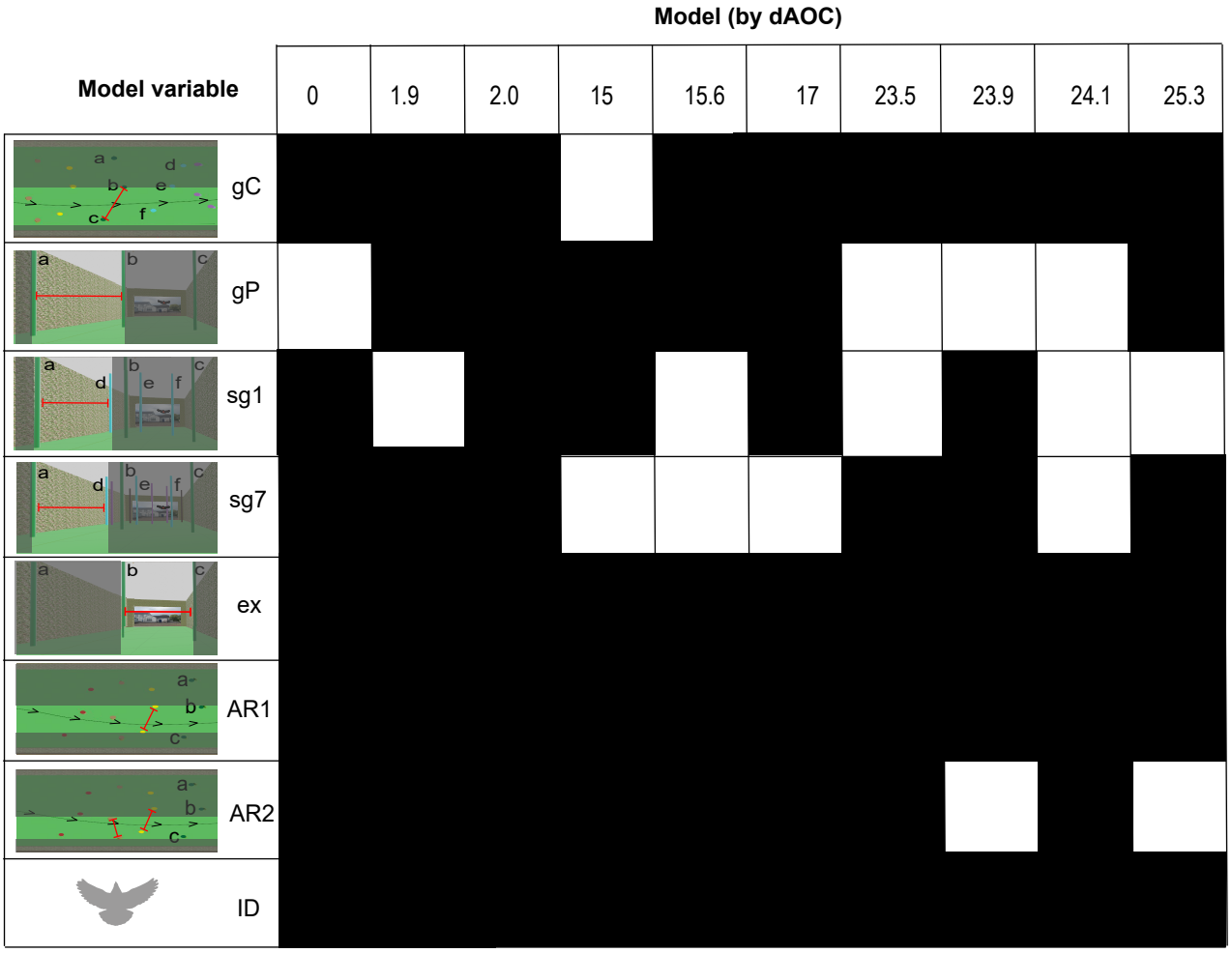


Figure 3.5: Model variables included in the top performing models. Each column represents one of the 10 top-performing models (refer to Table 3.5 for further information about each of the models). Dark boxes indicate the variable in that row is included in the given model. White boxes indicate the variable is not included in the model. Variable abbreviations: gC = cartesian gap size (V1); gP = polar (visual) gap size (V2a); sg1 = size of the gap formed by obstacles in the row to be crossed and row+1 (V2b); sg7 = size of the gap formed by all the remaining obstacles in front of the bird (variable 2c); ex = exit roller door (V3); AR1 and AR2 = autoregressive terms (V4a and V4b respectively); ID = bird identity (V6). Images depicting figures relate to the larger schematic shown in Fig. 3.2. See the main text and refer to Table 3.1 for further clarification.

	D.f.	Deviance	Resid. D.f.	Resid. Dev	Pr(>Chi)
			2843	3893.82	
$Gapchoice_{t-1}$	1	422.78	2842	3471.04	<0.001
$Gapchoice_{t-2}$	1	61.02	2841	3410.02	<0.001
Exit roller door	1	402.61	2840	3007.42	<0.001
$Largestsubgap_{t+1}$	1	86.32	2839	2921.10	<0.001
Largest gap (cart)	1	75.41	2838	2845.69	<0.001
$Largestsubgap_{allrows}$	1	14.79	2837	2830.90	<0.001
ID	16	74.99	2821	2755.91	<0.001

Table 3.3: Analysis of variance of factors included in the top-performing model of pigeon gap choice.

same individual responding to variations in obstacle positioning. When alternative gap options are presented, the decision is affected more by the structure of the environment and previous choices than by the handedness of individual birds. This finding suggests common mechanisms may underpin animals' negotiation of cluttered environments. We observe deliberate steering through the obstacle field, which pigeons traverse with nearly 100% proficiency (very few collisions or landings before the roller exit), and show that birds move through structured environments in predictable ways. Specifically, we find that pigeons select larger clearances containing the greatest view of the outside.

3.5.1 Estimating the size of apertures

The observation that birds choose wider gaps when weaving through obstacles is not surprising, as maximising clearance to objects in the environment is the safest way to avoid collisions. Moreover, even if the birds were paying no attention to the obstacles, we would expect to see more birds crossing the larger gap by chance. This is because it covers a wider proportion of the available space than the smaller gap (it has a larger capture area). We verified that the observation was not purely due to wider gaps having a larger capture area by including an additional term with information about the proportion of the total distance from the leftmost to the rightmost obstacle each gap subtended. While including this variable slightly reduced the size of the effect of gap size, all four definitions of gap size still showed a statistically significant effect of gap size on path choice ($p << 0.001$,

$z_{V1)} = -15.82, z_{V2a)} = -14.96, z_{V2b)} = -10.41, z_{V2c)} = -7.13$). Therefore based on our analysis, the birds seem to be positively choosing larger gaps.

Our experimental set-up provided several sources of visual information about the size and passability of gaps. Testing different definitions of gap size helped us tease apart what information the birds might be using. We also observe that the birds seem to attend to the size of gaps further down the room, which suggests the effect is independent of any sampling effects. If this is the case, our results would imply that birds are capable of estimating metric width, as gaps defined in Cartesian coordinates have a more significant effect on gap choice than those calculated based on polar coordinates. Humans are thought to use intrinsic knowledge of eyesight height and the visual angle subtended by the inside edges of obstacles at a certain distance to derive the distance to and width of an aperture [159]. However, this depends on the assumption of moving on a horizontal plane, so it is unlikely to apply to animals that fly at variable heights, particularly when the ground cannot be approximated by a horizontal plane. Stereo vision provides an alternative static information source to measure gaps' physical width and distance. However, the small region of binocular overlap in pigeons of approximately 20° [154],[160],[161] would be insufficient to utilise stereo to measure the distance between many obstacles in our set-up. Similarly, the low acuity of the pigeon's frontal visual field ($<$ 12 sinusoidal cycles/degree [162]) would preclude static cues of size, such as the width of poles, from being used to estimate the distance and width of gaps. This is consistent with our results, as the ability to measure metric distance implies that clearances are not just calculated based on static appearance. Conversely, bird eyes are well adapted for perceiving rapid motion, with flicker fusion frequencies above 100 Hz [23] (compared to 10 - 20 Hz in rats, for instance, [163]). Together, these suggest pigeons likely use dynamic information to measure gap size.

Dynamic information refers to that linked with self or externally generated movement, such as that arising from an animal translating through space or saccading. The use of visual expansion, or looming, cues has been used in robotics as an efficient mechanism for obstacle avoidance [164]. Looming cues are also known

to trigger collision avoidance in flies [34]. The sensory processing of looming stimuli is well understood in birds [165], and has already been suggested to help budgerigars determine whether or when to close their wings when traversing an aperture [166]. Our results provide further indirect evidence that birds may use visual expansion cues to negotiate structured environments. Such stimuli could be used to estimate gap widths by monitoring the profile of spatial frequency of an image (scale changes) or by sensing the rate of expansion of the stimuli at particular angular widths, such as through optic flow. The latter relies on changes in luminance over time (1st order motion), whereas scale change cues are contrast-defined (2nd order motion)[167]. Pigeons have relatively low contrast sensitivity [168], suggesting they would require a high contrast to detect changes in spatial frequencies. Such high contrast is unlikely to have been present in our experimental set-up in the time frames needed for the animals to estimate gap sizes. Conversely, the natural light from the roller door opening provided a pronounced luminance gradient that the birds could utilise to sense the rate of expansion of stimuli at particular angular widths. Together, these suggest optic flow may be used preferentially to process dynamic information about the environment. Optic flow is highly motion-dependent. Supposing pigeons are using optic flow to determine gap sizes, this feature may also partly account for the importance of time history (AR2 term in our model, representing the previous two gap choices) in determining pigeon gap choice.

3.5.2 Determining targets

Modelling movement through clutter as a process of gap selection has several distinct advantages over modelling the same behaviour as repellence from obstacles. In a naturalistic environment, multiple blocks are likely to be present. Whilst we can distinguish discrete obstacles by design in our set-up, the "obstacles" in a natural setting (tree trunks, branches, etc.) all blend into one another. Superposing their particular repellence effects is computationally challenging and likely to lead to unreasonable trajectories, such as oscillations in narrow passages. The more straightforward process of selecting an unobstructed direction to steer towards is

also safer than turning away from potential blocks, as it is likely to maximise the clearance to potential obstacles. Analytically, it allows the sensory and cognitive processes relevant to the task to be investigated independently of the mechanical implementation (steering). Established steering models for pigeons could then be combined with decision process models (target selection) to simulate trajectories through obstacle fields [158]. While the behavioural objective of avoiding obstacles is more apparent than the steering aims in flying through a structured environment, we can make some inferences about what pigeons might be aiming for based on our data.

Our model and data suggest that pigeons steering through forest-like obstacle fields do not just react to obstacles immediately in front of them. This finding is inherently independent of the sampling effect mentioned above. Moreover, the side they fly on their first decision point immediately before the first row of obstacles seems to have a disproportionate impact on the decisions in the rest of the flight. In many cases, most of the steering happens in this first section of the flight, with relatively straight paths thereafter. This is also the section in which birds seem to fly the slowest. The similarity of the portion of each flight immediately preceding the obstacle field with the trajectories observed in preceding experiments [158] is also worth noting. Despite the differences in experimental set-ups, the birds seem to initially fly forward until there is enough information to make a decision. In the first instance, our results still resemble those of experiments with flies and locusts presented with a choice of two spatially distinct options [144]. However, the theoretical modelling Sridhar *et al* suggest for selecting between more than two options does not seem to hold in our data. Their model predicts that when more than two options are available, these are broken down into sequential binary decisions, each averaging the available options. Thus their model would predict pigeons initially fly forwards, then bifurcate into two paths roughly centred between gaps 1 and 2 and 3 and 4, respectively, and continue following a straight path to the average position between gaps 1 and 2 or 3 and 4, before finally bifurcating again to select a final gap. A quick look at the histograms produced by superimposing the trajectories observed in our pigeons (Fig. 3.3, Supplementary Information

3.6.2) reveals this pattern is not followed. Later decision points similarly show a much stronger bias than predicted theoretically. This divergence might be due to broken symmetry, but given our observed effect of previous choices, we hypothesise birds' inertia to continue on the same path is more likely to account for this. Together, these observations suggest that the initial flight section might be where most decision-making happens in short obstacle fields. Flying based on an initial decision could allow birds to enhance the speed and safety with which they fly through clutter, which has been mathematically shown to be advantageous for birds moving through complex environments as individuals as well as in flocks [138]. In minimising steering and the need for further information updating, such a strategy is likely more energetically efficient than alternatives. How could birds choose a steering aim so early on?

The roller door at the end of the room provides a natural target for the birds. However, as pointed out, the roller door also provides abundant natural light. As a result, gaps aligned with the opening would appear brighter independent of any semantic knowledge about the roller door as an exit. Thus, based on brightness, the clearest path to the exit could, in principle, be located near-instantaneously from a single image, as phototactic information is much faster than motion vision to process. Rainforest-dwelling bees are known to use brightness cues to negotiate apertures. They have been suggested to use a brightness-based guidance strategy to identify and navigate through the most obstacle-free paths available [137]. Similarly, our pigeons could use brightness cues to decide which gaps to fly through. This single metric could, in theory, circumvent the potential issue of determining which of the many obstacles around are relevant to deciding between gaps at each time point, which we attempted to capture in our sub-gap variables. Our finding that the initial gap choice is strongly affected by the alignment of gaps with the exit roller door would support this theory. It could also partly explain why most of our pigeons chose the middle two gaps, despite the gaps formed between the walls and an obstacle often being bigger in absolute terms. Based on our data, we cannot distinguish between the roller door's effect being due to it being treated as a semantic goal or

brightness being an attractor in itself. Nonetheless, it is interesting to consider its potential as a complementary mechanism to motion vision for navigating cluttered environments, as each is processed separately [169]. Based on observations in the current and other studies, we hypothesise that brightness information might indeed play an essential role in helping birds quickly identify clear areas. Further studies might consider experimentally manipulating luminance to explore how birds might use brightness to guide their flight through complex environments.

3.5.3 Limitations

Any model of a biological problem is a simplification of reality. Our decision to simplify the analysis of gap selection into a binary choice inevitably conceals some of the complexity in the observed behaviour. This useful simplification allows us to draw comparisons with previous experiments [158]. However, multinomial regression might have been more appropriate to encompass all available options if the gaps closest to the walls had been selected more often. While to the best of our knowledge, the decision criteria we tested cover all measurable environmental characteristics that have been linked to moving through structured environments, it is possible that other factors affected the birds' decisions. In a limited number of trials, video recordings outside the flight hall showed people walking close to the roller door opening, which likely affected bird trajectories, particularly towards the end of the flight hall. Moreover, we did not attempt to include the physiological state of birds in our model, despite evidence that it affects decision-making in a range of contexts [170]. A complete model would likely include some representation of internal factors in a decision function. Here, we were interested primarily in determining how decisions are made in cluttered environments. For our purposes, and given the inherent noise present in biological data, the 86% accuracy of our model captures the data well. However, for predictive purposes, particularly if combining decision outcomes with steering controllers to model entire flights, more powerful models such as contextual bandits would be advantageous.

Another obvious simplification is the arbitrariness of the time points we defined as decision points. As alluded to previously, the timing of decisions is critical to determining the overall shape of a trajectory and therefore merits further investigation. The rich history of the pigeon as a study species is particularly beneficial here, as the neurological correlates of decision-making have been well-studied by cognitive psychologists. Combining recordings of brain activity in free flight with the behavioural modelling suggested here might be a fruitful way to explore real-time decision-making in naturalistic environments, as has been attempted in longer-range navigation studies [171].

3.6 Supplementary Information

3.6.1 Characteristics of animals used during data collection

Name	Ring number	Colour	Year	Weight (g)
A27	A36127	BB	2011	474
A33	A36133	RB	2011	432
B01	B46901	B DK CH	2012	508
B62	B46862	DK CH	2012	484
B65	B46865	BB Pied	2012	493
B69	B46869	BB WT	2012	466
B73	B46873	BB	2012	469
B80	B46880	B DK CH	2012	472
D00	D44800	CH	2010	465
D01	D44801	Red	2010	468
D10	D44810	BB	2010	501
D12	D44812	DK CH	2010	462
K03	K40603	BB	2011	453
S17	S21317	BB	2014	456
S28	S21328	B CH	2014	502
S84	S21284	BB Pied	2014	510
S86	S21286	B CH WT	2014	482

Table 3.4: Birds used for experiments.

3.6.2 2D histograms of routes taken through obstacle configurations

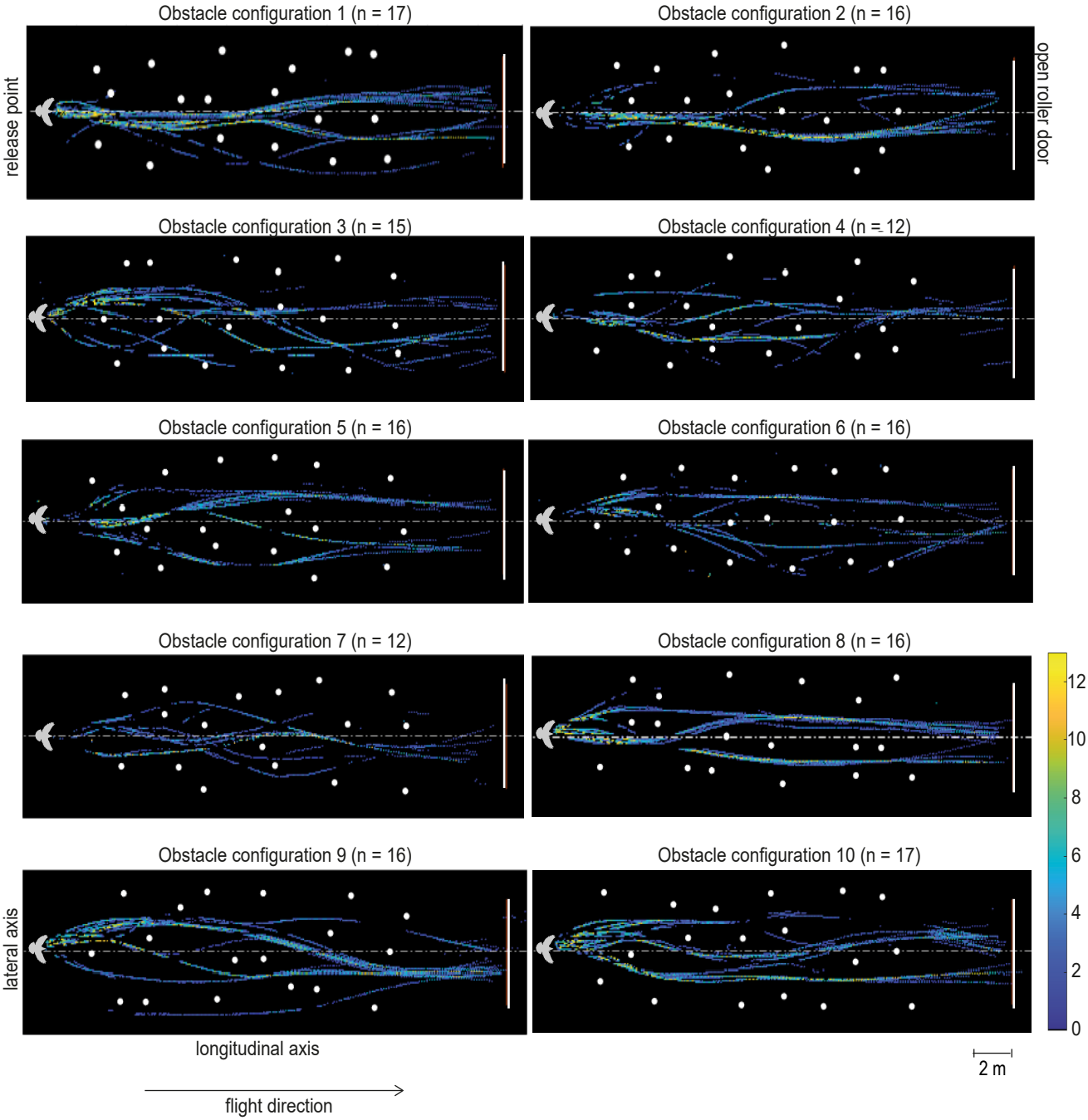


Figure 3.6: 2D histograms of routes taken through obstacle configurations 1-10 White dots represent obstacle positions. The white dashed line marks the midpoint along the transverse of the flight hall. The pigeon release point -represented by a bird silhouette shaded grey- is to the left end of the histogram, with the roller door opening -represented by a light grey line- at the right.

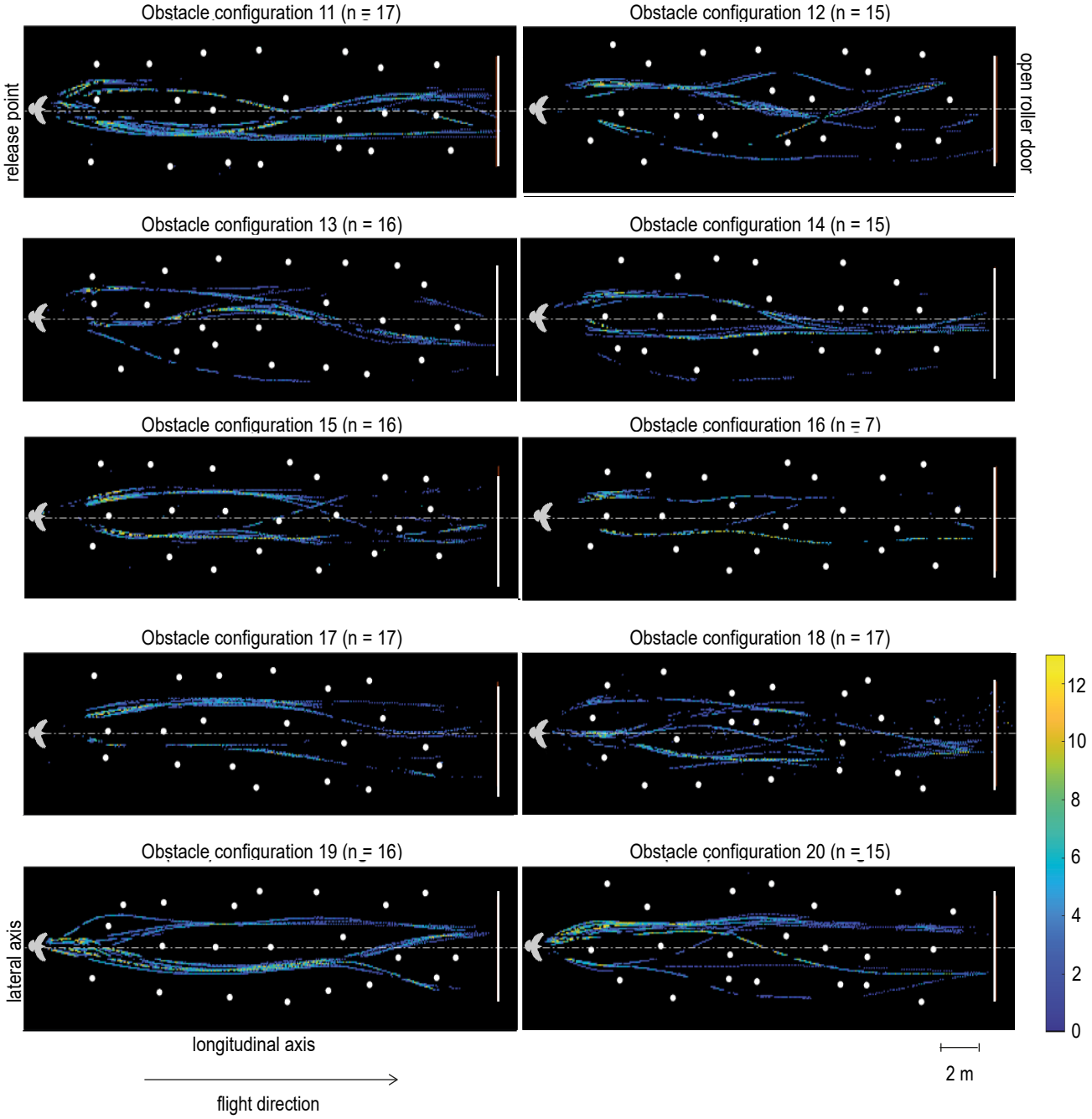


Figure 3.7: 2D histograms of routes taken through obstacle configurations 11-20. White dots represent obstacle positions. The white dashed line marks the midpoint along the transverse of the flight hall. The pigeon release point -represented by a bird silhouette shaded grey- is to the left end of the histogram, with the roller door opening -represented by a light grey line- at the right.

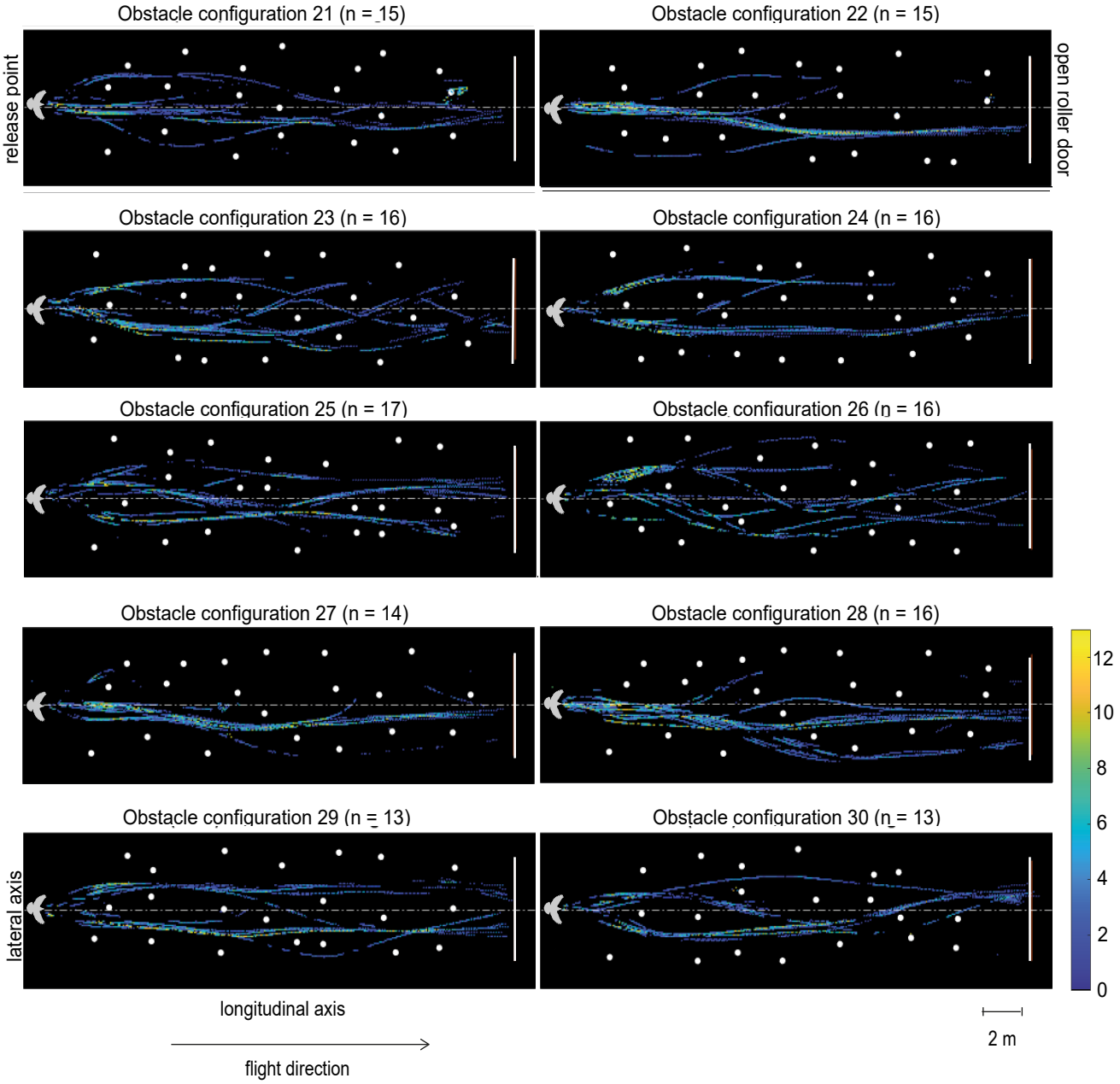


Figure 3.8: 2D histograms of routes taken through obstacle configurations 21-30 White dots represent obstacle positions. The white dashed line marks the midpoint along the transverse of the flight hall. The pigeon release point -represented by a bird silhouette shaded grey- is to the left end of the histogram, with the roller door opening -represented by a light grey line- at the right.

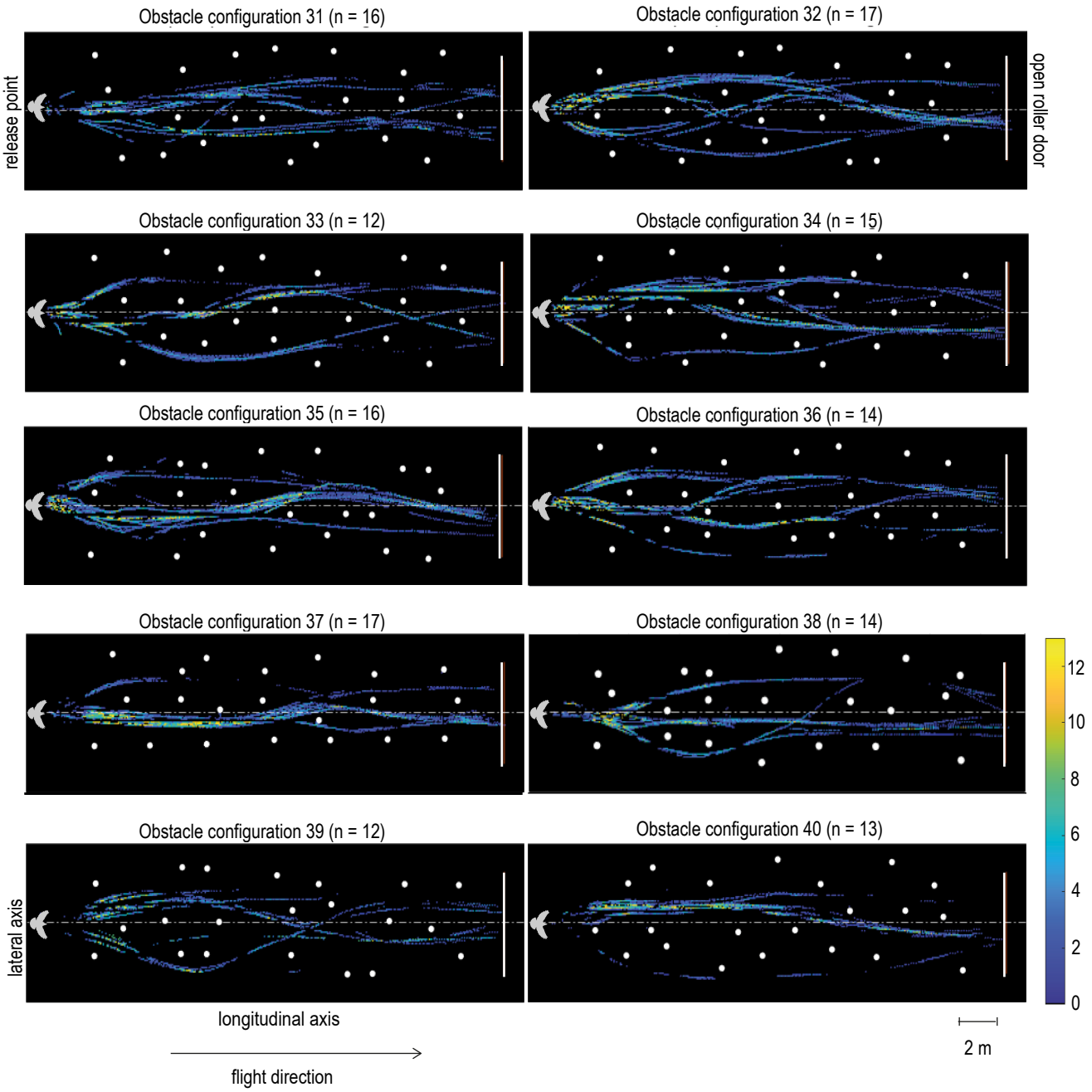


Figure 3.9: 2D histograms of routes taken through obstacle configurations 31-40 White dots represent obstacle positions. The white dashed line marks the midpoint along the transverse of the flight hall. The pigeon release point -represented by a bird silhouette shaded grey- is to the left end of the histogram, with the roller door opening -represented by a light grey line- at the right.

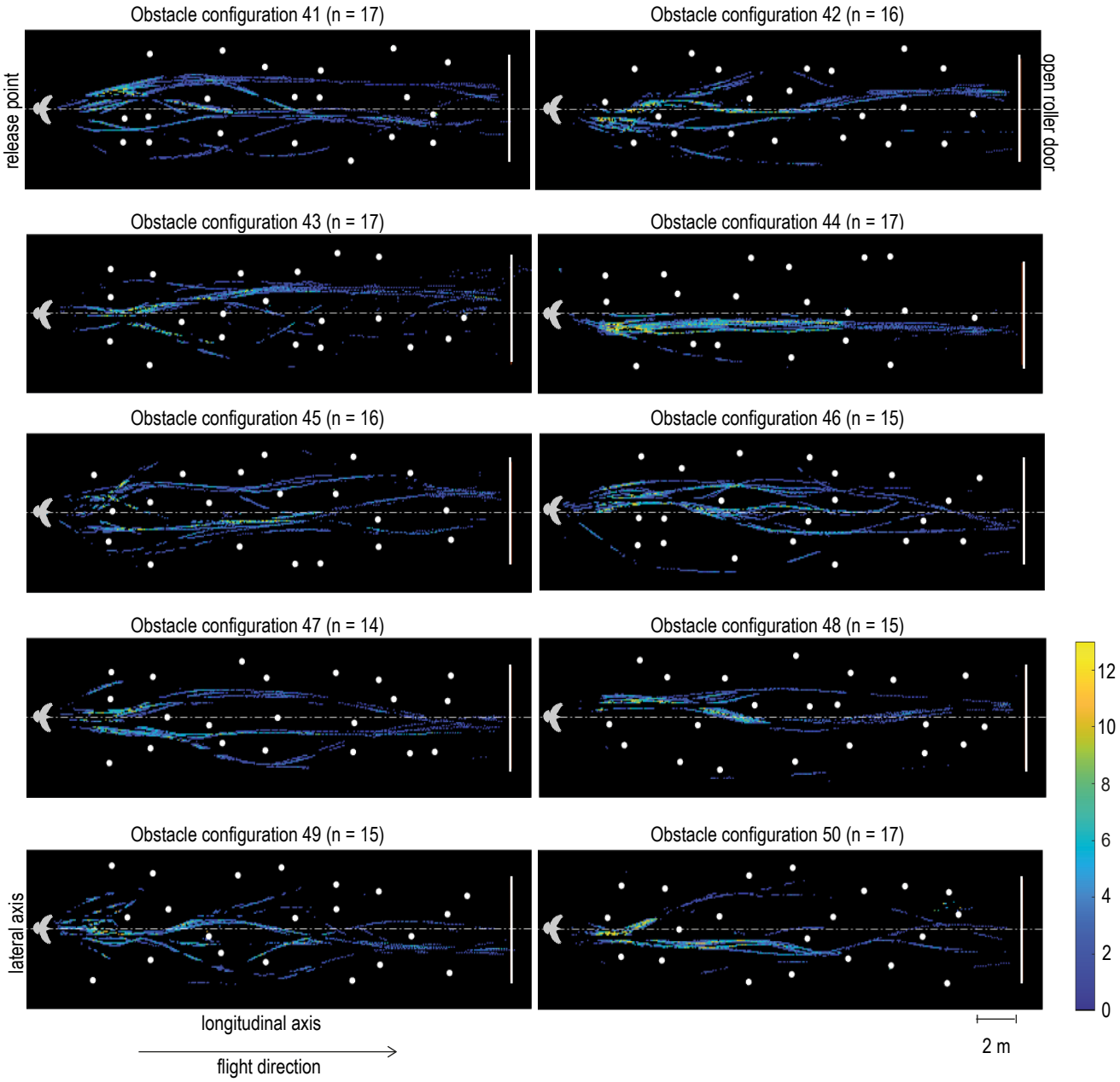


Figure 3.10: 2D histograms of routes taken through obstacle configurations 41-50 White dots represent obstacle positions. The white dashed line marks the midpoint along the transverse of the flight hall. The pigeon release point -represented by a bird silhouette shaded grey- is to the left end of the histogram, with the roller door opening -represented by a light grey line- at the right.

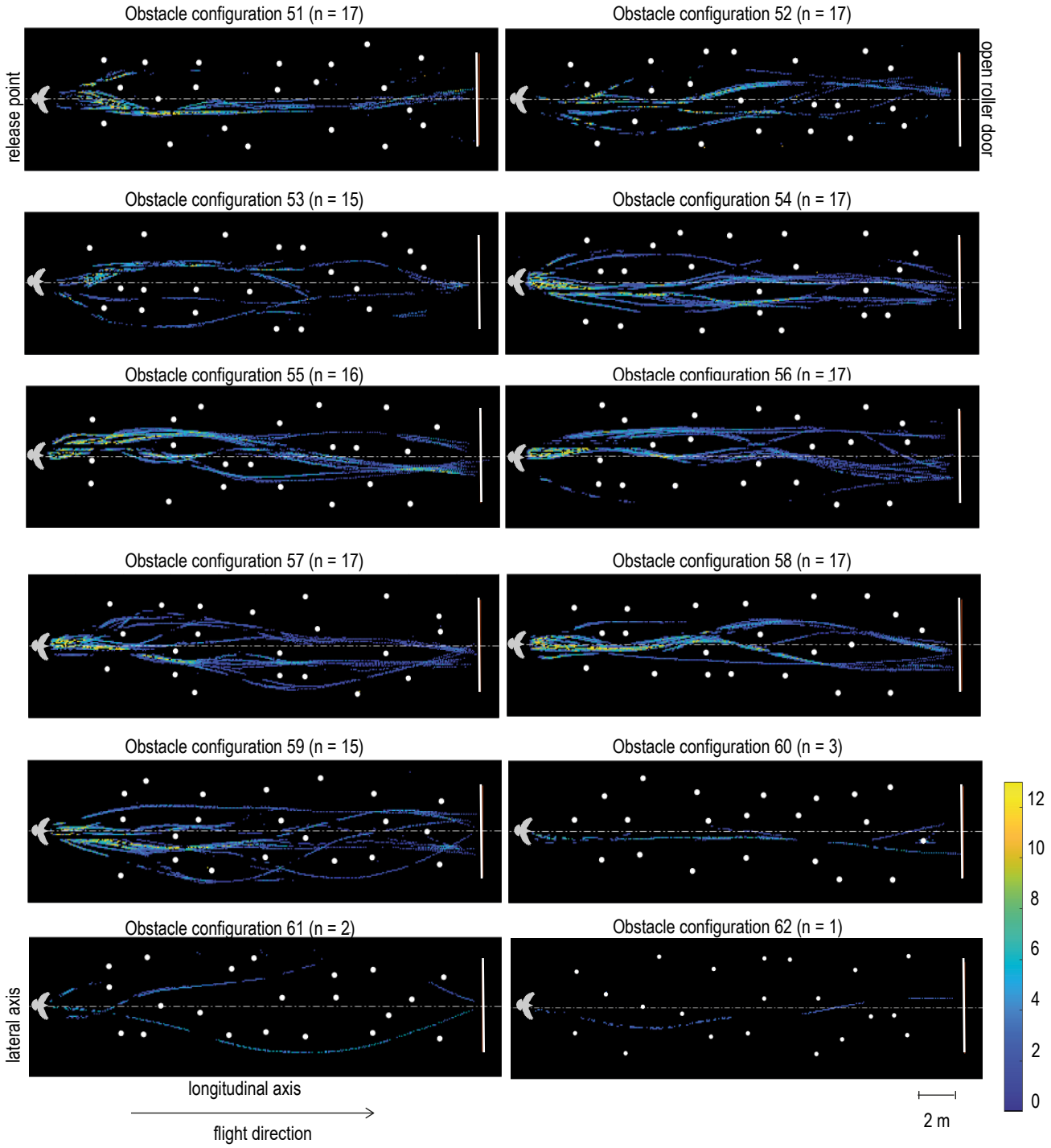


Figure 3.11: 2D histograms of routes taken through obstacle configurations 51-62 White dots represent obstacle positions. The white dashed line marks the midpoint along the transverse of the flight hall. The pigeon release point -represented by a bird silhouette shaded grey- is to the left end of the histogram, with the roller door opening -represented by a light grey line- at the right.

3.6.3 2D histograms of routes taken by individual

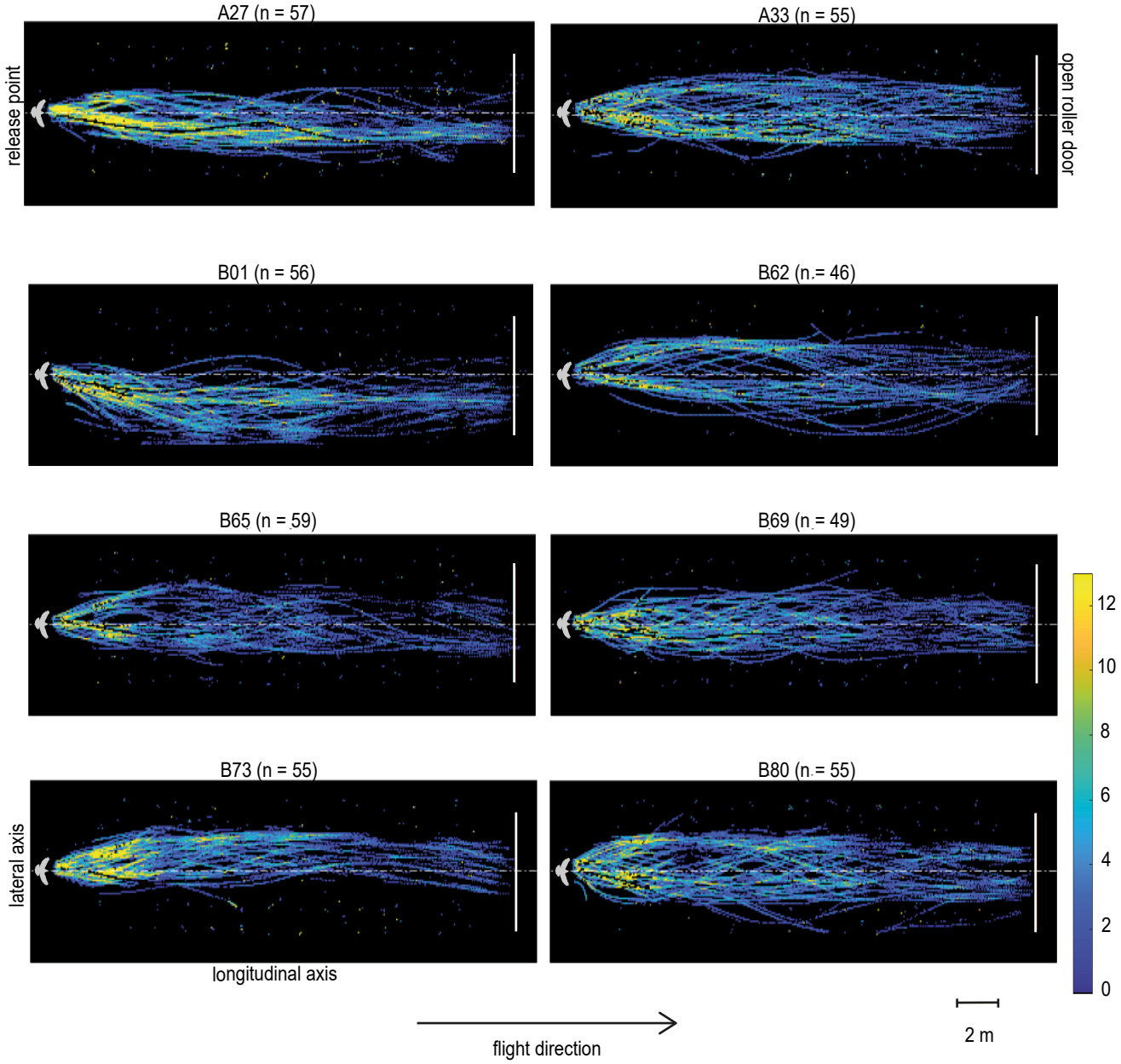


Figure 3.12: 2D histograms of routes taken by individuals A27-B80. Each plot represents all the flights of a single pigeon across different obstacle configurations. The white dashed line marks the midpoint along the transverse of the flight hall. The pigeon release point -represented by a bird silhouette shaded grey- is to the left end of the histogram, with the roller door opening -represented by a light grey line- at the right.

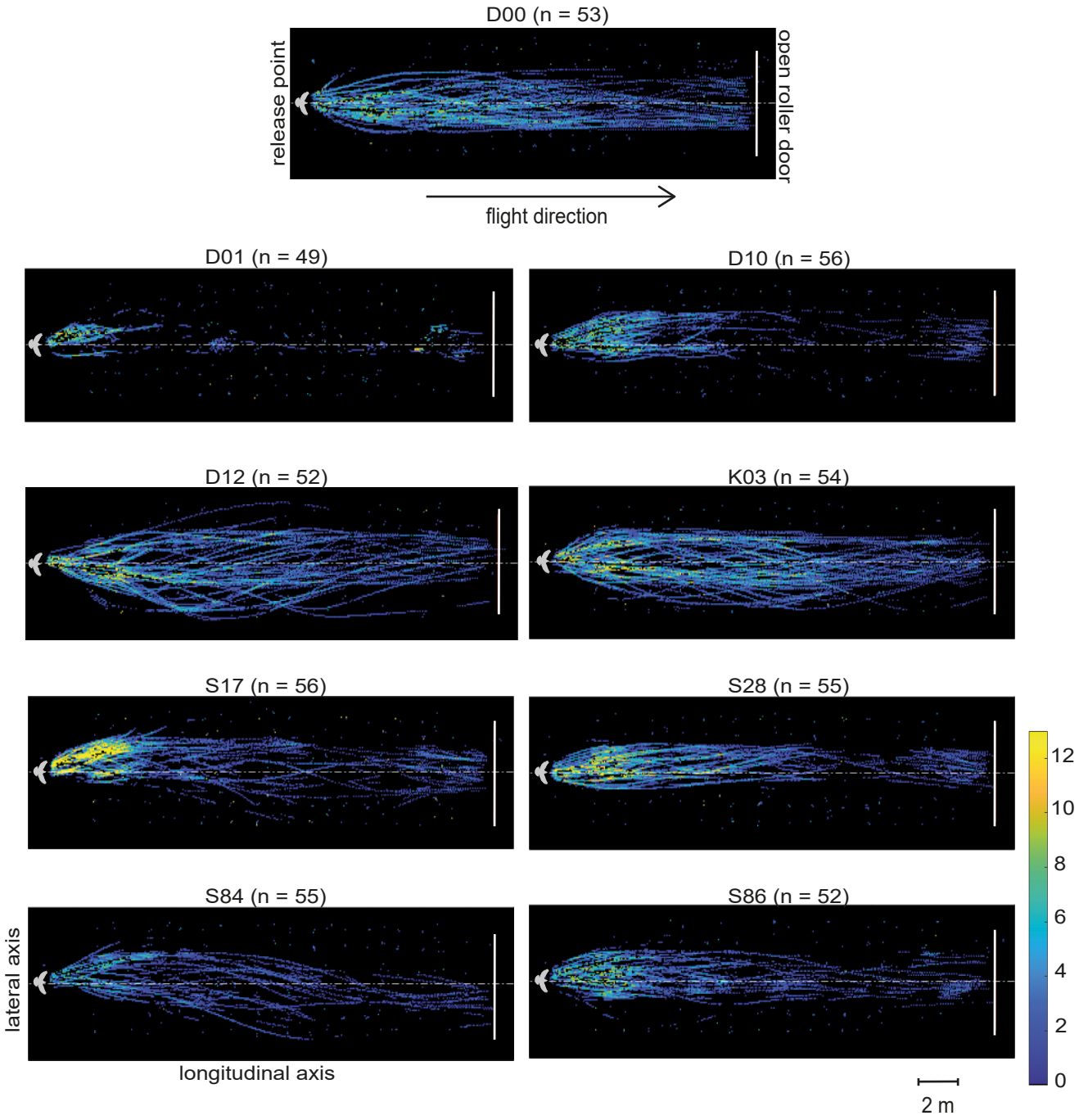


Figure 3.13: 2D histograms of routes taken by individuals D00-S86. Each plot represents all the flights of a single pigeon across different obstacle configurations. The white dashed line marks the midpoint along the transverse of the flight hall. The pigeon release point -represented by a bird silhouette shaded grey- is to the left end of the histogram, with the roller door opening -represented by a light grey line- at the right.

3.6.4 Performance of candidate binomial generalised linear models of pigeon gap choice in an artificial forest of obstacles task.

Table 3.5: Performance of candidate binomial generalised linear models of pigeon gap choice in an artificial forest of obstacles task. Autoregressive terms (AR1 and AR2 -V4a and V4b respectively), exit roller door (ex, V3), cartesian gap size (gC, V1), polar gap size (gP, V2a), size of the gap formed by obstacles in the row to be crossed and row+1 (sg1, V2b), and size of the gap formed by all the remaining obstacles in front of the bird (sg7, V2c) input as factors with two levels. Bird identity (ID, V6) has 17 levels. See the main text and refer to Table 3.1 for further clarification.

Model	**logLik**	**AICc**	dLogLik	**dAICc**	**df**	**weight**
AR1+AR2+ex+sg1+gC+sg7+ID	-1378.0	2802.3	462.7	0	23	0.57
AR1+AR2+ex+gP+gC+sg7+ID	-1378.9	2804.2	461.7	1.9	23	0.22
AR1+AR2+ex+sg1+gP+gC+sg7+ID	-1378.0	2804.3	462.7	2.0	24	0.21
AR1+AR2+ex+sg1+gP+ID	-1386.4	2817.3	454.1	15.0	22	<0.001
AR1+AR2+ex+gP+gC+ID	-1386.8	2817.9	453.8	15.6	22	<0.001
AR1+AR2+ex+sg1+gP+gC+ID	-1386.5	2819.3	454.1	17.0	23	<0.001
AR1+AR2+ex+gC+sg7+ID	-1390.7	2825.8	449.9	23.5	22	<0.001
AR1+ex+sg1+gC+sg7+ID	-1390.9	2826.2	449.7	23.9	22	<0.001
AR1+AR2+ex+gC+ID	-1392.0	2826.4	448.6	24.1	21	<0.001
AR1+ex+gP+gC+sg7+ID	-1391.6	2827.6	449.0	25.3	22	<0.001
AR1+ex+sg1+gP+gC+sg7+ID	-1390.9	2828.2	449.7	25.9	23	<0.001
AR1+ex+sg1+gP+ID	-1401.4	2845.1	439.2	42.8	21	<0.001
AR1+ex+gP+gC+ID	-1401.5	2845.3	439.1	43.1	21	<0.001
AR1+ex+sg1+gP+gC+ID	-1401.4	2847.1	439.2	44.8	22	<0.001
AR1+ex+gC+sg7+ID	-1402.7	2847.8	437.9	45.5	21	<0.001
AR1+ex+gC+ID	-1405.3	2850.9	435.3	48.6	20	<0.001
AR1+AR2+ex+gP+sg7+ID	-1418.3	2881.0	422.3	78.6	22	<0.001
AR1+AR2+ex+sg1+gP+sg7+ID	-1417.8	2882.0	422.8	79.7	23	<0.001
AR1+AR2+sg1+gC+sg7+ID	-1418.9	2882.1	421.7	79.8	22	<0.001
AR1+AR2+ex+sg1+sg7+ID	-1419.2	2882.8	421.4	80.5	22	<0.001
AR1+AR2+sg1+gP+gC+sg7+ID	-1418.6	2883.6	422.0	81.3	23	<0.001
AR1+AR2+gP+gC+sg7+ID	-1419.7	2883.8	420.9	81.5	22	<0.001
AR1+AR2+ex+gP+ID	-1427.1	2896.5	413.5	94.2	21	<0.001
AR1+AR2+ex+sg1+gC+ID	-1427.0	2898.4	413.6	96.1	22	<0.001
AR1+AR2+ex+sg1+ID	-1428.5	2899.3	412.1	97.0	21	<0.001
AR1+ex+gP+sg7+ID	-1430.1	2902.6	410.5	100.3	21	<0.001
AR1+ex+sg1+gP+sg7+ID	-1429.8	2904.0	410.8	101.7	22	<0.001
AR1+ex+sg1+sg7+ID	-1431.5	2905.2	409.2	102.9	21	<0.001
AR1+AR2+gP+gC+ID	-1432.1	2906.5	408.5	104.2	21	<0.001
AR1+AR2+sg1+gP+gC+ID	-1431.8	2908.0	408.8	105.7	22	<0.001
AR1+ex+gP+ID	-1440.9	2922.1	399.7	119.8	20	<0.001
AR1+ex+sg1+gC+ID	-1440.9	2924.1	399.7	121.9	21	<0.001

Table 3.5 – continued from previous page

Model	**logLik**	**AICc**	dLogLik	**dAICc**	**df**	**weight**
AR1+ex+sg1+ID	-1442.7	2925.6	397.9	123.3	20	<0.001
AR1+sg1+gC+sg7+ID	-1442.0	2926.4	398.6	124.1	21	<0.001
AR1+gP+gC+sg7+ID	-1442.3	2926.8	398.3	124.6	21	<0.001
AR1+sg1+gP+gC+sg7+ID	-1441.4	2927.2	399.2	125.0	22	<0.001
AR1+gP+gC+ID	-1458.7	2957.7	381.9	155.4	20	<0.001
AR1+sg1+gC+ID	-1459.4	2959.0	381.2	156.7	20	<0.001
AR1+AR2+sg1+gC+ID	-1459.4	2959.0	381.2	156.7	20	<0.001
AR1+sg1+gP+gC+ID	-1458.6	2959.6	382.0	157.3	21	<0.001
AR1+AR2+gC+ID	-1464.9	2970.2	375.7	167.9	20	<0.001
AR1+AR2+gC+sg7+ID	-1464.9	2972.2	375.7	169.9	21	<0.001
AR1+AR2+gP+sg7+ID	-1466.5	2975.4	374.1	173.1	21	<0.001
AR1+AR2+sg1+gP+sg7+ID	-1466.0	2976.3	374.6	174.0	22	<0.001
AR1+AR2+sg1+sg7+ID	-1470.1	2982.5	370.5	180.2	21	<0.001
AR1+AR2+ex+sg7+ID	-1472.7	2987.7	367.9	185.4	21	<0.001
AR1+AR2+ex+ID	-1475.1	2990.5	365.5	188.2	20	<0.001
AR1+AR2+gP+ID	-1480.6	3001.6	360.0	199.3	20	<0.001
AR1+AR2+sg1+gP+ID	-1480.6	3003.5	360.0	201.2	21	<0.001
AR1+ex+sg7+ID	-1482.5	3005.4	358.1	203.1	20	<0.001
AR1+ex+ID	-1483.8	3005.8	356.8	203.5	19	<0.001
AR1+AR2+sg1+ID	-1485.1	3010.6	355.5	208.3	20	<0.001
AR1+gP+sg7+ID	-1488.5	3017.3	352.1	215.0	20	<0.001
AR1+sg1+gP+sg7+ID	-1488.2	3018.6	352.5	216.3	21	<0.001
AR1+gC+ID	-1490.5	3019.3	350.1	217.0	19	<0.001
AR1+gC+sg7+ID	-1490.3	3020.9	350.3	218.6	20	<0.001
AR1+sg1+sg7+ID	-1493.4	3027.0	347.3	224.7	20	<0.001
AR1+gP+ID	-1506.7	3051.7	333.9	249.4	19	<0.001
AR1+sg1+gP+ID	-1506.7	3053.8	333.9	251.4	20	<0.001
AR1+sg1+ID	-1512.6	3063.4	328.0	261.1	19	<0.001
AR1+AR2+sg7+ID	-1636.8	3313.9	203.8	511.6	20	<0.001
AR1+AR2+ID	-1664.4	3367.1	176.2	564.8	19	<0.001
AR1+sg7+ID	-1665.5	3369.4	175.1	567.1	19	<0.001
AR1+ID	-1687.5	3411.1	153.2	608.8	18	<0.001
AR1+AR2	-1705.0	3416.0	135.6	613.7	3	<0.001
AR1	-1735.5	3475.0	105.1	672.7	2	<0.001
ID	-1840.6	3715.4	0	913.1	17	<0.001

3.6.5 Performance of candidate binomial generalised linear models of pigeon gap choice in an artificial forest of obstacles task.

Bird	Odds right (CI)	Odds largest (CI)	Odds door (CI)
A27	3.31 (1.8, 6.4)	3.67 (2, 7.2)	
A33	1.75 (0.41, 7.45)	9.99 (1.73, 57.97)	6.57 (0.96, 44.81)
B01	14.67 (2.10, 109.49)	2.13 (0.46, 9.79)	24.00 (1.26, 457.33)
B62	1 (0.23, 4.34)	3.6 (0.74, 17.58)	13.33 (1.46, 121.85)
B65	1.73 (0.41, 7.24)	5 (1.04, 24.04)	7.00 (1.03, 47.63)
B69	1.63 (0.38, 7.05)	9 (1.55, 52.38)	7.00 (0.98, 49.85)
B73	0.81 (0.19, 3.38)	6 (1.19, 30.38)	4.67 (0.72, 30.21)
B80	1.43 (0.34, 6.04)	5.22 (1.06, 25.75)	5.38 (0.81, 35.63)
D00	3.08 (0.69, 13.81)	2.79 (0.61, 12.76)	11.75 (1.45, 94.92)
D01	1.07 (0.22, 5.07)	1.38 (0.28, 6.83)	0.50 (0.03, 7.21)
D10	0.81 (0.19, 3.38)	3 (0.66, 13.69)	2.78 (0.42, 18.51)
D12	3.45 (0.74, 16.02)	4.44 (0.89, 22.08)	11.00 (1.20, 101.25)
K03	1.6 (0.37, 6.86)	2.71 (0.59, 12.45)	5.72 (0.83, 39.18)
S17	0.43 (0.10, 1.83)	2.35 (0.53, 10.47)	2.73 (0.43, 17.32)
S28	1.24 (0.30, 5.20)	4.09 (0.86, 19.39)	12.67 (1.38, 115.96)
S84	0.8 (0.19, 3.38)	3.5 (0.75, 16.38)	4.80 (0.62, 37.08)
S86	0.88 (0.21, 3.80)	4.44 (0.90, 22.08)	2.45 (0.38, 15.69)

Table 3.6: Odds ratios of individual birds choosing a gap on the first row based on handedness, gap size or alignment with roller door expressed as odds of choosing the right-hand gap, the largest gap, or the gap most aligned with the roller door with 95% confidence intervals.

References

[23] Eberhard Dodt and Alberto Wirth. “Differentiation Between Rods and Cones by Flicker Electroretinography in Pigeon and Guinea Pig”. In: *Acta Physiologica Scandinavica* 30.1 (1954), pp. 80–89. (Visited on 05/19/2022).

[34] Lance F. Tammero and Michael H. Dickinson. “Collision-Avoidance and Landing Responses Are Mediated by Separate Pathways in the Fruit Fly, Drosophila Melanogaster”. In: *Journal of Experimental Biology* 205.18 (Sept. 2002), pp. 2785–2798. (Visited on 05/18/2022).

[105] Huai-Ti Lin, Ivo G. Ros, and Andrew A. Biewener. “Through the Eyes of a Bird: Modelling Visually Guided Obstacle Flight”. In: *Journal of The Royal Society Interface* 11.96 (July 2014), p. 20140239. (Visited on 05/04/2022).

[111] Kevin J Rounsley and Sally A McFadden. “Limits of Visual Acuity in the Frontal Field of the Rock Pigeon (Columba Livia)”. In: *Perception* 34.8 (Aug. 2005), pp. 983–993. (Visited on 05/06/2022).

[137] Emily Baird and Marie Dacke. “Finding the Gap: A Brightness-Based Strategy for Guidance in Cluttered Environments”. In: *Proceedings of the Royal Society B: Biological Sciences* 283.1828 (Apr. 2016), p. 20152988. (Visited on 05/04/2022).

[138] Partha S. Bhagavatula et al. “Behavioral Lateralization and Optimal Route Choice in Flying Budgerigars”. In: *PLOS Computational Biology* 10.3 (Mar. 2014), e1003473. (Visited on 05/04/2022).

[139] M. Remy and J. Emmerton. “Behavioral Spectral Sensitivities of Different Retinal Areas in Pigeons”. In: *Behavioral Neuroscience* 103.1 (Feb. 1989), pp. 170–177.

[142] Ivo G. Ros et al. “Rules to Fly by: Pigeons Navigating Horizontal Obstacles Limit Steering by Selecting Gaps Most Aligned to Their Flight Direction”. In: *Interface Focus* 7.1 (Feb. 2017), p. 20160093. (Visited on 05/09/2022).

[144] Vivek H. Sridhar et al. “The Geometry of Decision-Making in Individuals and Collectives”. In: *Proceedings of the National Academy of Sciences* 118.50 (Dec. 2021), e2102157118. (Visited on 05/04/2022).

[150] Hans Wallraff. “Navigation by Homing Pigeons: Updated Perspective”. In: *Ethology Ecology & Evolution - ETHOL ECOL EVOL* 13 (Mar. 2001).

[151] Graham R. Martin. “The Subtlety of Simple Eyes: The Tuning of Visual Fields to Perceptual Challenges in Birds”. In: *Philosophical Transactions of the Royal Society B: Biological Sciences* 369.1636 (Feb. 2014), p. 20130040. (Visited on 03/04/2023).

[152] Gordon Lynn Walls. “THE VERTEBRATE EYE AND ITS ADAPTIVE RADIATION”. In: *The Journal of Nervous and Mental Disease* 100.3 (Sept. 1944), p. 332. (Visited on 05/20/2022).

[153] Kevin Healy et al. “Metabolic Rate and Body Size Are Linked with Perception of Temporal Information”. In: *Animal Behaviour* 86.4 (Oct. 2013), pp. 685–696. (Visited on 03/04/2023).

[154] Crlos Martinoya, Jacques Rey, and Susana Bloch. “Limits of the Pigeon’s Binocular Field and Direction for Best Binocular Viewing”. In: *Vision Research* 21.7 (Jan. 1981), pp. 1197–1200. (Visited on 05/06/2022).

[155] Emily Baird et al. “Visual Control of Flight Speed and Height in the Honeybee”. In: *From Animals to Animats 9*. Ed. by Stefano Nolfi et al. Lecture Notes in Computer Science. Berlin, Heidelberg: Springer, 2006, pp. 40–51.

[156] Nellie Linander, Emily Baird, and Marie Dacke. “Bumblebee Flight Performance in Environments of Different Proximity”. In: *Journal of Comparative Physiology A* 202.2 (Feb. 2016), pp. 97–103. (Visited on 03/04/2023).

[157] Partha S. Bhagavatula et al. “Optic Flow Cues Guide Flight in Birds”. In: *Current Biology* 21.21 (Nov. 2011), pp. 1794–1799. (Visited on 05/06/2022).

[158] Natalia Pérez-Campanero Antolin and Graham K. Taylor. *Gap Selection and Steering during Obstacle Avoidance in Pigeons*. Preprint. Animal Behavior and Cognition, Mar. 2022. (Visited on 09/01/2022).

[159] Aaron J Fath and Brett R Fajen. “Static and Dynamic Visual Information about the Size and Passability of an Aperture”. In: *Perception* 40.8 (Aug. 2011), pp. 887–904. (Visited on 05/05/2022).

[160] B. P. Hayes et al. “The Projection of the Visual Field upon the Retina of the Pigeon”. In: *Vision Research* 27.1 (Jan. 1987), pp. 31–40. (Visited on 05/06/2022).

[161] A. Charles Catania. “On the Visual Acuity of the Pigeon1”. In: *Journal of the Experimental Analysis of Behavior* 7.5 (1964), pp. 361–366. (Visited on 05/06/2022).

[162] U. Hahmann and O. Güntürkün. “The Visual Acuity for the Lateral Visual Field of the Pigeon (Columba Livia)”. In: *Vision Research* 33.12 (Aug. 1993), pp. 1659–1664.

[163] Yuichiro Nomura et al. “Evaluation of Critical Flicker-Fusion Frequency Measurement Methods Using a Touchscreen-Based Visual Temporal Discrimination Task in the Behaving Mouse”. In: *Neuroscience Research* 148 (Nov. 2019), pp. 28–33.

[164] M. Tistarelli and G. Sandini. “On the Advantages of Polar and Log-Polar Mapping for Direct Estimation of Time-to-Impact from Optical Flow”. In: *IEEE Transactions on Pattern Analysis and Machine Intelligence* 15.4 (Apr. 1993), pp. 401–410.

[165] Paul Carlile, Richard Peters, and Christopher Evans. “Detection of a Looming Stimulus by the Jacky Dragon: Selective Sensitivity to Characteristics of an Aerial Predator”. In: *Animal Behaviour* 72 (Sept. 2006), pp. 553–562.

[166] Ingo Schiffner et al. “Minding the Gap: In-Flight Body Awareness in Birds”. In: *Frontiers in Zoology* 11.1 (Sept. 2014), p. 64. (Visited on 05/19/2022).

[167] Finnegan J. Calabro, Kunjan D. Rana, and Lucia M. Vaina. “Two Mechanisms for Optic Flow and Scale Change Processing of Looming”. In: *Journal of Vision* 11.3 (Mar. 2011), p. 5. (Visited on 05/06/2022).

[168] W Hodos et al. “Spatiotemporal Contrast Sensitivity in Pigeons”. In: *Investigative Ophthalmology & Visual Science* 43.13 (Dec. 2002), p. 4712.

[169] Klaus Landwehr, Esther Brendel, and Heiko Hecht. “Luminance and Contrast in Visual Perception of Time to Collision”. In: *Vision Research* 89 (Aug. 2013), pp. 18–23. (Visited on 05/18/2022).

[170] Michael Mendl and Elizabeth S. Paul. “Animal Affect and Decision-Making”. In: *Neuroscience & Biobehavioral Reviews* 112 (May 2020), pp. 144–163. (Visited on 05/07/2022).

[171] Alexei L. Vyssotski et al. “EEG Responses to Visual Landmarks in Flying Pigeons”. In: *Current Biology* 19.14 (July 2009), pp. 1159–1166. (Visited on 05/07/2022).

4

Fish gap selection in rubble-like obstacle field

Contents

4.1 Abstract 134
4.2 Introduction 135
4.3 Methods 139
4.3.1 Subjects 139
4.3.2 Experimental tank 140
4.3.3 Experimental procedure 141
4.3.4 Data processing 143
4.3.5 Data analysis 144
4.4 Results 148
4.5 Discussion 153
4.5.1 Visual cues for clutter negotiation 153
4.5.2 Gap selection and individual characteristics 154
4.5.3 Limitations 155
4.6 Supplementary Information 157
References 157

4.1 Abstract

Animals are frequently faced with the challenge of negotiating structured environments during goal-oriented behaviours. Such behaviours may involve an initial search phase aimed at locating the goal, followed by a directed approach phase that

detours around obstacles to reach the goal. Recent work on visually-guided flight through clutter has conceptualised this as a process of identifying and negotiating visual gaps that are broadly aligned with the animal's expected or intended goal. These visual gaps are thereby conceived of as attractors in their own right rather than as features incidental to obstacles acting as repellers. Here we ask whether the foraging behaviour of a visually-guided reef fish, the Picasso triggerfish *Rhinecanthus aculeatus*, can be modelled using similar gap selection algorithms to those used to model visually-guided flight through clutter in birds and insects. Specifically, we test whether their swimming behaviour during goal search and approach is best modelled as a process of sequential gap selection and the extent to which the size of the available gaps and their alignment to the actual or expected direction of the target affects their attractiveness. We test different definitions of gap sizes to deduce the mechanisms triggerfish may be using to extract visual information from their environment during goal-oriented tasks.

4.2 Introduction

Coral reefs are some of the most diverse and structurally complex environments in the world. The heterogeneity and irregularity in topographic elements provide sheltered spaces [172] and physical niches [173] that can support a high level of biodiversity at different spatial scales due to reducing competition and predation. Accordingly, the relationship between structural complexity and species composition has received some attention in the ecological coral reef literature (eg [174] [175] [176] [177] amongst others). The variety of shapes of sessile organisms in reefs, such as scleractinian corals, provide highly complex physical structures for fish to negotiate. However, remarkably little is known about how fish safely move through such complex environments. This study addresses this gap using Picasso triggerfish *Rhinecantus aculeatus*, a shallow water, inter-tidal marine fish that occupies brightly lit coral reef areas in the Indo-Pacific ocean. Triggerfish are territorial invertivore predators that typically hunt in rubble areas around coral bommies (see figure 4.1 for an example of their natural habitat). They are known to overturn rubble and break

apart corals to expose hidden invertebrates [178]. Feeding in areas where physical obstacles often move around due to weather, tides and wave action makes triggerfish likely to have developed an efficient method to guide their movement through cluttered environments. Here, we ask what cues triggerfish may be attending to in identifying and locating clearances that they can safely traverse while homing in their desired direction. Studies in terrestrial species that habitually move through highly structured 3D environments such as rainforests and cities have suggested that birds aim toward the largest visual gaps available to avoid colliding with obstacles [105]. Likewise, insects use brightness cues to locate sufficiently large gaps to negotiate safely while flying [137]. For underwater species, light comes from a much narrower window from above than in animals living with a view of the sky, and triggerfish typically don't have overhanging structures as insects and birds do. As a result, different mechanisms may be at play. But, to the best of our knowledge, no such studies have yet been carried out in aquatic ecosystems to understand what cues animals may be using while navigating complex environments. Investigating how fish solve tasks that have been studied in air-dwelling and terrestrial organisms, we can learn whether mechanisms involved in negotiating structured environments are highly conserved, likely due to their robustness, or how they may have changed as a response to differing habitats. Such information could shed some light on how navigation systems evolved in animals.

In this study, we wanted to focus on how visual cues are used for obstacle negotiation. Vision is a powerful sensory system that guides a wide range of behaviours in many aquatic organisms, particularly in shallow coastal habitats such as coral reefs [179] where light is readily available. For this reason, we chose an intertidal species that live in shallow waters for our study. Accordingly, our study species have a highly developed visual system with high visual acuity alongside full-colour vision. *Rhinecanthus aculeatus* are trichromatic, housing three spectral types of visual pigments in single and double cones [115]. Behavioural experiments have estimated their visual acuity to be 1.75 cycles per degree [180], but anatomical investigations suggest a higher acuity of 6.8 cpd for ganglion cells [181]. However,

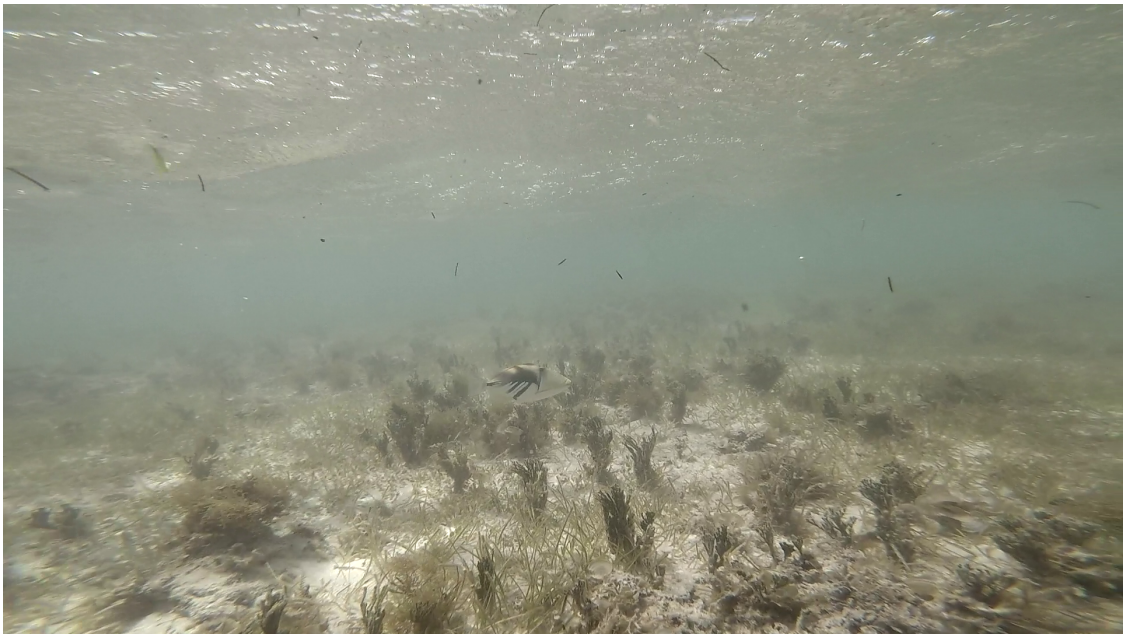


Figure 4.1: The natural habitat of Picasso triggerfish. Note the scene is mostly flat with many vertical obstacles. In low tide, when the water level is reduced (lower than depicted here), the navigational challenge of avoiding collisions takes place mostly along the horizontal axis. Our experimental design echoes these conditions.

the conditions of vision underwater can be more challenging than in air due to the optical properties of light propagation, namely absorption and scattering. These can cause problems in image formation in several ways. Firstly, suspended matter in water, such as bubbles, particles of sand, and tiny organisms, block light and generate noise. With wavelength-dependent light attenuation effects, this can reduce visibility and distort colours. The movement of tides uplifting sediment makes this a particular problem for intertidal species. Secondly, the refractive index of water changes with salinity and temperature, which can make position estimation difficult, particularly at a distance when environments between a viewer and an object might be different. Underwater visibility can be quite variable but is typically in the range of 1-10 metres. Therefore, in moving through structured environments, highly visual aquatic species such as triggerfish are likely to attend to features within a shorter range than might be expected in aerial environments. As with other species, triggerfish can also use information from other senses, such as the lateral line, a hydrodynamic receptor system found exclusively in aquatic vertebrates [182]. While experimental evidence suggests that the lateral line can detect small objects, it

is primarily used at very close range, and during poor visibility conditions [183]. Given their visual system and environment, *Rhinecanthus aculeatus* are therefore unlikely to use the lateral line to negotiate environmental clutter.

From a motor perspective, water is a much denser fluid than air. It follows that the frictional and pressure drag, lift and acceleration reaction -and as a result, the effective cost of transport- are typically more extensive in aquatic dwelling organisms than in air [184]. We might therefore expect manoeuvres to avoid obstacles to be harder to implement in water. Nevertheless, triggerfish display several adaptations suggestive of optimising for manoeuvrability. Like other balistids, they use median paired fin (MPF) locomotion, which is believed to allow greater agility and stability than the body caudal fin swimming typical of most fish, partly due to reducing drag [185]. MPF swimming involves undulating the paired pectoral fins located on the sides while keeping the body rigid. Together with the caudal fin, which provides rapid direct forward propulsion, these control steering in Rhinecanthus. The dependence on median fins for swimming has caused the triggerfish's 2nd dorsal and anal fins to enlarge and become very flexible, allowing undulatory waves that are passed through their length to produce thrust in several directions, including backwards [186]. Moreover, their laterally compressed bodies are thought to facilitate sharp turns, and rapid acceleration [187]. As a result of these adaptations, we expect triggerfish to be able to efficiently move through much narrower spaces than equivalently sized fish adapted to high-speed swimming might. Consequently, the size of clearances might have less impact than factors such as target location on which gaps they choose to move through than has been observed in birds and bees.

Conventional paradigms for navigating structurally complex environments are typically based on having an almost complete representation of the surrounding space, which is then used to plan the safest or most efficient path to a target. Triggerfish regularly navigate between their home nest in the highly structured reef zones and adjacent foraging areas over coral rubble that has been broken up by erosion. Waves and tidal movements create intermittent water currents of variable strength, direction and turbulence, which can cause the environment to undergo

sporadic and sometimes rapid changes. In this habitat, having almost-complete knowledge of the environment seems unlikely. Moreover, in intertidal areas, even obstacles that remain in roughly the same place tend to be in constant flux due to water movements. Taken together, these characteristics of the natural habitat of Picasso triggerfish suggest that they might be better adapted to reacting to obstacles in their environment rather than planning paths into the future to avoid them. We, therefore, hypothesise that R. aculeatus react to obstacles over short distances and time scales based on local information and simple rules. To test this, we explore the responses of triggerfish to complex environments in a task consisting of traversing an array of vertical poles in an experimental tank to reach a food reward. The simplified setup reduces steering responses to the horizontal plane, likely to be dominated by visual cues, to understand better the factors that affect route choice. The familiarity of the fish with the tank and its scale also minimises the global navigation challenge, as the fish know to expect a food reward on the side of the tank opposite to where they entered. We formulate the problem as a gap choice experiment, examining how characteristics of the visual environment (such as gap size) and individual characteristics of the fish (such as their body size) affect the sequence of gaps the fish selected. Simplifying the question of how fish move through highly structured environments such as coral reefs in this way allows us to make deductions about the mechanisms used for underwater navigation in a species highly adapted to moving in a complex 3D habitat.

4.3 Methods

4.3.1 Subjects

The Animal Welfare and Ethics Review Board (AWERB) of the University of Oxford's Department of Zoology approved all experimental and husbandry protocols. Methods were carried out following relevant regulations and the code of practice for the care and use of animals for scientific purposes. A total of five Picasso triggerfish *(Rhinecanthus aculeatus)* were used in this experiment. Fish were purchased from local suppliers and were originally wild-caught. Fish were housed in individual

aquaria ($360 \times 1040 \times 450mm$) in a flow-through marine aquarium system and fed a mixed diet of pellets (Ocean Nutrition, Formula One Marine Pellet), fish, prawn and cockles. All fish had live rock and a commercially available fish shelter in each tank. All five fish were large (total length: Fish $38I = 165mm$, fish $39J = 155mm$, fish $40M = 130mm$, fish $41N = 126mm$, Fish $30 = 128mm$), and all had previous experimental experience in the same tank used for this study [188].

4.3.2 Experimental tank

Experiments were run in an experimental tank ($600 \times 1000 \times 450mm$) divided into two sections with an opaque white acrylic board. The water in the experimental tank was kept at $200mm$ depth. It was removed at the end of every day and refilled from the same supply as the home tanks every morning. This ensured that the water in the home and experimental tanks had the same temperature and chemistry. The smaller section of the experimental tank ($600 \times 215 \times 450mm$) acted as a refuge for the fish and had two commercial aquarium rock shelters identical to those found in the fish's home tanks. An opaque white wall with a guillotine door divided the refuge from the main testing area. This wall had two perforated sections to allow water to flow through the tank. The main testing area ($600 \times 740 \times 450mm$) had an acrylic board on the bottom. A white acrylic board also covered the experimental tank's end opposite the refuge area and guillotine door. Hook and loop dots (Velcro Brand, $19mm$ coins) were attached to this backboard to hold food pots in place.

Food pots consisted of small plastic Petri dishes (diameter: $35mm$, depth: $10mm$) filled with agar jelly that held a single food pellet in the centre. Food pots were made by mixing 3 g of agar-agar powder (Special Ingredients Ltd) with $225mL$ of reversed osmosis filtered (RO) water and following package instructions. Approximately one teaspoon of the mixture was added to each petri dish with a single pellet. The mixture was allowed to set before starting experiments. Fresh pots were made daily to ensure the food reward remained attractive to the fish [188]. In the backboard of the experimental tank, three possible positions for the food pots (F1–F3 were spaced equally along the board at a height of $100mm$) 4.2. The

position of the food pot used for each trial was randomly allocated. All fish were given opportunities to explore these pots in their home tank before experiments started, and all subjects were able to find and remove the food pellet from within.

In experimental trials, 20 vertical obstacles were pseudo-randomly positioned between the opaque white wall that divided the experimental and shelter area and the backboard at the opposite end of the tank. Each obstacle consisted of a $250mm$ tall, $20mm$ diameter white acrylic cylinder positioned at the bottom of the tank to protrude vertically just above water level. The obstacles were arranged in a regular grid so that a fish's trajectory could be divided into distinct decision points at each row. However, we also wanted to have the obstacles change positions from trial to trial to allow for variation in environmental features and to preclude learning. Therefore, the grid locations consisted of chevrons with six available positions where an obstacle was semi-randomly placed in each trial (Fig 4.2). Within each chevron, the distance between the two forward-most and two back-most positions of a chevron was $80mm$. Neighbouring chevron locations were also separated by $80mm$. This positioning ensured the fish had enough space to manoeuvre while keeping a high density of obstacles. It also meant the first obstacle encountered would be at most one body length from the guillotine door, and the food pot would be approximately one body length from the last obstacle encountered.

4.3.3 Experimental procedure

At the beginning of each testing session, a fish was caught with a net and a bucket and moved from its home tank to the holding area of the testing tank with the guillotine door down. A video camera (GoPro Hero 5. Resolution: 1080p, frames per second: 60, field of view: linear) placed above the tank was turned on. The fish was given five minutes to acclimate to the experimental tank after which experimental trials could begin.

To begin the experiment, the guillotine door was opened. The trial start time was recorded as the time at which the fish's forward-most tip crossed the door. The end time was considered to be the point at which the fish bit the food pellet.

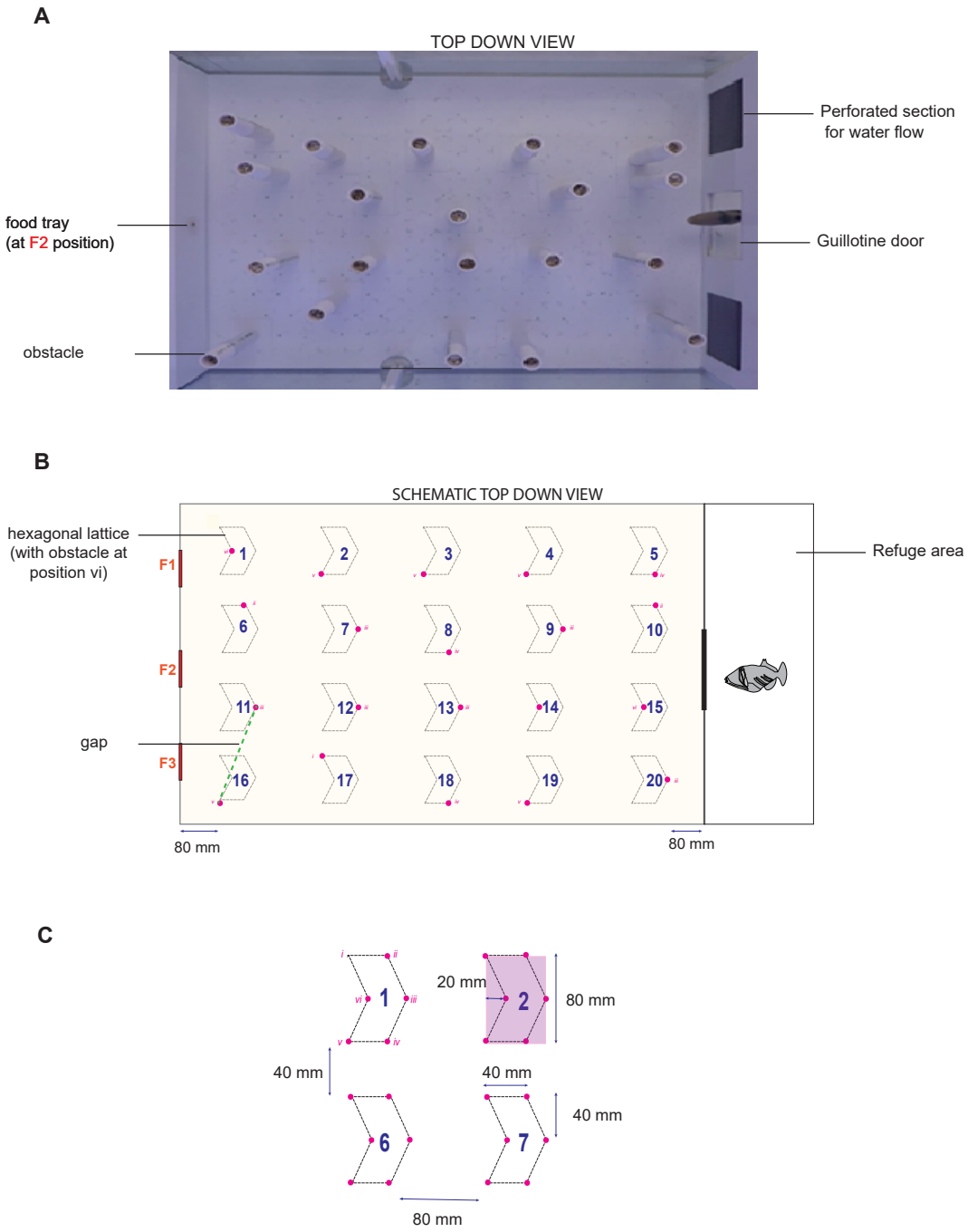


Figure 4.2: Experimental tank. Actual (A) and schematic (B) top-down view showing a sample obstacle distribution in the experimental tank. B) Schematic view of the tank showing grid arrangement used to semi-randomly position obstacles in each trial, formed by five rows of 4 chevrons each. Obstacle positions matching those in A) are shown as pink dots. Rows are formed by contiguous obstacles (eg row 1: obstacles 1-4, row 2: obstacles 5-8 etc). Gaps are defined as the vector between two contiguous obstacles in the same row (example shown in green dashed line). The three available food positions are marked as F1, F2 and F3. (C) Close-up of chevron arrangement.

The fish was allowed to swim freely until it returned to the refuge area, at which point the door was closed. The individual was left to acclimate for approximately five minutes before the next trial while obstacles were semi-randomly re-positioned within their chevrons. Each experimental session consisted of 10 trials, after which the fish was returned to its home tank. Experiments were conducted on weekdays, during which the ten pellets were adequate for daily feeding. On weekends, the fish were given pellets and fish pieces on the first day and a large cockle in the shell on the second day. Each fish completed 100 experimental trials.

4.3.4 Data processing

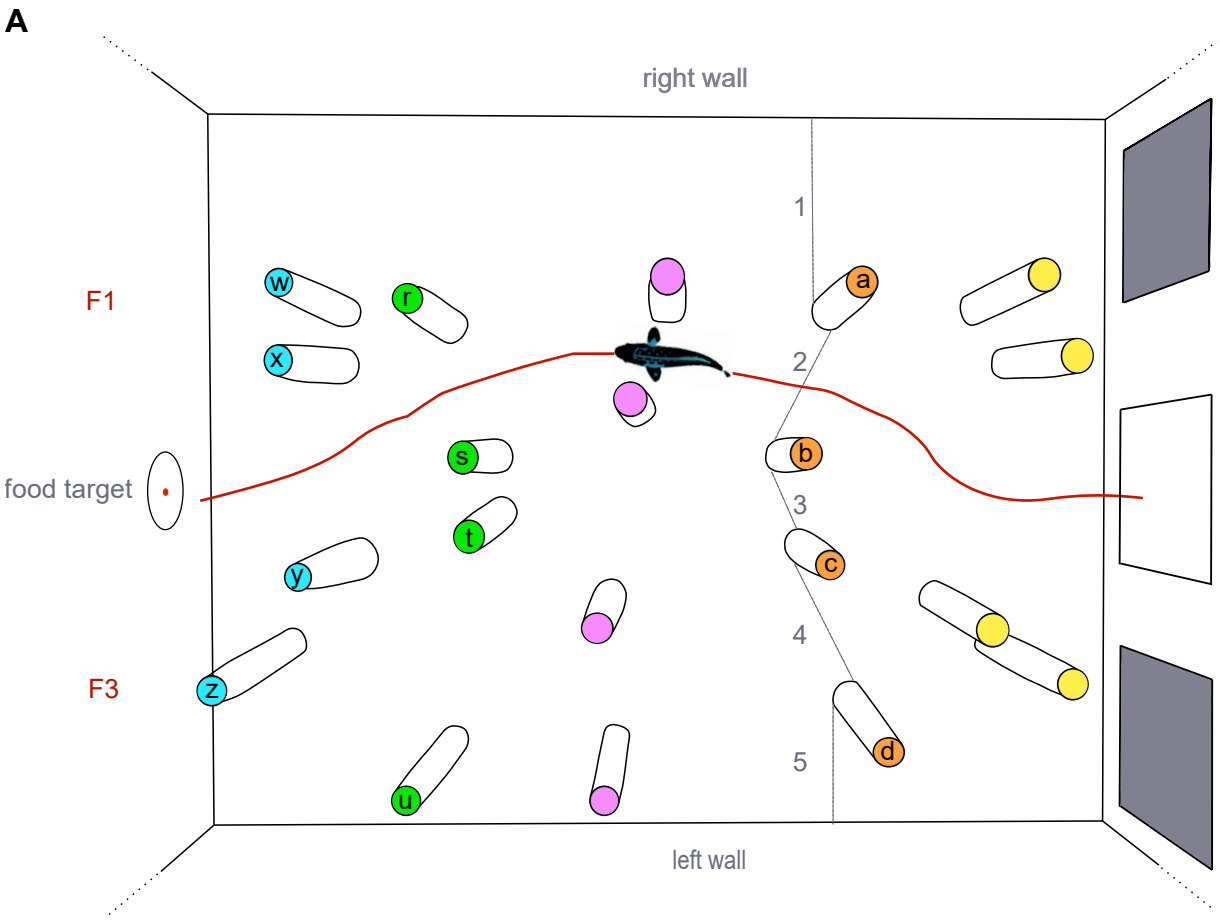
The recorded video covered the main testing area of the tank. The video data was processed using a custom-written program in MATLAB (MathWorks, Natick, MA). The program identified the fish's entire body through a background subtraction method and recorded the centroid of this collection of pixels at a rate of two frames per second. The experimenter manually corrected errors in the background subtraction method and fish tracking. Obstacle and food positions were obtained through manual tracking of the video data. Distance measurements were calculated based on changes in calibrated pixel values using a checkerboard of known dimensions for calibration. Time measurements were calculated to the nearest half-second based on the frame rate of the video analysis. Tracked positions were defined relative to the principal axes of the tank, as determined through the positions of the corners of the tank and floorboard. Any minor discrepancies in the alignment of the axis system between trials were corrected by applying a Procrustes transformation to the camera coordinates prior to further analysis so that the axis definitions for all trials were the same.

This method was however not completely robust to the variation in the experimental dataset due to perturbations in the water and obstacles occluding the fish leading to several trials being unusable. Consequent iterations of data processing, therefore, employed an improved pipeline, using deep learning to track the positions of obstacles and movements of the fish. This was done in collaboration with

Dr Abhiskeh Dutta in the Department of Computer Science. Examples of the outcome of this process are provided in section 4.5 (Fig 4.6). However, the improved data processing could not be completed in time to include a full analysis of the experimental dataset in this thesis. As a result, the analysis presented here is based on a subset of the recorded trials: 10 trials for each fish (a total of 50 trials) that could be reliably tracked in over 80% of frames using the background subtraction method.

4.3.5 Data analysis

To analyse trajectories, each trial was divided into five decision points corresponding to the five rows of obstacles in the experimental set-up (Fig 4.2). For statistical analysis purposes, the decision point was taken to be the position in a fish's trajectory at which it swam past the mean longitudinal position of the obstacles in the previous row (Fig 4.3). While this may not reflect the actual decision point, it provides an objective position at which the fish would have mostly cleared the row of obstacles it was swimming through and would likely shift its focus to the obstacles ahead. Based on the position of the fish at each decision point, we calculated the polar coordinates of the remaining obstacles in front of the fish and those of the food reward. For the first row of obstacles, the decision point was taken to be the position at which the fish's forward-most tip crossed the open guillotine door. This represented roughly the same distance to the first row of obstacles as the median distance between the mean longitudinal position of obstacles in contiguous rows ($\approx 40mm$). At each row, the decision outcomes were determined as gap "choices", where gaps were defined as the virtual gate that would be formed by connecting contiguous obstacles in a row. Thus, each row had five available gap choices. In row 1 these would consist of the virtual gates formed by connecting the right wall with obstacle 1 (gap 1), obstacle 1 with obstacle 2 (gap 2), obstacle 2 with obstacle 3 (gap 3) and obstacle 3 with obstacle 4 (gap 4), and obstacle 4 with the left wall (gap 4) (see Fig 4.2 and 4.3 for reference). Therefore the "choice" of a fish swimming between obstacles 2 and 3 would be recorded as gap 3. This process resulted in 250 observations for initial analysis from 50 trials.


A
right wall
F1
food target
F3
left wall
1
2
3
4
5
w
r
x
s
t
y
z
u
a
b
c
d

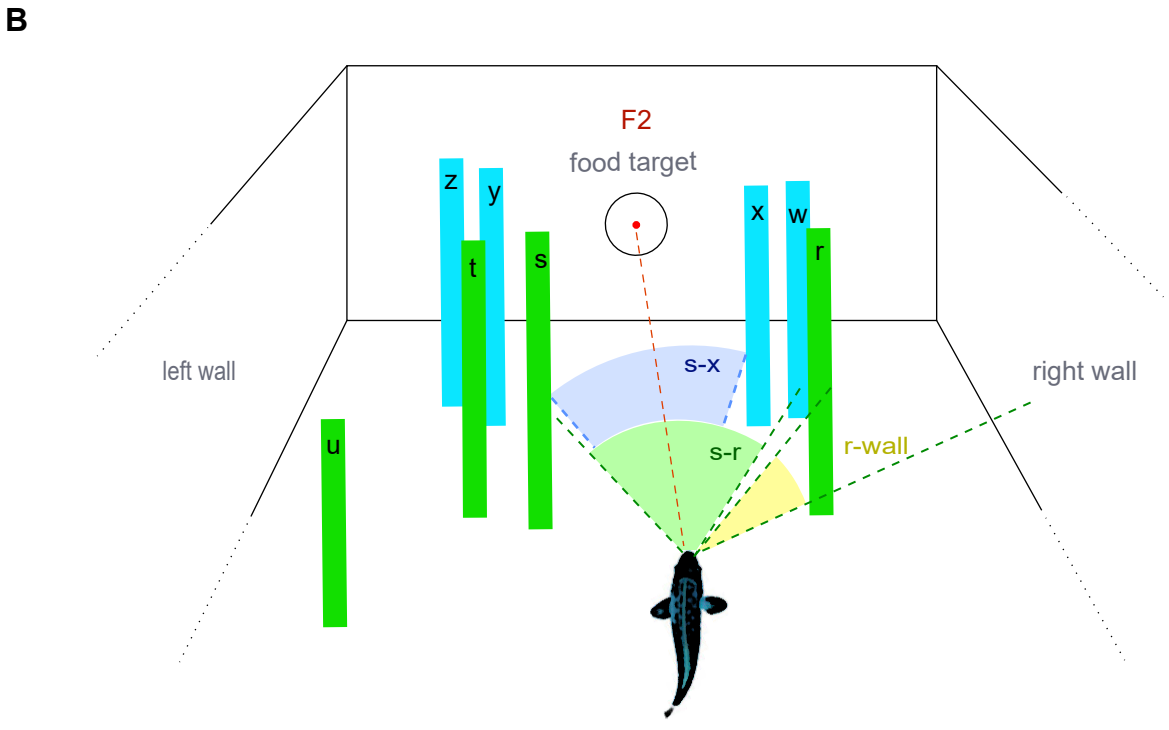

B
F2
food target
left wall
right wall
z
y
t
s
x
w
r
u
s-x
s-r
r-wall

Figure 4.3: Depiction of trial variables captured in statistical model. **A** Top-down illustration of the experimental tank during a sample trial. Obstacle positions are shown as columns coloured by row. The tracked path is shown as a red line. The path spans from the opening of the gate that connects the experimental area and the refuge area, depicted as a rectangle to the right, to the petri dish containing a food reward to the left (shown as a red dot). The petri dish shown is depicted in the middle out of the three positions for the food reward, F2. The other two alternative positions for the food reward are marked on the illustration as F1 and F3. A fish is shown swimming between obstacles in the third row of obstacles (coloured pink). This position, at which the fish has cleared the midpoint of the obstacles in row 3, would be considered the "decision point" for the next row of obstacles (row 4, shown in green). Numbered gap choices are depicted for row 2 only for clarity. The grey lines connecting contiguous obstacles in row 1 depict the physical gap between obstacles (model predictor 1). **B** Frontal view of the inside of the tank depicting the fish in the same position as in (A). From this "decision point", visual gap sizes are measured to determine model predictors **2a), 2b), 2c)** (see main text). Green dashed lines to two of the obstacles in the row and to the right wall show how angles are obtained using the polar vectors to obstacles, and to a virtual position in the wall of the tank matching the mean longitudinal position of the obstacles in that row. The largest angle between these vectors (**2a)**) is shaded in green, corresponding to gap 2 of the fourth row of obstacles (predictor **2a)**: gap 2). Visual gap 1 in row 4, formed between the wall and the rightmost obstacle (r) is shaded yellow. The red dotted line shows the vector to the food reward from the fish's vantage point at the decision point for row 4, which falls between obstacles s and r (predictor **3)**: gap 2). Blue dotted lines show vectors to obstacles in rows_t and row_{t+1}, taken as an ensemble to calculate the size of 'sub-gaps'. In this case, the largest visual gap between obstacles in rows 4 and 5 from the vantage point of the fish is between obstacles s and x, shaded blue, which falls within gap 2 of row 4 (s-r). Predictor **2b)** would therefore be recorded as gap 2. The same process is followed to determine predictor **2c)**. In this example, gap choice at $\text{row}_{t\text{-}1}$ (row 3) would be recorded as gap 2.

To develop an empirical model of fish behaviour through cluttered environments, three physical features of the obstacle-laden tank were identified and then tested for their ability to predict fish behaviour: **1)** physical distance between obstacles, **2)** visual (angular) distance between obstacles, **3)** alignment with a food reward. 1) and 2) (depicted in Fig. 4.3) were chosen to verify whether larger gaps are chosen and to determine what sensory cues fish may use to judge gap size. Due to the virtual nature of visual gaps, **2)** was further subdivided into three alternative definitions of a visual gap: **2a)** visual distance between obstacles in the row immediately ahead of the fish, **2b)** visual distance between obstacles in the two rows immediately ahead of the fish and **2c)** visual distance between all the obstacles lying between the fish and the end of the tank containing the food (see Fig 4.3). These divisions were made to indicate the rough distance at which obstacles in front of the fish affected its trajectory, with **2a)** representing the most myopic view of the obstacles and **2c)** representing the most long-sighted view of the obstacles. **3)** was chosen to indicate the role of directionality on the fish paths. Successful navigation involves getting closer to a desired location

over time, which following a strategy of choosing gaps based on size alone would not provide. The variation in food position allowed us to test the effect of target position on fish trajectories. Additionally, we tested for **4)** the effect that previous gap choices had on the current choice, as we hypothesised fish would be more likely to continue swimming in the same direction they were in due to momentum. The variables were determined as follows: **1)** was calculated based on the Cartesian coordinates of the obstacles in the row to be crossed; **2a)**, **2b)** and **2c)** were calculated using the polar coordinates of the obstacles ahead from the fish's vantage point at the defined decision coordinate (see Fig. 4.3); **3)** the polar coordinates of the food target were used to determine which gap it was viewable through; **4)** gap choices were determined by identifying the positions at which the fish's trajectory intersected virtual lines connecting contiguous obstacles within a row.

Generalised linear mixed effect models were used to test for the effects of gap size, alignment with food target and previous gap choice (**1), 2a), 2b), 2c), 3)** and **4)** above) on the gap fish swam through, with fish as a random variable to control for repeated measures. Predictor variables were coded as factors with two levels, corresponding to whether or not the fish went through the largest gap, the gap most aligned with food or the same gap as in the previous row. Odds ratios from the logistic regressions were computed by exponentiating the logistic regression coefficients. We used likelihood ratio tests to assess the significance of the model factors at $\alpha = 0.05$; Wald tests to compute the significance of differences between levels, and profile-likelihood 95% confidence intervals to quantify the uncertainty in the parameter estimates. We approximated a null expectation of how likely a fish was to go through a particular gap based on each gap's "capture area": its width relative to that of the tank. We tested our predictors including this term as a fixed effect in our model to control for the expected chance level of random movement falling into the chosen gap (sampling effect). We used Cramer's V to quantify the associations between the gap chosen and the numbered gaps with the highest level of each of the explanatory variables per row (see Fig 4.3). All statistical analyses were conducted in R version 4.1.1 (RCoreTeam 2021), using the packages lme4

to construct generalised mixed effects models (GLMMs) and bblme to estimate generalised linear model (GLM) parameters using maximum likelihood.

4.4 Results

The trajectories of fish were recorded as they traversed the obstacle set-up. Upon the guillotine door being opened, the fish entered the main experimental area of the tank. All fish successfully retrieved the food pellets on the opposite side of the tank.

The fish swam mostly through the middle of the tank (fig 4.5), with 51.2% of the 250 observed gap crossings being through the middle gap (gap 3). This preference was even more pronounced in the first row, where the fish chose the middle gap on 74% of the gap crossings and did not go through the outermost gaps (gaps 1 and 5) in any of the 50 trials (Fig 4.4). To check whether this bias may have been a result of our obstacle positioning, we checked the size distribution of gaps formed by the pseudo-randomly positioned obstacles. We found the gaps formed by the three rightmost obstacles and the right wall had roughly equal probabilities of having the greatest absolute clearance out of all the gaps in a given row (from right to left: 23.2%, 26%, 24.4%, 23.6%), but the gap formed by the leftmost obstacle and the left wall was the largest in only 2.8% of the 250 instances of rows. This effect was therefore unlikely to be caused by the absolute distance between obstacles alone. Indeed, out of the four definitions of gap size we tested (**1), 2a), 2b), 2c)**), the absolute distance between adjacent obstacles (**1)**) was the least likely to have an effect on gap choice (GLME estimate: -0.5, CI: -0.7, -0.2).

The explanatory variables that were most likely to have an effect on gap choice were the position of the largest clearance looking a row ahead (**2b)**, GLME estimate: -2.2, CI: -2.6, -1.8), and the position of the food pellet (**3)**, GLME estimate: 2.1, CI: 1.7, 2.5). Including these in a model of the data led to the largest decrease in AIC value (**2b)** dAIC: 186; **3)** dAIC: 173). These were closely followed by the other two variables measured based on the fish's vantage point: the angular size of the gaps ahead (**2c)**, GLME estimate: -1.8, CI: -2.2, -1.5, dAIC: 143) and the largest angular clearance when all obstacles ahead were taken into account (**2a)**,

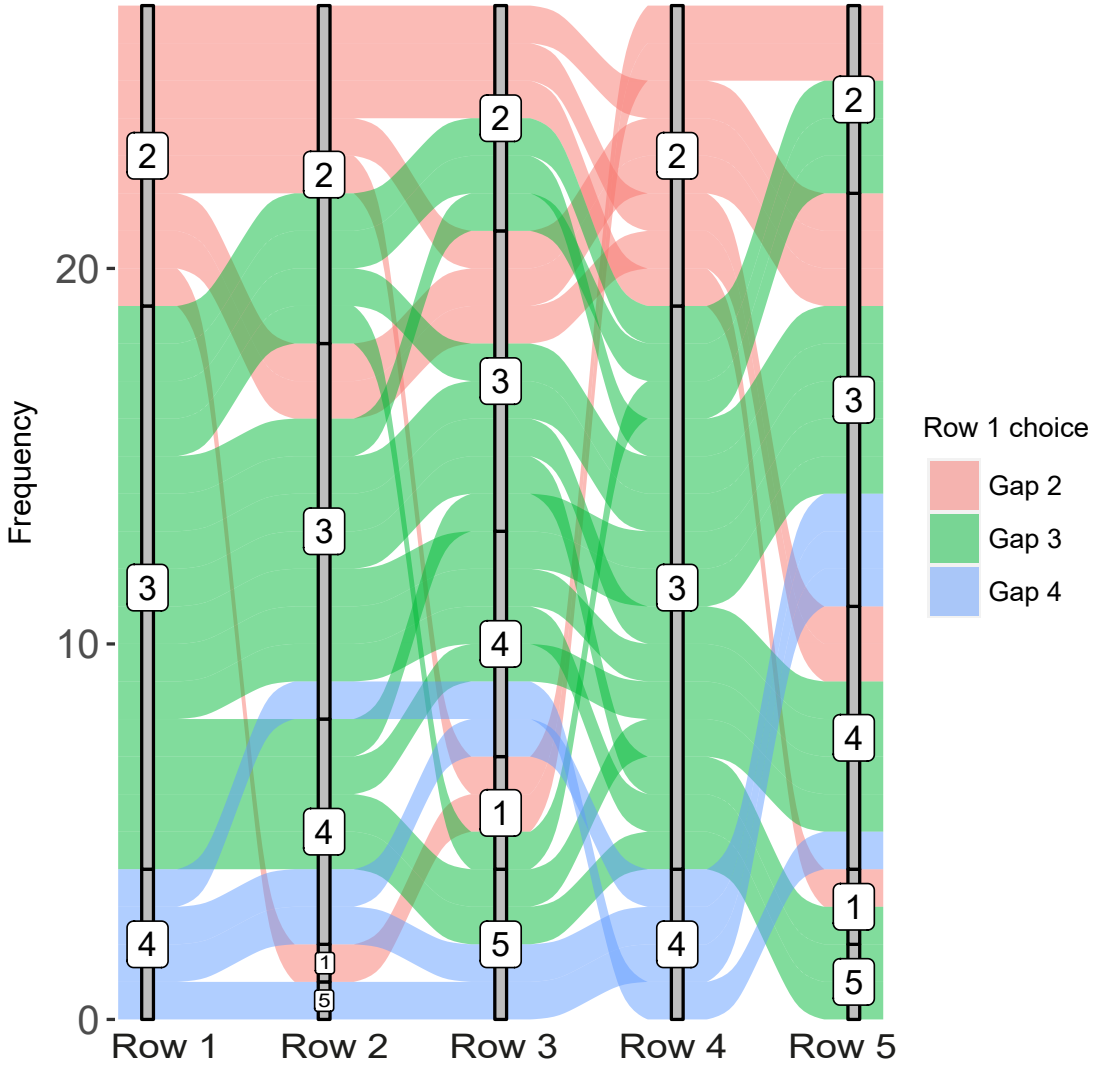


Figure 4.4: Alluvial plot depicting the frequency of gap choices. Grey bars show the proportion of each gap choice for each row. The small (or nonexistent in rows 1 and 4) portion of the grey bars for gaps 1 and 5 shows the fish barely swam down the sides of the tank. The flow of gap choices is represented by alluvia, with each alluvium representing an observed sequence of gaps. The width of alluvium represents the frequency of a given sequence. Colour represents the choice taken at row 1.

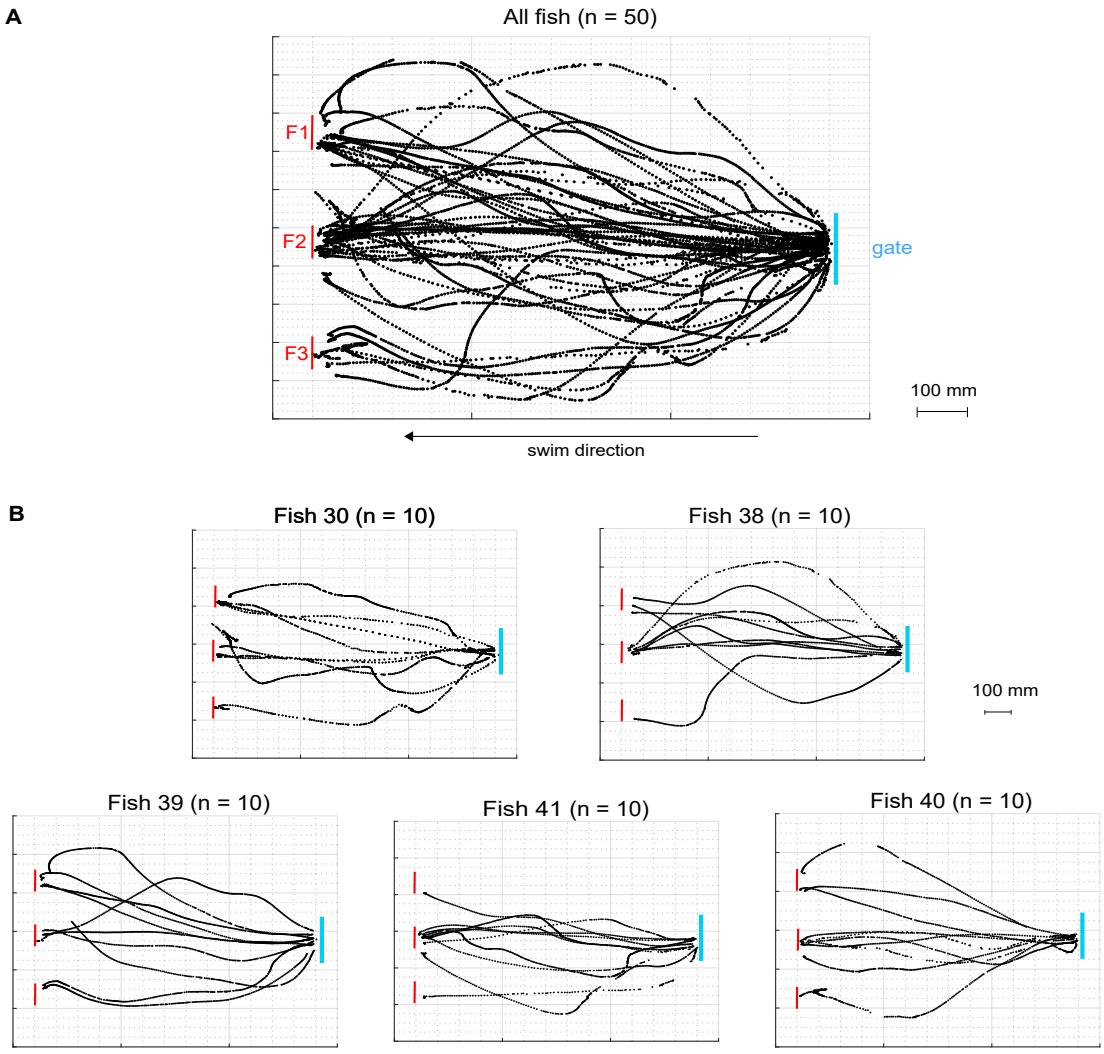


Figure 4.5: Fish trajectories during recorded trials included in the analysis. Fish swim from the right to the left. Their start position is recorded as the position at which they first cross the guillotine door, depicted as a light blue line to the right of the diagram. The end position is recorded as the position when they reach the food reward, with the three possible positions of food rewards (F1-F3) depicted as red lines to the right in the diagram (see main text). The top of each graph corresponds to the right tank wall, and the bottom corresponds to the left tank wall. (A) All trials (n = 50) for all fish, with a scale bar for reference. (B) Trials recorded by individual fish, with a scale bar for reference.

GLME estimate: 1.75, CI: 1.4,2.1, dAIC: 150). As expected, being aligned with the food reward (**3)**) and having a larger angular size (**2a)**) increased the likelihood of the fish choosing a gap. All fish chose the gap most aligned with the food in over 85% of observations (odds of choosing food gap: 7.6, CI: 5.2, 11.2), and the largest angular gap on over 80% of observations (odds of the largest gap being chosen: 5.8, CI: 4.1,8.2). However, **2b)** and **2c)** had the opposite effect. Gaps with the largest clearance beyond the immediate obstacles (**2b), 2c)**) were less likely to be chosen (they were picked in <20% of observations). The odds of choosing such gaps when all obstacles were taken into account (**2c)**) was 0.16 (CI: 0.11, 0.23), and 0.12 (CI: 0.08, 0.17) when the row to be crossed and the row beyond that were considered (**2b)**). The effect directions and magnitudes of food position (**3)**) and gap size (**1,2a),2b),2c)**) remained statistically significant when the width of the chosen gap relative to the width of the tank was controlled for ($p < 0.05$).

This pattern suggests there is a correlation between the gap with the largest angular size and that containing the food. The strength of the association between variables was quantified using Cramer's V, which indicated a stronger association between the angular size of a gap and the food being in view through that gap than between either of those variables and gap choice (Table 4.1). The observed associations between variables further indicated strong associations between the gap crossed in $\text{row}_{(t-1)}$ (**4)**), which would correspond to the decision point from which polar distances were measured, the largest gap (in angular terms, **2a)**) and the gap through which food was theoretically visible (**3)**). These were the three variables most associated with the observed gap choice. When tested individually, we found a statistically significant likelihood of the choice made in any given row being the same as the choice made in the row immediately before (**4)** GLME estimate: z=6.4, p«0.001), with the odds of the fish choosing the same gap as in the previous row being 2.5 (CI: 0.4, 13.8). However, once the width of the chosen gap relative to the room was controlled for, the effect of the previous choice was no longer statistically significant (z= 1.9, p=0.06).

						Gap crossed
					1)	0.19
				2a)	0.08	0.64
			2b)	0.05	0.13	0.10
		2c)	0.81	0	0.11	0.07
	3)	0.06	0.08	0.75	0.15	0.69
4)	0.58	0.18	0.13	0.67	0.03	0.48

Table 4.1: Association between variables extracted from each flight, measured using Cramer's V. **1)**: Largest metric gap; **2a)**: largest visual (angular) gap; **2b)**: largest visual subgap (row_t- row_{t+1}); **2c)**: largest visual subgap (row_t- row_{end}); **3)** Gap most aligned with food target; **4)** Gap crossed at row_{t-1}.

The mixed models indicated fish identity was not likely to affect gap choice. However, to check whether there might be any individual differences in the observed trials, we calculated odds ratios for individual fish using a general linear model with fish identity as a fixed effect (table 4.2). These showed little individual differences, and all fish responded in the same direction. We also regressed the size of each fish against the absolute size of the gaps it went through but found no correlation between these (Pearson correlation coefficient = -0.07).

Fish	Odds $row_t = row_{t-1}$ (CI)	Odds largest ang (CI)	Odds food (CI)
30	1.4 (0.7, 2.5)	1.5 (0.7, 3.1)	1.6 (0.6, 4.1)
38	2.3 (0.5, 10.3)	5.25 (0.8, 32.6)	5.25 (0.5, 10.3)
39	2.1 (0.5, 9.3)	5.25 (0.8, 32.6)	9 (0.5, 9.3)
40	2.8 (0.6, 12.7)	11.5 (1.5, 87.3)	9 (0.6, 12.8)
41	2.3 (0.5, 10.3)	4.6 (0.8, 27.6)	7.3 (0.5, 10.3)

Table 4.2: Odds ratios of fish choosing a gap given the same gap was crossed in the row before, that the gap is the largest available, and that the gap contains a view of the food target expressed as odds of choosing the same gap as before, the largest gap, or the gap most aligned with the food pellet with 95% confidence intervals.

We found the position at which the fish crossed two adjacent obstacles to follow a normal distribution, with fish mostly centering their position between obstacles (normalised median position of fish, where 0 represents a centred response and 1 and -1 the positions of adjacent obstacles: -0.06, Q1: -0.3, Q3: 0.2).

4.5 Discussion

This is, to my knowledge, the first study on obstacle avoidance in fish. Our results indicate that triggerfish respond similarly to each other in structured spaces. They are likely to choose between available clearances in obstacle-laden environments based on the relative angular size of a clearance compared to that of other possible routes and whether their target is viewable through the visual gaps between obstacles.

4.5.1 Visual cues for clutter negotiation

In their natural habitat, triggerfish appear to swim above obstacles if enough space is available in the water column (unless they are foraging; personal observation). Therefore, we hypothesize that coming into contact with obstacles while navigating is undesirable. However, there are scenarios in which this can't be avoided (e.g. low tide). It makes sense in these cases for triggerfish to aim for larger apertures, reducing their risk of coming into contact with extraneous objects or lurking predators. Therefore, our finding that triggerfish preferentially choose to go through the largest gaps immediately in front of them is not surprising. Interestingly, this preference seems to be based on angular size rather than metric distance. Metric distance is measured in world coordinates, whereas angular size is the apparent size based on the observer's position and is therefore an egocentric measure. What appears as the largest gap from the vantage point of the fish may not represent the largest physical gap. Fish are known to display size constancy and are therefore capable of estimating size [189]. As with the pigeons, binocular mechanisms are unlikely to be used for distance estimation by our fish due to their relatively small binocular visual field of about 35°, and the observation that fish frequently use one eye only to look at an object [190]. The question is, what other cues might they be using? Visual contrast and image blur both provide rapid monocular cues for visual distance perception: contrast tends to decrease, and blur tends to increase with viewing distance [191]. However, these cues would be less prominent underwater than in air due to the light-propagating properties of water described above. Moreover,

the high variability of visibility conditions in inter-tidal areas would likely make these unreliable cues for *R. acauleatus* to use for distance estimation. Accommodation, or the ability to change the focal length of the eye and detect changes in the distance of focal objects, has been shown in several teleosts but is unlikely to be useful for distance estimation in the time scales needed for obstacle negotiation [192]. Motion parallax -the difference in the apparent position of an object viewed along two different lines of sight- is another possible monocular mechanism for distance estimation, but little is known about motion parallax use in fish. Previous studies in goldfish have found that in situations where the size of an object is expected to remain constant, such as visual landmarks or the poles in our experiment, they rely solely on visual angles as a proxy for size rather than measuring absolute distance [193]. Our observation that gap choice is much more associated with the relative size of a gap's visual angle than with the physical distance between obstacles might indicate that the triggerfish are using visual angle as a proxy for size instead of calculating absolute distance. Neurologically, space is represented in an egocentric reference frame in the optic tectum before the sensory information is anchored to the external environment further downstream in the lateral pallium (see section 1.3.3) [84]. Representing size in angular rather than metric terms is therefore less computationally complex, as it does not require converting sensory information into a different reference frame. The preferential use of angular over absolute size might thus suggest simpler mechanisms are favoured in situations requiring fast reaction times, such as during obstacle avoidance. Further work might consider explicitly testing this hypothesis by investigating differences in reaction times when each of these cues is used.

4.5.2 Gap selection and individual characteristics

We expected to find bigger fish would tend to go through larger gaps, but this was not the case. Neither the size nor the fish's identity were likely to bias the observed responses. This finding was surprising because other animals are known to adjust the apertures they move through based on their size. Humans and

birds tend to be conservative in their estimates (i.e. overestimating rather than underestimating their size as the safer of the two options) ([145], [194]). However, the fish tested were fairly similar in size. Therefore future work might consider testing fish with a wider range of sizes to determine whether the pattern observed in other animals is also present in fish.

The apertures available to the fish were, for the most part, significantly more expansive than their body width. However, the fish were still observed attempting to traverse obstacles too close together for them to get through. This was only observed in the two rows closest to the food reward. It could be that close to the food reward, the fish weighed the potential costs of collision differently than in earlier sections. This would be consistent with the observation that their tendency to avoid contact with obstacles happens only when fish are not foraging. When foraging, triggerfish will enter small crevices searching for food. Such a behavioural shift highlights the importance of including physiological factors in any model of animal movement through complex spaces. When the full deep learning dataset is available, we intend to take behavioural states into consideration. During data collection and processing, we observed that fish tended to swim more slowly in certain parts of the trials. We plan to look at how changes in the fish's speed may indicate changes in behavioural strategies, such as shifting from an exploratory state to a goal-directed state. We hypothesise the fish might start swimming slowly in an initial "search stage", followed by faster, directed swimming once the position of the food reward is in direct view. Differences in searching and directed movement have already been observed in response to increasing levels of water turbidity, which makes targets harder to see [188]. Making this distinction would allow us to quantify potential differences in how apertures are selected based on behavioural state.

4.5.3 Limitations

The most obvious limitation in our current analysis is the limited sample size. Analysing the full collected dataset will improve our confidence in our results. We have approached the analysis of this reduced dataset by comparing the odds

ratios of going through gaps with particular properties. Looking at the variables independently suffers from the problem of having strong associations between the variables. The way to resolve this would be to use multinomial multiple regression. This was the originally intended analysis method to construct a model of the collected data. However, the limited data available at the time of the present analysis would make this a weak model. Therefore we have opted to wait until the full dataset is available to carry out a more thorough analysis. Data processed through the deep learning pipeline (example of the output of this process provided in figure 4.6) tracks the position and velocity of the fish, detects the positions of poles, and identifies all the "virtual gates" the fish crossed rather than being limited to the gaps (virtual gates) available per row (in Fig. 4.6, available "virtual gates" labelled in yellow, virtual gates/gaps crossed by the fish shaded green). Nevertheless, deductions about how fish negotiate cluttered environments can still be made based on the present dataset.

Within the dataset analysed, issues may have arisen from how the subsample to be tracked using the background subtraction method was selected. As previously stated, several of the trials were not reliably tracked using this method. These tended to be trials with more complex-looking trajectories (e.g. fish reversing). This will inevitably bias our analysis and limit our ability to predict paths where fish might not move between rows as they were ordered in our experimental set-up. Possibly partly as a result of this, a much higher number of the trials included in this analysis than would be expected by chance had the food reward in the central position (40/120/90 for positions F1/F2/F3). Both of these effects are likely to lead to the trajectories included in the analysis being on average straighter than the average of the full dataset would be.

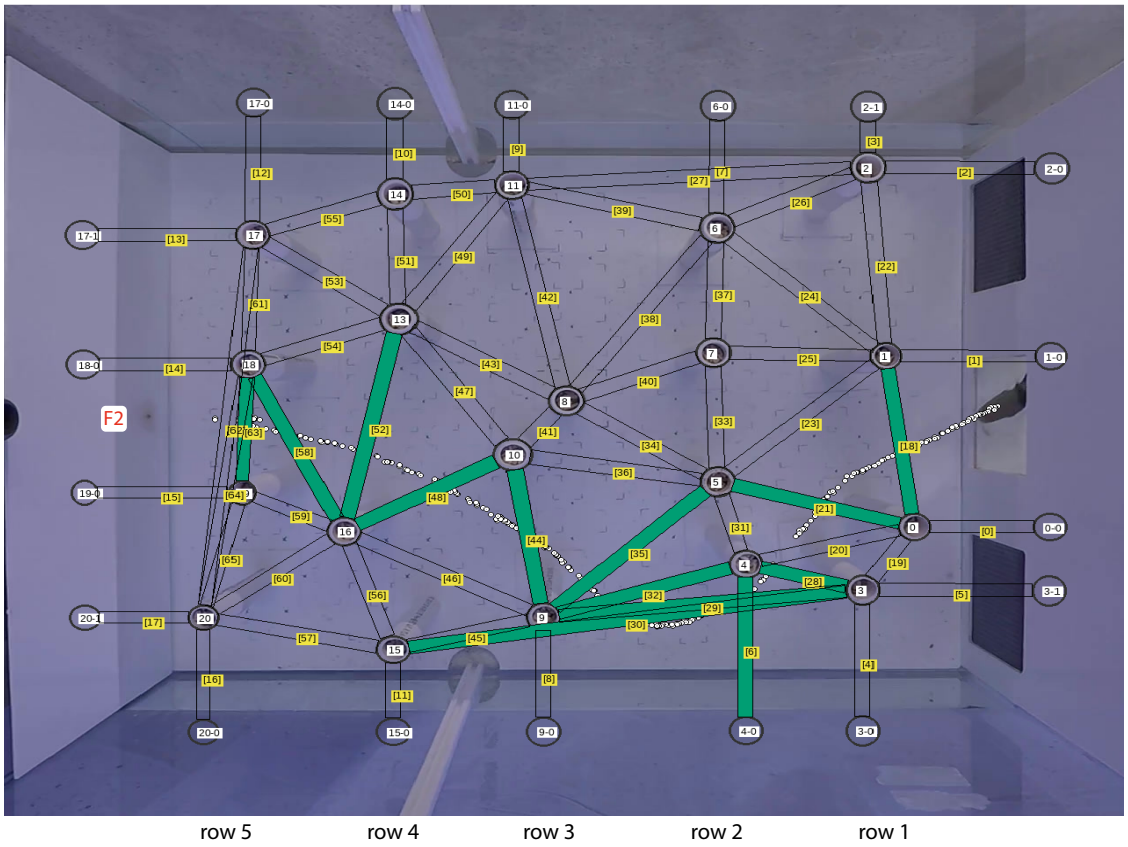


Figure 4.6: Example output of processing recorded video data using a deep learning pipeline. The background image is the first frame of the video analysed. Fish position over the length of the trial is shown as white dots. Obstacles (real, as in poles, and virtual, as in the positions of the wall from which the size of clearances are measured) are labelled in white. Available gaps ("virtual gates") are labelled in yellow. Virtual gates/gaps crossed by the fish shaded green. The food position is labelled in red. Row numbers are indicated for comparison with the experimental setup.

4.6 Supplementary Information

The manuscript associated with the processing of the full dataset collected has been submitted for publication under the title "Keeping an Eye on a Picasso Triggerfish". The full associated dataset is available at https://robots.ox.ac.uk/ vgg/research/fish. A further manuscript outlining the results of the analysis of gap choices from the full dataset is currently *in prep*.

References

[84] Haleh Fotowat et al. “Neural Activity in a Hippocampus-like Region of the Teleost Pallium Is Associated with Active Sensing and Navigation”. In: *eLife* 8

(Apr. 2019). Ed. by Vatsala Thirumalai, Timothy E Behrens, and Maurice J Chacron, e44119. (Visited on 05/06/2022).

[105] Huai-Ti Lin, Ivo G. Ros, and Andrew A. Biewener. "Through the Eyes of a Bird: Modelling Visually Guided Obstacle Flight". In: *Journal of The Royal Society Interface* 11.96 (July 2014), p. 20140239. (Visited on 05/04/2022).

[115] Karen L. Cheney et al. "Colour Vision and Response Bias in a Coral Reef Fish". In: *Journal of Experimental Biology* 216.15 (Aug. 2013), pp. 2967–2973. (Visited on 05/19/2022).

[137] Emily Baird and Marie Dacke. "Finding the Gap: A Brightness-Based Strategy for Guidance in Cluttered Environments". In: *Proceedings of the Royal Society B: Biological Sciences* 283.1828 (Apr. 2016), p. 20152988. (Visited on 05/04/2022).

[145] J. M. Warren. "Handedness and Laterality in Humans and Other Animals". In: *Physiological Psychology* 8.3 (Sept. 1980), pp. 351–359. (Visited on 05/04/2022).

[172] Glenn R. Almany. "Differential Effects of Habitat Complexity, Predators and Competitors on Abundance of Juvenile and Adult Coral Reef Fishes". In: *Oecologia* 141.1 (Sept. 2004), pp. 105–113. (Visited on 05/08/2022).

[173] M. Willis et al. "Infrasonic Observations of Open Ocean Swells in the Pacific: Deciphering the Song of the Sea". In: *Geophysical Research Letters* 31.19 (2004). (Visited on 05/19/2022).

[174] S. C. Willis, K. O. Winemiller, and H. Lopez-Fernandez. "Habitat Structural Complexity and Morphological Diversity of Fish Assemblages in a Neotropical Floodplain River". In: *Oecologia* 142.2 (Jan. 2005), pp. 284–295. (Visited on 05/08/2022).

[175] Valeriya Komyakova, Philip L. Munday, and Geoffrey P. Jones. "Relative Importance of Coral Cover, Habitat Complexity and Diversity in Determining the Structure of Reef Fish Communities". In: *PLOS ONE* 8.12 (Dec. 2013), e83178. (Visited on 05/19/2022).

[176] Darren J. Coker, Morgan S. Pratchett, and Philip L. Munday. "Influence of Coral Bleaching, Coral Mortality and Conspecific Aggression on Movement and Distribution of Coral-Dwelling Fish". In: *Journal of Experimental Marine Biology and Ecology* 414–415 (Mar. 2012), pp. 62–68. (Visited on 05/19/2022).

[177] Karen M. Chong-Seng et al. "The Influence of Coral Reef Benthic Condition on Associated Fish Assemblages". In: *PLOS ONE* 7.8 (Aug. 2012), e42167. (Visited on 05/19/2022).

[178] Matthew Tietbohl et al. "Intentional Partial Beaching in a Coral Reef Fish: A Newly Recorded Hunting Behaviour of Titan Triggerfish, Balistoides Viridescens". In: *Journal of Fish Biology* 97 (Aug. 2020).

[179] Fabio Cortesi et al. "Visual System Diversity in Coral Reef Fishes". In: *Seminars in Cell & Developmental Biology*. Vertebrate Vision: Lessons from Non-Model Species 106 (Oct. 2020), pp. 31–42. (Visited on 05/19/2022).

[180] Connor Champ et al. "Visual Acuity in a Species of Coral Reef Fish: Rhinecanthus Aculeatus". In: *Brain, Behavior and Evolution* 83.1 (2014), pp. 31–42. (Visited on 05/19/2022).

[181] Karen L. Cheney et al. “Seeing Picasso: An Investigation into the Visual System of the Triggerfish Rhinecanthus Aculeatus”. In: *Journal of Experimental Biology* 225.7 (Apr. 2022), jeb243907. (Visited on 05/19/2022).

[182] Siby Philip et al. “Fish Lateral Line Innovation: Insights into the Evolutionary Genomic Dynamics of a Unique Mechanosensory Organ”. In: *Molecular Biology and Evolution* 29.12 (Dec. 2012), pp. 3887–3898. (Visited on 05/20/2022).

[183] Horst Bleckmann and Randy Zelick. “Lateral Line System of Fish”. In: *Integrative Zoology* 4.1 (Mar. 2009), pp. 13–25.

[184] MARK W. DENNY. “Terrestrial Versus Aquatic Biology: The Medium and Its Message1”. In: *American Zoologist* 30.1 (Feb. 1990), pp. 111–121. (Visited on 05/19/2022).

[185] Paul W. Webb. “Form and Function in Fish Swimming”. In: *Scientific American* 251.1 (1984), pp. 72–83. JSTOR: 24969414. (Visited on 05/19/2022).

[186] PW Webb. “Entrainment by River Chub Nocomis Micropogon and Smallmouth Bass Micropterus Dolomieu on Cylinders”. In: *Journal of Experimental Biology* 201.16 (Aug. 1998), pp. 2403–2412. (Visited on 05/19/2022).

[187] Peter B. Moyle et al. “Biology and Population Dynamics of Sacramento Splittail (Pogonichthys Macrolepidotus) in the San Francisco Estuary: A Review”. In: *San Francisco Estuary and Watershed Science* 2.2 (2004). (Visited on 05/19/2022).

[188] Cait Newport, Oliver Padget, and Theresa Burt de Perera. “High Turbidity Levels Alter Coral Reef Fish Movement in a Foraging Task”. In: *Scientific Reports* 11.1 (Mar. 2021), p. 5976. (Visited on 05/08/2022).

[189] R. H. Douglas, J. Eva, and N. Guttridge. “Size Constancy in Goldfish (Carassius Auratus)”. In: *Behavioural Brain Research* 30.1 (Sept. 1988), pp. 37–42. (Visited on 05/18/2022).

[190] A. Meesters. “Über Die Organisation Des Gesichtsfeldes Der Fische. [On the Organization of the Visual Field in the Fish.]” In: *Zeitschrift für Tierpsychologie* 4 (1940), pp. 84–149.

[191] S. Chaudhuri. *Depth From Defocus: A Real Aperture Imaging Approach*. 2004. (Visited on 05/18/2022).

[192] MARGOT E Andison and JACOB G Sivak. “The Naturally Occurring Accommodative Response of the Oscar, Astronotus Ocellatus, to Visual Stimuli”. In: *Vision Research* 36.19 (Oct. 1996), pp. 3021–3027. (Visited on 05/18/2022).

[193] R. H. Douglas. “Goldfish Use the Visual Angle of a Familiar Landmark to Locate a Food Source”. In: *Journal of Fish Biology* 49.3 (1996), pp. 532–536. (Visited on 05/18/2022).

[194] Partha S. Bhagavatula et al. “Behavioral Lateralization and Optimal Route Choice in Flying Budgerigars”. In: *PLOS Computational Biology* 10.3 (Mar. 2014), e1003473. (Visited on 05/04/2022).

5 General discussion

Contents

5.1 Modelling decision-making in space 161
5.2 Spatial decision-making in distinct taxa 164
5.2.1 Limitations 164
5.2.2 State dependence 167
5.2.3 Timing and geometry of decisions 168
5.3 Concluding remarks 170
References 170

This thesis set out to better understand how animals guide their movements through cluttered environments. Previous work framed clutter negotiation as a gap-aiming problem [105] [142], greatly simplifying modelling such behaviours, but failed to provide a realistic decision model to determine how animals select between available gaps. Studies looking at what cues animals may be using to move through apertures have previously provided only one or two options for animals to choose between [137] [157] [138]. In this thesis, I have broken down clutter negotiation into a decision-making stage and a steering implementation stage, using a gap-aiming approach to model animal behaviour in two species. This approach has shown how seemingly complex behaviours can be successfully broken down into components to model decision-making in spatial tasks.

5.1 Modelling decision-making in space

In ethological research, animal decision-making processes, and the sensory or internal cues that inform them, can only be understood through observation of behavioural outcomes. Experimentally, perceptual decision-making has typically been studied in laboratory settings, with standard protocols in psychology, behavioural ecology and neurobiology typically involving training and testing a small number of options with straightforward relationships between stimuli, actions and consequences. Simplifying and experimentally manipulating the information an animal might encounter in the natural environment, such as through psychophysics studies, is an important process that allows researchers to isolate key variables. However, such settings are unlikely to represent the structure of the environment an animal is adapted to. Similarly, in behavioural and evolutionary ecology, models of decision-making typically consider highly simplified environments, where the availability of different options does not change over time and is known to the animal. Both of these are therefore unrealistic in their own ways. While simplification and abstraction of scientific problems is a key element in understanding them, there is a risk of over-simplifying to the point of failing to capture features of natural environments necessary to understand behaviour.

An obvious way in which this happens is by removing the decision-making process from its spatiotemporal context. As was noted in the introduction to this thesis, perception and motion are closely intertwined. Both behavioural evidence from navigational studies and neurobiological evidence from the characterisation of hippocampus cells show a range of animals use vectorial representations of desired directions (such as targets) [195] [196] [197]. Egocentric representations of spatial relationships necessarily change as animals move through space. However, to the best of my knowledge, with the exception of a single study published late last year, decision processes have not been modelled as a dynamic process with respect to space before [144]. A large part of this thesis' contribution lies in providing a framework in which to do so, integrating knowledge from the sensory biology and control literature. This is a more ecologically relevant way of considering how

animals may make decisions, and, while the experimental set-ups are inevitably a simplification of natural environments, study species were chosen whose habitats most closely resemble the spatial challenge we used to tackle this problem in chapters 3 and 4. The value of such an approach has become increasingly evident over the course of this thesis in conversing with colleagues. For instance, our collaborator in computer science, whom we are working with on the fish data processing, remarked how framing the question this thesis is trying to solve in terms of analysing characteristics of gaps as potential targets helped design the computer vision methods that resulted in the video analysis depicted in figure 4.6 and a new framework for processing similar kinds of data using computer vision. Likewise, another collaborator in computer science is now testing a drone using a k_N controller to steer a path between pre-planned waypoints, as a computationally efficient approach to the problem.

Our decision model can be integrated with our steering model to create realistic simulations of how an animal might react to novel cluttered environments based on the characteristics of the physical space alone. An example of how this can be done in the experimental set-up used in chapter 3 is shown in figure 5.1. Here, we use the predictions from the regression model to give us the sequence of gap choices the bird would fly through. We use the midpoint of each predicted gap choice as the input targets to the kN steering controller proposed in chapter 2. We give the controller the initial release position of the pigeon, and assume constant velocity for simplicity. This is used to simulate the trajectory to the midpoint of the predicted gap choice in the first row of obstacles. The last position of that simulation is in turn used as the starting condition for simulating the trajectory to the midpoint of the next gap choice, and so forth. Beyond the experimental setup, this approach could be used to predict the trajectories of animals in other settings where features of the environment are known. This would be a particularly interesting avenue to follow in more natural environments. For instance, the forest structure in Wytham Woods has already been mapped out using LiDAR techniques. Using our model, we could theoretically predict based on this mapping the trajectories that pigeons are likely

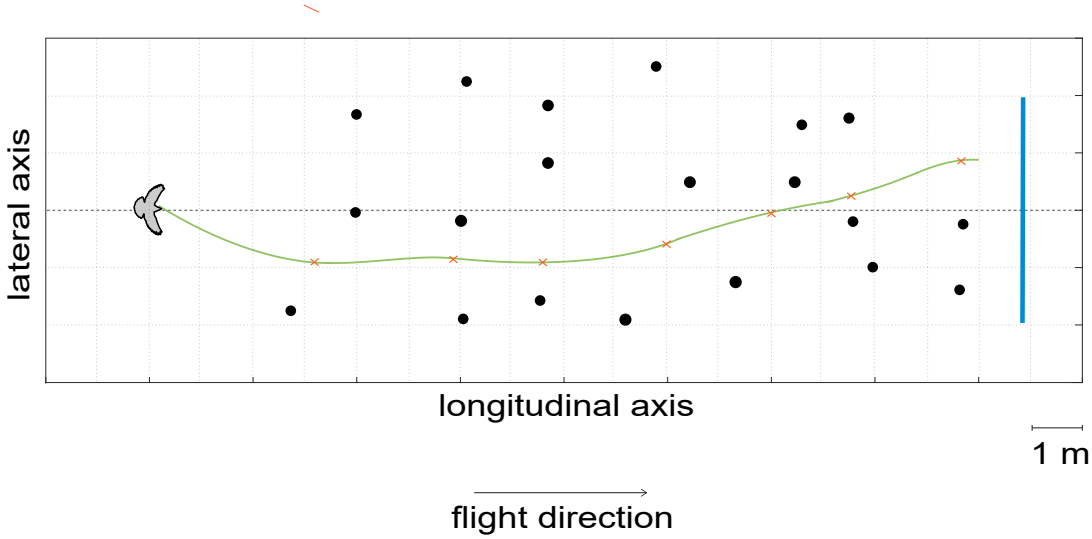


Figure 5.1: Incorporating models of gap choice and steering into a simulated trajectory. The release point of the flight used as the starting position of the steering controller is marked as a grey bird silhouette on the left of the graph. Obstacle positions are shown as black circles. The grey dashed line marks the midpoint along the transverse of the flight hall. The open roller is depicted as a solid blue line to the right of the graph. Obstacle configuration corresponds to that marked as 31 in Figure 3.9. Original histogram of all flights recorded in this obstacle configuration is shown again in Figure 5.2. Steering controller simulations based on a k_N controller, using the mean parameter estimate obtained from fitting flight sections in Chapter 2 globally to all flights ($\tilde{k}_N = 2.05$), but no delay ($\tau = 0$), and constant speed for simplification. The controller aim is set as the midpoint of the gaps predicted by the best model in chapter 3 (binomial GLM with structure $Gapchoice \sim Gapchoice_{(t-1)} + Gapchoice_{(t-2)} + rollerdoor + subgap_{(row+1)} + subgap_{(allrowsahead)} + Gapsize_{cartesian} + BirdID$). These are marked as orange crosses at each time-step.

to take. Our predictions could in turn be verified experimentally by releasing birds in the woods, and the recorded tracks used to further improve our existing model.

While our choice of steering controller is based on simulations of very short sections of flight in chapter 2, classical steering laws in engineering, originating in missile guidance, are typically variations of a pure proportional navigation controller. Proportional navigation controllers are known to implement all the basic geometries observed in animal pursuit behaviour, making them valuable models in animal behaviour [122]. They also reduce the complexity of steering, as the agent need only retain the target at a constant bearing, without regard to cues about distance, velocity or size. There are thus clear benefits of using such a well-established controller. Processing of sensory information would be minimised to that necessary to make perceptual decisions, such as which gap to aim for, rather than having to

process any additional information to implement said decisions in space. Moreover, it unifies pursuit and obstacle avoidance behaviours under the same framework.

5.2 Spatial decision-making in distinct taxa

Having studied the same problem in two different species opens up interesting possibilities for comparisons. Before any further discussion on this, however, the differences in the experiments must be acknowledged.

5.2.1 Limitations

While the experiments were designed to be as comparable as possible, the arrangement of obstacles ended up being slightly different between the flight hall in chapter 3 and the tank in chapter 4. There were several reasons for this, not least that a tank of the appropriate aspect ratio could not be located in time for experiments to take place. Given the constraints of the dimension discrepancies, our first iteration of the experimental set-up attempted to scale the obstacle grid used for the pigeon experiments down to the size of the tank. However, this did not take into account differences in species locomotion, and the task proved too easy for the triggerfish. In the second iteration, we instead chose to keep separations between the grid positions of chevrons the same between experiments relative to the dimensions of the animals. Following this approach, the spacing would relate to each animal in similar ways. For instance, a separation of 2 wingspans in the grid of the bird set-up would correspond to a separation of 2 body lengths in the grid of the fish set-up. These are of course not directly equivalent, but given triggerfish can move in all directions, body-length was used as a rough measure of the space an iteration of movement might take up. Keeping both experimental areas equally densely populated with obstacles using this measure meant a different number of rows and columns of obstacles were needed for each set-up, despite the total number of obstacles being almost identical (21 for the pigeons, 20 for the fish). This meant a different number of gap options and sequential choices were available to each species. Therefore the results are not directly comparable. These differences are also reflected in the analysis of each

chapter. As noted in the individual chapters, assessing how the animals choose between all the available gap options would be better tackled using a multinomial multiple regression, but comparing the results of this in each of the datasets would still suffer from the issues listed above. This is only partially addressed in the chapters by the inclusion of a measure of the sampling effect in each of the models.

Both species seemed to attend to obstacles within relatively close-range. Going back to one of the questions we posed in the introduction, this tells us about how the animals might be perceiving cluttered environments. The much larger effect of explanatory variables that only considered the row of obstacles immediately ahead of the animal suggests that close obstacles are weighted more heavily in spatial decisions. This can be illustrated as attending primarily to obstacles within the red limit of attention in the diagram in figure 5.2B, with objects falling within the green limit of attention also having some impact on the decisions taken at a given timepoint (in both species, the row of obstacles immediately after that to be crossed was also statistically likely to affect gap choice, albeit less so than obstacles in the row to be crossed). If this is true, those objects falling in the blue area of attention are unlikely to affect how an animal perceives available opportunities (gaps or clearances) in a cluttered environment. Thus, gaps to be aimed for would likely be identified based on something like the left two projections on the retina depicted in figure 5.2C. In approaching movement through clutter as iterative gap-aiming, it is therefore essential to define how gaps are determined. Again, this can be seen in figure 5.2B. Models such as FGM in robotics (see section 1.4) and that proposed by Lin et al [105] would generate different steering commands depending on which retinal projection is used. This would in turn shape the overall predicted trajectory. In both datasets, the position of an animal within the gap was found to be normally distributed with a mean centered at the midpoint of the chosen gap. Therefore while on average, simplifying the steering aim as aiming to the center of the gap is a useful approximation, this is not always the case, and, again, will depend on how a gap is defined. Qualitatively, looking at the spatial histograms suggests there are occasions where the animals may well have been displaying a centering response

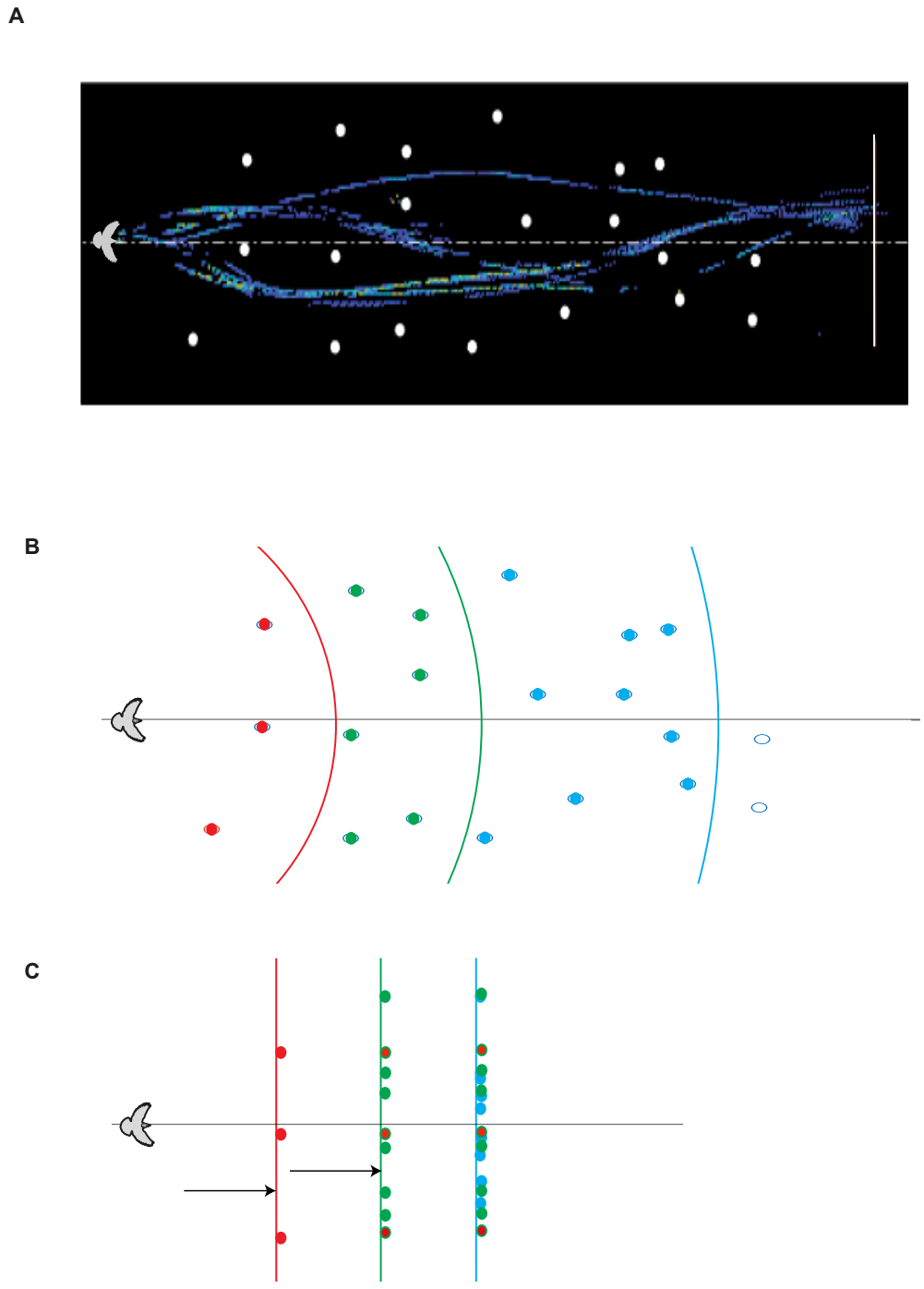


Figure 5.2: Determining the mid-point of gaps to aim towards (A) Histogram of all flights recorded for obstacle configuration 30 (see Chapter 3, Figure 3.8). The white dashed line marks the midpoint along the transverse of the flight hall. The pigeon release point -represented by a bird silhouette shaded grey- is to the left end of the histogram, with the roller door opening -represented by a light grey line- at the right. (B) Diagrammatic view of obstacle set-up in (A). The black line marks the midpoint along the transverse of the flight hall. Coloured lines mark limits of areas of attention. Obstacles are shaded according to the area of attention they would fall under (akin to Figure 1.3 in section 1.5 of the general introduction). (C) Projections of the obstacles in (B) on the pigeon's retina from the designated position marked with a pigeon drawing in all three panels. The black line marks the midpoint along the transverse of the flight hall. Black arrows mark the midpoint of the largest visual gap at each area of attention. The arrow at the green area of attention is further left than that at the red area of attention.

towards a visual gap, but one which would not have been reflected in our measure of centrality due to only taking the closest obstacles into account. This is illustrated in figure 5.2A, where, for instance, birds flying to the right of the room (bottom) in the first row of obstacles clearly do not centre their flight going through the gap formed by the closest two obstacles (shown as red dots). However, the position of crossing that first gap does seem to be centred when obstacles further afield in the green area of attention are also considered. Thus, if this flight were to be modelled as the birds aiming to the midpoint between the obstacles in red, the simulated bird would steer further right (downwards in Fig. 5.2) than the actual birds do (compare position marked in Fig. 5.2C to trajectories in Fig. 5.2A). To the best of my knowledge, this has not been explicitly addressed before. Clarifying the optimal distance from the agent at which objects in the environment are considered of interest to making spatial decisions, therefore, has clear benefits to robotics algorithms beyond the inherent biological interest in how animals do this.

5.2.2 State dependence

Comparing observations of the different experiments in this thesis also highlighted the importance of factoring behavioural states into models of animal behaviour. In the experiments with fish, we observed that there seemed to be a more scattered explorative phase in at least some of the trials, followed by a more directed approach towards the food reward. In robotics, the only models of navigation through cluttered environments that reflect different states are those based on nearness diagram approaches (summarised in section 1.4). The clearest behavioural state in the original Nearness Diagram (ND) navigation model is when the target is in the line of sight of the agent, and the path to it is unobstructed [97]. This is associated with a different guidance rule than would be applied if the agent was in an area of dense clutter and not in direct view of its target. In a similar way, animal behaviour might be better captured by associating guidance rules to different states, and only guiding movement based on the rules associated with a given state. For instance, in the data presented in this thesis, a fish trajectory could be divided into two distinct

states, such as search and targeted behavioral states, and guidance rules applied to each accordingly. In our pigeon data, behavioural state may partly account for the differences in responses observed between experiments in chapters 2 and 3. In chapter 3, the birds had a clear view of the exit roller door from the release point. In this case, we found the birds seemed to choose the largest gaps most aligned with the exit gate, and responses to the same obstacle set-ups were consistent across individuals. In chapter 2, the curtain obstructed the pigeons' view of the exit roller door from the release point. In these experiments, we found instead that gap choice seemed to be more associated with the pigeons' inherent handedness than with the size of the available gaps. It could be that responding with handedness is the preferred rule for states in which the target is unclear (e.g. pigeons released into a room facing a curtain), but choosing gaps based on the target position is favoured when a clear target is in view (e.g. pigeons being released in a room with clutter but a direct view of the outside). This would be consistent with the observation that birds avoid mid-air collisions during head-on encounters by steering in an individually preferred direction, with most birds having a preference for veering right [198]. Just like in our experimental set-up in chapter 2, in this paradigm, there is no clear target to aim towards, and the birds respond based on a preset preference.

5.2.3 Timing and geometry of decisions

The close interplay between an animal's movement, the structure of an environment, and how the space the animal is moving in is perceived has been a constant theme in this thesis. Nevertheless, all three data chapters made assumptions about the timing or position of the animal choosing a target to move towards. This is a clear limitation in the work, for all the reasons that have already been outlined. While every attempt was made to choose an objective timepoint that made sense within the context of the experiment, the point at which the environment is sampled inevitably affects model outcomes. In reality, sensory information is time-varying and likely to be sampled continuously rather than at isolated decision points. Accordingly,

in human decision-making studies, evidence accumulation (also known as drift-diffusion) models have emerged as the dominant explanation for the mechanisms underlying forced choice decisions. Drift diffusion models (DDM) assume decisions are made by continuously sampling noisy evidence until a decision boundary in favour of one of the options is reached [199]. Recent work on human collision threat detection has shown the applicability of DDMs to locomotor decisions both behaviourally and neurologically [200]. Sridhar et al's [144] work on the geometry of decisions, while not explicitly based on DDMs, adopts a similar approach. In their modelling of the trajectories of flies and locusts, the authors propose the animal adopts the average path between two options until some critical phase transition occurs, at which point the system decides spontaneously between them. It is interesting to note that while the shape of the trajectories observed in chapter 2 closely resembles those predicted by the modelling of these insect experiments, those of chapters 3 and 4 mostly do not. As noted in the discussion of the relevant chapters, this is likely due to the symmetry of the available choices being broken. Sections of the summed trajectories that return to bifurcating-like shapes, as predicted for flies and locusts, seem to most closely correspond to areas where the relative positions of the animals and obstacles are returning to symmetry.

This intriguing observation precipitated further thinking about the broader applicability of Sridhar et al's model. In talking to the authors, it was revealed that their model is only able to predict choices in situations of perfect symmetry but breaks down in more complicated scenarios. We hypothesise this may be because where configurations are asymmetrical, the rate of accumulation of sensory information changes as animals move through space. In the real world, perfect symmetry is unlikely to be achieved in natural scenarios. Therefore the capacity to model how changes in sensory evidence accumulation affect spatial decisions could provide exciting developments to the work that has already been established in the field. The work in chapters 3 and 4 helped to determine what cues animals may be attending to when making decisions about what gaps to aim for in cluttered environments. As seen in figure 3.1 and covered in the introduction (section 1.2.1),

visual information changes in predictable ways with motion. Therefore, it is possible to determine the visual information available to animals at each position in space. The motion of an animal could thus be used to determine how it accumulates sensory information through space. This could in turn be combined with models established in the psychological and neurobiological literature that predict timings of decisions based on rates of sensory accumulation (for examples, see references [199] and [201]) to predict when a decision is likely to be made.

5.3 Concluding remarks

Natural environments are wonderfully complex, yet animals, humans, and sometimes even robots manage to move through them seemingly effortlessly. Many disciplines have tackled this problem in their own way, but I hope my work makes a case for the value of using interdisciplinary approaches to tackle difficult questions. I have been fortunate in being exposed to experts in many areas that feed into obstacle avoidance, such as decision-making, sensory biology and control engineering among many others. The work in this thesis represents only a small fraction of what could be achieved by combining models from different fields, and opens a lot of avenues for further research. I can only hope some of my research might inspire future work in some of the directions outlined throughout this concluding chapter.

References

[97] J. Minguez and L. Montano. "Nearness Diagram (ND) Navigation: Collision Avoidance in Troublesome Scenarios". In: *IEEE Transactions on Robotics and Automation* 20.1 (Feb. 2004), pp. 45–59. (Visited on 05/20/2022).

[105] Huai-Ti Lin, Ivo G. Ros, and Andrew A. Biewener. "Through the Eyes of a Bird: Modelling Visually Guided Obstacle Flight". In: *Journal of The Royal Society Interface* 11.96 (July 2014), p. 20140239. (Visited on 05/04/2022).

[122] Caroline H. Brighton, Adrian L. R. Thomas, and Graham K. Taylor. "Terminal Attack Trajectories of Peregrine Falcons Are Described by the Proportional Navigation Guidance Law of Missiles". In: *Proceedings of the National Academy of Sciences* 114.51 (Dec. 2017), pp. 13495–13500. (Visited on 05/04/2022).

[137] Emily Baird and Marie Dacke. "Finding the Gap: A Brightness-Based Strategy for Guidance in Cluttered Environments". In: *Proceedings of the Royal Society B: Biological Sciences* 283.1828 (Apr. 2016), p. 20152988. (Visited on 05/04/2022).

[138] Partha S. Bhagavatula et al. “Behavioral Lateralization and Optimal Route Choice in Flying Budgerigars”. In: *PLOS Computational Biology* 10.3 (Mar. 2014), e1003473. (Visited on 05/04/2022).

[142] Ivo G. Ros et al. “Rules to Fly by: Pigeons Navigating Horizontal Obstacles Limit Steering by Selecting Gaps Most Aligned to Their Flight Direction”. In: *Interface Focus* 7.1 (Feb. 2017), p. 20160093. (Visited on 05/09/2022).

[144] Vivek H. Sridhar et al. “The Geometry of Decision-Making in Individuals and Collectives”. In: *Proceedings of the National Academy of Sciences* 118.50 (Dec. 2021), e2102157118. (Visited on 05/04/2022).

[157] Partha S. Bhagavatula et al. “Optic Flow Cues Guide Flight in Birds”. In: *Current Biology* 21.21 (Nov. 2011), pp. 1794–1799. (Visited on 05/06/2022).

[195] Ayelet Sarel et al. “Vectorial Representation of Spatial Goals in the Hippocampus of Bats”. In: *Science* 355.6321 (Jan. 2017), pp. 176–180. (Visited on 05/20/2022).

[196] Johannes D. Seelig and Vivek Jayaraman. “Neural Dynamics for Landmark Orientation and Angular Path Integration”. In: *Nature* 521.7551 (May 2015), pp. 186–191. (Visited on 05/20/2022).

[197] David Andel and Rüdiger Wehner. “Path Integration in Desert Ants, Cataglyphis: How to Make a Homing Ant Run Away from Home.” In: *Proceedings of the Royal Society B: Biological Sciences* 271.1547 (July 2004), pp. 1485–1489. (Visited on 05/19/2022).

[198] Ingo Schiffner, Tristan Perez, and Mandyam V. Srinivasan. “Strategies for Pre-Emptive Mid-Air Collision Avoidance in Budgerigars”. In: *PLOS ONE* 11.9 (Sept. 2016), e0162435. (Visited on 05/20/2022).

[199] Roger Ratcliff. “A Note on Modeling Accumulation of Information When the Rate of Accumulation Changes over Time”. In: *Journal of Mathematical Psychology* 21.2 (1980), pp. 178–184.

[200] Gustav Markkula et al. “Accumulation of Continuously Time-Varying Sensory Evidence Constrains Neural and Behavioral Responses in Human Collision Threat Detection”. In: *PLOS Computational Biology* 17.7 (July 2021), e1009096. (Visited on 05/20/2022).

[201] Scott D. Gronlund and Roger Ratcliff. “Time Course of Item and Associative Information: Implications for Global Memory Models”. In: *Journal of Experimental Psychology: Learning, Memory, and Cognition* 15.5 (1989), pp. 846–858.

Appendices

A

Visual and vestibular input use in perching

Contents

A.1 Abstract 173
A.2 Introduction 174
A.3 Materials and methods 175
A.3.1 Animals 175
A.3.2 Videography 176
A.3.3 Treatment 178
A.3.4 Torque measurements 178
A.3.5 Statistical analysis 179
A.4 Results 179
A.5 Discussion 180
References 182

A.1 Abstract

Birds have outstanding abilities to balance on two legs and maintain upright posture on both rigid and highly flexible moving perches. However, to our knowledge, there has been no formal study investigating which sensory modalities are used to control upright posture in birds and, more importantly, how these are combined. From observation, we hypothesized that birds use a combination of visual, vestibular and proprioceptive information to balance on a perch. We used a perch torque

sensor to measure the torques and forces exerted on the perch under different circumstances to explore this question.

To test the degree to which vision contributes to balancing ability, we compared perching ability in the light and dark. Zebra finches *(Taeniopygia guttata)* were assessed for their ability to perch using high speed infrared videography and perch torque measurements in light and dark conditions over several weeks. In the dark perch torque root-mean-squared (RMS) deviation from 0 was higher in light conditions ($p=0.003$), suggesting that perching ability was impaired in the dark. We then assessed the role of the vestibular system in maintaining upright posture while perched by damaging vestibular hair cells with amino glycoside antibiotics, and measuring perching ability in the light and dark over a period of 8 weeks, over which loss of vestibular function and consequent recovery as inner ear hair cells regenerated was recorded. Again, we found root-mean-squared deviation from 0 was higher in light conditions than in the dark, but not significantly so ($p=0.06$). This was attributed to birds being overall less active after treatment, as reflected both in the videography and RMS data ($p=0.01$), which was especially evident in light conditions.

A.2 Introduction

In nature, birds can easily maintain their position on both rigid and flexible branches of trees even in stormy weather or when asleep. However, we are still unsure about what mechanisms allow them to stay balanced under such circumstances. The sensory inputs typically associated with balance are those arising from the eyes (vision), the vestibular organs (motion, equilibrium, spatial orientation) and motion in muscles and joints (proprioreception). In humans, vision and the vestibular system seem to have the strongest influence on balance.

Over the past few decades, songbirds, and particularly zebra finches *(Taeniopygia guttata)*, have become a widely used model organism for neuroscientists and ethologists studying complex sequential behaviours and sensory-guided motor learning. While the main focus of study in this bird has been its song learning

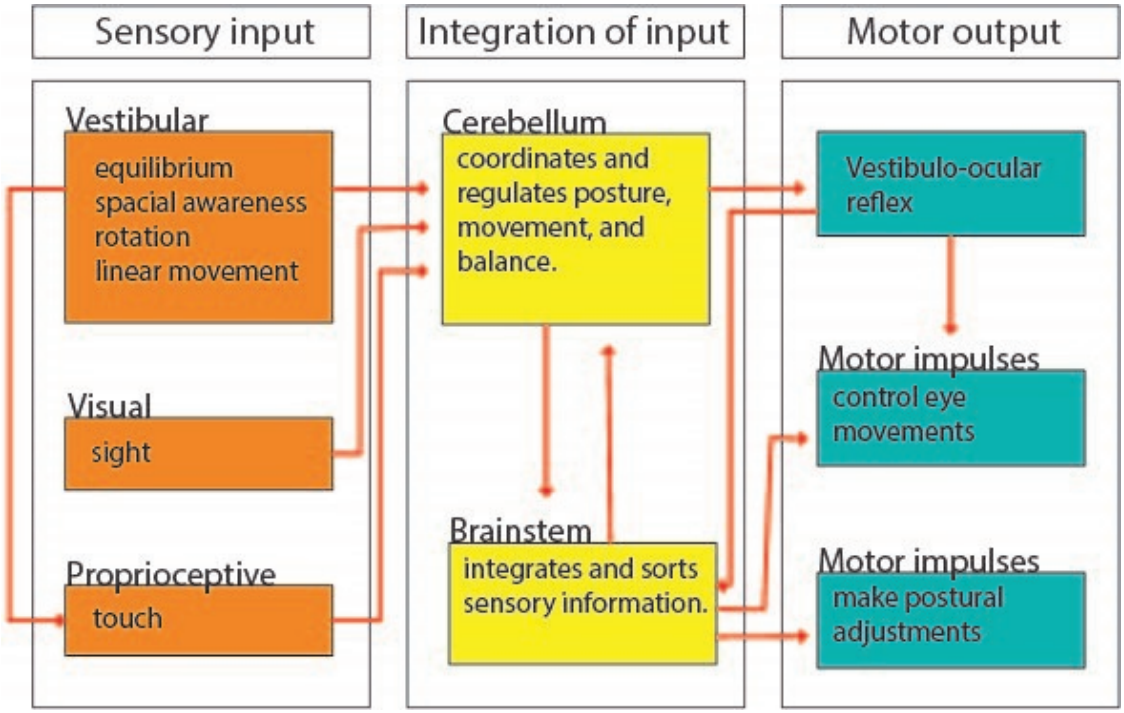


Figure A.1: Diagram of sensory modalities associated with maintaining upright posture and how these translate into a motor output.

system, the knowledge accumulated on zebra finches, as well as its proclivity to breed in captivity, its rapid maturation, and its natural flight behaviour make it an ideal system on which to study sensory control of perching.

Therefore, we set out to test the degree to which vision and vestibular sensory input contribute to balancing ability in zebra finches by removing visual and vestibular sensory inputs, singly and in combination, and consequently testing perching ability.

A.3 Materials and methods

A.3.1 Animals

Subjects were sourced from our breeding colony at the University of Washington, Seattle, USA, operated under university and government research permits, where all birds were given *ad lib* food and water. The Institutional Animal Care and Use Committee at the University of Washington approved all procedures used in this study. Adult birds were kept in single-sex cages in the same colony room until used

in the experiments. Throughout the duration of the experiments, all the birds used in this study were kept in a new colony room in single-sex (size) cages while they were not being recorded. Prior to the experiment, the birds were labelled using 1-mm diameter dots of non-toxic white paint positioned on the top of the head, the tip of the beak, and at the end of the central tail feather.

A.3.2 Videography

A videography session was considered to be a period of 45-75mins when a single bird was allowed to freely fly inside a 20cm x 20cm x 40cm flight arena made of mesh walls, occasionally landing on an available perch. The 10cm perch protruded from the back wall of the arena, and was attached to a torque sensor to measure the forces exerted on the perch by the bird. Videos were taken at 200fps, using two IR cameras (Phantom v7.1, Vision Research Inc., Wayne, NJ, USA) placed orthogonally to each other (Figure A.2). The videos were used to track the birds' head, beak and tail positions frame-by-frame during each videography session, and where possible, to extract their three-dimensional coordinates using DLTdv5 script [202] in MATLAB (v. 2017b).

Within this set-up, each bird was recorded under two conditions: light and dark (only infrared illumination available). The two conditions were alternated at 5 minute intervals during each session. To be included in data analysis, a flight to the perch had to be followed by the bird balancing on the perch for at least 5 seconds after initial contact with the perch. This was considered to be one perching event. For dark trials, as birds would not fly to the perch in complete darkness, the flight to the perch itself happened with the lights on, and the lights were turned off as soon as the bird made contact with the perch. Before a flight recording session, the bird to be tested was taken from its single-sex cage into the flight arena and then returned to the colony room immediately after the session. All recording sessions took place during daylight hours, and each bird was assigned a new time slot for its recording session each consecutive day, to equalise possible circadian effects. Two cages were placed contiguous to the flight arena (on the left and right, outside the

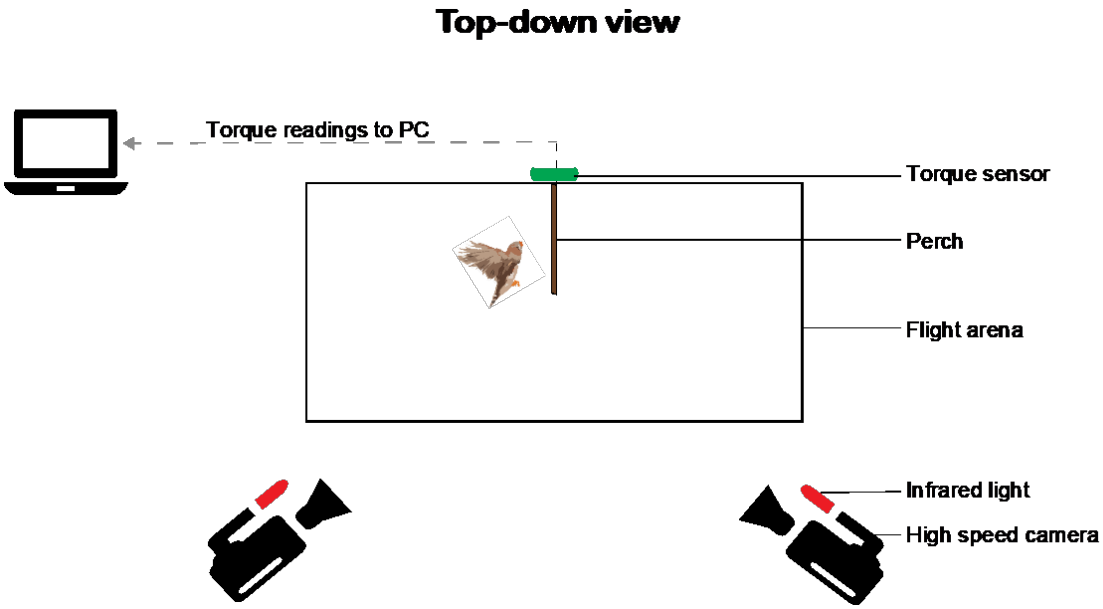


Figure A.2: Top-down schematic view of experimental set-up. Only the cage (flight arena) being recorded is shown here. In the set-up, two additional cages were placed at either side of the flight arena with birds of the opposite sex to that of the subject bird for social input (see text, Figure A.3).

camera plane), each containing a bird of the opposite sex to the bird being recorded (Figure 3). Their positioning was designed to provide social stimuli to encourage flying in the bird being recorded. All birds had access to ad lib food and water.

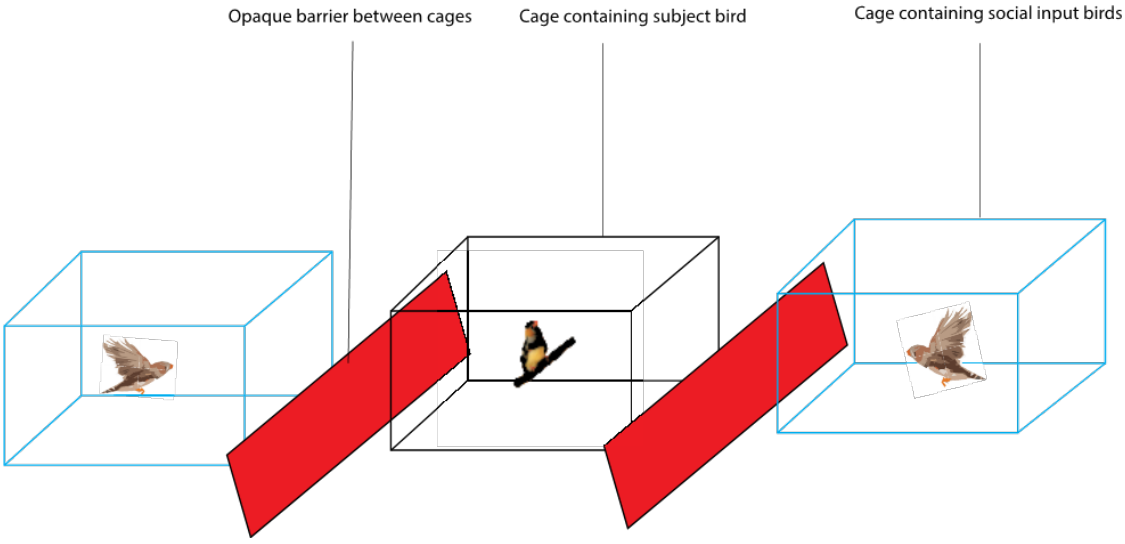


Figure A.3: Bird cage set-up for social input with birds of opposite sex in contiguous cages. A barrier was used in between each cage to encourage the subject bird to fly up to the perch, the only place in the cage from which the other two birds were visible in this set-up.

A.3.3 Treatment

After three days of flight recordings, birds were divided into three treatment groups, each consisting of one male and one female: control group; low-dose antibiotic group; and medium-dose antibiotic group. Each bird received a daily intramuscular injection of under 1ml of saline or gentamicin solution for four consecutive days. Gentamicin is an aminoglycoside antibiotic known to be toxic to inner ear hair cells, causing vestibular lesion. The doses administered were: 0 (control group), 5mg/kg (low dose group), and 10mg/kg (medium-dose group). Each bird was then followed for 8 weeks to document the loss of vestibular function and consequent recovery of such function (as bird hair cells regenerate). During this period, as well as during the three days of pre-treatment flight recordings, birds were weighed daily and monitored for inactivity, inability to eat and any other behavioural changes that may have resulted from the treatment or otherwise. Loss of 20% of body weight or inability to feed or drink were considered grounds for euthanasia by isoflurane anaesthesia and decapitation.

A.3.4 Torque measurements

The torque meter perch was custom built for the purposes of this study. Torque measurements were fed into a computer from the perch via an Arduino Uno interface, and the DC offset was removed using a high pass filter. We discarded any recordings with obviously erratic variation in peak forces, as well as those were the bird balanced on the perch for less than 5s. For each recording, the first 3s after the bird landed and the last 3s before take-off were discarded, to avoid confusing balancing forces with landing or take off forces. The remaining section of each recording was transformed into the frequency domain using a chirpse-Z transform at frequency points from 0 to 100 Hz in 0.1 Hz steps, using Welch's method for window averaging with 80% overlapping Hanning windows of 1 s duration. This allowed us to compute the magnitude of the response.

A.3.5 Statistical analysis

All data processing, statistics and figure plotting were performed using MATLAB (v. 2017b), and Python (v. 2.7.12). An initial inspection of the data was carried out in the frequency domain, and power spectral density was plotted using Welch's method to compare each condition for the whole group, for each bird individually, and for the subset of birds that were tested in all four conditions. However, given the nature of the data, we opted to carry out further analyses using simpler summary measures such as root mean square (RMS) and peak derivative values of torque measurements. The former is a standard measurement used for analysis of sensory experiments. This left us with two measurements for each trial on which to perform statistical analyses. Two sample t-tests were conducted to compare the performance of individual birds in light and dark conditions prior to treatment, as well as group data. The group data prior to treatment was also tested using a repeated measures ANOVA, and a two way repeated measures analysis of variance was carried out on the RMS and peak derivative values of the four birds that experienced all four conditions.

A.4 Results

A total of 456 perching events were recorded from 6 subjects over 8 weeks, out of which half were discarded due to the bird being perched for less than 5 seconds or due to obviously erratic measurements. Frequency domain analyses on the remaining data indicated that the greatest differences in perch balancing between conditions were in the 10-20 Hz range, at which the torque meter registered higher power in the light than in the dark. This pattern was maintained across treatments and individuals.

At a group level, there was a significant difference in the RMS values in the light ($\bar{x} = 0.488, s = 0.3$) and dark ($\bar{x} = 0.352, s = 0.3$); ($t_{(202)} = -3.07, p = 0.003$). At an individual level, however, only two of the birds tested (one male, one female) showed a significant difference in RMS values between light and dark conditions

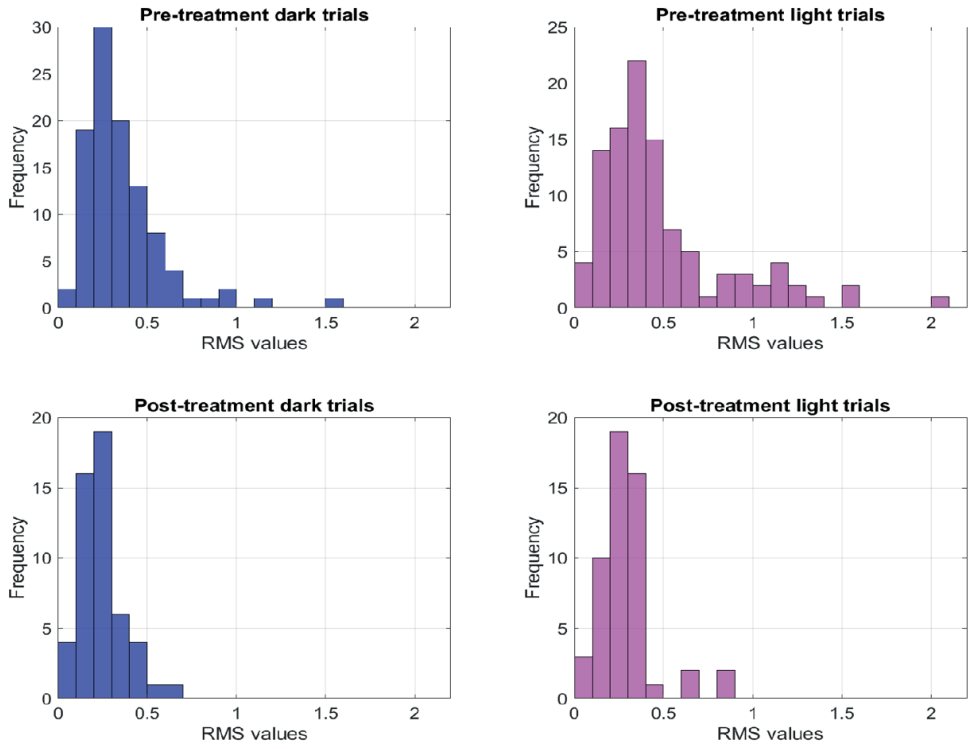


Figure A.4: Histograms of root mean square (RMS) values of torque in light and dark conditions before and after antibiotic treatment. RMS values were significantly higher when perching in the light compared to perching in the dark only before gentamicin treatment was applied.

(male: $t_{(41)} = -4.2, p = 0.0001$; female: $t_{(10)} = -8.9, p < 0.0008$). Neither of these were birds that later received gentamicin treatment.

A two-way repeated measures ANOVA was carried out to test the effects of light levels and treatment on the torque data of the four individuals that experienced all four conditions. There was a significant effect of light level on RMS at the p<.05 level ($F_{(1,1)} = 3.91, p = 0.04$), but the gentamicin treatment did not seem to have any significant effect ($p = 0.13$)

A.5 Discussion

Birds were consistently able to balance on the rotating perch under all experimental conditions, illustrating the robustness of their perching abilities. While availability of light significantly increased RMS ($t_{(202)} = -3.07, p = 0.003$), we hypothesise that this was most likely due to increased interest in social interactions in the light rather than on light affecting perching ability. The videography data supports this,

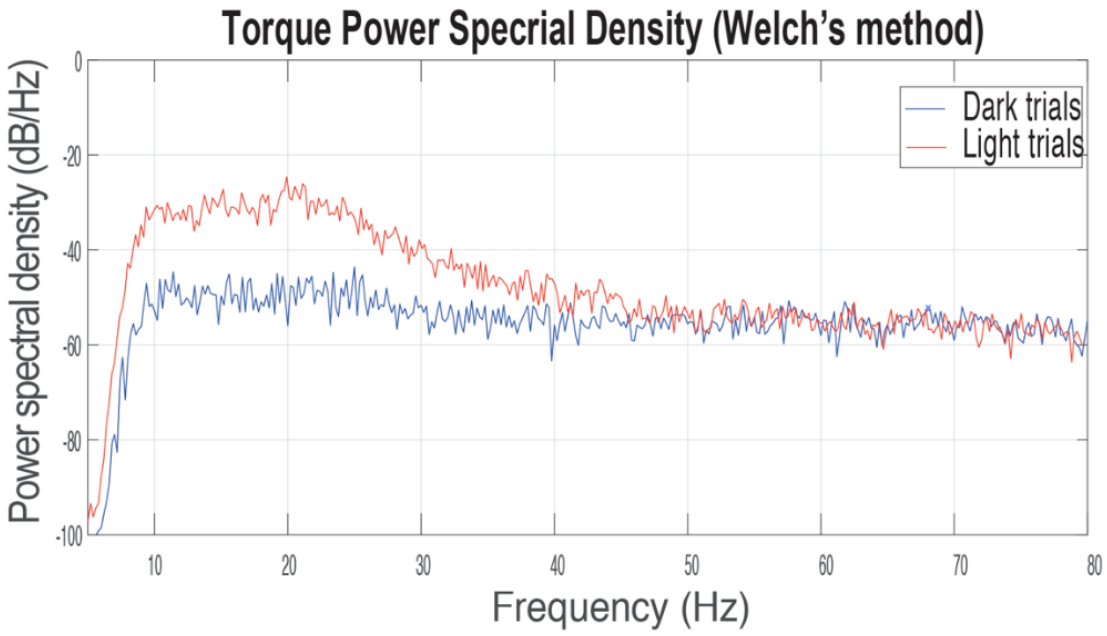


Figure A.5: Example of power spectral density estimate for one individual. The greatest differences in perch balancing between conditions are reflected in the 10-20 Hz range, at which the torque meter registered higher power in the light than in the dark. This pattern was maintained across individuals before antibiotic treatment.

as the subject birds were found to stretch out to look at birds in the contiguous cages during many light trials pre-treatment and some of the post treatment trials, but failed to do so in the dark. Also consistent with this hypothesis, the skewed distribution of RMS of each trial in the dark indicates that the birds had a higher RMS value in only a subset of trials in the light, rather than having an increase in RMS of torque across the board, as each RMS measurement refers to the entirety of a single perching episode. Those trials with higher RMS also coincide with the trials in which videography data shows most movement of the birds' head during a perching bout so as to look at nearby cages.

While the antibiotic treatment reduced birds' social activity, it did not have a significant effect on their perching ability. We found after the treatment, birds' movements tended to be softer, as reflected in peak derivative values and power spectral density plots, but not significantly so ($t_{(202)} = -1.92, p = 0.064$). It is important to note that due to complications experienced in the early stages of this study, the planned gentamicin dose given to the birds was reduced, and we

did not dissect birds at each stage, so we cannot conclusively say we damaged the vestibular system. For this reason, further studies are needed to draw any conclusions about whether the vestibular system has any effect on perching ability. A possible alternative to dissection would have been to test auditory ability of the birds during each week, as damaging inner ear hair cells would also have affected hearing. Moreover, during the 8 weeks post treatment that we intended to record, we were unable to collect enough data to conduct analyses of how perching ability improved over time due to logistical issues. This further limited the scope of this study, further indicating the need for further studies to draw any conclusions about the effect of the vestibular system. One further limitation of our study was that we failed to take into account the potential role of the lumbosacral organ. The lumbosacral organ, a specialised organ within the pelvis unique to birds, has recently been suggested to function as a sense organ of equilibrium [203] that exists in addition to the vestibular system, and which would affect any conclusions drawn from the treatment data. Given the lumbosacral organ is well-developed in terrestrial birds and that it has been suggested to facilitate balance control in perching and terrestrial locomotion [204], it is unsurprising that the gentamicin treatment did not have a significant effect on the birds' perching ability. Our results would therefore support, within the limitations stated above, the suggestion that the two different sense organs play a role in different kinds of locomotion, with the vestibular organ being predominantly used during flight and the lumbosacral system being predominantly used during walking and balancing on perches [205].

References

[202] Tyson L. Hedrick. "Software Techniques for Two- and Three-Dimensional Kinematic Measurements of Biological and Biomimetic Systems". In: *Bioinspiration &amp$\mathsemicolon$ Biomimetics* 3.3 (July 2008), p. 034001. (Visited on 05/20/2022).

[203] R Necker. "Specializations in the Lumbosacral Spinal Cord of Birds: Morphological and Behavioural Evidence for a Sense of Equilibrium". In: *European journal of morphology* 37.2-3 (Apr. 1999), pp. 211–214. (Visited on 05/19/2022).

[204] Darío Urbina-Meléndez et al. “A Physical Model Suggests That Hip-Localized Balance Sense in Birds Improves State Estimation in Perching: Implications for Bipedal Robots”. In: *Frontiers in Robotics and AI* 5 (2018). (Visited on 05/19/2022).

[205] Reinhold Necker. “Specializations in the Lumbosacral Vertebral Canal and Spinal Cord of Birds: Evidence of a Function as a Sense Organ Which Is Involved in the Control of Walking”. In: *Journal of Comparative Physiology A* 192.5 (Feb. 2006), p. 439. (Visited on 05/19/2022).

Bibliography

[1] John M McNamara and Alasdair I Houston. "Optimal Annual Routines: Behaviour in the Context of Physiology and Ecology". In: *Philosophical Transactions of the Royal Society B: Biological Sciences* 363.1490 (Jan. 2008), pp. 301–319. (Visited on 05/19/2022).

[2] Douglas G. Wallace et al. "Vestibular Information Is Required for Dead Reckoning in the Rat". In: *Journal of Neuroscience* 22.22 (Nov. 2002), pp. 10009–10017. (Visited on 05/19/2022).

[3] Douglas R. W. Wylie and Barrie J. Frost. "Complex Spike Activity of Purkinje Cells in the Ventral Uvula and Nodulus of Pigeons in Response to Translational Optic Flow". In: *Journal of Neurophysiology* 81.1 (Jan. 1999), pp. 256–266. (Visited on 05/19/2022).

[4] Elhanan Ben-Yishay et al. "Directional Tuning in the Hippocampal Formation of Birds". In: *Current biology: CB* 31.12 (June 2021), 2592–2602.e4.

[5] M. -L. Mittelstaedt and H. Mittelstaedt. "Homing by Path Integration in a Mammal". In: *Naturwissenschaften* 67.11 (Nov. 1980), pp. 566–567. (Visited on 05/06/2022).

[6] Martin Müller and Rüdiger Wehner. "Path Integration in Desert Ants, Cataglyphis Fortis". In: *Proceedings of the National Academy of Sciences* 85.14 (July 1988), pp. 5287–5290. (Visited on 05/19/2022).

[7] null Collett. "Insect Navigation En Route to the Goal: Multiple Strategies for the Use of Landmarks". In: *The Journal of Experimental Biology* 199.Pt 1 (1996), pp. 227–235.

[8] Carole Parron and Etienne Save. "Evidence for Entorhinal and Parietal Cortices Involvement in Path Integration in the Rat". In: *Experimental Brain Research* 159.3 (Dec. 2004), pp. 349–359. (Visited on 05/19/2022).

[9] Soyun Kim et al. "Contrasting Effects on Path Integration after Hippocampal Damage in Humans and Rats". In: *Proceedings of the National Academy of Sciences* 110.12 (Mar. 2013), pp. 4732–4737. (Visited on 05/06/2022).

[10] Xiaoli Chen et al. "Bias in Human Path Integration Is Predicted by Properties of Grid Cells". In: *Current biology: CB* 25.13 (June 2015), pp. 1771–1776.

[11] Ehud Vinepinsky, Opher Donchin, and Ronen Segev. "Wireless Electrophysiology of the Brain of Freely Swimming Goldfish". In: *Journal of Neuroscience Methods* 278 (Feb. 2017), pp. 76–86. (Visited on 05/06/2022).

[12] Rickesh N. Patel and Thomas W. Cronin. "Mantis Shrimp Navigate Home Using Celestial and Idiothetic Path Integration". In: *Current Biology* 30.11 (June 2020), 1981–1987.e3. (Visited on 05/06/2022).

[13] null Dittman and null Quinn. “Homing in Pacific Salmon: Mechanisms and Ecological Basis”. In: *The Journal of Experimental Biology* 199.Pt 1 (1996), pp. 83–91.

[14] Dora Biro, Jessica Meade, and Tim Guilford. “Familiar Route Loyalty Implies Visual Pilotage in the Homing Pigeon”. In: *Proceedings of the National Academy of Sciences* 101.50 (Dec. 2004), pp. 17440–17443. (Visited on 05/06/2022).

[15] Anthony Inder Mazeroll and W. Linn Montgomery. “Daily Migrations of a Coral Reef Fish in the Red Sea (Gulf of Aqaba, Israel): Initiation and Orientation”. In: *Copeia* 4 (Dec. 1998), pp. 893–905. (Visited on 05/06/2022).

[16] Hans G. Wallraff. “The Effect of Directional Experience on Initial Orientation in Pigeons”. In: *The Auk* 91.1 (1974), pp. 24–34. JSTOR: 4084658. (Visited on 05/19/2022).

[17] Roswitha Wiltschko and Wolfgang Wiltschko. “Avian Navigation: From Historical to Modern Concepts”. In: *Animal Behaviour* 65.2 (Feb. 2003), pp. 257–272. (Visited on 05/19/2022).

[18] Stephen C. Levinson. “Language and Space”. In: *Annual Review of Anthropology* 25.1 (1996), pp. 353–382. (Visited on 05/19/2022).

[19] Tim Guilford and Dora Biro. “Route Following and the Pigeon’s Familiar Area Map”. In: *Journal of Experimental Biology* 217.2 (Jan. 2014), pp. 169–179. (Visited on 05/19/2022).

[20] Stephen T. Emlen. “The Influence of Magnetic Information on the Orientation of the Indigo Bunting, Passerina Cyanea”. In: *Animal Behaviour* 18 (May 1970), pp. 215–224. (Visited on 05/19/2022).

[21] Roswitha Wiltschko. “Über Den Einfluß Statischer Magnetfelder Auf Die Zugorientierung Der Rotkehlchen (Erithacus Rubecula)”. In: *Zeitschrift für Tierpsychologie* 25 (Apr. 2010), pp. 537–558.

[22] Kramer. “EXPERIMENTS ON BIRD ORIENTATION AND THEIR INTERPRETATION. - Kramer - 1957 - Ibis - Wiley Online Library”. In: (1957). (Visited on 05/19/2022).

[23] Eberhard Dodt and Alberto Wirth. “Differentiation Between Rods and Cones by Flicker Electroretinography in Pigeon and Guinea Pig”. In: *Acta Physiologica Scandinavica* 30.1 (1954), pp. 80–89. (Visited on 05/19/2022).

[24] James A. Simmons, Michael J. Ferragamo, and Cynthia F. Moss. “Echo-Delay Resolution in Sonar Images of the Big Brown Bat, Eptesicus Fuscus”. In: *Proceedings of the National Academy of Sciences of the United States of America* 95.21 (Oct. 1998), pp. 12647–12652. (Visited on 05/20/2022).

[25] Lasse Jakobsen, Signe Brinkløv, and Annemarie Surlykke. “Intensity and Directionality of Bat Echolocation Signals”. In: *Frontiers in Physiology* 4 (2013). (Visited on 05/17/2022).

[26] Te K. Jones and Cynthia F. Moss. “Visual Cues Enhance Obstacle Avoidance in Echolocating Bats”. In: *Journal of Experimental Biology* 224.9 (May 2021), jeb241968. (Visited on 05/14/2022).

[27] Robert B. Welch and David H. Warren. “Immediate Perceptual Response to Intersensory Discrepancy”. In: *Psychological Bulletin* 88.3 (1980), pp. 638–667.

[28] Jan J. Koenderink. “Optic Flow”. In: *Vision Research* 26.1 (Jan. 1986), pp. 161–179. (Visited on 05/19/2022).

[29] J. J. Gibson. “The Perception of Visual Surfaces. By James J. Gibson, 1950”. In: *The American Journal of Psychology* 100.3-4 (1987 Fall-Winter), pp. 646–664.

[30] D. N. Lee et al. “The Optic Flow Field: The Foundation of Vision”. In: *Philosophical Transactions of the Royal Society of London. B, Biological Sciences* 290.1038 (July 1980), pp. 169–179. (Visited on 05/19/2022).

[31] James J. Gibson. *The Ecological Approach to Visual Perception*. New York: Psychology Press, 1979.

[32] Dennis Eckmeier et al. “Gaze Strategy in the Free Flying Zebra Finch (Taeniopygia Guttata)”. In: *PLOS ONE* 3.12 (Dec. 2008), e3956. (Visited on 05/09/2022).

[33] David N Lee. “A Theory of Visual Control of Braking Based on Information about Time-to-Collision”. In: *Perception* 5.4 (Dec. 1976), pp. 437–459. (Visited on 05/19/2022).

[34] Lance F. Tammero and Michael H. Dickinson. “Collision-Avoidance and Landing Responses Are Mediated by Separate Pathways in the Fruit Fly, Drosophila Melanogaster”. In: *Journal of Experimental Biology* 205.18 (Sept. 2002), pp. 2785–2798. (Visited on 05/18/2022).

[35] Melissa J Kearns et al. “Path Integration from Optic Flow and Body Senses in a Homing Task”. In: *Perception* 31.3 (Mar. 2002), pp. 349–374. (Visited on 05/18/2022).

[36] Jonathan C Horton and Daniel L Adams. “The Cortical Column: A Structure without a Function”. In: *Philosophical Transactions of the Royal Society B: Biological Sciences* 360.1456 (Apr. 2005), pp. 837–862. (Visited on 05/19/2022).

[37] Michael B. Orger et al. “Perception of Fourier and Non-Fourier Motion by Larval Zebrafish”. In: *Nature Neuroscience* 3.11 (Nov. 2000), pp. 1128–1133. (Visited on 05/17/2022).

[38] Erich D. Jarvis et al. “Avian Brains and a New Understanding of Vertebrate Brain Evolution”. In: *Nature Reviews Neuroscience* 6.2 (Feb. 2005), pp. 151–159. (Visited on 05/17/2022).

[39] Michael P. Jones, Kenneth E. Pierce, and Daniel Ward. “Avian Vision: A Review of Form and Function with Special Consideration to Birds of Prey”. In: *Journal of Exotic Pet Medicine* 16.2 (Apr. 2007), pp. 69–87. (Visited on 05/04/2022).

[40] Scott Husband and Toru Shimizu. “Evolution of the Avian Vision”. In: *Avian Visual Cognition* (Jan. 2001).

[41] Ann B. Butler and William Hodos. *Comparative Vertebrate Neuroanatomy: Evolution and Adaptation*. John Wiley & Sons, Sept. 2005.

[42] Andrew N. Iwaniuk and Douglas R.W. Wylie. “Neural Specialization for Hovering in Hummingbirds: Hypertrophy of the Pretectal Nucleus Lentiformis Mesencephali”. In: *Journal of Comparative Neurology* 500.2 (2007), pp. 211–221. (Visited on 03/18/2023).

[43] J. D. Pettigrew, K. J. Sanderson, and W. R. Levick. *Visual Neuroscience*. CUP Archive, Dec. 1986.

[44] Robert van der Willigen, Barrie Frost, and Hermann Wagner. “Stereoscopic Depth Perception in the Owl”. In: *Neuroreport* 9 (May 1998), pp. 1233–7.

[45] H J Bischof and S Watanabe. “On the Structure and Function of the Tectofugal Visual Pathway in Laterally Eyed Birds”. In: *European journal of morphology* 35.4 (Oct. 1997), pp. 246–254. (Visited on 05/19/2022).

[46] B. J. Frost, D. R. Wylie, and Y. -C. Wang. “The Processing of Object and Self-Motion in the Tectofugal and Accessory Optic Pathways of Birds”. In: *Vision Research*. Optics Physiology and Vision 30.11 (Jan. 1990), pp. 1677–1688. (Visited on 05/17/2022).

[47] Qian Xiao and Barrie J. Frost. “Looming Responses of Telencephalic Neurons in the Pigeon Are Modulated by Optic Flow”. In: *Brain Research* 1305 (Dec. 2009), pp. 40–46. (Visited on 05/17/2022).

[48] E. Pascal Malkemper et al. “Neuronal Circuits and the Magnetic Sense: Central Questions”. In: *Journal of Experimental Biology* 223.21 (Nov. 2020), jeb232371. (Visited on 03/18/2023).

[49] Dom Miceli et al. “Distribution of Ganglion Cells in the Pigeon Retina Labeled via Retrograde Transneuronal Transport of the Fluorescent Dye Rhodamine β-Isothiocyanate from the Telencephalic Visual Wulst”. In: *Brain Research* 1098.1 (July 2006), pp. 94–105. (Visited on 05/19/2022).

[50] Jin Yang, Chuan Zhang, and Shu-Rong Wang. “Comparisons of Visual Properties between Tectal and Thalamic Neurons with Overlapping Receptive Fields in the Pigeon”. In: *Brain, Behavior and Evolution* 65.1 (2005), pp. 33–39. (Visited on 05/13/2022).

[51] Cheri A. Budzynski et al. “Participation of the Homing Pigeon Thalamofugal Visual Pathway in Sun-Compass Associative Learning”. In: *European Journal of Neuroscience* 15.1 (2002), pp. 197–210. (Visited on 02/18/2023).

[52] P. Chand, R. C. Maurya, and U. C. Srivastava. “Neuronal Morphology and Spine Density of the Visual Wulst of the Strawberry Finch, Estrilda Amandava”. In: *Proceedings of the National Academy of Sciences, India Section B: Biological Sciences* 83.4 (Dec. 2013), pp. 627–642. (Visited on 02/18/2023).

[53] Nathan A. Crowder and Douglas R. Wylie. “Responses of Optokinetic Neurons in the Pretectum and Accessory Optic System of the Pigeon to Large-Field Plaids”. In: *Journal of Comparative Physiology A* 188.2 (Mar. 2002), pp. 109–119. (Visited on 02/18/2023).

[54] J. Martin Wild. “Pretectal and Tectal Projections to the Homologue of the Dorsal Lateral Geniculate Nucleus in the Pigeon: An Anterograde and Retrograde Tracing Study with Cholera Toxin Conjugated to Horseradish Peroxidase”. In: *Brain Research* 479.1 (Feb. 1989), pp. 130–137. (Visited on 02/18/2023).

[55] Nathan A. Crowder, Michael R.W. Dawson, and Douglas R.W. Wylie. “Temporal Frequency and Velocity-Like Tuning in the Pigeon Accessory Optic System”. In: *Journal of Neurophysiology* 90.3 (Sept. 2003), pp. 1829–1841. (Visited on 02/18/2023).

[56] B. J. Winterson and S. E. Brauth. “Direction-Selective Single Units in the Nucleus Lentiformis Mesencephali of the Pigeon (Columba Livia)”. In: *Experimental Brain Research* 60.2 (1985), pp. 215–226.

[57] W. Graf, J. I. Simpson, and C. S. Leonard. “Spatial Organization of Visual Messages of the Rabbit’s Cerebellar Flocculus. II. Complex and Simple Spike Responses of Purkinje Cells”. In: *Journal of Neurophysiology* 60.6 (Dec. 1988), pp. 2091–2121. (Visited on 05/17/2022).

[58] David J. Graham and Douglas R. Wylie. “Zebrin-Immunopositive and -Immunonegative Stripe Pairs Represent Functional Units in the Pigeon Vestibulocerebellum”. In: *The Journal of Neuroscience* 32.37 (Sept. 2012), pp. 12769–12779. (Visited on 05/17/2022).

[59] Curtis Hardyck et al. “The Eyes Have It: Exposure Times and Saccadic Movements in Visual Half-Field Experiments”. In: *Brain and Cognition* 4.4 (Oct. 1985), pp. 430–438. (Visited on 05/19/2022).

[60] Kevin Laland, Jens Krause, and Culum Brown. *Fish Cognition and Behavior*. John Wiley & Sons, June 2011.

[61] K. V. Fite. “Pretectal and Accessory-Optic Visual Nuclei of Fish, Amphibia and Reptiles: Theme and Variations”. In: *Brain, Behavior and Evolution* 26.2 (1985), pp. 71–90.

[62] Alexey T. Aliper et al. “Updated Functional Segregation of Retinal Ganglion Cell Projections in the Tectum of a Cyprinid Fish—Further Elaboration Based on Microelectrode Recordings”. In: *Fish Physiology and Biochemistry* 45.2 (Apr. 2019), pp. 773–792. (Visited on 03/04/2023).

[63] Greg Lemke and Michaël Reber. “RETINOTECTAL MAPPING: New Insights from Molecular Genetics”. In: *Annual Review of Cell and Developmental Biology* 21.1 (2005), pp. 551–580. (Visited on 05/19/2022).

[64] Tobias Roeser and Herwig Baier. “Visuomotor Behaviors in Larval Zebrafish after GFP-Guided Laser Ablation of the Optic Tectum”. In: *Journal of Neuroscience* 23.9 (May 2003), pp. 3726–3734. (Visited on 05/19/2022).

[65] Ethan Gahtan, Paul Tanger, and Herwig Baier. “Visual Prey Capture in Larval Zebrafish Is Controlled by Identified Reticulospinal Neurons Downstream of the Tectum”. In: *Journal of Neuroscience* 25.40 (Oct. 2005), pp. 9294–9303. (Visited on 05/19/2022).

[66] Estuardo Robles, Stephen Smith, and Herwig Baier. “Characterization of Genetically Targeted Neuron Types in the Zebrafish Optic Tectum”. In: *Frontiers in Neural Circuits* 5 (2011). (Visited on 03/04/2023).

[67] M Van Der Marel et al. “Changes in Skin Mucus of Common Carp, Cyprinus Carpio L., after Exposure to Water with a High Bacterial Load”. In: *Journal of Fish Diseases* 33.5 (2010), pp. 431–439. (Visited on 05/19/2022).

[68] J I Simpson. “The Accessory Optic System”. In: *Annual Review of Neuroscience* 7.1 (1984), pp. 13–41. (Visited on 03/04/2023).

[69] Olivia Andrea Masseck and Klaus-Peter Hoffmann. “Question of Reference Frames: Visual Direction-Selective Neurons in the Accessory Optic System of Goldfish”. In: *Journal of Neurophysiology* 102.5 (Nov. 2009), pp. 2781–2789. (Visited on 03/04/2023).

[70] Kun Wang et al. “Parallel Channels for Motion Feature Extraction in the Pretectum and Tectum of Larval Zebrafish”. In: *Cell Reports* 30.2 (Jan. 2020), 442–453.e6. (Visited on 03/04/2023).

[71] Kun Wang et al. “Selective Processing of All Rotational and Translational Optic Flow Directions in the Zebrafish Pretectum and Tectum”. In: *BMC Biology* 17.1 (Mar. 2019), p. 29. (Visited on 05/19/2022).

[72] Hongyuan Wu, Xiaoye Michael Wang, and Jing Samantha Pan. “Perceiving Blurry Scenes with Translational Optic Flow, Rotational Optic Flow or Combined Optic Flow”. In: *Vision Research* 158 (May 2019), pp. 49–57. (Visited on 05/19/2022).

[73] Eva A. Naumann et al. “From Whole-Brain Data to Functional Circuit Models: The Zebrafish Optomotor Response”. In: *Cell* 167.4 (Nov. 2016), 947–960.e20. (Visited on 05/19/2022).

[74] Adrienn G. Varga et al. “Spatial Navigation and the Central Complex: Sensory Acquisition, Orientation, and Motor Control”. In: *Frontiers in Behavioral Neuroscience* 11 (2017). (Visited on 05/06/2022).

[75] Ehud Vinepinsky et al. “Representation of Edges, Head Direction, and Swimming Kinematics in the Brain of Freely-Navigating Fish”. In: *Scientific Reports* 10.1 (Sept. 2020), p. 14762. (Visited on 05/06/2022).

[76] Js Taube, Ru Muller, and Jb Ranck. “Head-Direction Cells Recorded from the Postsubiculum in Freely Moving Rats. I. Description and Quantitative Analysis”. In: *The Journal of Neuroscience* 10.2 (Feb. 1990), pp. 420–435. (Visited on 05/06/2022).

[77] Jeffrey S. Taube. “The Head Direction Signal: Origins and Sensory-Motor Integration”. In: *Annual Review of Neuroscience* 30 (2007), pp. 181–207.

[78] J. O’Keefe and D. H. Conway. “Hippocampal Place Units in the Freely Moving Rat: Why They Fire Where They Fire”. In: *Experimental Brain Research* 31.4 (Apr. 1978), pp. 573–590. (Visited on 05/19/2022).

[79] Torkel Hafting et al. “Microstructure of a Spatial Map in the Entorhinal Cortex”. In: *Nature* 436.7052 (Aug. 2005), pp. 801–806. (Visited on 05/19/2022).

[80] James G. Canfield and Sheri J. Y. Mizumori. “Methods for Chronic Neural Recording in the Telencephalon of Freely Behaving Fish”. In: *Journal of Neuroscience Methods* 133.1-2 (Feb. 2004), pp. 127–134.

[81] Jennifer J. Siegel, Douglas Nitz, and Verner P. Bingman. “Lateralized Functional Components of Spatial Cognition in the Avian Hippocampal Formation: Evidence from Single-Unit Recordings in Freely Moving Homing Pigeons”. In: *Hippocampus* 16.2 (2006), pp. 125–140.

[82] H. L. Payne, G. F. Lynch, and D. Aronov. “Neural Representations of Space in the Hippocampus of a Food-Caching Bird”. In: *Science* 373.6552 (July 2021), pp. 343–348. (Visited on 05/19/2022).

[83] Francesco Savelli, JD Luck, and James J Knierim. “Framing of Grid Cells within and beyond Navigation Boundaries”. In: *eLife* 6 (Jan. 2017). Ed. by Upinder S Bhalla, e21354. (Visited on 05/19/2022).

[84] Haleh Fotowat et al. “Neural Activity in a Hippocampus-like Region of the Teleost Pallium Is Associated with Active Sensing and Navigation”. In: *eLife* 8 (Apr. 2019). Ed. by Vatsala Thirumalai, Timothy E Behrens, and Maurice J Chacron, e44119. (Visited on 05/06/2022).

[85] Tom Hartley et al. “Space in the Brain: How the Hippocampal Formation Supports Spatial Cognition”. In: *Philosophical Transactions of the Royal Society B: Biological Sciences* 369.1635 (Feb. 2014), p. 20120510. (Visited on 05/06/2022).

[86] Bruce L. McNaughton et al. “Path Integration and the Neural Basis of the 'Cognitive Map'”. In: *Nature Reviews. Neuroscience* 7.8 (Aug. 2006), pp. 663–678.

[87] Bruno Siciliano and Oussama Khatib, eds. *Springer Handbook of Robotics*. Springer Handbooks. Springer, 2016.

[88] Steven M. LaValle. *Planning Algorithms*. Cambridge University Press, May 2006.

[89] A. Elshamli, H.A. Abdullah, and S. Areibi. “Genetic Algorithm for Dynamic Path Planning”. In: *Canadian Conference on Electrical and Computer Engineering 2004 (IEEE Cat. No.04CH37513)*. Vol. 2. May 2004, 677–680 Vol.2.

[90] Adham Atyabi and David Powers. “Review of Classical and Heuristic-Based Navigation and Path Planning Approaches”. In: *International Journal of Advancements in Computing Technology (IJACT)* 5 (Jan. 2013), pp. 1–14.

[91] Rodney A. Brooks. “Planning Collision- Free Motions for Pick-and-Place Operations”. In: *The International Journal of Robotics Research* 2.4 (Dec. 1983), pp. 19–44. (Visited on 04/05/2023).

[92] Sertac Karaman and Emilio Frazzoli. “Sampling-Based Algorithms for Optimal Motion Planning”. In: *The International Journal of Robotics Research* 30.7 (June 2011), pp. 846–894. (Visited on 03/20/2023).

[93] Oussama Khatib. “Real-Time Obstacle Avoidance for Manipulators and Mobile Robots”. In: *The International Journal of Robotics Research* 5.1 (Mar. 1986), pp. 90–98. (Visited on 05/20/2022).

[94] Volkan Sezer and Metin Gokasan. “A Novel Obstacle Avoidance Algorithm: “Follow the Gap Method””. In: *Robotics and Autonomous Systems* 60.9 (Sept. 2012), pp. 1123–1134. (Visited on 05/19/2022).

[95] A Arbib. “Sensorimotor Transformations in the Worlds of Frogs and Robots”. In: (1995), p. 27.

[96] Brett R Fajen et al. “A Dynamical Model of Visually-Guided Steering, Obstacle Avoidance, and Route Selection | SpringerLink”. In: 54 (2003), pp. 13–34. (Visited on 05/18/2022).

[97] J. Minguez and L. Montano. “Nearness Diagram (ND) Navigation: Collision Avoidance in Troublesome Scenarios”. In: *IEEE Transactions on Robotics and Automation* 20.1 (Feb. 2004), pp. 45–59. (Visited on 05/20/2022).

[98] L. Kavraki and J.-C. Latombe. “Randomized Preprocessing of Configuration Space for Path Planning: Articulated Robots”. In: *Proceedings of IEEE/RSJ International Conference on Intelligent Robots and Systems (IROS'94)*. Vol. 3. Sept. 1994, 1764–1771 vol.3.

[99] Steven M. LaValle and James J. Kuffner. “Randomized Kinodynamic Planning”. In: *The International Journal of Robotics Research* 20.5 (May 2001), pp. 378–400. (Visited on 03/20/2023).

[100] Vladimir J. Lumelsky and Alexander A. Stepanov. “Path-Planning Strategies for a Point Mobile Automaton Moving amidst Unknown Obstacles of Arbitrary Shape”. In: *Algorithmica* 2.1 (Nov. 1987), pp. 403–430. (Visited on 05/19/2022).

[101] John H. Holland. *Adaptation in Natural and Artificial Systems: An Introductory Analysis with Applications to Biology, Control, and Artificial Intelligence.* Adaptation in Natural and Artificial Systems: An Introductory Analysis with Applications to Biology, Control, and Artificial Intelligence. Oxford, England: U Michigan Press, 1975, pp. viii, 183.

[102] M. Dorigo and L.M. Gambardella. “Ant Colony System: A Cooperative Learning Approach to the Traveling Salesman Problem”. In: *IEEE Transactions on Evolutionary Computation* 1.1 (Apr. 1997), pp. 53–66.

[103] Dervis Karaboga. “An Idea Based on Honey Bee Swarm for Numerical Optimization, Technical Report - TR06”. In: *Technical Report, Erciyes University* (Jan. 2005).

[104] M. Zohaib et al. *Control Strategies for Mobile Robot With Obstacle Avoidance.* June 2013. arXiv: 1306.1144 [cs]. (Visited on 05/13/2022).

[105] Huai-Ti Lin, Ivo G. Ros, and Andrew A. Biewener. “Through the Eyes of a Bird: Modelling Visually Guided Obstacle Flight”. In: *Journal of The Royal Society Interface* 11.96 (July 2014), p. 20140239. (Visited on 05/04/2022).

[106] Hosein Houshyari and Volkan Sezer. “A New Gap-Based Obstacle Avoidance Approach: Follow the Obstacle Circle Method”. In: *Robotica* (Nov. 2021), pp. 1–24. (Visited on 05/19/2022).

[107] Shigeru Watanabe, Junko Sakamoto, and Masumi Wakita. “Pigeons’ Discrimination of Paintings by Monet and Picasso”. In: *Journal of the Experimental Analysis of Behavior* 63.2 (Mar. 1995), pp. 165–174. (Visited on 05/06/2022).

[108] Wolfgang Wiltschko and Roswitha Wiltschko. “Magnetic Compass Orientation in Birds and Its Physiological Basis”. In: *Naturwissenschaften* 89.10 (Oct. 2002), pp. 445–452. (Visited on 05/19/2022).

[109] Ken Cheng et al. “Small-Scale Spatial Cognition in Pigeons”. In: *Behavioural Processes* 72.2 (May 2006), pp. 115–127.

[110] Jerry A. Waldvogel. “The Bird’s Eye View”. In: *American Scientist* 78.4 (1990), pp. 342–353. JSTOR: 29774120. (Visited on 05/20/2022).

[111] Kevin J Rounsley and Sally A McFadden. “Limits of Visual Acuity in the Frontal Field of the Rock Pigeon (Columba Livia)”. In: *Perception* 34.8 (Aug. 2005), pp. 983–993. (Visited on 05/06/2022).

[112] Monika Remy and Jacky Emmerton. “Directional Dependence of Intraocular Transfer of Stimulus Detection in Pigeons (Columba Livia)”. In: *Behavioral Neuroscience* 105.5 (1991), pp. 647–652.

[113] Melvyn A. Goodale. “Visuomotor Organization of Pecking in the Pigeon”. In: *Advances in Vertebrate Neuroethology* (1983), pp. 349–357. (Visited on 05/20/2022).

[114] Thomas J. Near et al. “Resolution of Ray-Finned Fish Phylogeny and Timing of Diversification”. In: *Proceedings of the National Academy of Sciences* 109.34 (Aug. 2012), pp. 13698–13703. (Visited on 05/20/2022).

[115] Karen L. Cheney et al. “Colour Vision and Response Bias in a Coral Reef Fish”. In: *Journal of Experimental Biology* 216.15 (Aug. 2013), pp. 2967–2973. (Visited on 05/19/2022).

[116] C. Karlsson et al. *Teleost Fish Can Accurately Estimate Distance Travelled*. Nov. 2019. (Visited on 03/18/2023).

[117] Laurie Mitchell et al. “Triggerfish Uses Chromaticity and Lightness for Object Segregation”. In: *Royal Society Open Science* 4.12 (), p. 171440. (Visited on 05/19/2022).

[118] S. R. Matchette et al. “Underwater Caustics Disrupt Prey Detection by a Reef Fish”. In: *Proceedings of the Royal Society B: Biological Sciences* 287.1924 (Apr. 2020), p. 20192453. (Visited on 05/19/2022).

[119] J. H. Capshew. “Engineering Behavior: Project Pigeon, World War II, and the Conditioning of B. F. Skinner”. In: *Technology and Culture* 34.4 (Oct. 1993), pp. 835–857.

[120] Andrew M. Hein et al. “An Algorithmic Approach to Natural Behavior”. In: *Current Biology* 30.11 (June 2020), R663–R675. (Visited on 05/04/2022).

[121] Kaushik Ghose et al. “Echolocating Bats Use a Nearly Time-Optimal Strategy to Intercept Prey”. In: *PLOS Biology* 4.5 (Apr. 2006), e108. (Visited on 05/04/2022).

[122] Caroline H. Brighton, Adrian L. R. Thomas, and Graham K. Taylor. “Terminal Attack Trajectories of Peregrine Falcons Are Described by the Proportional Navigation Guidance Law of Missiles”. In: *Proceedings of the National Academy of Sciences* 114.51 (Dec. 2017), pp. 13495–13500. (Visited on 05/04/2022).

[123] Caroline H. Brighton and Graham K. Taylor. “Hawks Steer Attacks Using a Guidance System Tuned for Close Pursuit of Erratically Manoeuvring Targets”. In: *Nature Communications* 10.1 (June 2019), p. 2462. (Visited on 05/04/2022).

[124] Caroline H. Brighton et al. “Attack Behaviour in Naive Gyrfalcons Is Modelled by the Same Guidance Law as in Peregrine Falcons, but at a Lower Guidance Gain”. In: *Journal of Experimental Biology* 224.5 (Mar. 2021), jeb238493. (Visited on 05/04/2022).

[125] Samuel T. Fabian et al. “Interception by Two Predatory Fly Species Is Explained by a Proportional Navigation Feedback Controller”. In: *Journal of The Royal Society Interface* 15.147 (Oct. 2018), p. 20180466. (Visited on 05/04/2022).

[126] T. S. Collett and M. F. Land. “How Hoverflies Compute Interception Courses”. In: *Journal of Comparative Physiology ? A* 125.3 (1978), pp. 191–204. (Visited on 05/04/2022).

[127] Suzanne Amador Kane, Andrew H. Fulton, and Lee J. Rosenthal. “When Hawks Attack: Animal-Borne Video Studies of Goshawk Pursuit and Prey-Evasion Strategies”. In: *Journal of Experimental Biology* 218.2 (Jan. 2015), pp. 212–222. (Visited on 03/20/2023).

[128] Caroline H. Brighton et al. “Raptors Avoid the Confusion Effect by Targeting Fixed Points in Dense Aerial Prey Aggregations”. In: *Nature Communications* 13.1 (Aug. 2022), p. 4778. (Visited on 03/24/2023).

[129] Norbert Boeddeker and Martin Egelhaaf. “Steering a Virtual Blowfly: Simulation of Visual Pursuit”. In: *Proceedings. Biological Sciences* 270.1527 (Sept. 2003), pp. 1971–1978.

[130] Andreas F. Haselsteiner, Cole Gilbert, and Z. Jane Wang. “Tiger Beetles Pursue Prey Using a Proportional Control Law with a Delay of One Half-Stride”. In: *Journal of The Royal Society Interface* 11.95 (June 2014), p. 20140216. (Visited on 05/04/2022).

[131] S. W. Zhang et al. “Visual Tracking of Moving Targets by Freely Flying Honeybees”. In: *Visual Neuroscience* 4.4 (Apr. 1990), pp. 379–386.

[132] Bart R. H. Geurten et al. “A Syntax of Hoverfly Flight Prototypes”. In: *The Journal of Experimental Biology* 213.Pt 14 (July 2010), pp. 2461–2475.

[133] Matthew J. McHenry et al. “The Pursuit Strategy of Predatory Bluefish (Pomatomus Saltatrix)”. In: *Proceedings of the Royal Society B: Biological Sciences* 286.1897 (Feb. 2019), p. 20182934. (Visited on 05/04/2022).

[134] R. M. Olberg et al. “Eye Movements and Target Fixation during Dragonfly Prey-Interception Flights”. In: *Journal of Comparative Physiology. A, Neuroethology, Sensory, Neural, and Behavioral Physiology* 193.7 (July 2007), pp. 685–693.

[135] M. F. Land and T. S. Collett. “Chasing Behaviour of Houseflies (Fannia Canicularis)”. In: *Journal of comparative physiology* 89.4 (Dec. 1974), pp. 331–357. (Visited on 05/06/2022).

[136] N. A. Shneydor. *Missile Guidance and Pursuit: Kinematics, Dynamics and Control*. Elsevier, Jan. 1998.

[137] Emily Baird and Marie Dacke. “Finding the Gap: A Brightness-Based Strategy for Guidance in Cluttered Environments”. In: *Proceedings of the Royal Society B: Biological Sciences* 283.1828 (Apr. 2016), p. 20152988. (Visited on 05/04/2022).

[138] Partha S. Bhagavatula et al. “Behavioral Lateralization and Optimal Route Choice in Flying Budgerigars”. In: *PLOS Computational Biology* 10.3 (Mar. 2014), e1003473. (Visited on 05/04/2022).

[139] M. Remy and J. Emmerton. “Behavioral Spectral Sensitivities of Different Retinal Areas in Pigeons”. In: *Behavioral Neuroscience* 103.1 (Feb. 1989), pp. 170–177.

[140] C. David Williams and Andrew A. Biewener. “Pigeons Trade Efficiency for Stability in Response to Level of Challenge during Confined Flight”. In: *Proceedings of the National Academy of Sciences* 112.11 (Mar. 2015), pp. 3392–3396. (Visited on 05/04/2022).

[141] Yongchang Wang and Barrie J. Frost. “Time to Collision Is Signalled by Neurons in the Nucleus Rotundus of Pigeons”. In: *Nature* 356.6366 (Mar. 1992), pp. 236–238. (Visited on 05/04/2022).

[142] Ivo G. Ros et al. “Rules to Fly by: Pigeons Navigating Horizontal Obstacles Limit Steering by Selecting Gaps Most Aligned to Their Flight Direction”. In: *Interface Focus* 7.1 (Feb. 2017), p. 20160093. (Visited on 05/09/2022).

[143] C. J. PENNYCUICK. “Power Requirements for Horizontal Flight in the Pigeon Columba Livia”. In: *Journal of Experimental Biology* 49.3 (Dec. 1968), pp. 527–555. (Visited on 05/04/2022).

[144] Vivek H. Sridhar et al. “The Geometry of Decision-Making in Individuals and Collectives”. In: *Proceedings of the National Academy of Sciences* 118.50 (Dec. 2021), e2102157118. (Visited on 05/04/2022).

[145] J. M. Warren. “Handedness and Laterality in Humans and Other Animals”. In: *Physiological Psychology* 8.3 (Sept. 1980), pp. 351–359. (Visited on 05/04/2022).

[146] Promode R. Bandyopadhyay, Henry A. Leinhos, and Aren M. Hellum. “Handedness Helps Homing in Swimming and Flying Animals”. In: *Scientific Reports* 3.1 (Jan. 2013), p. 1128. (Visited on 05/04/2022).

[147] Dora Biro, Jessica Meade, and Tim Guilford. “Route Recapitulation and Route Loyalty in Homing Pigeons: Pilotage From 25 Km?” In: *Journal of Navigation* 59 (Jan. 2006), pp. 43–53.

[148] Daniel Kress, Evelien van Bokhorst, and David Lentink. “How Lovebirds Maneuver Rapidly Using Super-Fast Head Saccades and Image Feature Stabilization”. In: *PLOS ONE* 10.6 (June 2015), e0129287. (Visited on 05/04/2022).

[149] Sofía Miñano and Graham K. Taylor. *Through Hawks’ Eyes: Reconstructing a Bird’s Visual Field in Flight to Study Gaze Strategy and Attention during Perching and Obstacle Avoidance*. June 2021. (Visited on 05/19/2022).

[150] Hans Wallraff. “Navigation by Homing Pigeons: Updated Perspective”. In: *Ethology Ecology & Evolution - ETHOL ECOL EVOL* 13 (Mar. 2001).

[151] Graham R. Martin. “The Subtlety of Simple Eyes: The Tuning of Visual Fields to Perceptual Challenges in Birds”. In: *Philosophical Transactions of the Royal Society B: Biological Sciences* 369.1636 (Feb. 2014), p. 20130040. (Visited on 03/04/2023).

[152] Gordon Lynn Walls. “THE VERTEBRATE EYE AND ITS ADAPTIVE RADIATION”. In: *The Journal of Nervous and Mental Disease* 100.3 (Sept. 1944), p. 332. (Visited on 05/20/2022).

[153] Kevin Healy et al. “Metabolic Rate and Body Size Are Linked with Perception of Temporal Information”. In: *Animal Behaviour* 86.4 (Oct. 2013), pp. 685–696. (Visited on 03/04/2023).

[154] Crlos Martinoya, Jacques Rey, and Susana Bloch. “Limits of the Pigeon’s Binocular Field and Direction for Best Binocular Viewing”. In: *Vision Research* 21.7 (Jan. 1981), pp. 1197–1200. (Visited on 05/06/2022).

[155] Emily Baird et al. “Visual Control of Flight Speed and Height in the Honeybee”. In: *From Animals to Animats 9*. Ed. by Stefano Nolfi et al. Lecture Notes in Computer Science. Berlin, Heidelberg: Springer, 2006, pp. 40–51.

[156] Nellie Linander, Emily Baird, and Marie Dacke. “Bumblebee Flight Performance in Environments of Different Proximity”. In: *Journal of Comparative Physiology A* 202.2 (Feb. 2016), pp. 97–103. (Visited on 03/04/2023).

[157] Partha S. Bhagavatula et al. “Optic Flow Cues Guide Flight in Birds”. In: *Current Biology* 21.21 (Nov. 2011), pp. 1794–1799. (Visited on 05/06/2022).

[158] Natalia Pérez-Campanero Antolin and Graham K. Taylor. *Gap Selection and Steering during Obstacle Avoidance in Pigeons*. Preprint. Animal Behavior and Cognition, Mar. 2022. (Visited on 09/01/2022).

[159] Aaron J Fath and Brett R Fajen. “Static and Dynamic Visual Information about the Size and Passability of an Aperture”. In: *Perception* 40.8 (Aug. 2011), pp. 887–904. (Visited on 05/05/2022).

[160] B. P. Hayes et al. “The Projection of the Visual Field upon the Retina of the Pigeon”. In: *Vision Research* 27.1 (Jan. 1987), pp. 31–40. (Visited on 05/06/2022).

[161] A. Charles Catania. “On the Visual Acuity of the Pigeon1”. In: *Journal of the Experimental Analysis of Behavior* 7.5 (1964), pp. 361–366. (Visited on 05/06/2022).

[162] U. Hahmann and O. Güntürkün. “The Visual Acuity for the Lateral Visual Field of the Pigeon (Columba Livia)”. In: *Vision Research* 33.12 (Aug. 1993), pp. 1659–1664.

[163] Yuichiro Nomura et al. “Evaluation of Critical Flicker-Fusion Frequency Measurement Methods Using a Touchscreen-Based Visual Temporal Discrimination Task in the Behaving Mouse”. In: *Neuroscience Research* 148 (Nov. 2019), pp. 28–33.

[164] M. Tistarelli and G. Sandini. “On the Advantages of Polar and Log-Polar Mapping for Direct Estimation of Time-to-Impact from Optical Flow”. In: *IEEE Transactions on Pattern Analysis and Machine Intelligence* 15.4 (Apr. 1993), pp. 401–410.

[165] Paul Carlile, Richard Peters, and Christopher Evans. “Detection of a Looming Stimulus by the Jacky Dragon: Selective Sensitivity to Characteristics of an Aerial Predator”. In: *Animal Behaviour* 72 (Sept. 2006), pp. 553–562.

[166] Ingo Schiffner et al. “Minding the Gap: In-Flight Body Awareness in Birds”. In: *Frontiers in Zoology* 11.1 (Sept. 2014), p. 64. (Visited on 05/19/2022).

[167] Finnegan J. Calabro, Kunjan D. Rana, and Lucia M. Vaina. “Two Mechanisms for Optic Flow and Scale Change Processing of Looming”. In: *Journal of Vision* 11.3 (Mar. 2011), p. 5. (Visited on 05/06/2022).

[168] W Hodos et al. “Spatiotemporal Contrast Sensitivity in Pigeons”. In: *Investigative Ophthalmology & Visual Science* 43.13 (Dec. 2002), p. 4712.

[169] Klaus Landwehr, Esther Brendel, and Heiko Hecht. “Luminance and Contrast in Visual Perception of Time to Collision”. In: *Vision Research* 89 (Aug. 2013), pp. 18–23. (Visited on 05/18/2022).

[170] Michael Mendl and Elizabeth S. Paul. “Animal Affect and Decision-Making”. In: *Neuroscience & Biobehavioral Reviews* 112 (May 2020), pp. 144–163. (Visited on 05/07/2022).

[171] Alexei L. Vyssotski et al. “EEG Responses to Visual Landmarks in Flying Pigeons”. In: *Current Biology* 19.14 (July 2009), pp. 1159–1166. (Visited on 05/07/2022).

[172] Glenn R. Almany. “Differential Effects of Habitat Complexity, Predators and Competitors on Abundance of Juvenile and Adult Coral Reef Fishes”. In: *Oecologia* 141.1 (Sept. 2004), pp. 105–113. (Visited on 05/08/2022).

[173] M. Willis et al. “Infrasonic Observations of Open Ocean Swells in the Pacific: Deciphering the Song of the Sea”. In: *Geophysical Research Letters* 31.19 (2004). (Visited on 05/19/2022).

[174] S. C. Willis, K. O. Winemiller, and H. Lopez-Fernandez. “Habitat Structural Complexity and Morphological Diversity of Fish Assemblages in a Neotropical Floodplain River”. In: *Oecologia* 142.2 (Jan. 2005), pp. 284–295. (Visited on 05/08/2022).

[175] Valeriya Komyakova, Philip L. Munday, and Geoffrey P. Jones. “Relative Importance of Coral Cover, Habitat Complexity and Diversity in Determining the Structure of Reef Fish Communities”. In: *PLOS ONE* 8.12 (Dec. 2013), e83178. (Visited on 05/19/2022).

[176] Darren J. Coker, Morgan S. Pratchett, and Philip L. Munday. “Influence of Coral Bleaching, Coral Mortality and Conspecific Aggression on Movement and Distribution of Coral-Dwelling Fish”. In: *Journal of Experimental Marine Biology and Ecology* 414–415 (Mar. 2012), pp. 62–68. (Visited on 05/19/2022).

[177] Karen M. Chong-Seng et al. “The Influence of Coral Reef Benthic Condition on Associated Fish Assemblages”. In: *PLOS ONE* 7.8 (Aug. 2012), e42167. (Visited on 05/19/2022).

[178] Matthew Tietbohl et al. “Intentional Partial Beaching in a Coral Reef Fish: A Newly Recorded Hunting Behaviour of Titan Triggerfish, Balistoides Viridescens”. In: *Journal of Fish Biology* 97 (Aug. 2020).

[179] Fabio Cortesi et al. “Visual System Diversity in Coral Reef Fishes”. In: *Seminars in Cell & Developmental Biology*. Vertebrate Vision: Lessons from Non-Model Species 106 (Oct. 2020), pp. 31–42. (Visited on 05/19/2022).

[180] Connor Champ et al. “Visual Acuity in a Species of Coral Reef Fish: Rhinecanthus Aculeatus”. In: *Brain, Behavior and Evolution* 83.1 (2014), pp. 31–42. (Visited on 05/19/2022).

[181] Karen L. Cheney et al. “Seeing Picasso: An Investigation into the Visual System of the Triggerfish Rhinecanthus Aculeatus”. In: *Journal of Experimental Biology* 225.7 (Apr. 2022), jeb243907. (Visited on 05/19/2022).

[182] Siby Philip et al. “Fish Lateral Line Innovation: Insights into the Evolutionary Genomic Dynamics of a Unique Mechanosensory Organ”. In: *Molecular Biology and Evolution* 29.12 (Dec. 2012), pp. 3887–3898. (Visited on 05/20/2022).

[183] Horst Bleckmann and Randy Zelick. “Lateral Line System of Fish”. In: *Integrative Zoology* 4.1 (Mar. 2009), pp. 13–25.

[184] MARK W. DENNY. “Terrestrial Versus Aquatic Biology: The Medium and Its Message1”. In: *American Zoologist* 30.1 (Feb. 1990), pp. 111–121. (Visited on 05/19/2022).

[185] Paul W. Webb. “Form and Function in Fish Swimming”. In: *Scientific American* 251.1 (1984), pp. 72–83. JSTOR: 24969414. (Visited on 05/19/2022).

[186] PW Webb. “Entrainment by River Chub Nocomis Micropogon and Smallmouth Bass Micropterus Dolomieu on Cylinders”. In: *Journal of Experimental Biology* 201.16 (Aug. 1998), pp. 2403–2412. (Visited on 05/19/2022).

[187] Peter B. Moyle et al. “Biology and Population Dynamics of Sacramento Splittail (Pogonichthys Macrolepidotus) in the San Francisco Estuary: A Review”. In: *San Francisco Estuary and Watershed Science* 2.2 (2004). (Visited on 05/19/2022).

[188] Cait Newport, Oliver Padget, and Theresa Burt de Perera. “High Turbidity Levels Alter Coral Reef Fish Movement in a Foraging Task”. In: *Scientific Reports* 11.1 (Mar. 2021), p. 5976. (Visited on 05/08/2022).

[189] R. H. Douglas, J. Eva, and N. Guttridge. “Size Constancy in Goldfish (Carassius Auratus)”. In: *Behavioural Brain Research* 30.1 (Sept. 1988), pp. 37–42. (Visited on 05/18/2022).

[190] A. Meesters. “Über Die Organisation Des Gesichtsfeldes Der Fische. [On the Organization of the Visual Field in the Fish.]” In: *Zeitschrift für Tierpsychologie* 4 (1940), pp. 84–149.

[191] S. Chaudhuri. *Depth From Defocus: A Real Aperture Imaging Approach*. 2004. (Visited on 05/18/2022).

[192] MARGOT E Andison and JACOB G Sivak. “The Naturally Occurring Accommodative Response of the Oscar, Astronotus Ocellatus, to Visual Stimuli”. In: *Vision Research* 36.19 (Oct. 1996), pp. 3021–3027. (Visited on 05/18/2022).

[193] R. H. Douglas. “Goldfish Use the Visual Angle of a Familiar Landmark to Locate a Food Source”. In: *Journal of Fish Biology* 49.3 (1996), pp. 532–536. (Visited on 05/18/2022).

[194] Partha S. Bhagavatula et al. “Behavioral Lateralization and Optimal Route Choice in Flying Budgerigars”. In: *PLOS Computational Biology* 10.3 (Mar. 2014), e1003473. (Visited on 05/04/2022).

[195] Ayelet Sarel et al. “Vectorial Representation of Spatial Goals in the Hippocampus of Bats”. In: *Science* 355.6321 (Jan. 2017), pp. 176–180. (Visited on 05/20/2022).

[196] Johannes D. Seelig and Vivek Jayaraman. “Neural Dynamics for Landmark Orientation and Angular Path Integration”. In: *Nature* 521.7551 (May 2015), pp. 186–191. (Visited on 05/20/2022).

[197] David Andel and Rüdiger Wehner. “Path Integration in Desert Ants, Cataglyphis: How to Make a Homing Ant Run Away from Home.” In: *Proceedings of the Royal Society B: Biological Sciences* 271.1547 (July 2004), pp. 1485–1489. (Visited on 05/19/2022).

[198] Ingo Schiffner, Tristan Perez, and Mandyam V. Srinivasan. “Strategies for Pre-Emptive Mid-Air Collision Avoidance in Budgerigars”. In: *PLOS ONE* 11.9 (Sept. 2016), e0162435. (Visited on 05/20/2022).

[199] Roger Ratcliff. “A Note on Modeling Accumulation of Information When the Rate of Accumulation Changes over Time”. In: *Journal of Mathematical Psychology* 21.2 (1980), pp. 178–184.

[200] Gustav Markkula et al. “Accumulation of Continuously Time-Varying Sensory Evidence Constrains Neural and Behavioral Responses in Human Collision Threat Detection”. In: *PLOS Computational Biology* 17.7 (July 2021), e1009096. (Visited on 05/20/2022).

[201] Scott D. Gronlund and Roger Ratcliff. “Time Course of Item and Associative Information: Implications for Global Memory Models”. In: *Journal of Experimental Psychology: Learning, Memory, and Cognition* 15.5 (1989), pp. 846–858.

[202] Tyson L. Hedrick. “Software Techniques for Two- and Three-Dimensional Kinematic Measurements of Biological and Biomimetic Systems”. In: *Bioinspiration &amp$\mathsemicolon$ Biomimetics* 3.3 (July 2008), p. 034001. (Visited on 05/20/2022).

[203] R Necker. “Specializations in the Lumbosacral Spinal Cord of Birds: Morphological and Behavioural Evidence for a Sense of Equilibrium”. In: *European journal of morphology* 37.2-3 (Apr. 1999), pp. 211–214. (Visited on 05/19/2022).

[204] Darío Urbina-Meléndez et al. “A Physical Model Suggests That Hip-Localized Balance Sense in Birds Improves State Estimation in Perching: Implications for Bipedal Robots”. In: *Frontiers in Robotics and AI* 5 (2018). (Visited on 05/19/2022).

[205] Reinhold Necker. “Specializations in the Lumbosacral Vertebral Canal and Spinal Cord of Birds: Evidence of a Function as a Sense Organ Which Is Involved in the Control of Walking”. In: *Journal of Comparative Physiology A* 192.5 (Feb. 2006), p. 439. (Visited on 05/19/2022).